w/dwr w/a letter dtd 12/20/95

Milestone 0BB02
Results of Geophysical Surveys along the North-South and South ESF Alignment

Milestone 0BB03
Summary Report: Interpretation of Multiple Geophysical Surveys

WBS 1.2.3.11.2 Surface Geophysics

Principal Investigator - Ernest L. Majer, LBNL

M. Feighner, L. Johnson, K. Lee, T. Daley, E. Karageorgi, P. Parker, T. Smith, K. Williams, A. Romero, and T. McEvilly

Ernest Orlando Lawrence Berkeley National Laboratory
Berkeley, California 94720

102.8

TABLE OF CONTENTS

Milestone 0BB02
Results of Geophysical Surveys along the North-South and South ESF Alignment

Milestone 0BB03
Summary Report: Interpretation of Multiple Geophysical Surveys

WBS 1.2.3.11.2 Surface Geophysics

Principal Investigator - Ernest L. Majer, LBNL

M. Feighner, L. Johnson, K. Lee, T. Daley, E. Karageorgi, P. Parker, T. Smith, K. Williams, A. Romero, and T. McEvilly

Ernest Orlando Lawrence Berkeley National Laboratory
Berkeley, California 94720

SCOPE OF REPORT

It should be noted that two milestones are being reported on in this document. To properly process and interpret the gravity data along the Exploratory Studies Facility (ESF) North-South ramp alignment (lines YMP-10 and YMP-11), it was necessary to process all of the repository lines. Therefore, the milestone report dealing with the data along the North-South, and South Ramp projections is being reported on with the data from the other lines. It should also be noted that the USGS milestone for the magnetic results fell after this milestone and therefore the magnetic results are not included in this report.

The scope of this report is to present the results of all geophysical measurements taken by LBNL in Phase I of the high resolution geophysical studies over and near the repository block. As explained below, as of the date of the submittal of this report, measurements are still in progress over the repository block, however, this report covers all work carried out in FY 1995 to the end of July 1995. The main content of this report is the processing results of the gravity electrical, and high resolution seismic reflection work carried out over and near the the repository block. Interpretation is included on the seismic, gravity and electrical (magneto-telluric, (MT)) data. An overall interpretation and synthesis including the magnetic results, previous relevant geophysical work and the data collected in late FY 1995 will be performed in the next phase of the geophysical characterization of the repository block. This work follows the technical procedures outlined in GPP-01, GPP-18, and SP-10.

OBJECTIVE OF WORK/BACKGROUND

In August of 1993 a relatively small program was initiated by LBNL at the direction of the DOE/YMSCO in evaluating the use of high resolution geophysics for the detection and mapping of lithology, structure, faults, and fractures in the repository area at Yucca Mountain site. This initial work (Daley and Majer, 1993, Majer and Karageorgi, 1993, Daley, et. al.,

1994, Majer et. al., 1994) involved two Vertical Seismic Profiles (WT-2 and NRG-6) utilizing three component recording, P- and S-wave vibrator sources at multiple offsets, and the recording of three high resolution surface reflection lines (approximately 4.5 kilometers at 12 meter station intervals using an accelerated weight drop: LINE 1 across the Ghost Dance Fault, LINE 2 up Drill Hole Wash and LINE 3 on the top of Yucca Mt.). The location of these lines and the drill holes used for the VSP work is shown in Figure 1. The objective of the initial work was to provide seismic imaging from the near surface (100 m) to the depth of the repository horizon and below, if possible. Among the issues addressed by this seismic imaging work was the location and depth of fracturing and faulting, geologic identification of reflecting horizons, and spatial continuity of reflecting horizons. The results were generally positive, with some specific successes. This was also the first attempt at this scale using modern seismic imaging techniques to determine geologic features on Yucca Mountain. At the conclusion of the initial work it was recognized that we still had not fully optimized the data acquisition and processing, however, compared to previous efforts of seismic reflection studies in the Yucca Mt. vicinity (e.g. Harding, 1988, McGovern, et al., 1983), we felt that we had made significant progress in defining the optimal application of high resolution geophysical imaging methods at the Yucca Mt. site. In addition to the seismic data, there were also gravity and magnetic data (Oliver et. al. 1994) acquired along the central portion of LINE 1 (from WT-2 past UZ-16) by the USGS that confirmed the major faults detected by the seismic survey, and led to the conclusion that gravity and magnetic data could also be useful in the geophysical characterization effort.

Because of the above mentioned conclusions and success, a larger scale seismic, and gravity program was considered for FY 1995. However, because the past work did show that the seismic and gravity data alone could not provide information on the the conductive (hydrologic and electrical) nature of the faults, magnetic and electrical work was added for FY 1995. Past electrical work at Yucca Mt. had mixed success at best, considering the resolution required in the repository block area (The Tuff is very resistive and the structure is very difficult to resolve using electrical methods). However, a new approach of using "continuous" profiling magnetotellurics (MT) could possibly resolve important conductive features. Past efforts at MT (Frischknecht and Raab, 1984) were encouraging , but lacked resolution and depth penetration at the scales required. The "continuous" profiling MT approach is similar to seismic reflection, in that a profile of stations at relatively close spacing (50 to 100 meters, which is close for MT) is acquired. Recent advances in interpretation and inversion methods have allowed this approach to be performed. The approach adopted in the MT work was to perform a preliminary profile on several kilometers of line across the Ghost Dance Fault (GDF) region to determine its sensitivity and resolution. After performing the work and comparing the results to other techniques, and known geology, a decision will then be made on where to use this methodology. This MT technique is relatively expensive (two to three times the cost of seismic coverage) and its use may not be justified in the same quantity as the seismic reflection. However, over critical features such as the Ghost Dance fault and the sharp water table gradient to the north of the repository block, it may provide critical information on hydrogeologic parameters.

Therefore, in FY 1995 at the direction of DOE/YMSCO, LBNL embarked on a more ambitious program of utilizing high resolution geophysics on and around the repository block. This program is currently using high resolution seismic imaging using surface reflection and VSP, gravity, electrical (MT), and magnetic methods. LBNL is currently responsible for the

seismic, gravity, and electrical work in FY 1995, and the USGS is responsible for all of the magnetic work.

FY 1995 Activities

Figures 2a and 2b show the location of the repository lines on which various geophysical surveys were performed. Table 1 summarizes the data acquired through July of 1995. The results of the geophysical work carried out on these lines will be the subject of this report (except for the magnetic work, as mentioned above). Seismic reflection data acquisition was started in mid December of 1994 and continued until late February of 1995. Data on lines YMP-1, 2, 3, 4, 5, 6, 7, 7a, 8, 9, 12, 13a, 13b, 14a and 14b were acquired during this period. The plan for the electrical work was to perform the initial work on YMP-3, across the Ghost Dance Fault region, to determine the sensitivity and resolution of the MT technique. Gravity was to be run on all lines shown in Figure 2a, (except on Lines 7, which has already been run) and on the regional seismic lines acquired by the USGS. Magnetic data was also scheduled to be collected on all lines in Figure 2a by the USGS. It should be noted that as of the date of the writing of this report additional seismic and gravity data are in the process of being collected. Specifically, gravity and seismic reflection lines to extend lines YMP-3 and YMP-4 west in order to tie line YMP-5 to YMP-6, two additional very high resolution 600 meter surface reflection lines (HR-1 and HR-2) across the GDF at 2 meter intervals on YMP-4 and the 1993 LINE-1, one 5 kilometer long surface reflection, and two gravity/magnetic lines in Rock Valley to investigate the faulting in that region associated with the Little Skull Mt. earthquake sequence. Also, due to poor data quality, portions of the seismic reflection line along YMP-3 are being re-run with higher resolution and tighter shot spacing because of its importance. In addition to the seismic reflection and gravity data, check shot P- and S-wave VSP surveys are being performed in boreholes RF-4, RF 7-a, G-4, G-2, and SD-12. The purpose of the VSP is to collect median P- and S-wave velocity data from the surface to the repository depth for use in seismic ground motion studies, and to examine the variation of these velocities across the mountain. A secondary purpose of the VSP is to collect velocity information for constraining the processing velocities for the seismic reflection results. All of the additional work is scheduled to be complete by September 30, 1995.

SEISMIC REFLECTION

Reported here are results from high resolution seismic reflection on lines YMP-1, 2, 4, 5, 6, 7, 7a, (short cross line perpendicular to the Yucca Wash faulting) 8, 9, 12, 13a, 13b, 14a, and 14b. It should be noted that the depth and resolution targets was not the same for all lines. The results of line YMP-3 are not included due to equipment problems in the data acquisition of this line. As explained below, it is being re-shot as of the writing of this report in another phase of geophysical data collection. These lines sample a variety of geologic conditions and features of interest to the project. The target depth for the majority of the lines was from 100 meters to repository depth and below if possible. Lines YMP-1, 2, 3, 4, 5, and 6 were designed to look at structure, faulting, and lithology in or near the repository block over this depth range. Lines YMP-7, 7a, 8, and 9 were designed to investigate lithology and structure that could provide insight into the "steep water table gradient" at the north end of Yucca Mt. Line YMP-12 was a short line over a small section of the north ramp designed to look at very shallow structure (20 meters to a few hundred meters) in an area that would have

subsurface mapping, i.e., the ESF. The four short lines on the pad of UZ-7a (approximately 100 meters each) were acquired at very high resolution (1 meter group spacing, using a hammer source) to determine the detailed fault structure in this region, hopefully to a depth of at least 500 meters, i.e., lines YMP-13a, 13b, 14a, and 14b.

Data Acquisition

Fifteen high resolution surface reflection lines were carried out at Yucca Mountain. The data acquisition took place between Dec 1994 and Feb 1995, as listed in Table 2. The locations of the lines are shown in Figure 2a. The total number of stations, line length for each line, and the precise locations of the first and last CDP stations in Nevada State Plane coordinates are also listed in Table 2 (Note: all line station numbers started with 101). Each geophone location along the seismic reflection lines was surveyed by conventional optical survey methods to within 0.1 foot. In total, this phase of the surface reflection work had 39 days of recording with a total of 2003 shotpoints acquired over a total line length of 34.18 km.

A number of the lines were also surveyed with Global Positioning Survey (GPS). The values agreed to within 0.1 foot, therefore, we have a high degree of confidence in the survey coordinates. All the surveying was conducted by Raytheon Services, Nevada (RSN). The lines were chosen in various geologic conditions, perpendicular to major faulting (line YMP-3 and YMP-4, across the southern structure of the Ghost Dance fault (GDF)), almost parallel to major faulting (eg. lines 2, 6, and 9, along the Bow Ridge, Solitario Canyon and Drill Hole Wash Faults, respectively), and in areas of assumed relative sparse faulting (Line 5, along the crest of Yucca Mountain). In all cases, except on lines YMP-12, 13, 13a, 14, and 14a, the depth of investigation was focused from 100 meters to about 1 kilometer depth.

We designed the 1995 data acquisition using information obtained from the 1994 seismic reflection surveys (Daley, Majer and Karageorgi, 1994), which were carried out with an impact source, a single 30 Hz geophone per station, and 40 ft station spacing and 48 channel recording. We attempted to improve the data quality in a number of ways. We believed improvement would be gained by the use of sensor arrays, a more powerful source, and a larger number of recorded channels per shot. The standard 1995 acquisition set up was 12 m station spacing with 6 geophones per station in a linear array spaced 2 m per geophone. Mark product model L25D 30 Hertz geophones with 3 inch spikes were used and care was taken to lay the cables such that wind noise was reduced. There were 144 stations recorded on a OYO DAS-1 (serial number 19) for each source shot point.

The source was a modified Bison EWG-4 accelerated weight drop. This is an accelerated weight drop source in which a weight is raised (about one meter) and accelerated down onto a steel plate (about 0.6 m square) with two large "rubber bands". Approximately 30,000 pounds of force is generated on this strike plate. This was chosen over a vibrator due to its high frequency content, and the necessity to reduce source noise at the near offset geophones. Also field tests showed that the trigger jitter was less than one millisecond, which for most applications allowed stacking in the field. We also felt that our best data would come from the near offset points and although a vibrator may give deeper penetration at the far offsets, the structure at Yucca Mt. varies to such a high degree in a lateral sense (Daley et. al. 1994), it is difficult to properly use the far offset information. The source was typically used eight times at each shot point with the eight source "pops" stacked in the field to yield one shot record of 144 sensor channels. Typically 240 stations were laid out at a time and rolled through. Because of varying data quality, the actual number of shots stacked ranged from 6

to 16. The first shot was not recorded, it was used to "set" the strike plate. The shotpoint spacing was normally 24 m, although this spacing was reduced to 12 m in certain cases (such as near the Ghost Dance Fault, or on short lines such as YMP-7A and YMP-9). Line 12 had shot and receiver spacings of 3 m. The high resolutions lines YMP-13a, 13b and YMP-14a, 14b (which were acquired on the UZ-7A well pad) used 1 m station spacing. Data was usually recorded in a "split spread" with 72 stations behind the source and 72 stations ahead of the source. At times a source array was used with two source locations stacked together for a single shot record. The source array was used to reduce ground roll noise. Typically, each stack of eight shots was played back in the field for data quality monitoring. At the beginning of the survey, noise tests were carried out along Line 2 to determine the frequency range that could be obtained and the optimal source and and receiver spacing and other acquisition variables. This resulted in a standard recording of 3 seconds of data with a sampling rate of 1000 samples/seconds using an OYO DAS-1 (144 channel, 24 bit digital recorder).

Data Processing

For the seismic lines with a 3-meter and 12-meter station spacing (YMP-1, 2, 4, 5, 6, 7, 7a, 8, 9, and 12) the processing sequence in Table 3a was used. For lines YMP 13a, 13b, 14a, and 14b the processing sequence in Table 3b was used. There were small differences for YMP-12 that are noted in the table. The raw field tapes were provided in SEG-D format. These tapes were converted to SEG-Y format using the ProMAX version 40.29 seismic software. All processing after this step used the CogniSeis Focus 3.0 seismic software. As of the date of this work, the Focus 3.0 software is still in the qualification process, however, the only data that can be considered unqualified are the migrated results. The line geometry was produced by creating a spreadsheet of the locations of the shots and receivers, based on the observers logs. The geometry was applied to each trace header by using the PROFILE command. Figures 3a-g show a common shot gather for some of the lines, with reflection events highlighted by an arrow. As can be seen, most of the reflectors tend to be seen at longer offsets and lower frequency (about 40-50 Hz). It is difficult to identify a reflector that spans the entire offset range. This indicates that the reflectivity of the rock interfaces varies significantly over 2800 feet (the length of the 144 channels). Since most of these lines are crooked, the CDPLINE program was used to generate a smooth CDP line through the source-to-receiver midpoint locations and bin the traces accordingly. Next, REMSPK was used to remove spikes in the data, which had been observed on some shot gathers. IEDIT was the interactive trace editing program that was used to remove noisy or bad traces.

The next step was to use DATUM which calculates a running average of the surface elevations over the length of 144 stations. This produces a floating datum, to which STATIC applied the shot and receiver field statics, above or below this floating datum. The amplitudes of the traces were equalized by using a 400 ms AGC window. A number of deconvolution tests were done with the best result obtained from a predictive gap deconvolution operator that was 51 points in length with a gap of 24 ms. The traces were then filtered and sorted into CDP gathers.

The interactive velocity picking program, VELDEF, was used to pick the stacking velocities. The top of Figure 4 shows the velocity picks for one CDP gather for Line YMP-1, with NMO applied. The bottom of Figure 4 shows the stack of these CDPs with the indicated velocity function in red and two other stacks faster and slower than this function. This was an important quality control method in picking the stacking velocities. Figure 5 shows the

stacking velocities for each line. It should be noted that YMP-8, 9, and 12 had noticeably slower stacking velocities than the other lines. YMP-12 in particular had stacking velocities below 5000 ft/sec. All these lines are located on the northern portion of mountain and these slow stacking velocities may indicate highly fractured and/or weathered zones.

A number of special processing techniques were tried to enhance the signal, including residual statics, partial prestack migration, and Radon velocity filtering. Residual statics were tried on several lines, but without much success. This was probably due to the fact that the signal was not continuous across the full range of offsets. In all the residual statics tests, the data quality was not improved, but was often degraded. We use YMP-1 as an example in Figure 6 (top) to show a regular stack with only field statics applied. Next, we look at two special processing schemes that were tried in order to enhance the signal.

The first was partial prestack migration (PPM or also referred to as DMO - "Dip Moveout"). In this procedure, the traces are sorted into common offset gathers, NMO is applied, and then input into a finite difference DMO program, MIGRATE. The program corrects for the effect of dip on reflectors so that the data properly stacks when using a normal moveout function. The DMO section is shown in Figure 6 (middle). The process did improve the data in places, but did not do a very good job in the shallow section. This is because the effect of DMO becomes greater at increasingly shallow depths.

The next test was Radon Velocity Filtering, also referred to as a "tau-p transform". In this procedure, the CDP data is transformed using the ray parameter, p, which is the inverse of the horizontal phase velocity. A velocity filter passes events from -20% to +20% of the input velocity function, which in this case was the stacking velocities. The program RADSTK performs the transform, filtering, inverse transform, and stacking of the data. Figure 6 (bottom) shows a much improved section, especially at the shallow depths, probably due to the removal of the coherent noise trains. All the lines showed improvement in signal quality with this procedure and Radon Filtering was used in all the stacked plots to follow. A mild F-X Decon filter was used on YMP-12 after stack to give better coherency to the reflectors.

Migrated depth sections were also produced using a smooth average function hung from the surface. Figure 5 shows the migration velocity function used for all the lines, with YMP-1 given as an example. The function starts at 5000 ft/sec at the surface and increased by 0.5 feet/sec for each foot in depth. The exception to this is YMP-12, which used a slower migration function starting at 4000 ft/sec at the surface and increased by 0.5 feet/sec for each foot in depth (Figure 5). The migration velocity will effect the depth to reflectors; a 10% error in the velocity function could change the calculated depth by as much as 100 feet. Better migration velocity functions, incorporating VSP data and well data are being developed now to give more accurate depths to reflectors.

The processing flow for the 1-meter spacing lines (YMP-13a, 13b, 14a, and 14b) is given in Table 3b and a detailed location map of the CDP locations is show in Figure 2b. The processing of these lines used the ProMAX version 40.29 seismic software. This flow differed substantially from the previous flow, mainly due to the coherent noise trains present in the data. Examples of shot gathers for YMP-13a and YMP-14a are given in Figure 3h and Figure 3i, respectively. Following Table 3b, the noise trains were removed by using an air-wave mute, F-K filtering to suppress reflected energy, and 2-D spatial filtering to enhance the signal. After stack, the section is converted to depth using the VSP velocity data from well WT-2. No migration was performed as this tended to blur fault features.

Results and Interpretations

The goal of the surface seismic work is, like the other geophysical studies, to provide information on certain physical parameters between points of known properties. For example, VSP uses well logs or core information to "tie" the reflectors to known geologic structure. >From our previous work and experience on the lines shown in Figure 1, and from the VSP work in WT-2 and NRG-6, we knew that certain segments of the volcanics were reflective. We also knew that the volcanic sequences do not appear as a continuous seismic reflector in the subsurface, either as a result of faulting, depositional changes, or lithology changes. While the processing of the reflection lines was performed with minimal geologic input (other than assuming approximately horizontal interfaces), the interpretation of the final sections requires geologic constraints. However, it should be noted that from our previous work we knew that in this faulted, laterally heterogeneous environment certain reflection events would most certainly be from out of plane reflectors, thus from this viewpoint the processing did take into account the geologic environment.

It should be strongly noted that in all cases in this report the seismic interpreted sections ARE NOT OUR FINAL INTERPRETATIONS, the interpretations presented at this time are just one possible interpretation. Not until all of the geophysical data are synthesized into a self consistent geophysical model, and interpreted with the aid of geologic input, will our "best" interpretation be forth coming.

The first step of interpretation was to identify the significant reflection events which we believed represented lithologic or structural variations. We then attempted the initial geologic interpretation of the various seismic lines. Our strategy for this initial interpretation was to use the geologic information contained in the USGS computer based 3-D Lynx model (version 2.0) (Buesch et al., 1995) to constrain each individual reflection line. In most cases the Lynx model was of little constraint and it is plotted on the sections only as a reference for the reader and not intended to be the interpretation. The Lynx model and associated data base contains information from both surface mapping and borehole logging and coring. It represents a self-consistent 3-D geologic model, providing a starting point for the geophysical interpretation. Table 4 shows the lithologic units in the Lynx model and the colors associated with each horizon. Table 4 also shows the color scheme used in this paper and how it relates to the Lynx model. We use five colors in our interpretation as follows:

Pink - Tiva Canyon Tuffs

Orange - Bedded Tuffs
(incl. Pah Canyon Tuff and Yucca Mountain Tuff)

Blue - Topopah Spring Tuffs

Yellow - Calico Hills Formation

Green - Prow Pass Tuff

This color scheme is followed throughout this report, except for YMP-12, which is a high resolution line, and the color-coded lithologies used for this line are given in Figure 16c.

For each line, a cross-section was obtained from the Lynx data base connecting the beginning and ending points of the seismic line. Within the seismic section we attempted to maintain the general geologic structure shown by the geologic cross-section, however, we modified the geologic interpretation to match the structure indicated by the seismic reflection events. This modification could consist of locally varying the dip and thickness of certain lithologies. As noted in the seismic processing section, the conversion of seismic data from time to depth is an inexact process, and the depth errors may affect the lithologic interpretation of the seismic reflectivity.

The quality of seismic reflectivity varied substantially from line to line and also within any one line. As we observed in the 1994 work (Daley et al., 1994), there were no reflections which were laterally continuous across an entire line. However, with the improvements described in the data acquisition section above, we were able to significantly improve the imaging in some cases. In particular, line YMP-2 showed a reflection which was nearly continuous along the entire line. However, most lines had breaks in the reflectors and were not laterally continuous.

We start with Line YMP-1, which is the southernmost of the repository lines (Figure 2a). The stacked CDP section is shown in Figure 7a, the migrated depth section in Figure 7b, the Lynx geologic model in Figure 7c, the highlighted reflectors in Figure 7d, and an interpreted section in Figure 7e. The Ghost Dance Fault crosses the line near CDP 642 and the Dune Wash Fault crosses near CDP 402. There are good shallow reflectors over much of the line associated with the Topopah Spring Tuffs (blue), as well as deeper Calico Hills Formation (yellow) and Prow Pass Tuff (green). The offset across the Ghost Dance Fault is small at this point (about 50 feet) but across the Dune Wash Fault the offset is about 500 feet, from the Lynx model. There is a small gravity anomaly that indicates the Ghost Dance Fault is down to the west, in agreement with the Lynx model. There also may be a fault at about CDP 323, or this may also be the Dune Wash Fault again, since his line crosses the Dune Wash Fault at such an oblique angle. One could with ease plot other faults in this region at the diffractor points, however, at this point in the interpretation we were conservative in our fault interpretation.

The stacked section of YMP-2, migrated depth, Lynx model, reflector highlight, and interpreted section are shown in Figures 8a-e. This north-south line has a continuous reflector we interpret as the top of the Topopah Spring Tuffs (blue color) on the northern end of the line. If this correlation is correct, then the Topopah Spring Tuffs may be deeper to the south than in the Lynx model. As compared to other lines the quality of the data is quite good. We attribute this higher quality due to the lack of any large fault structures, and the good conditions of low wind during the acquisition phase of the data collection.

YMP-4 sections are shown in Figure 9a-e. This line runs east-west up Yucca Mountain and traverses over 1100 feet in elevation. The data quality is generally poor with a few patches of reflectors. It is worthwhile to note that the acquisition conditions were not that different from YMP-2. We attribute the poorer quality due to geologic conditions, rather than shooting conditions. Although the rapid change in topography on the west end of YMP-4 did make processing more difficult. Most shallow events are missing, but a few deeper reflections are spotty and dip to the east. The Ghost Dance Fault crosses at about CDP 396 with little offset and the Bow Ridge Fault crosses at about CDP 782 with unknown offset, from the Lynx model. A few strong reflectors to the west appear to correlate with the bottom of the Topopah Spring Tuffs (blue). If so, then these tuffs may be shallower to the east than in the

Lynx model.

YMP-5 sections are shown in Figures 10a-e. This line runs along the crest of Yucca Mountain and the reflectors tend to be near horizontal with limited lateral continuity. There are no major faults from the Lynx model. The Topopah Spring Tuffs (blue) appear to have a number of reflectors at the top and at the base. The Yucca Mountain Tuff (orange) appears to be a reflector in places as well. This is an interesting sections from several viewpoints. This is an example of how a change in depositional characteristics may affect the seismic data. Buesch (per communication) mapped the thickness of the lithostratigraphic contacts along this line. He mapped the base of the crystal-poor vitric nonwelded subzone of the Tiva Canyon Tuff, the base of the crystal-rich vitric moderately welded subzone of the Topopah Springs Tuff, and the contacts where the amount of lithophysae drop below one percent in the crystal-poor upper lithophysal zone of the Topopah Spring Tuff. Preliminary results from this work indicate that there are variations in thickness and lateral continuity of units. Buesch has indicated that the thickness of the deposits increases as one goes northward, but this thickening increases sharply north of N 761500, or at CDP point 460, where there is a loss of reflectivity. In addition, Buesch generally confirmed the locations of the Scott and Bonk (1984) mapped faults in position, but in the preliminary interpretations the nature of the faulting was not confirmed. The seismic data also indicate laterally varying thickness of the stratigraphic units and possibly thickening to the north. Also of note is the correlation of the flattening of the residual gravity data (between CDP 703 and 723 on Figure 10a) and an increase in reflectivity. This change in reflectivity is due to a change in material properties, either due to faulting changing the rock properties at this point or depositional changes.

YMP-6 sections are shown in Figures 11a-e. This line runs up Solitario Canyon, just west of the Solitario Canyon Fault. The near continuous shallow reflector to the south appears to correlate with the bottom of the Topopah Spring Tuffs (blue). If so, then the data suggests that these units are draped over the topography of the Calico Hills (yellow), with a relief of about 50-75 feet. At about CDP 713, there appears to be a break in the shallow reflector, possibly indicating the presence of a fault. The Lynx model does not show a fault here, but the fault geometry is complicated to the north, and this could be a splay fault crossing Solitario Canyon.

YMP-7 sections are shown in Figures 12a-e. This line is the northernmost line and traverses up Yucca Wash, just south of the Yucca Wash Fault. The Solitario Canyon Fault barely crosses this line to the northwest, and the Bow Ridge Fault is to the southeast at about CDP 253. Nice reflectors appear to correlate with the top and bottom of the Topopah Spring Tuffs (blue), although patchy. Some reflectors also appear in the Calico Formation (yellow), and possibly, the Prow Pass Tuff (green).

YMP-7a sections are shown in Figure 13. This is a very short line across the Yucca Wash Fault at about CDP 252. There are a few shallow reflectors in the Topopah Spring Tuffs (blue) and they may truncate at the Yucca Wash Fault, but the fold coverage quickly drops near the edges of the section and this is uncertain.

YMP-8 sections are shown in Figures 14a-e. This line runs along the crest of the ridge between Pagany Wash and Sever Wash. Data quality is generally poor for this line, but some reflectors appear to correlate with the Topopah Spring Tuffs (blue) and dip to the southeast, in agreement with the Lynx model.

YMP-9 sections are shown in Figure 15. This line strikes northwest up Drill Hole Wash. There are a few reflectors in the Topopah Spring Tuffs (blue) that appear to truncate at about CDP 303, but no faulting in noted in the Lynx model. Since no reflectors are seen to the southeast, it is uncertain whether this is a fault, but the gravity shows no anomaly here.

YMP-12 sections are shown in Figures 16a-d. This line is a high resolution line with a station spacing of 3 meters and is located just above the north ramp tunnel through Exile Hill. The stacked time section (Figure 16a) shows a break in the reflectors at the location of the Bow Ridge Fault. The gravity also shows a 1 mgal signal here. When this section is migrated (Figure 16b) the fault becomes less distinct. The geologic model in Figure 16c is from (Beason, 1995) and is a cross-section based on information obtained from drilling of the tunnel. In our interpretation (Figure 16d), we see reflectors associated with individual east dipping units of the Tiva Canyon Tuffs, west of the Bow Ridge Fault. However, east of the Bow Ridge Fault, we see a strong reflector dipping to the west, in opposition to the cross-section. We tried a number of different processing flows to compare to this one (DMO, FK filter, different stacking velocities) and all of them showed this west dipping reflector. Most likely this reflector represents out of the plane energy bouncing off a fault plane and coherently stacking in the section.

A great deal of effort was placed on careful processing and interpretation of the lines across the UZ-7a pad. These lines were presented in an earlier report (milestone 0bb03c), however, additional processing and interpretation has been carried since that report has been submitted. Figures 17 through 19 present the processed and interpreted results of the data acquired on the UZ-7a pad. Figure 2b shows the location of these lines relative to UZ-7a and UZ-8 boreholes. It appears that the GDF is not N-S trending at this location. depending on where one picks the intersection of the GDF on Line 14a, (either CDP 270 or 226) it is either trending NE or NW. Our preferred pick is around 270, thus making the GDF trending slightly NE. Although the trace of the GDF looks like there is a large dip and some curvature, the large horizontal exaggeration should be noted (almost 10 to 1). The faulting at around CDP 225 On line 14a may be an extension of the east dipping faulting at CDP 320 on line 13a. Correlation with the results of the drilling from UZ-7a have not been carried out, however, one would expect UZ-7a to intersect significant fracturing.

Conclusions

In summary, we review the possible correlation of the reflectors with lithology, starting from the top down. The Tiva Canyon Tuffs (pink) were generally not reflectors on the seismic lines with 12-meter spacing. For YMP-12, with 1-meter station spacing, reflective individual units were observed. The Pah Canyon Tuff and Yucca Mountain Tuff (orange) were weak reflectors, with the possible exception of the southern part of YMP-5. The greatest amount of reflections appear to come from within the Topopah Spring Tuffs (blue). From Table 4, the uppermost tuff is Tptrv, a crystal-rich, vitric, non-welded tuff, which may be a reflector (YMP-2, southeast YMP-7). The bottom reflectors of this unit frequently appear as a doublet (portions of YMP-4, 5, 6, and 7) and this could represent the alternating lithophysal/non-lithophysal character of these tuffs, such as the Tptul and Tptpln units. Deeper reflectors appeared on most sections, probably associated with the units of Calico Hills Formation (yellow) and Prow Pass Tuff (green). However, the continuity of these reflectors was poor. Locations of known faults from the Lynx model generally corresponded to breaks in reflectors for lines YMP-1, 4, 7a, and 12. In addition, some possible faults (YMP-1, 6, and

9) were seen that are not in the Lynx model. However, care must be taken in inferring faults where reflectors end, since the general pattern of reflectivity seems to be patchy.

The interpretations presented here are only preliminary; improved migration velocity functions incorporating VSP well data will be carried out in order to identify reflectors with confidence. For this milestone report, emphasis was placed on obtaining the best possible stacked time sections for the lines.

GRAVITY

Introduction

This report describes the initial phase of a surface gravity survey performed by Lawrence Berkeley National Laboratory (LBNL) at Yucca Mountain. It presents the data obtained for twelve repository gravity lines and gives a preliminary interpretation of the crustal and basement structure which is consistent with the observed data. Particular attention is given to the areas where the gravity lines cross mapped faults to determine if the gravity anomalies can place constraints on the location and amount of offset on the faults. This work is also meant to complement the other geophysical surveys currently being conducted and has, as general goals, the broad interpretation of geologic substructure, the delineation and interpretation of faults and fault systems, and the nature of recent movement along such faults. In particular, most of the gravity lines coincide with seismic reflection lines.

Equipment and Calibration

The vertical acceleration of gravity was measured with two LaCoste and Romberg Model G gravity meters. The serial numbers of these meters are 244 and 531. The meters were read manually for all of the data collected in this project.

The meter calibration factors for the general region that includes Yucca Mountain were determined on the basis of four different runs on the Charleston Peak gravity calibration loop (Ponce and Oliver, 1981). The results of these calibration runs are contained in Tables G1 and G2. The mean values shown in these tables were obtained as maximum likelihood estimates of the average of the four individual runs. These mean values were used in the reduction of all the data collected as part of this project.

All gravity measurements were tied to the absolute gravity station MERCA, which is located in the U.S. Geological Survey Core Library building in Mercury, Nevada (Zumberge et al., 1988). The value of gravity at floor level which was used for this station was:

$$g = 979518.874 \ cm/sec^2$$

Each day of gravity measurements began and ended with a reading at this station, which served as the primary base station for all gravity measurements for this project.

Data Acquisition Procedures

The two gravity meters were operated in tandem for all of the survey lines. The meters were used in a leap frog fashion with the measurement at a minimum of every tenth station being duplicated by both meters. This provided redundancy in at least 10% of the readings and helped identify any possible tares in meter operation. All key points, such as the beginning and ending stations on all survey lines and the first and last stations for each day, were

always read with both meters.

Data Reduction Procedures

After the removal of the effects of the solid earth tides, a drift correction was estimated for each meter for each day. This correction was based on all stations which had been occupied more than once by the same meter in the same day and assumed that the drift was linear in time. The drift rate was estimated with a least squares procedure using a weighting factor proportional to the time duration between two measurements at the same station. This calculated drift, which typically had a maximum value of less than 0.05 mgals/day, was then removed from the readings for that day.

After correction for solid earth tides and meter drift, all measurements were referenced to the value at the base station MERCA. The data collected with the two meters were then combined for each station where gravity had been measured more than once. For these stations a mean and standard error was obtained and the mean value used in all further calculations for that station. The standard errors were used to detect any errors in the reading or recording of the data.

Basic Observational Data

The locations of repository lines 1 through 12 are shown on Figure 2a. Table G3 lists the parameters of the gravity collection procedures along each of these lines. About 750 total gravity readings were collected. The basic observational data for these lines, which are observed gravity referenced to the base station MERCA, are listed in Tables G4 through G15.

Density Data

Interpretation of the gravity data in terms of geological structure requires assumptions about density as a function of depth below the surface. These assumptions are aided by sampling of surface rocks, sampling of drill cores, gamma ray logs, and borehole gravity measurements. Snyder and Carr (1984) have summarized these results available in the vicinity of Yucca Mountain. They found that the Cenozoic deposits have a density of about 2.0 gm/cm^3 near the surface which increases with depth at a rate of about 0.26 $gm/cm^3/km$. The average density of the sedimentary deposits can thus be described by the equation

$$\rho(z) = 1.95 + 0.26\, z \quad (gm/cm^3)$$

where z is depth below the surface in km. Their sampling of older basement rocks at the surface gave a mean density of 2.66 gm/cm^3. In a similar study of the area immediately north of Yucca Mountain, Reamer and Ferguson (1989) found that the tuff units within the Silent Canyon caldera have densities that can be described by

$$\rho(z) = 1.75 + 0.42\, z \quad (gm/cm^3)$$

Calculation of Gravity Anomalies

Standard methods were used to convert the observed gravity values into a Bouguer gravity anomaly that could be used to obtain a geologic interpretation (International Association of Geodesy, 1971; Morelli, 1974; Oliver, 1980). The value of a reference ellipsoid and the effect of elevation above this ellipsoid were first removed. In calculating the Bouguer

anomaly it was clear that the standard density of 2.67 gm/cm^3 was not appropriate for the surficial rocks of Yucca Mountain. Snyder and Carr (1984) used a value of 2.0 gm/cm^3 for the Bouguer correction. Our procedure was to use a value of 2.1 gm/cm^3 for the rocks above an elevation of 0.8 km and a value of 2.67 gm/cm^3 for the interval between this elevation and sea level. On the basis of a number of experimental calculations, these density values appeared to be optimum in the sense of producing a Bouguer anomaly which showed the minimum correlation with elevation.

The original plan was to perform all terrain corrections with digital data. Topography data for Yucca Mountain and its immediate vicinity created from 1:6000 orthophotos were obtained, but these data have not yet been successfully modified to a form suitable for the terrain correction. Therefore the data in this report were reduced with estimates of the terrain corrections that were provided by the US Geological Survey (Langenheim, 1995). These terrain corrections do not include the effects from zones A and B (within 68 meters of the station).

Interpretation of Gravity Anomalies

The basic objective of this phase of the analysis was to provide a gravity data which could be used in the interpretation of the geological structure at Yucca Mountain. A critical element of this task is to remove the effects of regional structure from the gravity observations. The results obtained in WBS 1.2.3.11.2, which was an analysis of gravity data on two regional lines that crossed Yucca Mountain, were used to achieve this task. In that report a model of the regional structure which explained the main features of the observed gravity along the two regional lines was derived. This regional structure consisted of two basic elements, the general crust and upper mantle structure in the western US and variations in depth to basement near the regional lines. For the crust and upper mantle structure, a model for central and western North America was used which consisted of density versus depth for the upper 200 km of the earth in about 20 different regions. However, the main contribution came from only three regions, the Sierra Nevada, the Basin and Range, and the Colorado Plateau. The net effect from this element was about -132 mgal, with a variation of less than 1 mgal over the extent of the regional lines. The second element of the regional structure was a model of the upper few kilometers of the crustal structure in the vicinity of Yucca Mountain, with the primary parameter of interest being depth to basement. A model consisting of 12 different regions was constructed which accounts for all areas within about 10 km of the regional lines, with density versus depth down to a depth of 4 km below sea level specified for each region. The effect of this basement structure was a variation in gravity of up to 40 mgal over the extent of the regional lines. All of these calculations were performed with the method of Johnson and Litehiser (1972) for three-dimensional structures in a spherical earth.

The geological structures which were needed to explain the observed gravity data along the regional lines are primarily related to changes in depth to basement. Along the east side of the Bare Mountains there appears to be an eastward dipping normal fault with a minimum of almost 3 km of vertical offset. To the east of Yucca Mountain the basement shallows in the vicinity of Busted Butte and Fran Ridge, with about 2 km offset of basement on the west side of this feature and about 1 km on the east. The elevation of basement along this feature is 0.2 km below sea level, in agreement with the depth to basement of 1.2 km found in drill hole P1. The sediments that cover the basement were modeled as fairly uniform in the horizontal direction, with a slight decrease in density east of Solitario Canyon. The sediments

have a continuous increase in density with depth, with the density anomaly ranging from -0.5 gm/cm^3 at the surface to -0.2 gm/cm^3 at the depth of basement. The only exception to this was in the Amargosa Desert where a thin layer of low density material was used to model the alluvium. It should be pointed out that in general there is a trade-off between the density of the sediments and the depth to basement, so that the depth to basement in our model could be increased somewhat by increasing the density of the sediments.

For all of the gravity plots shown in this report the effects of the regional and basement structure have been removed. Thus, what is termed the "residual anomaly" is the Bouguer anomaly with the calculated effects of the model derived from the regional lines removed. To the extent that the regional model is correct, this residual anomaly should only contain the effects of density variations in the upper few kilometers of the sediments at Yucca Mountain. This permits a direct comparison with the seismic reflection data, which contain information on this same region of the shallow crust.

Repository lines 1, 11, 3, 4, 12, and 9 are all predominantly east-west lines on the east slope of Yucca Mountain (see Figure 2a). Line 1 begins in Dune Wash to the west of Boundary Ridge and proceeds southeast alongside Yucca Mountain Road before branching off into Abandoned Wash. Line 11 begins near the H-3 well pad on the crest of Yucca Mountain and proceeds due east into Ghost Dance Wash, crosses Boundary Ridge, and ends in Midway Valley. Line 3 begins near the crest and proceeds along the north flank of Whaleback Ridge before descending into Midway Valley. Line 4 also begins near the crest of Yucca Mountain and proceeds eastward to the south of Live Yucca Ridge into Split Wash and finishes in Midway Valley. Line 12 is a short line which crosses the North Portal in an east-west direction. Lines 9 lies north of the main repository and has a general northwest-southeast trend, being located within Drill Hole Wash. Cross sections of the basement structure and the residual gravity anomalies along these six lines are shown in Figures G1 to G6. Prominent surface features and the approximate locations of mapped faults are also shown in these figures. The sediments between the basement and the surface are colored to show variations in density anomalies, ranging from -0.5 gm/cc (yellow) at the surface to -0.2 gm/cc (blue) at the contact with the basement (red).

Line 1' is the most southerly of this group of east-west lines and follows a more southeasterly direction. Near its west end where it crosses the Ghost Dance Fault there is a slight depression and a possible offset of 0.5 mgal, which would be consistent with downward displacement on the west side of this fault (Figure G1). There are other local variations in gravity along this line, with a possible offset of about 1 mgal slightly to the west of the point where the Dune Wash Fault intersects the gravity line at a low angle. Line 11 (Figure G2) crosses the mapped trace of the Ghost Dance Fault, but does not extend as far east as the Bow Ridge Fault. There is a small depression in the gravity anomaly near the Ghost Dance Fault, but a more prominent feature is located a few hundred meters to the west. The largest local anomalies, up to about 1 mgal, are located in the vicinity of Boundary Ridge. There are a series of mapped but unnamed faults in this area which appear to join up with the Bow Ridge Fault further to the south. Lines 3 and 4 both cross mapped traces of the Ghost Dance Fault and Bow Ridge Fault (see Figures G3 and G4). The Ghost Dance Fault does not cause any clearly identifiable anomaly in the gravity data on either of the lines. However, the Bow Ridge Fault produces a distinctive feature on both lines, consisting of a negative dip a few hundred meters wide having a maximum deviation of about 1 mgal. This is not the type of anomaly one would expect for a simple change in density across the fault, but is more

suggestive of a zone of low density along the fault. Even though Line 12 is quite short (Figure G5), it appears to show an anomaly associated with the Bow Ridge Fault, similar to those present on Lines 3 and 4. Line 9 is also rather short (Figure 6) and does not show any clear anomaly where it crosses the Ghost Dance Fault.

Repository Lines 6, 5, 10, 8, and 2 are all predominantly north-south lines that parallel the Yucca Mountain crest on either side. Line 6 runs up the floor of Solitario Canyon. Line 5 runs along the crest of Yucca Mountain. Line 10 runs along the east side of Yucca Mountain, crossing about six major ridges that extend eastward from the crest. Line 8 is further to the north and runs along the crest of the ridge bounded by Pagany Wash and Sever Wash. Line 2 extends along the base of Yucca Mountain to the west of Midway Valley. Cross sections of the basement structure and the residual gravity anomalies along these four lines are shown in Figures G7 to G11. All five of these north-south gravity lines exhibit quite similar residual gravity anomalies, characterized by a general negative trend in the anomaly as one proceeds from south to north and then a transition to an interval of almost constant values near the northern ends of the lines. Aside from these general features, the north-south lines do not show any significant local features that could be reliably associated with the crossing of a fault.

The negative trend in these north-south lines could possibly be modeled by a deepening of the basement towards the north. Note that basement structure shown in Figures G7 - G11 shows no relief in a north-south direction, reflecting the fact that the regional gravity lines provided very little control on north-south structure changes. The repository gravity data may require that some north-south features be added to the basement structure. However, with a simple deepening of the basement, it would be difficult to explain the inflection point which marks the transition from decreasing to constant values, particularly prominent on line 6 (Figure G7). Thus an alternative explanation may be possible in terms of a general change in density in the shallow sediments. It is also worth noting that the inflection points on these gravity lines correlate roughly with positions where the depth to water table begins to decrease. By incorporating geologic data and other types of geophysical data, it should be possible to decide between these various possible interpretations, or perhaps demonstrate that a combination of more than one is required.

Repository Line 7a is a very short line located well north of the main repository area in Yucca Wash. A cross section of the basement structure and the residual gravity anomaly is shown in Figure G12. This line shows a steep trend in the anomaly, but it is difficult to give a reliable interpretation of this feature, primarily because of the short length of the line.

Conclusions

During this stage of the analysis, the major emphasis has been on collecting and reducing the raw gravitational data. Using a model which was derived with the aid of data collected along the regional lines, the gravity data in the repository area have been reduced to residual anomalies which should only be a function of density variations in the upper couple of kilometers of the sedimentary section at Yucca Mountain. For the purposes of this report, there has not been an attempt to further interpret these residual anomalies in terms of fine-scale geological features within the repository area of Yucca Mountain. That task will performed later as part of a joint interpretation of all the geophysical data. However, it is possible to give a preliminary interpretation of the gravity data in the sense of noting where there is a correlation or lack of correlation between mapped faults and significant features in the residual

anomalies.

In every instance where it crosses the gravity lines the Bow Ridge Fault exhibits a negative anomaly of about 1 mgal, which could possibly be explained by a region of low density along the fault. The Ghost Dance Fault, on the other hand, shows a small gravity feature to the south where it crosses Lines 1 and 11, but appears to have very little if any effect upon the gravity further north in the main repository area..

One deficiency in the gravity analysis performed so far is the fact that the regional lines crossed the repository area in primarily an east-west direction, thus giving only limited control on regional gravity gradients in a north-south direction. This deficiency has become apparent in the analysis of the repository gravity lines, as there remains in the residual anomalies for the north-south lines a general trend of decreasing values from south to north. Further analysis will be required to determine the cause of this feature. Of note also is the lack of gravity anomalies on the East-West lines YMP-3 and YMP-4. On these two lines the seismic data were indicative of complicated structure and lithology. The gravity data indicate that the tuffs are relatively consistent in their density, but the seismic data indicate quite varied acoustic properties. If the gravity anomalies that do exist are due to faulting in the basement, the the offsets are relatively small and only in a few places.

MAGNETOTELLURICS

Objective

Hidden faults and geological heterogeneities at Yucca Mt. can be of great concern for the long-term integrity of the performance of potential repository. An attempt was made to detect and characterize these features using the magnetotelluric (MT) method. The utility of the MT method can be greatly enhanced if the method is coupled with other geophysical techniques, such as gravity and magnetic, and in particular the seismic method for structural constraints.

FY95 Task description

The overall task at LBNL consists of designing the MT field survey, oversight and quality control during the data acquisition period, and the actual interpretation of the data using the inversion code. The following is a summary of FY95 activities.

(1) A 2 mile line (YMP-3, see Figure 2a) was covered during the survey period May 31 - June 8, 1995. The contractor was Electromagnetic Instruments, Inc. (EMI).

(2) A multi-channel MT system was used for data acquisition in continuous mode.

(3) It was necessary to use non-polarizable electrodes, such as copper-copper sulfate electrode to collect data at low frequencies using the natural field. An initial 3-day survey in January of 1995 along a small section of YMP-3 used iron rods (rebar), which led to unsatisfactory results.

(4) Given the relatively shallow depth of investigation (repository depth) and high-resolution requirements (50 to 100 meters), we also used a controlled-source to achieve

high-frequency data.

(5) An initial data evaluation and preliminary interpretation was carried out.

The bandwidth of the final data is 0.01 Hz to 25kHz. Natural field energy provided data from 0.01 Hz up to 2 kHz, with a sampling rate of 6 points per decade. The controlled source covered the bandwidth from 460 Hz up to 25 kHz, with a maximum of 13 frequency data. There is a frequency overlap between MT and controlled source in the range of 460 Hz to 2 kHz. Only one data acquisition unit was necessary to collect data from both type of sources, natural and controlled.

At the end of the survey, the contractor provided impedance data, cross power, as well as the original time series. In addition the contractor provided EMAP filtered TM-mode data, and cross section of apparent resistivity for both the TM- and TE- mode.

Survey Procedure

An MT set-up consisting of eight electric and two magnetic measurements (8E-2H) was used (Figure MT1). One set-up covered four (4) stations. The electric dipole length used was 48 m, (same as the gravity stations, and every fourth seismic reflection point) and two models of the EMI induction coils were used to measure magnetic fields; EMi models BF-4 and BF-6.

MT Field Set Up

The BF-4 coils are for measuring low-frequency magnetic fields between 0.01 and 500 Hz. These coils were buried at least two to three feet below the surface of the earth to reduce noise. Since low-frequency magnetic fields can be assumed to be uniform over a 192 m interval (one set-up coverage), only one set of two orthogonal coils is needed for each set-up. To reduce polarization and noise we used copper-copper sulfate electrodes for measuring low-frequency electric fields. Each of the BF-6 locations marked by an x consists of two orthogonal high- frequency coils. A pair of BF-6 coils was placed at every station since the high-frequency magnetic fields could vary over the distance of single electric dipole spacing. These coils measure high-frequency natural field (MT) magnetic fields (170 Hz to 2 kHz), as well as the controlled-source magnetic fields up to 25 kHz.

After laying out all electrodes and coils, the measurements began by first making records for the low-frequency MT. All eight (8) electrodes and BF-4 coils are involved along with remote magnetic fields. The location of the remote magnetic fields with another pair of BF-4s is at the flag 250 for the entire YMP-3 line coverage (Figure 2a). Upon completing the low-frequency MT measurement, we next measured high-frequency MT and controlled-source field at the same time. For high-frequency magnetic fields we used BF-6 coils. At high frequencies, it was not necessary to use copper-copper sulfate electrodes.

To retain directional consistency at all stations, the electric dipoles and magnetic coils are always oriented S50*deg*E (X- direction) and N40*deg*E (Y-direction) along the entire coverage. The orientation of the YMP-3 profile was roughly parallel to the X- direction of the MT survey. Throughout the survey the contact resistance between electrodes and ground was kept below 1.6 kohms.

Characterization of data

The raw data are summarized in color 2-D sections, plotted as a function of frequency (vertical) and horizontal position along the transect from west to east. The apparent resistivity and impedance phase derived from the XY-mode impedance are shown in Figures MT2 and MT3. The XY-mode impedance is the ratio of the electric field along profile (X-direction) to magnetic field normal to the profile (Y-direction). Also plotted (Figures MT5 and MT6) are the apparent resistivity and phase derived from the YX- mode impedance, the ratio of the electric field normal to the profile and magnetic field parallel to the profile. Figure MT4 shows the cross section of the 1-D Bostick inversion of the EMAP filtered XY-mode impedance.

I. Controlled source data (above 500 Hz)

Above 4 kHz several conductive regions are apparent in the data, with apparent resistivities between 10 ohm-m and 100 ohm-m, and phases below 38 degrees (or 218 degrees), evidently corresponding to surficial structures, including the visible trace of the Ghost Dance Fault at the 800 m point on YMP-3. Between 4 kHz and 1 kHz, there are a number of small localized regions of low apparent resistivity, particularly between 400m and 1100m from the western end of the survey. Very rapid variation with frequency as well as some very high phases, suggest that these values may be spurious. Between 1 kHz and 500 Hz very low apparent resistivities may be attributed to near source effects from the magnetic dipole sources. Between 5 kHz and 800 Hz, XY apparent resistivities, ρxy, are very high (approximately 600 ohm-m) over much of the survey line. YX apparent resistivities are also higher at these frequencies, but generally significantly lower than the XY values. To the east, between 2600m and 3100m, only weak natural magnetic fluctuations were available as a source and data are unreliable.

II. Ambient source data (below 500 Hz)

Overall, the ambient source MT data is characterized by relatively lower apparent resistivities at 500 Hz, higher values from 300 Hz to 30 Hz (ρxy) or 400 Hz to 40 Hz (ρyx). The ρxy apparent resistivities return to low values, from 30 Hz to 0.3 Hz on the western end of the survey, and from about 80 Hz to 0.6 Hz on the eastern end. Between about 500m and 1300m from the western end, the ρxy values extend from 80 Hz to 0.3 Hz, with a pronounced offset at 1350m where the range of low values is from 80 Hz to 0.6 Hz. The ryx apparent resistivities are generally low in about the same frequency ranges, but show a much greater range in values from site to site, presumably due to effects of off-line variations in surficial conductivity which would offset the ryx curves in the manner observed.

The phase of the XY impedance, ϕxy, starts a bit below 45 degrees at 500 Hz, increases to values of about 65 degrees at the western end at about 30 Hz, and to values closer to 60 degrees at the eastern end. Some much higher phase values observed around 2500m are thought to be spurious. XY phases fall to a low of about 25 degrees centered about 0.4 Hz from the western end to about 1350m. At 1350m there is an abrupt change in the mid- frequency xy phase with the range of low phases spread over a broader frequency range, and centered at a higher frequency (~0.7 Hz). This transition is coincident with a large offset in XY apparent resistivity. The sharpness of the transition in the behavior of the mid-frequency XY phase is possibly an artifact due to varying amounts of mode mixing with varying ρxy to ρyx ratios. Mid-frequency YX phases attain a low of about 35 degrees, and show a similar

trend from west to east with low phases at slightly higher frequencies in the east.

At lower frequencies, apparent resistivities again increase, with a high centered at about 0.1 Hz, ρxy attaining values between 100 Wm and 800 Wm, with ryx remaining at much lower values. At the lowest frequencies (0.01 Hz) ρxy attains values between 100 Wm and 40 Wm, while ryx ranges from 100 Wm to 10 Wm. At the low frequencies, XY phase rises to as much as 70 degrees, and the YX phases to 65 degrees.

Interpretation

A spatial numerical filter was applied to the XY apparent resistivity results and subsequently transformed from frequency to depth using a 1-D Bostick transform to obtain an initial estimate of the conductivity structure beneath the survey line YMP-3 (Figure MT-4). This shows a 20m to 100m thick conductive layer at the surface (10 ohm-m to 100 ohm-m) with lower resistivities at the surface. This does not coincide with resistivity well logs for H-4, which is on line YMP-3. At the near surface it is difficult to obtain reliable data from this method. Between 100m and 300m depths resistivities tend more to a 200 ohm-m to 1000 ohm-m range, with an indication of enhanced conductivity in the vicinity of the Ghost Dance Fault (at x=800 m in Figure MT4). These values are in the same range as the well logs from H-4. The existence of a conductor shown between x=260 m and x=3100 m at intermediate depths is dubious, given the poor data quality there. The Bostick transformed data show a region of fairly uniform conductivity from 300m to about 900m depth, with resistivities around 100 ohm-m. It is not clear whether variations in the depth to the top of this zone are resolvable by the data. Beneath this is a conductive zone with inferred resistivities about 30 ohm-m in the west and closer to 50 ohm-m in the east, with resistivities greatly increasing below the first few kilometers.

An initial alternative model to the Bostick transformed ρxy data has been developed. The 2-D model and its responses in XY- mode and YX-mode are shown in Figures MT7, MT8 and MT9, respectively. The model (Figure MT7) consists of a surficial conductive layer (50 ohm-m) with thickness varying between 25m and 50m. Additional conductive material (10 ohm-m) has been added at 50m depth to increase the amplitude of responses at 800m and 1400m. The surficial layer of variable conductance is placed on top of 200 ohm-m material to 100m depth, above 2000 ohm-m material to 1 km depth. A layer of 10 ohm-m material was placed at 1km depth. To model the observation of larger 1Hz XY apparent resistivities beyond 1350m east and the smaller frequency range of low apparent resistivities there, and the observed trends in mid-frequency XY and YX phases, the layer was made 1 km thick west of 1350m and 250m thick to the east. The model was underlain by 2000 ohm-m material over 20 ohm-m material at 20 km depth (not shown in Figure MT7).

The response of the initial alternative model matches many aspects of the observed magnetotelluric data. One of its short comings is it results in high 500 Hz phases on the order of 20 to 30 degrees in the XY-mode and 15 to 30 degrees in the YX- mode. The XY phases are a bit too low and the YX phases not low enough. Apparent resistivities, particularly ryx, at 500 Hz are a bit too high. There needs to be quite a bit more surface conductance to carry currents in the Y-direction (normal to the profile), such as would be provided by thin isolated conductors in that direction. To avoid a pronounced effect on the XY-mode (TM) apparent resistivities at all periods, the conductors would need to be substantially thinner than the 48m dipole length used in the survey. The model (Figure MT7) is not able to match the sharp offset in XY phase response at 1350m at around 1 Hz, but rather results in a smooth variation

of phases from a minimum of 33 degrees at 0.8 Hz in the west to a minimum of 23 degrees at 1.4 Hz in the east, not as low as the values observed around 20 degrees. The marked site-to-site offsets in ryx have not been modeled, as they are thought to be simple static effects due to off-line surficial conductance variations.

The surface conductive layer may be due to enhanced conductivity of a weathered zone containing residual humidity, and should be able to be resolved quite well. The transition between very resistive rocks and the moderately conductive rocks at around 300m depth suggested in the Bostick transformed data is tantalizing, however we are uncertain that it is actually resolved by the data. The transition between a thick zone of porous rock below the water table to a thinner one east of 1350m has been chosen as more geologically plausible than a transition between a uniform thickness layer much more conductive to the west than east.

SUMMARY AND CONCLUSIONS

The major general conclusions regarding the character of the geologic structure from using seismic, gravity and electrical methods are:

(1). In terms of the seismic reflection work, it appears that the Tiva Canyon Tuffs were generally not reflectors on the seismic lines with 12-meter spacing. For YMP-12, with 1-meter station spacing, reflective individual units were observed. The Pah Canyon Tuff and Yucca Mountain Tuff were weak reflectors, with the possible exception of the southern part of YMP-5. The greatest amount of reflections appear to come from within the Topopah Spring Tuffs. From Table 4, the uppermost tuff is Tptrv, a crystal-rich, vitric, non-welded tuff, which may be a reflector (YMP-2, southeast YMP-7). The bottom reflectors of this unit frequently appear as a doublet (portions of YMP-4, 5, 6, and 7) and this could represent the alternating lithophysal/non-lithophysal character of these tuffs, such as the Tptul and Tptpln units. Deeper reflectors appeared on most sections, probably associated with the units of Calico Hills Formation and Prow Pass Tuff. However, the continuity of these reflectors was poor. Locations of known faults from the Lynx model generally corresponded to breaks in reflectors for lines YMP-1, 4, 7a, and 12. In addition, some possible faults (YMP-1, 5, 6, and 9) were seen that are not in the Lynx model. However, care must be taken in inferring faults where reflectors end, since the general pattern of reflectivity seems to be patchy. Again, at his point in the construction of the geophysical model for Yucca Mt. we are being conservative in our placement of faults. One must take care in order to balance the geologic sections and conserve the structure. This cannot be done until all the data are examined and interpreted.

(2). On the very high resolution lines across the UZ-7a pad, the seismic image indicated a steeply dipping graben-like structure with the Ghost Dance Fault (GDF) intersecting an eastward dipping fault. It appears that the GDF is fairly straight with little curvature. The faulting in this region appears to be complicated by cross-faulting and thus the images are difficult to interpret. Faulting could also be inferred to the east of the GDF.

(3). A one mgal gravity anomaly is associated with The Bow Ridge Fault on lines YMP-3, 4, and 12. The nature of the anomaly (shallow high frequency) indicates that it is due to a shallow low density region along the fault. The correlation with the seismic data was inconclusive for YMP-4, since the data in the shallow section was poor. However, there is good seismic evidence for faulting on YMP-12. However, the evidence is only shallow, and no there is no information to suggest a deeper anomaly indicating any large offset in the Bow

Ridge Fault at depth.

(4). The Ghost Dance Fault best appears on YMP-1, the southern most line, where the offset along this fault is the greatest. It can be seen in the gravity and seismic data. However, the Ghost Dance Fault is not clearly identifiable in the gravity and seismic to the north (YMP-3 and 4) where the offset is much less. The electrical methods found an indication of enhanced conductivity in the vicinity of this fault along YMP-3.

(5). The gravity studies did not find evidence for significant abundant faulting in the repository block area. This is in conflict with the seismic evidence that indicated a large variation in structure, either due to faulting or due to depositional and lithology changes. The gravity results may be indicating that the discontinuity in the reflectors shown in the seismic results (faulting?) may exist only in the tuffs (which have little density contrast, and thus any displacement across beds would not show up in the gravity data) and not in the underlying basement.

(6). No reflectors were identified to be basement paleozoic material. The depth of the basement from the seismic data appears to be at least 4000 feet under the repository block region.

(7). The steep water table gradient at the northern end of Yucca Mountain still remains a question, but the gravity and seismic data are providing critical clues. YMP-8 is located in the steep water table gradient, where the water table shallows to the northwest, from about 2400 feet elevation at CDP 202 to about 3300 feet elevation at CDP 667 (Bandurraga, 1995). The gravity data profile along this line shows a sharp inflection, which may indicate a basement fault. Interesting, the YMP-8 seismic section shows reflectors at about 3000 feet elevation which are slightly dipping to the northwest, between CDP's 203 and 343, possibly suggesting a buried fault. For the other seismic line in the water table gradient area, YMP-7, there appear to be a few reflectors slightly dipping to the northwest, against the southeastern regional dip, between CDP's 403 and 583 at 2500 feet elevation. The gravity data for YMP-7 was processed by the USGS (Langenheim and Ponce, 1994) and their gravity profile shows a sharp inflection about midpoint on the section near the anomalously dipping seismic reflectors. Integration of all the geophysical data into a consistent model may help explain the water table gradient.

(8). Due to the limited control on the regional gravity gradients in the north-south direction, there remains an unmodeled regional or basement effect in these north-south lines. For example, the gravity profile of YMP-5 also show an inflection point and it appears to correlate with an inflection point in the magnetic anomalies for this line published by Ponce et al. (1995). Further integrated modeling will be necessary to help explain these and other features.

In general, the geophysical results indicate that Yucca Mt. is made up of a complex overlapping structure of tuffs that vary in physical properties as a function of distance from their point of origin. The variation in seismic properties both as a function of depth and and lateral extent indicates that welding, the lithophysal content, and mineralogy are highly variable. It is difficult to distinguish this effect from fracturing and faulting, however in such data as the UZ-7a pad seismic lines where there is good surface evidence for faulting, it appears that the faulting is classic basin and range faulting with cross-cutting faults intersecting the normal faulting.

In order to put a coherent geophysical model together for the repository block the seismic, gravity, magnetic, and electrical lines discussed in this report, in addition to the data collected at the end of of FY 1995 (most notably the very high resolution 600 meter lines across the UZ-7a pad and on YMP-4, the VSP data at SD-12, G-4, G-2, and UZ-16) must now be all jointly interpreted with previous geophysical results. Future work will focus on this effort.

ACKNOWLEDGEMENTS

This work was carried out under U.S. Department of Energy Contract No. DE-AC03-76SF00098 for the Director, Office of Civilian Radioactive Waste Management, Office of Geologic Disposal, and was administered by the Nevada Operations Office, U.S. Department of Energy, in cooperation with the U.S. Geological Survey, Denver. The authors would like to thank David Buesch, Rick Spengler, Clay Hunter, and Warren Day of the U.S.G.S. for their input and reviews. We would also like to thank Ponce of the U.S.G.S. for assistance in the gravity work and in the interpretation of the gravity and magnetic data. Don Lippert, assisted with and facilitated the collection of all data in the field. David Jefferis provided the location and elevation data used in the reduction of the gravity data. Vicki Langenheim very kindly performed the calculation of the terrain corrections.

REFERENCES

Bandurraga, M., personal communication, September, 1995.

Beason, S., ESF North Ramp characterization project cross-section through Exile Hill, USBR Mapping Team, Preliminary Information Only, personal communication, May, 1995.

Buesch, D.C., Dickerson, R.P., Drake, R.M., and Spengler, R.W., 1994, Integrated geology and preliminary cross section along the north ramp of the exploratory studies facility, Yucca Mountain, in Proceedings of the Fifth Annual International Conference on High Level Radioactive Waste Management, Las Vegas, Nevada, volume 2.

Buesch, D.C., J.E. Nelson, R.P. Dickerson, R.M. Drake, R.W. Spengler, J.K. Geslin, T.C. Moyer, and C.A. San Juan, Distribution of lithostratigraphic units within the central block of Yucca Mountain, Nevada: A three-dimensional computer-based model, version YMP.R2.0, U.S. Geol. Survey Open File Report 95-124, 1995.

Daley, T.M. and Majer, E.L., 1993, Analysis Paper: Data Reduction NRG-6/WT-2 VSP, Interim Report for Activity: 8.3.1.4.2.2.5, Yucca Mountain Project.

Daley, T.M., Majer, E.L., and Karageorgi, E., 1994, Analysis Paper: Combined Analysis of Surface Reflection Imaging and Vertical Seismic Profiling, Interim Report for Activity: 8.3.1.4.2.2.5, Yucca Mountain Project, Milestone 3GGf241M.

Frischknecht, F. C., and Raab, P. V., 1984, Time-Domain electromagnetic soundings at the Nevada Test Site, Nevada, Geophysics, V. 49, no. 7, pp 981-992.

Gelsin, J.K., Moyer, T.C., and Beusch, D.C., Summary of lithologic logging of new and existing boreholes at Yucca Mountain, Nevada, August 1993 to February 1994, U.S. Geological Survey Open File Report 94-342., in press.

Gelsin, J.K., Moyer, T.C., 1994, written communication, Graphical lithologic log of borehole NRG-7/7A, DTN: GS940408314211.020.

Harding, S.T., 1988, Preliminary results of high-resolution seismic-reflection surveys conducted across the Beatty and Crater Flat fault scarps, Nevada, in Geologic and Hydrologic Investigations of a Potential Nuclear Waste Disposal Site at Yucca Mountain, Southern Nevada, M.D. Carr and J.C. Yount (editors), U.S. Geological Survey Bulletin 1790, p. 121-127.

International Association of Geodesy, 1971, Geodetic references system 1967, Special Publication 3, 116 p., 1971.

Johnson, L. R., and J. J. Litehiser, A method for computing the gravitational attraction of three-dimensional bodies in a spherical and ellipsoidal earth, J. Geophys. Res., 77, 6999-7009, 1972.

Langenheim, V. E. and D. A. Ponce, Gravity and magnetic investigations of Yucca Wash, Southwest Nevada, High Level Radioactive Waste Management, Proc. of the Fifth Ann. Int. Conf., Amer. Soc. of Civil Eng., Vol. 4, 2272-2278, 1994.

Langenheim, V. E., personal communication, September, 1995.

Majer, E.L. and Karageorgi, E., 1993, Analysis Paper: Ghost Dance Surface Reflection Profiles, Milestone Report for Activity 8.3.1.4.2.2.5. Yucca Mountain Project.

Majer, E.L., Johnson, L.R., Karageorgi, E.K., Peterson, J.E., 1994, High-resolution seismic imaging of Rainier Mesa using surface reflection and surface-to-tunnel tomography, in Proceedings of the Symposium on the Non-Proliferation Experiment Results and

Implications, M.D. Denny et. al., editors, Lawrence Livermore National Laboratory, Livermore, CA, CONF-9404100.

Martin III, R.J., 1993, personnel communication, Summary data sheet: NRG-6 Borehole.

McGovern, T.F., Pankratz, L.W., and Ackerman, H.D., 1983, An evaluation of seismic reflection studies in the Yucca Mountain area, Nevada Test Site, U.S. Geological Survey Open-file Report 83-912.

Morelli, C., editor, The International Gravity Standardization Net 1971, International Association of Geodesy Special Publication 4, 194 p., 1974.

Nelson, P.H., Muller, D.C., Schimschal, U., Kibler, J.E., 1991, Geophysical logs and core measurements from forty boreholes at Yucca Mountain, Nevada, U.S. Geological Survey, Geophysical Investigations, Map GP-1001, 64p.

Oliver, H. W., editor, Interpretation of the gravity map of California and its California margin, California Division of Mines and Geology Bulletin 205, 52 p., 1980.

Oliver, H.W., Majer, E.L., and Spengler, R.W., 1994, Geophysical investigations of the Ghost Dance Fault, Yucca Mountain, Nevada, abstract in Geological Society of America Cordilleran section meeting, San Bernardino, Ca., March 1994, p.78.

Ponce, D. A., and H. W. Oliver, Charleston Peak gravity calibration loop, Nevada, U.S. Geological Survey Open File Report 81-985, 20 p., 1981.

Ponce, D. A., R. F. Sikora, C. W. Roberts, R. L. Morin, and P. F. Halvorson, Magnetic investigations along selected high-resolution seismic traverses in the central block of Yucca Mountain, Nevada, USGS Open-File Report, preliminary draft, 1995.

Reamer, S. K., and J. F. Ferguson, Regularized two-dimensional Fourier gravity inversion method with application to the Silent Canyon caldera, Nevada, Geophysics, 54, 486-496, 1989.

Scott, R.B. and Bonk, J., 1984, Preliminary geologic map of Yucca Mountain, Nye County, Nevada with geologic sections, U.S. Geological Survey Open File Report 84-494.

Snyder, D. B., and W. J. Carr, Interpretation of gravity data in a complex volcano-tectonic setting, southwest Nevada, J. Geophys. Res., 89, 10,193-10,206, 1984.

Spengler, R.W. and Fox Jr., K.F., 1989, Stratigraphic and structural framework of Yucca Mountain, Nevada, Radioactive Waste Management and the Nuclear Fuel Cycle, vol 13(1-4), pp 21-36.

Spengler, R.W., 1994, personnel communication to authors.

USGS Rock Characteristics Section, 1994, written communication through L.R. Hayes to E.L. Majer, Methodology and Source Data used to construct the demonstration lithostratigraphic model: Second Progress Report, and L.R. Hayes to S. Jones, Early submittal of 3-D site scale lithostratigraphic model, version YMP.R2.0 Please. be advised that there may be uncorrected errors within this preliminary model as no quality checking or technical review has been performed on this version, YMP.R2.0

Zumberge, M. A., R. N. Harris, H. W. Oliver, G. S. Sasagawa, and D. A. Ponce, Preliminary results of absolute and high-precision gravity measurements at the Nevada Test Site and vicinity, Nevada, U.S. Geological Survey Open File Report 88-242, 29 p., 1988.

Table 1

Summary of Geophysical Lines in the Repository Area

Line	1	2	3	4	5	6	7,7a	8	9	10	11	12	13a	13b	14a	14b
Gravity (50m spacing)	X	X	X	X	X	X	X	X	X	X	X	X				
Magnetic (50m spacing)	X	X	X	X	X	X	X	X	X	X		X				
Seismic (meter spacing)	12	12	12	12	12	12	12	12	12			3	1	1	1	1
MT 50m, 3 comp			X													

Table 2
Seismic Line Information

						First CDP			Last CDP		
Line	Date	Station Spacing	Last Source Station	Last Sensor Station	Total Length (km)	Station	East	North	Station	East	North
YMP-1	1995 Jan 31-Feb 2	12m	363	365	3.18	202	567725	748189	713	560828	755179
YMP-2	1994 Dec 14-17	12m	286	310	2.52	202	568667	766721	596	567064	759172
YMP-3*	1994 Dec 17-20	12m	379	415	3.78						
YMP-4	1994 Dec 21-22, 1995 Jan 12-14	12m	436	436	4.03	282	560426	764781	848	570595	760268
YMP-5	1995 Jan 25-29	12m	485	490	4.68	202	558368	756862	964	558849	771827
YMP-6	1995 Feb 8-13	12m	506	524	5.09	202	553879	755327	1011	557883	770724
YMP-7	1995 Jan 17-20	12m	562	562	5.54	202	570706	772318	1054	559438	784574
YMP-7a	1995 Feb 7	12m	131	132	0.38	202	563462	780507	264	564523	781107
YMP-8	1995 Jan 15-17	12m	338	338	2.86	202	565027	770877	667	560348	778611
YMP-9	1995 Jan 14-15	12m	196	196	1.15	202	563116	768874	390	560290	771244
YMP-12	1995 Jan 21-22	3m	248	301	0.60	202	569565	765513	542	568078	766290
YMP-13a YMP-13b	1995 Feb 3-4	1m	232	232	0.13	187 383	562456 562269	760699 760629	342 463	562169 562257	760633 760759
YMP-14a YMP-14b	1995 Feb 5-6	1m	241	241	0.24	181 393	562187 562405	760727 760800	346 481	562496 562391	760745 760657

*Due to poor data quality, YMP-3 was reacquired in summer of 1995 and was not processed in time for this report.

Table 3a - DATA PROCESSING FLOW FOR YMP-1, 2, 4, 5, 6, 7, 7a, 8, 9, 12

PROCESSING STEP*	DESCRIPTION
SEGD to SEGY Conversion	Demultiplex data
PROFILE	Apply field geometry to trace headers
CDPLINE	Create a smooth CDP line through common midpoint locations to provide for more equal binning of CDP locations for crooked line geometry
REMSPK	Remove spikes in data
IEDIT	Interactive trace editing
DATUM	Calculate floating datum. Reference Datum is 5000 feet above sea level with a 5000 ft/sec replacement velocity (YMP-12 - 4000 ft Reference Datum)
STATIC	Apply shot and receiver statics to Floating Datum
AGC	Automatic Gain Control with 400 ms window
DECON	Predictive Gap Deconvolution
FILTER	Bandpass 12 - 100 Hz
SORT	Sort traces by CDP
VELDEF	Interactive Velocity Analysis Program. Pick stacking velocities
RADSTK	Radon velocity filtering using stacking velocities. Also stacks data
STATIC	Apply floating datum
FILTER	Bandpass 12 - 100 Hz
AGC	Automatic Gain Control with 400 ms window
PLOT	**Plot Stacked Section** (YMP-12 has additional F-X Decon after stack to enhance reflectors)
MIGZWE	Finite Difference Depth Migration of Time Section using smooth function hung from the surface
MUTE	Mute to station elevations
PLOT	**Plot Migrated Depth Section**

*All processing step names are from Focus 3.0 from CogniSeis Development, Inc., except SEGD to SEGY conversion which was done with Promax 40.29 from Advance Geophysical Corp.

Table 3b - MAIN PROCESSING STEPS FOR YMP-13a, 13b, 14a, 14b

PROCESSING STEP*	DESCRIPTION
Visual Editing	Bad shots and or traces were zeroed.
Band-pass Filtering	Different bandwidths were tried; for these lines the range 80-300 Hz gave the best results. Note that this is a substantially higher range than the one applied to the other lines.
Elevation Statics	
Mute of First Breaks	
Air-wave Mute	The shot gathers showed the air-wave (and the reflected energy from the wall at the pad) to be very strong. This was a particular critical step in the processing sequence.
Deconvolution	
F-K Filtering	To suppress negative slope events (reflected energy from the wall, etc.).
2-D Spatial Filtering	This step was more important in improving the signal-to-noise ratio in those lines with poorer data quality.
NMO	Simple velocity function used: 3000-4000 ft/sec at the fault zone and 7000-9000 ft/sec at other locations.
Stacking	
Post-stack Dip Filter	Removal of F-K artifact noise.
F-X Decon	
AGC	
Depth Conversion	Using WT-2 VSP velocity function.
PLOT	**Plot Depth Section**

*All processing was done with Promax 40.29 from Advance Geophysical Corp.

TABLE 4. COLOR SCHEMES OF LITHOLOGIC UNITS USED IN THIS PAPER

LYNX 2.0 COLOR SCHEME

	Modeled units	Lithostratigraphic units	Thermal-mechanical units	Hydrogeologic units
		PAINTBRUSH GROUP		
		Tiva Canyon Tuff (Tpc)	Undifferentiated overburden (UO)	Unconsolidated Surficial Materials (UO)
		Crystal-rich		
		Vitric		
		Nonwelded (rv3)		
		Moderately (rv2)		
		Densely welded (rv1[4], includes vitrophyre)		
		Nonlithophysal (rn)		
		Crystal-poor	Tiva Canyon welded unit (TCw)	Tiva Canyon welded hydrogeologic unit (TCw)
		Upper lithophysal (pul)		
	Tpcun	Middle nonlithophysal (pmn)		
		Lower lithophysal (pll)		
		Lower nonlithophysal (pln)		
		Hackly (plnh)		
		Columnar (plnc)		
		Vitric		
Aqua		Densely welded (pv3)[5]		
		Moderately welded (pv2)		
	Tpcpv	Partially welded to		
Red		nonwelded, (pv1)	Upper Paintbrush nonwelded unit (PTn)	Paintbrush nonwelded hydrogeologic unit (PTn)
		Pre-Tpc bedded tuff (Tpbt4)		
Blue	Tpy	**Yucca Mountain Tuff** (Tpy)		
Black	Tpbt3	Pre-Tpy bedded tuff (Tpbt3)		
Maroon	Tpp	**Pah Canyon Tuff** (Tpp)		
		Pre-Tpp bedded tuff (Tpbt2)		
		Topopah Spring Tuff (Tpt)		
	Tptrv	Crystal-rich		
		Vitric		
		Nonwelded welded (rv3)		
		Moderately welded (rv2)		
Yellow		Incipient devitrified		
		Densely welded (rv1)		
Purple	Tptrn	Nonlithophysal (rn)	Topopah Spring welded unit lithophysae-rich (TSw1)[6]	Topopah Spring welded hydrogeologic unit (TSw)
		Lithophysal (rl)		
	Tptpul	Crystal-poor		
Pink		Upper lithophysal (pul)		
		Middle nonlithophysal (pmn)	Topopah Spring welded unit lithophysae-poor (TSw2)	
	Tptpln	Lower lithophysal (pll)		
Cyan		Lower nonlithophysal (pln)		
		Vitric	Topopah Spring welded unit vitrophyre (TSw3)	
Coral	Tptpv3	Densely welded (pv3)		
		Moderately welded (pv2)	Calico Hills and Lower Paintbrush nonwelded unit (CHn1 + CHn2)	Calico Hills nonwelded hydrogeologic unit (CHn)
Green	Tptpv1&2	Nonwelded (pv1)		
		Pre-Tpt bedded tuff (Tpbt1)		
Blue	Tac	**Calico Hills Formation**		
	Tcp	**Prow Pass Tuff**	Calico Hills and Lower Paintbrush nonwelded unit (CHn3), Prow Pass welded unit (PPw), Upper Crater Flat nonwelded unit (CFUn)	
Red				

COLOR SCHEME USED IN THIS REPORT

Table G1. Calibration Runs for Meter 244				
No.	Date m/d/y	Drift mgal	Factor	Standard Error
1	12/01/94	-0.011	1.000705	0.000058
2	12/10/94	0.018	1.000810	0.000159
3	01/31/95	0.006	1.000745	0.000128
4	02/24/95	0.068	1.000806	0.000064
	Mean		1.000754	0.000039

Table G2. Calibration Runs for Meter 531				
No.	Date m/d/y	Drift mgal	Factor	Standard Error
1	12/01/94	-0.071	1.000570	0.000074
2	12/10/94	0.002	1.000559	0.000057
3	01/31/95	0.148	1.000631	0.000096
4	02/24/95	0.437	1.000439	0.000231
	Mean		1.000571	0.000040

Table G3. Repository Gravity Lines

No.	Date m/d/y	No. Stations	Station Spacing meters	Total Length km
1	02/03-04/95	67	48	3.0
2	02/01/95	55	48	2.7
3	02/01-02/95	79	48	4.0
4	02/04-05/95	84	48	4.0
5	02/02-03/95	98	48	5.0
6	02/14/95	106	48	5.0
7a	02/13/95	16	24	0.4
8	02/15/95	60	48	2.8
9	02/04/95	25	48	1.2
10	02/22-23/95	91	50	4.5
11	02/15-16/95	41	50	2.7
12	02/14-15/95	27	24	0.6

TABLE G4. OBSERVED GRAVITY FOR REPOSITORY LINE 1

Station	Latitude deg N	Longitude deg E	Elevation km	Gravity cm/sec**2
1-364	36.82460022	-116.45886230	1.274765	979480.476
1-361	36.82456589	-116.45846558	1.272022	979481.157
1-357	36.82452774	-116.45793152	1.268120	979482.116
1-353	36.82448196	-116.45739746	1.265042	979483.035
1-349	36.82442856	-116.45686340	1.262360	979483.690
1-345	36.82432175	-116.45634460	1.258672	979484.526
1-341	36.82424545	-116.45582581	1.254252	979485.686
1-337	36.82415390	-116.45529175	1.249497	979487.160
1-333	36.82408524	-116.45478058	1.243797	979488.814
1-329	36.82402802	-116.45425415	1.239865	979489.909
1-325	36.82397079	-116.45372772	1.237061	979490.828
1-321	36.82380676	-116.45323944	1.233038	979491.790
1-317	36.82353592	-116.45281982	1.229807	979492.746
1-313	36.82325745	-116.45242310	1.227094	979493.535
1-309	36.82297516	-116.45201874	1.224382	979494.252
1-305	36.82270050	-116.45160675	1.220693	979495.301
1-301	36.82242584	-116.45119476	1.216944	979496.327
1-297	36.82214737	-116.45077515	1.213439	979497.280
1-293	36.82188797	-116.45034027	1.210239	979498.082
1-289	36.82160950	-116.44992828	1.207099	979498.931
1-285	36.82131577	-116.44952393	1.203503	979499.725
1-281	36.82103348	-116.44911194	1.200912	979500.391
1-277	36.82075882	-116.44869232	1.198169	979500.935
1-273	36.82047653	-116.44827271	1.195029	979501.773
1-269	36.82020187	-116.44784546	1.191829	979502.438
1-265	36.81991959	-116.44742584	1.188263	979503.419
1-261	36.81963730	-116.44700623	1.185032	979504.184
1-257	36.81935501	-116.44659424	1.181374	979505.082
1-253	36.81908035	-116.44616699	1.177991	979505.990
1-249	36.81877136	-116.44578552	1.175492	979506.764
1-245	36.81844330	-116.44542694	1.172748	979507.488
1-241	36.81801605	-116.44530487	1.170127	979508.171
1-237	36.81758499	-116.44521332	1.167902	979508.780
1-233	36.81715012	-116.44512939	1.165708	979509.379
1-229	36.81671524	-116.44503021	1.163086	979510.098
1-225	36.81629562	-116.44486237	1.160404	979510.847
1-221	36.81601334	-116.44465637	1.157874	979511.631
1-217	36.81558990	-116.44420624	1.155405	979512.249
1-213	36.81527328	-116.44384003	1.153942	979512.526
1-209	36.81491089	-116.44351196	1.152693	979512.860

1-205	36.81452942	-116.44323730	1.150529	979513.571
1-201	36.81414413	-116.44297028	1.148182	979514.229
1-197	36.81376266	-116.44270325	1.146139	979514.733
1-193	36.81337357	-116.44245911	1.144250	979515.199
1-189	36.81297684	-116.44222260	1.141872	979515.798
1-185	36.81257629	-116.44202423	1.139739	979516.465
1-181	36.81216812	-116.44186401	1.137849	979516.929
1-177	36.81180191	-116.44158173	1.135350	979517.599
1-173	36.81148148	-116.44122314	1.133490	979518.121
1-169	36.81104660	-116.44088745	1.131143	979518.889
1-165	36.81077194	-116.44059753	1.128796	979519.524
1-161	36.81037903	-116.44035339	1.126175	979520.240
1-157	36.80996323	-116.44018555	1.124864	979520.604
1-153	36.80956268	-116.43996429	1.122883	979521.149
1-149	36.80918884	-116.43967438	1.121054	979521.611
1-145	36.80883789	-116.43934631	1.118860	979522.178
1-141	36.80845642	-116.43906403	1.117458	979522.626
1-137	36.80807877	-116.43878937	1.114684	979523.292
1-133	36.80772781	-116.43846893	1.112154	979523.918
1-129	36.80739212	-116.43811798	1.110295	979524.348
1-125	36.80704880	-116.43778992	1.107948	979524.860
1-121	36.80671692	-116.43743896	1.106211	979525.240
1-117	36.80641174	-116.43705750	1.104382	979525.677
1-113	36.80613709	-116.43663788	1.102766	979526.095
1-109	36.80587006	-116.43621063	1.100968	979526.538
1-105	36.80561829	-116.43576813	1.099383	979526.810
1-101	36.80535889	-116.43532562	1.098255	979527.249

TABLE G5. OBSERVED GRAVITY FOR REPOSITORY LINE 2

Station	Latitude deg N	Longitude deg E	Elevation km	Gravity cm/sec**2
2-317	36.83408737	-116.43824768	1.186312	979503.447
2-313	36.83448791	-116.43804169	1.178113	979505.258
2-309	36.83488464	-116.43785095	1.175979	979505.676
2-305	36.83528900	-116.43764496	1.174273	979506.049
2-301	36.83568573	-116.43743896	1.176741	979505.508
2-297	36.83608627	-116.43725586	1.177534	979505.240
2-293	36.83649445	-116.43707275	1.177747	979505.131
2-289	36.83687973	-116.43685150	1.176040	979505.350
2-285	36.83723450	-116.43653870	1.174059	979505.779
2-281	36.83763123	-116.43632507	1.170889	979506.309
2-277	36.83802414	-116.43611145	1.167841	979506.956
2-273	36.83843231	-116.43592072	1.164976	979507.535
2-269	36.83884811	-116.43579102	1.162660	979508.038
2-265	36.83926773	-116.43568420	1.159977	979508.524
2-261	36.83966827	-116.43549347	1.157996	979508.981
2-257	36.84006500	-116.43528748	1.155344	979509.404
2-253	36.84045792	-116.43506622	1.153881	979509.860
2-249	36.84085464	-116.43486023	1.154156	979509.716
2-245	36.84125137	-116.43466187	1.154064	979509.751
2-241	36.84165192	-116.43444824	1.153363	979509.923
2-237	36.84204102	-116.43423462	1.152784	979509.988
2-233	36.84244156	-116.43403625	1.152296	979510.056
2-229	36.84283829	-116.43383026	1.151047	979510.291
2-225	36.84323120	-116.43360901	1.151473	979510.096
2-221	36.84362793	-116.43355560	1.152875	979509.674
2-217	36.84402084	-116.43318939	1.153759	979509.505
2-213	36.84441757	-116.43298340	1.155497	979508.940
2-209	36.84480667	-116.43276978	1.156228	979508.687
2-205	36.84521103	-116.43256378	1.156807	979508.449
2-201	36.84560394	-116.43235016	1.157569	979508.220
2-197	36.84599686	-116.43212128	1.157844	979507.970
2-193	36.84636307	-116.43182373	1.157326	979508.108
2-189	36.84677887	-116.43173981	1.159398	979507.579
2-185	36.84720993	-116.43173981	1.159977	979507.367
2-181	36.84763718	-116.43175507	1.160831	979507.089
2-177	36.84806824	-116.43177032	1.161196	979506.881
2-173	36.84849548	-116.43177032	1.160800	979506.877
2-169	36.84892654	-116.43178558	1.161196	979506.633
2-165	36.84935761	-116.43180084	1.161044	979506.546
2-161	36.84978867	-116.43181610	1.160648	979506.522

2-157	36.85021973	-116.43181610	1.159276	979506.816
2-153	36.85065460	-116.43182373	1.158545	979506.897
2-149	36.85108185	-116.43183899	1.157508	979507.091
2-145	36.85151291	-116.43184662	1.156838	979507.052
2-141	36.85194016	-116.43186188	1.155680	979507.290
2-137	36.85237122	-116.43186951	1.155466	979507.192
2-133	36.85280228	-116.43186951	1.155466	979507.114
2-129	36.85322952	-116.43187714	1.155893	979506.852
2-125	36.85366440	-116.43190002	1.156228	979506.766
2-121	36.85409546	-116.43190002	1.156106	979506.623
2-117	36.85452652	-116.43190765	1.156045	979506.520
2-113	36.85495758	-116.43192291	1.155436	979506.616
2-109	36.85539627	-116.43193054	1.154796	979506.642
2-105	36.85582352	-116.43193054	1.154186	979506.785
2-101	36.85625839	-116.43195343	1.153942	979506.745

TABLE G6. OBSERVED GRAVITY FOR REPOSITORY LINE 3

Station	Latitude deg N	Longitude deg E	Elevation km	Gravity cm/sec**2
3-101	36.84739685	-116.46549988	1.487150	979426.451
3-109	36.84731293	-116.46443939	1.469532	979431.354
3-113	36.84724045	-116.46392822	1.456243	979434.754
3-117	36.84717941	-116.46342468	1.441155	979438.447
3-121	36.84714127	-116.46292877	1.421313	979443.079
3-125	36.84708786	-116.46240997	1.408999	979446.026
3-129	36.84703445	-116.46188354	1.404366	979447.355
3-133	36.84698105	-116.46136475	1.396289	979449.307
3-137	36.84692764	-116.46084595	1.383883	979452.345
3-141	36.84687805	-116.46032715	1.372880	979454.763
3-145	36.84682083	-116.45980072	1.364285	979456.809
3-149	36.84676743	-116.45927429	1.359317	979458.046
3-153	36.84671402	-116.45875549	1.352489	979459.719
3-157	36.84666061	-116.45822144	1.344137	979461.524
3-161	36.84661865	-116.45770264	1.333073	979464.104
3-165	36.84656143	-116.45718384	1.330361	979464.934
3-169	36.84649277	-116.45665741	1.325545	979466.283
3-173	36.84642029	-116.45613861	1.325697	979466.461
3-177	36.84638596	-116.45561981	1.315608	979468.773
3-181	36.84634018	-116.45510101	1.308811	979470.235
3-185	36.84602356	-116.45475769	1.304361	979471.503
3-189	36.84571838	-116.45439148	1.299149	979472.710
3-193	36.84540558	-116.45402527	1.295491	979473.752
3-197	36.84507751	-116.45367432	1.291285	979474.648
3-201	36.84482193	-116.45326233	1.287902	979475.681
3-205	36.84463501	-116.45277405	1.285890	979476.062
3-209	36.84453201	-116.45226288	1.282446	979477.059
3-213	36.84445572	-116.45173645	1.278209	979478.011
3-217	36.84430313	-116.45123291	1.273576	979479.210
3-221	36.84409332	-116.45076752	1.269919	979480.130
3-225	36.84386826	-116.45031738	1.266231	979481.251
3-229	36.84361649	-116.44987488	1.262908	979481.988
3-233	36.84331894	-116.44949341	1.260013	979483.066
3-237	36.84295654	-116.44921112	1.256172	979483.978
3-241	36.84259033	-116.44893646	1.252454	979484.922
3-245	36.84227753	-116.44857788	1.248491	979485.934
3-249	36.84198380	-116.44818878	1.248674	979486.263
3-253	36.84171677	-116.44776916	1.245443	979486.998
3-257	36.84152985	-116.44728851	1.240505	979488.423
3-261	36.84127045	-116.44686890	1.236848	979489.285

3-265	36.84095001	-116.44652557	1.233678	979490.355
3-269	36.84060669	-116.44619751	1.230599	979490.984
3-273	36.84031677	-116.44581604	1.227460	979491.890
3-277	36.84008789	-116.44536591	1.224260	979492.593
3-281	36.83985138	-116.44491577	1.220815	979493.542
3-285	36.83963013	-116.44446564	1.217859	979494.203
3-289	36.83940125	-116.44400787	1.215085	979495.059
3-293	36.83917236	-116.44355774	1.211854	979495.679
3-297	36.83895111	-116.44309998	1.208562	979496.503
3-301	36.83870697	-116.44266510	1.206429	979497.050
3-305	36.83849335	-116.44219971	1.203198	979498.065
3-309	36.83828354	-116.44174194	1.200668	979498.659
3-313	36.83805466	-116.44128418	1.198199	979499.429
3-317	36.83783722	-116.44082642	1.195822	979499.940
3-321	36.83761978	-116.44036865	1.193902	979500.646
3-325	36.83739853	-116.43991852	1.191737	979501.157
3-329	36.83720398	-116.43943787	1.188842	979502.159
3-333	36.83702087	-116.43896484	1.185916	979502.888
3-337	36.83677292	-116.43856049	1.183630	979503.597
3-341	36.83658981	-116.43807983	1.181435	979504.073
3-345	36.83639526	-116.43759918	1.179698	979504.727
3-349	36.83619308	-116.43713379	1.177595	979505.161
3-353	36.83598328	-116.43666840	1.175370	979505.857
3-357	36.83578110	-116.43619537	1.172809	979506.376
3-361	36.83557892	-116.43572235	1.170737	979506.998
3-365	36.83537674	-116.43524933	1.168085	979507.529
3-369	36.83517075	-116.43478394	1.165494	979508.208
3-373	36.83497620	-116.43431091	1.163361	979508.496
3-377	36.83477402	-116.43383789	1.160953	979508.980
3-381	36.83457184	-116.43336487	1.159307	979509.237
3-385	36.83436584	-116.43289185	1.157356	979509.622
3-389	36.83416748	-116.43241882	1.155314	979509.983
3-393	36.83396530	-116.43194580	1.154095	979510.277
3-397	36.83376694	-116.43147278	1.157996	979510.148
3-401	36.83356857	-116.43100739	1.168177	979508.500
3-405	36.83338165	-116.43054199	1.178692	979506.067
3-409	36.83317947	-116.43006897	1.179210	979505.892
3-413	36.83297729	-116.42961884	1.169975	979508.084
3-417	36.83277512	-116.42915344	1.162081	979510.290

TABLE G7. OBSERVED GRAVITY FOR REPOSITORY LINE 4

Station	Latitude deg N	Longitude deg E	Elevation km	Gravity cm/sec**2
4-101	36.85242081	-116.46520996	1.476177	979428.649
4-105	36.85234451	-116.46469116	1.470416	979430.560
4-109	36.85228348	-116.46417999	1.464168	979432.180
4-113	36.85221863	-116.46366119	1.457096	979434.019
4-117	36.85216141	-116.46314240	1.449598	979435.723
4-121	36.85210419	-116.46263885	1.437345	979438.608
4-125	36.85206223	-116.46218109	1.416497	979443.630
4-129	36.85202408	-116.46170807	1.395801	979448.574
4-133	36.85198212	-116.46124268	1.375288	979453.268
4-137	36.85192108	-116.46067047	1.368217	979454.990
4-141	36.85187531	-116.46020508	1.365961	979455.770
4-145	36.85182571	-116.45966339	1.362761	979456.464
4-149	36.85177231	-116.45912170	1.363584	979456.621
4-153	36.85171509	-116.45861816	1.359256	979457.568
4-157	36.85167313	-116.45810699	1.347399	979460.439
4-161	36.85163116	-116.45761108	1.335055	979463.160
4-165	36.85157394	-116.45709991	1.325209	979465.622
4-169	36.85152435	-116.45657349	1.316919	979467.517
4-173	36.85147476	-116.45607758	1.306068	979470.025
4-177	36.85142899	-116.45555878	1.294120	979472.455
4-181	36.85131454	-116.45507050	1.295187	979472.577
4-185	36.85107040	-116.45462799	1.291651	979473.323
4-189	36.85078812	-116.45423126	1.285921	979474.731
4-193	36.85049057	-116.45384216	1.282233	979475.642
4-197	36.85019302	-116.45346832	1.278605	979476.589
4-201	36.84995651	-116.45303345	1.273942	979477.567
4-205	36.84973907	-116.45258331	1.268669	979478.894
4-209	36.84962463	-116.45204926	1.266292	979479.470
4-213	36.84955215	-116.45151520	1.263426	979480.286
4-217	36.84946823	-116.45098877	1.261232	979480.883
4-221	36.84940338	-116.45046997	1.257331	979481.924
4-225	36.84936523	-116.44994354	1.254130	979482.647
4-229	36.84918594	-116.44946289	1.250229	979483.771
4-233	36.84889603	-116.44906616	1.247120	979484.552
4-237	36.84877396	-116.44857025	1.244620	979485.344
4-241	36.84865570	-116.44805908	1.241420	979486.262
4-245	36.84849167	-116.44756317	1.238128	979487.181
4-249	36.84838486	-116.44705963	1.234867	979488.079
4-253	36.84826279	-116.44654846	1.231422	979489.068
4-257	36.84811401	-116.44590759	1.228131	979489.998

4-261	36.84799194	-116.44554138	1.224869	979490.874
4-265	36.84780884	-116.44505310	1.222157	979491.599
4-269	36.84760666	-116.44459534	1.219200	979492.479
4-273	36.84738159	-116.44412994	1.216365	979493.134
4-277	36.84716797	-116.44366455	1.213165	979494.071
4-281	36.84687042	-116.44329071	1.209812	979494.936
4-285	36.84655380	-116.44292450	1.206124	979495.904
4-289	36.84624481	-116.44258881	1.202680	979496.787
4-293	36.84593201	-116.44220734	1.200302	979497.383
4-297	36.84562302	-116.44183350	1.197742	979498.018
4-301	36.84531021	-116.44146729	1.195273	979498.728
4-305	36.84501266	-116.44107056	1.192682	979499.363
4-309	36.84475708	-116.44063568	1.190000	979500.156
4-313	36.84453201	-116.44018555	1.187074	979500.887
4-317	36.84432602	-116.43970490	1.184209	979501.645
4-321	36.84412003	-116.43923950	1.181222	979502.469
4-325	36.84391022	-116.43876648	1.177900	979503.400
4-329	36.84372330	-116.43828583	1.175095	979504.074
4-333	36.84355545	-116.43778992	1.171743	979504.996
4-337	36.84344864	-116.43727112	1.168939	979505.606
4-341	36.84336853	-116.43674469	1.166287	979506.363
4-345	36.84323502	-116.43624878	1.163696	979506.991
4-349	36.84304047	-116.43576813	1.160983	979507.812
4-357	36.84263992	-116.43481445	1.156076	979509.108
4-361	36.84243011	-116.43434906	1.153698	979509.701
4-365	36.84218216	-116.43390656	1.151748	979510.181
4-369	36.84198380	-116.43342590	1.149157	979510.799
4-373	36.84177399	-116.43296051	1.147206	979511.213
4-377	36.84156799	-116.43248749	1.145774	979511.484
4-381	36.84136200	-116.43201447	1.143671	979511.890
4-385	36.84115982	-116.43154144	1.141354	979512.408
4-389	36.84095764	-116.43107605	1.138977	979513.159
4-393	36.84075165	-116.43059540	1.137422	979513.697
4-397	36.84055328	-116.43013000	1.136111	979514.307
4-401	36.84034729	-116.42964935	1.134252	979514.893
4-405	36.84013748	-116.42916870	1.132972	979515.503
4-409	36.83993149	-116.42868805	1.131631	979515.920
4-413	36.83972168	-116.42821503	1.131021	979516.181
4-417	36.83956528	-116.42774200	1.129345	979516.607
4-421	36.83930969	-116.42726898	1.127303	979517.123
4-425	36.83910751	-116.42679596	1.125078	979517.724
4-429	36.83890152	-116.42632294	1.122853	979518.302
4-433	36.83869553	-116.42584229	1.120871	979518.827
4-436	36.83854675	-116.42548370	1.119439	979519.157

TABLE G8. OBSERVED GRAVITY FOR REPOSITORY LINE 5

Station	Latitude deg N	Longitude deg E	Elevation km	Gravity cm/sec**2
5-101	36.82923889	-116.46723175	1.486052	979428.627
5-105	36.82966995	-116.46713257	1.485565	979428.748
5-109	36.83010101	-116.46716309	1.486083	979428.535
5-113	36.83053207	-116.46721649	1.486205	979428.627
5-117	36.83096313	-116.46730804	1.486723	979428.226
5-121	36.83139801	-116.46735382	1.487089	979428.162
5-125	36.83183289	-116.46737671	1.487546	979427.917
5-129	36.83226395	-116.46745300	1.488582	979427.679
5-133	36.83267975	-116.46759796	1.490167	979427.083
5-137	36.83308792	-116.46778107	1.491996	979426.541
5-141	36.83347321	-116.46801758	1.493550	979425.710
5-145	36.83388519	-116.46820831	1.493520	979425.716
5-149	36.83430099	-116.46835327	1.491234	979426.291
5-153	36.83472824	-116.46845245	1.491173	979426.439
5-157	36.83515930	-116.46852875	1.492270	979426.009
5-161	36.83557129	-116.46868134	1.494495	979425.429
5-165	36.83599854	-116.46877289	1.496781	979424.557
5-169	36.83641815	-116.46861267	1.499799	979423.829
5-173	36.83684158	-116.46848297	1.504249	979422.695
5-177	36.83726120	-116.46833801	1.507358	979422.014
5-181	36.83768082	-116.46820831	1.507907	979421.594
5-185	36.83810425	-116.46806335	1.506962	979422.056
5-189	36.83852386	-116.46794891	1.505956	979422.204
5-193	36.83893967	-116.46780396	1.505895	979422.251
5-197	36.83935928	-116.46765137	1.505986	979422.177
5-201	36.83977890	-116.46752930	1.504798	979422.516
5-205	36.84019852	-116.46743011	1.504340	979422.528
5-209	36.84062195	-116.46733093	1.504188	979422.485
5-213	36.84104538	-116.46724701	1.503426	979422.599
5-217	36.84146881	-116.46714783	1.502969	979422.671
5-221	36.84189606	-116.46705627	1.502024	979422.870
5-225	36.84231567	-116.46694183	1.500591	979423.245
5-229	36.84273529	-116.46685028	1.499006	979423.604
5-233	36.84316254	-116.46674347	1.498092	979423.832
5-237	36.84358978	-116.46664429	1.497239	979424.023
5-241	36.84402084	-116.46654510	1.496446	979424.155
5-245	36.84444427	-116.46644592	1.495836	979424.210
5-249	36.84487152	-116.46633148	1.495562	979424.191
5-253	36.84529495	-116.46621704	1.494282	979424.507
5-257	36.84571457	-116.46611023	1.492880	979424.855

5-261	36.84613419	-116.46599579	1.492026	979425.059
5-265	36.84655380	-116.46585846	1.490533	979425.494
5-269	36.84696960	-116.46572876	1.489131	979425.901
5-273	36.84738541	-116.46561432	1.487576	979426.211
5-277	36.84780121	-116.46549225	1.485504	979426.797
5-281	36.84822083	-116.46536255	1.483401	979427.313
5-285	36.84863663	-116.46522522	1.481541	979427.837
5-289	36.84906006	-116.46512604	1.480078	979428.252
5-293	36.84948730	-116.46514130	1.479530	979428.238
5-297	36.84991837	-116.46521759	1.479469	979428.165
5-301	36.85035706	-116.46525574	1.479103	979428.234
5-305	36.85078812	-116.46525574	1.478859	979428.118
5-309	36.85122299	-116.46525574	1.478249	979428.270
5-313	36.85165787	-116.46526337	1.477792	979428.300
5-317	36.85208893	-116.46526337	1.476878	979428.586
5-321	36.85253143	-116.46529388	1.475963	979428.826
5-325	36.85296249	-116.46531677	1.475506	979428.845
5-329	36.85339355	-116.46533966	1.475811	979428.764
5-333	36.85383224	-116.46534729	1.475933	979428.721
5-337	36.85426712	-116.46535492	1.476116	979428.657
5-341	36.85470200	-116.46536255	1.476847	979428.391
5-345	36.85514069	-116.46537018	1.477305	979428.318
5-349	36.85557938	-116.46540833	1.478189	979427.899
5-353	36.85600662	-116.46545410	1.478646	979427.763
5-357	36.85644531	-116.46543121	1.478585	979427.689
5-361	36.85687637	-116.46540070	1.478707	979427.667
5-365	36.85730743	-116.46540833	1.479652	979427.456
5-369	36.85774612	-116.46540833	1.480383	979426.972
5-373	36.85817719	-116.46539307	1.480261	979427.039
5-377	36.85861206	-116.46540833	1.480718	979426.969
5-381	36.85905075	-116.46540833	1.480779	979426.867
5-385	36.85948181	-116.46539307	1.480292	979427.001
5-389	36.85991669	-116.46539307	1.480322	979427.066
5-393	36.86035156	-116.46536255	1.479652	979427.322
5-397	36.86077881	-116.46527863	1.478798	979427.589
5-401	36.86119843	-116.46516418	1.477945	979427.963
5-405	36.86163712	-116.46506500	1.476969	979428.213
5-409	36.86206818	-116.46495819	1.475628	979428.623
5-413	36.86249161	-116.46484375	1.474013	979429.043
5-417	36.86291504	-116.46475220	1.472580	979429.462
5-421	36.86334229	-116.46465302	1.471239	979429.869
5-425	36.86376572	-116.46453857	1.470233	979430.114
5-429	36.86418915	-116.46443939	1.469319	979430.338
5-433	36.86461258	-116.46434784	1.468770	979429.757
5-437	36.86503983	-116.46431732	1.469014	979430.414
5-441	36.86548233	-116.46434021	1.469227	979430.377

5-445	36.86592102	-116.46439362	1.469989	979430.146
5-449	36.86634064	-116.46452332	1.471087	979429.864
5-453	36.86675262	-116.46469116	1.471788	979429.639
5-457	36.86716843	-116.46486664	1.472733	979429.444
5-461	36.86758041	-116.46504211	1.474074	979429.092
5-465	36.86801147	-116.46515656	1.474653	979428.755
5-469	36.86844635	-116.46517181	1.476360	979428.552
5-473	36.86887360	-116.46516418	1.477792	979428.214
5-477	36.86931610	-116.46518707	1.479530	979427.712
5-481	36.86974716	-116.46530914	1.481054	979427.375
5-485	36.87017441	-116.46543884	1.481876	979427.158
5-487	36.87038040	-116.46548462	1.481999	979427.100

TABLE G9. OBSERVED GRAVITY FOR REPOSITORY LINE 6

Station	Latitude deg N	Longitude deg E	Elevation km	Gravity cm/sec**2
6-101	36.82505035	-116.48257446	1.191128	979496.270
6-105	36.82537460	-116.48222351	1.193231	979495.812
6-109	36.82571030	-116.48189545	1.194115	979495.645
6-113	36.82604599	-116.48156738	1.195578	979495.270
6-117	36.82638168	-116.48122406	1.197498	979494.795
6-121	36.82670593	-116.48091125	1.198474	979494.441
6-125	36.82713699	-116.48076630	1.200028	979494.057
6-129	36.82755661	-116.48081207	1.201643	979493.626
6-133	36.82798767	-116.48088837	1.202436	979493.467
6-137	36.82841110	-116.48091125	1.204234	979492.966
6-141	36.82884216	-116.48087311	1.205697	979492.556
6-145	36.82926559	-116.48081207	1.207191	979492.217
6-149	36.82969666	-116.48078156	1.209446	979491.732
6-153	36.83012390	-116.48072052	1.210879	979491.342
6-157	36.83055115	-116.48066711	1.211702	979491.110
6-161	36.83095169	-116.48046112	1.213287	979490.740
6-165	36.83133698	-116.48022461	1.214567	979490.367
6-169	36.83171844	-116.47998047	1.215939	979489.998
6-173	36.83210373	-116.47973633	1.216487	979489.831
6-177	36.83248520	-116.47949982	1.217615	979489.580
6-181	36.83288956	-116.47930908	1.219688	979489.066
6-185	36.83330536	-116.47919464	1.221791	979488.599
6-189	36.83373261	-116.47914124	1.223802	979488.045
6-193	36.83415985	-116.47906494	1.225814	979487.539
6-197	36.83457947	-116.47893524	1.226759	979487.191
6-201	36.83499527	-116.47879028	1.229441	979486.594
6-205	36.83541107	-116.47866058	1.231118	979486.081
6-209	36.83582306	-116.47851562	1.232733	979485.657
6-213	36.83624649	-116.47836304	1.234318	979485.201
6-217	36.83666229	-116.47821045	1.236391	979484.750
6-221	36.83708191	-116.47807312	1.237793	979484.312
6-225	36.83747864	-116.47785187	1.238555	979484.110
6-229	36.83786774	-116.47762299	1.239378	979483.838
6-233	36.83824921	-116.47736359	1.241389	979483.384
6-237	36.83865738	-116.47717285	1.243035	979482.988
6-241	36.83907318	-116.47700500	1.244773	979482.550
6-245	36.83948517	-116.47686768	1.246632	979482.076
6-249	36.83991241	-116.47673035	1.248217	979481.830
6-253	36.84033203	-116.47660828	1.249893	979481.253
6-257	36.84075165	-116.47644806	1.251326	979481.015

6-261	36.84115982	-116.47625732	1.252789	979480.510
6-265	36.84154892	-116.47604370	1.255410	979480.024
6-269	36.84195709	-116.47583771	1.257757	979479.365
6-273	36.84231567	-116.47555542	1.258214	979479.283
6-277	36.84271622	-116.47537231	1.260135	979478.749
6-281	36.84315109	-116.47530365	1.261567	979478.444
6-285	36.84358215	-116.47525024	1.263701	979477.864
6-289	36.84402084	-116.47519684	1.265499	979477.489
6-293	36.84445190	-116.47512817	1.267450	979476.895
6-297	36.84487915	-116.47506714	1.269675	979476.444
6-301	36.84529877	-116.47492981	1.271687	979475.887
6-305	36.84571457	-116.47476196	1.273241	979475.515
6-309	36.84613800	-116.47463226	1.274795	979475.047
6-313	36.84655380	-116.47454071	1.275588	979474.808
6-317	36.84697342	-116.47441864	1.277965	979474.264
6-321	36.84739304	-116.47433472	1.280434	979473.582
6-325	36.84779358	-116.47412872	1.281775	979473.101
6-329	36.84816360	-116.47386169	1.282629	979472.861
6-333	36.84826660	-116.47359467	1.283208	979472.549
6-337	36.84893417	-116.47338104	1.285189	979472.113
6-341	36.84934235	-116.47315216	1.287201	979471.555
6-345	36.84974670	-116.47298431	1.289121	979471.085
6-349	36.85016251	-116.47283936	1.290401	979470.736
6-353	36.85057831	-116.47269440	1.291986	979470.399
6-357	36.85099792	-116.47257996	1.293510	979469.950
6-361	36.85142517	-116.47249603	1.295644	979469.561
6-365	36.85185242	-116.47240448	1.296741	979469.212
6-369	36.85224533	-116.47217560	1.299179	979468.802
6-373	36.85266876	-116.47210693	1.301008	979468.393
6-377	36.85309982	-116.47211456	1.302868	979468.141
6-381	36.85351944	-116.47200012	1.303904	979467.787
6-385	36.85396576	-116.47196198	1.306556	979467.208
6-389	36.85438156	-116.47183990	1.308689	979466.731
6-393	36.85479736	-116.47171021	1.310579	979466.348
6-397	36.85522461	-116.47164917	1.312499	979465.794
6-401	36.85565567	-116.47155762	1.314206	979465.492
6-405	36.85607910	-116.47145844	1.316279	979464.988
6-409	36.85649109	-116.47132874	1.318382	979464.596
6-413	36.85689926	-116.47121429	1.320637	979464.028
6-417	36.85732651	-116.47107697	1.322436	979463.707
6-421	36.85773468	-116.47091675	1.324630	979463.126
6-425	36.85813904	-116.47073364	1.326825	979462.702
6-429	36.85854340	-116.47055054	1.328714	979462.143
6-433	36.85897064	-116.47045898	1.330635	979461.943
6-437	36.85939026	-116.47053528	1.332433	979461.453
6-441	36.85973740	-116.47081757	1.335512	979460.812

6-445	36.86015701	-116.47089386	1.337706	979460.043
6-449	36.86051559	-116.47062683	1.338377	979460.053
6-453	36.86087418	-116.47031403	1.338986	979459.874
6-457	36.86124802	-116.47005463	1.340785	979459.549
6-461	36.86162949	-116.46980286	1.342949	979459.031
6-465	36.86205292	-116.46968842	1.344930	979458.582
6-469	36.86247635	-116.46961975	1.348222	979457.845
6-473	36.86289978	-116.46952820	1.351483	979457.074
6-477	36.86329269	-116.46934509	1.350904	979457.217
6-481	36.86371613	-116.46926117	1.354623	979456.348
6-485	36.86412048	-116.46919250	1.356695	979455.909
6-489	36.86453629	-116.46929932	1.358920	979455.311
6-493	36.86496735	-116.46921539	1.361054	979454.893
6-497	36.86539841	-116.46917725	1.363614	979454.150
6-501	36.86582947	-116.46913147	1.366967	979453.523
6-509	36.86664581	-116.46887970	1.368918	979453.013
6-513	36.86706924	-116.46878815	1.373093	979452.019
6-517	36.86749268	-116.46883392	1.377208	979451.279
6-521	36.86792374	-116.46875000	1.379830	979450.601
6-524	36.86821747	-116.46857452	1.381201	979450.176

TABLE G10. OBSERVED GRAVITY FOR REPOSITORY LINE 7a

Station	Latitude deg N	Longitude deg E	Elevation km	Gravity cm/sec**2
7a-101	36.88983154	-116.44311523	1.332281	979465.319
7a-103	36.88989639	-116.44304657	1.330452	979465.812
7a-105	36.88995743	-116.44283295	1.328776	979466.157
7a-107	36.89001846	-116.44269562	1.326520	979466.717
7a-109	36.89008331	-116.44255066	1.324752	979467.111
7a-111	36.89014816	-116.44240570	1.323320	979467.470
7a-113	36.89020920	-116.44226837	1.321856	979467.812
7a-115	36.89027786	-116.44212341	1.320028	979468.229
7a-117	36.89033890	-116.44197845	1.318931	979468.497
7a-119	36.89040375	-116.44184113	1.319845	979468.387
7a-121	36.89046478	-116.44169617	1.319144	979468.521
7a-123	36.89053726	-116.44155121	1.317833	979468.877
7a-125	36.89059830	-116.44141388	1.317346	979468.992
7a-127	36.89065933	-116.44126892	1.316218	979469.325
7a-129	36.89072800	-116.44113159	1.314633	979469.757
7a-131	36.89078903	-116.44098663	1.314480	979469.832

TABLE G11. OBSERVED GRAVITY FOR REPOSITORY LINE 8

Station	Latitude deg N	Longitude deg E	Elevation km	Gravity cm/sec**2
8-338	36.88895798	-116.46026611	1.556827	979412.584
8-333	36.88866806	-116.45970917	1.551706	979413.480
8-329	36.88843155	-116.45925903	1.549573	979413.933
8-325	36.88819122	-116.45880127	1.545915	979414.895
8-321	36.88794708	-116.45836639	1.541861	979415.476
8-317	36.88774109	-116.45787811	1.537503	979416.410
8-313	36.88751221	-116.45742798	1.534180	979416.949
8-309	36.88724899	-116.45700836	1.528694	979417.785
8-305	36.88697433	-116.45658875	1.525890	979418.347
8-301	36.88668823	-116.45619202	1.521836	979419.365
8-297	36.88638306	-116.45580292	1.517538	979420.027
8-293	36.88609314	-116.45540619	1.513606	979421.063
8-289	36.88580322	-116.45501709	1.509674	979421.730
8-285	36.88551331	-116.45459747	1.506139	979422.741
8-281	36.88519287	-116.45423889	1.502847	979423.299
8-277	36.88484573	-116.45391846	1.500043	979424.163
8-273	36.88448334	-116.45361328	1.497025	979424.641
8-269	36.88410950	-116.45333099	1.494130	979425.486
8-265	36.88373566	-116.45307159	1.490777	979426.090
8-261	36.88333893	-116.45285034	1.487546	979427.022
8-257	36.88293839	-116.45264435	1.483797	979427.630
8-253	36.88256454	-116.45236969	1.479834	979428.709
8-249	36.88219833	-116.45207214	1.475628	979429.431
8-245	36.88185501	-116.45173645	1.472153	979430.286
8-241	36.88151550	-116.45141602	1.468770	979431.001
8-237	36.88116837	-116.45107269	1.464930	979431.884
8-233	36.88082123	-116.45075989	1.461425	979432.627
8-229	36.88045120	-116.45046997	1.457828	979433.569
8-225	36.88007736	-116.45020294	1.454353	979434.243
8-221	36.87968063	-116.44997406	1.450909	979435.202
8-217	36.87928391	-116.44976044	1.447282	979435.861
8-213	36.87887955	-116.44956970	1.443259	979436.887
8-209	36.87846756	-116.44939423	1.438473	979437.916
8-205	36.87805176	-116.44924927	1.433505	979439.238
8-201	36.87763214	-116.44911194	1.428079	979440.347
8-197	36.87720108	-116.44902039	1.423660	979441.488
8-193	36.87677002	-116.44895172	1.419850	979442.196
8-189	36.87633514	-116.44893646	1.416284	979443.065
8-185	36.87590408	-116.44886017	1.412138	979443.919
8-181	36.87547684	-116.44876099	1.408450	979444.833

8-177	36.87505722	-116.44863129	1.404976	979445.314
8-173	36.87463379	-116.44849396	1.400495	979446.241
8-169	36.87423325	-116.44827271	1.396167	979447.239
8-165	36.87383270	-116.44807434	1.392936	979447.908
8-161	36.87342072	-116.44789886	1.389827	979448.511
8-157	36.87303543	-116.44766998	1.386078	979449.471
8-153	36.87267685	-116.44734192	1.380622	979450.684
8-149	36.87230682	-116.44709778	1.375989	979451.962
8-145	36.87188721	-116.44689178	1.370594	979453.119
8-141	36.87148285	-116.44668579	1.366357	979454.309
8-137	36.87108994	-116.44646454	1.362273	979455.104
8-133	36.87072372	-116.44618988	1.357945	979456.312
8-129	36.87034607	-116.44590759	1.351879	979457.562
8-125	36.86994934	-116.44567871	1.346972	979459.048
8-121	36.86957550	-116.44541168	1.343223	979459.685
8-117	36.86922455	-116.44508362	1.339291	979460.951
8-113	36.86890793	-116.44471741	1.334963	979461.778
8-109	36.86855698	-116.44442749	1.330879	979463.068
8-105	36.86813736	-116.44439697	1.326916	979463.853
8-101	36.86769867	-116.44436646	1.325087	979464.409

TABLE G12. OBSERVED GRAVITY FOR REPOSITORY LINE 9

Station	Latitude deg N	Longitude deg E	Elevation km	Gravity cm/sec**2
9-197	36.86873627	-116.46060181	1.348313	979457.360
9-193	36.86839294	-116.46026611	1.345448	979457.999
9-189	36.86804962	-116.45993805	1.340175	979459.256
9-185	36.86770248	-116.45960999	1.337158	979460.045
9-181	36.86735916	-116.45929718	1.333988	979460.799
9-177	36.86702347	-116.45895386	1.331123	979461.511
9-173	36.86672592	-116.45857239	1.327739	979462.350
9-169	36.86654282	-116.45808411	1.325758	979463.012
9-165	36.86639023	-116.45758057	1.322375	979463.849
9-161	36.86622620	-116.45707703	1.318839	979464.637
9-157	36.86605453	-116.45657349	1.316309	979465.415
9-153	36.86589050	-116.45608521	1.313536	979466.172
9-149	36.86567307	-116.45561981	1.310152	979466.964
9-145	36.86539841	-116.45520782	1.307287	979467.693
9-141	36.86509705	-116.45481873	1.304331	979468.464
9-137	36.86480713	-116.45442200	1.301191	979469.181
9-133	36.86452103	-116.45401764	1.297899	979469.883
9-129	36.86423492	-116.45360565	1.295065	979470.681
9-125	36.86398315	-116.45317841	1.291925	979471.342
9-121	36.86370850	-116.45275879	1.289609	979472.052
9-117	36.86344910	-116.45232391	1.286683	979472.504
9-113	36.86323166	-116.45185852	1.283939	979473.399
9-109	36.86294556	-116.45144653	1.281105	979473.967
9-105	36.86259842	-116.45113373	1.278423	979474.732
9-101	36.86220932	-116.45091248	1.277843	979475.003

TABLE G13. OBSERVED GRAVITY FOR REPOSITORY LINE 10

Station	Latitude deg N	Longitude deg E	Elevation km	Gravity cm/sec**2
10-92	36.82468033	-116.45693970	1.261079	979484.012
10-91	36.82512665	-116.45690918	1.260897	979483.766
10-90	36.82558441	-116.45687866	1.279977	979479.537
10-89	36.82603455	-116.45683289	1.302593	979474.551
10-88	36.82648468	-116.45680237	1.324539	979469.673
10-87	36.82692719	-116.45677948	1.323594	979470.004
10-86	36.82738495	-116.45674133	1.308781	979473.322
10-85	36.82782745	-116.45671844	1.293693	979476.317
10-84	36.82828140	-116.45668030	1.312530	979472.278
10-83	36.82873154	-116.45665741	1.338163	979466.362
10-82	36.82918167	-116.45661926	1.355964	979462.334
10-81	36.82962799	-116.45658875	1.352946	979462.990
10-80	36.83007431	-116.45655823	1.333378	979467.531
10-79	36.83052826	-116.45653534	1.311493	979472.173
10-78	36.83097839	-116.45650482	1.300795	979474.562
10-77	36.83143616	-116.45647430	1.300002	979473.635
10-76	36.83187866	-116.45644379	1.308659	979472.857
10-75	36.83232880	-116.45641327	1.323259	979469.546
10-74	36.83277893	-116.45638275	1.313200	979471.721
10-73	36.83322525	-116.45635986	1.308720	979472.490
10-72	36.83367920	-116.45632935	1.317254	979470.492
10-71	36.83412933	-116.45629883	1.337036	979466.167
10-70	36.83457565	-116.45626831	1.350599	979463.122
10-69	36.83502960	-116.45623779	1.347399	979463.693
10-68	36.83547211	-116.45621490	1.334841	979466.559
10-67	36.83592606	-116.45618439	1.342400	979464.618
10-66	36.83637619	-116.45614624	1.363828	979459.794
10-65	36.83682632	-116.45612335	1.374099	979457.195
10-64	36.83727646	-116.45608521	1.371661	979457.827
10-63	36.83772659	-116.45606232	1.369497	979458.164
10-62	36.83817291	-116.45603180	1.357183	979460.959
10-61	36.83861923	-116.45600891	1.335634	979465.523
10-60	36.83906937	-116.45597076	1.312743	979470.442
10-59	36.83951950	-116.45594025	1.320058	979468.980
10-58	36.83996964	-116.45590973	1.314511	979470.048
10-57	36.84041977	-116.45587921	1.310457	979470.706
10-56	36.84086990	-116.45584869	1.334536	979465.618
10-55	36.84132004	-116.45582581	1.354348	979460.985
10-54	36.84177017	-116.45578766	1.366418	979457.975
10-53	36.84221649	-116.45575714	1.360261	979459.199

10-52	36.84266663	-116.45573425	1.339413	979464.123
10-51	36.84311676	-116.45569611	1.319083	979468.536
10-50	36.84356689	-116.45566559	1.316767	979469.092
10-49	36.84401703	-116.45563507	1.335755	979464.744
10-48	36.84446716	-116.45560455	1.338712	979464.144
10-47	36.84491730	-116.45557404	1.317742	979468.398
10-46	36.84536743	-116.45554352	1.321643	979467.791
10-45	36.84581757	-116.45551300	1.326551	979466.497
10-44	36.84626770	-116.45548248	1.314938	979469.001
10-43	36.84671783	-116.45545197	1.320637	979467.410
10-42	36.84717178	-116.45541382	1.346241	979461.750
10-41	36.84761810	-116.45539093	1.357884	979458.783
10-40	36.84806061	-116.45536041	1.346119	979461.552
10-39	36.84851074	-116.45535278	1.324905	979466.187
10-38	36.84897614	-116.45529938	1.296253	979472.221
10-37	36.84942627	-116.45526886	1.303782	979470.701
10-36	36.84986496	-116.45523834	1.319601	979467.359
10-35	36.85031509	-116.45520782	1.326337	979465.661
10-34	36.85076523	-116.45517731	1.314450	979468.343
10-33	36.85121536	-116.45514679	1.298539	979471.622
10-32	36.85167313	-116.45513153	1.297137	979471.843
10-31	36.85211182	-116.45508575	1.321034	979466.680
10-30	36.85256958	-116.45504761	1.335877	979463.427
10-29	36.85301971	-116.45501709	1.316462	979467.395
10-28	36.85346222	-116.45498657	1.319510	979466.903
10-27	36.85391617	-116.45495605	1.341821	979461.395
10-26	36.85436249	-116.45494080	1.363462	979456.169
10-25	36.85481262	-116.45489502	1.357244	979457.509
10-24	36.85526276	-116.45486450	1.338925	979462.039
10-23	36.85571289	-116.45484161	1.318870	979465.264
10-22	36.85617065	-116.45481110	1.322070	979465.748
10-21	36.85661697	-116.45477295	1.343375	979460.859
10-20	36.85705948	-116.45474243	1.336853	979462.476
10-19	36.85750580	-116.45471191	1.334963	979462.664
10-18	36.85796738	-116.45468140	1.361816	979456.065
10-17	36.85840988	-116.45465088	1.346241	979459.721
10-16	36.85886002	-116.45462036	1.322984	979465.046
10-15	36.85931778	-116.45458984	1.300216	979469.501
10-14	36.85976410	-116.45455933	1.289395	979471.667
10-13	36.86021805	-116.45447540	1.315760	979465.972
10-12	36.86065674	-116.45439911	1.344259	979459.847
10-10	36.86155319	-116.45423126	1.386444	979449.784
10-9	36.86199188	-116.45414734	1.385438	979449.520
10-8	36.86243057	-116.45407867	1.360597	979455.875
10-7	36.86289215	-116.45398712	1.336274	979461.297
10-6	36.86333084	-116.45388794	1.312652	979466.700

10-5	36.86377716	-116.45381165	1.297777	979469.691
10-4	36.86422348	-116.45372772	1.295461	979470.494
10-3	36.86466980	-116.45364380	1.297107	979470.038
10-2	36.86511612	-116.45355988	1.297869	979469.997
10-1	36.86556625	-116.45346069	1.302746	979468.989

TABLE G14. OBSERVED GRAVITY FOR REPOSITORY LINE 11

Station	Latitude deg N	Longitude deg E	Elevation km	Gravity cm/sec**2
11-101	36.82896423	-116.46694946	1.483248	979429.551
11-102	36.82895660	-116.46639252	1.474866	979432.005
11-104	36.82893753	-116.46527100	1.451275	979438.282
11-106	36.82891846	-116.46414948	1.419362	979446.045
11-108	36.82890320	-116.46303558	1.380622	979455.091
11-110	36.82888794	-116.46190643	1.369192	979458.116
11-112	36.82886505	-116.46078491	1.368765	979458.808
11-114	36.82884598	-116.45966339	1.385133	979454.868
11-116	36.82883072	-116.45854187	1.370686	979458.572
11-118	36.82881165	-116.45742798	1.351483	979463.297
11-119	36.82880402	-116.45686340	1.343985	979465.069
11-120	36.82879257	-116.45630646	1.339901	979466.217
11-122	36.82877350	-116.45517731	1.323350	979470.450
11-124	36.82876205	-116.45406342	1.293876	979477.480
11-126	36.82873917	-116.45293427	1.272449	979482.619
11-128	36.82872391	-116.45182037	1.264310	979484.804
11-130	36.82870865	-116.45069885	1.259830	979486.125
11-132	36.82869339	-116.44962311	1.239835	979490.597
11-133	36.82868195	-116.44902039	1.236604	979490.983
11-134	36.82867432	-116.44846344	1.236817	979490.839
11-135	36.82866669	-116.44790649	1.260348	979485.768
11-136	36.82865524	-116.44734192	1.279489	979481.606
11-137	36.82864761	-116.44677734	1.272113	979483.438
11-138	36.82863998	-116.44622040	1.251722	979488.240
11-139	36.82863235	-116.44566345	1.239256	979490.681
11-140	36.82862091	-116.44509888	1.239073	979491.039
11-141	36.82861328	-116.44454193	1.234166	979491.839
11-142	36.82860184	-116.44397736	1.241816	979490.285
11-143	36.82859421	-116.44342041	1.263548	979485.624
11-144	36.82859039	-116.44285584	1.284092	979481.244
11-145	36.82857895	-116.44230652	1.282294	979481.565
11-146	36.82857895	-116.44173431	1.265621	979485.725
11-147	36.82855988	-116.44116974	1.249771	979489.392
11-148	36.82854843	-116.44062042	1.234105	979493.273
11-149	36.82853699	-116.44005585	1.220633	979496.361
11-150	36.82852936	-116.43949127	1.210513	979498.900
11-151	36.82852173	-116.43893433	1.203046	979500.539
11-152	36.82851028	-116.43837738	1.198717	979501.834
11-153	36.82850647	-116.43781281	1.196462	979502.288
11-154	36.82849121	-116.43724823	1.187440	979504.416
11-155	36.82848740	-116.43669128	1.174669	979507.436

TABLE G15. OBSERVED GRAVITY FOR DEPOSITORY LINE 12

Station	Latitude deg N	Longitude deg E	Elevation km	Gravity cm/sec**2
12-308	36.85547638	-116.43490601	1.205911	979494.965
12-301	36.85539627	-116.43471527	1.200851	979496.091
12-293	36.85529327	-116.43448639	1.193566	979497.866
12-285	36.85520172	-116.43426514	1.186586	979499.522
12-277	36.85510254	-116.43403625	1.181374	979500.810
12-269	36.85500717	-116.43379974	1.176955	979501.922
12-261	36.85490799	-116.43357086	1.171986	979503.024
12-253	36.85480881	-116.43334198	1.167475	979503.975
12-245	36.85470963	-116.43311310	1.164824	979504.666
12-237	36.85461044	-116.43288422	1.162294	979505.378
12-229	36.85451508	-116.43265533	1.160709	979505.891
12-221	36.85441589	-116.43242645	1.159032	979506.063
12-213	36.85432053	-116.43219757	1.157935	979506.497
12-205	36.85422134	-116.43196106	1.156594	979506.480
12-197	36.85411835	-116.43172455	1.155344	979506.921
12-189	36.85401535	-116.43148804	1.153973	979506.995
12-181	36.85391617	-116.43125153	1.153302	979507.274
12-173	36.85382080	-116.43102264	1.152601	979507.350
12-165	36.85371780	-116.43078613	1.150986	979507.834
12-157	36.85362625	-116.43054962	1.154338	979507.048
12-149	36.85352325	-116.43031311	1.155009	979507.073
12-141	36.85342789	-116.43008423	1.160496	979506.012
12-133	36.85332870	-116.42984772	1.164336	979505.606
12-125	36.85322952	-116.42961121	1.168756	979504.884
12-117	36.85313034	-116.42937469	1.172718	979503.941
12-109	36.85302734	-116.42913818	1.175979	979503.246
12-101	36.85293198	-116.42889404	1.175461	979503.236

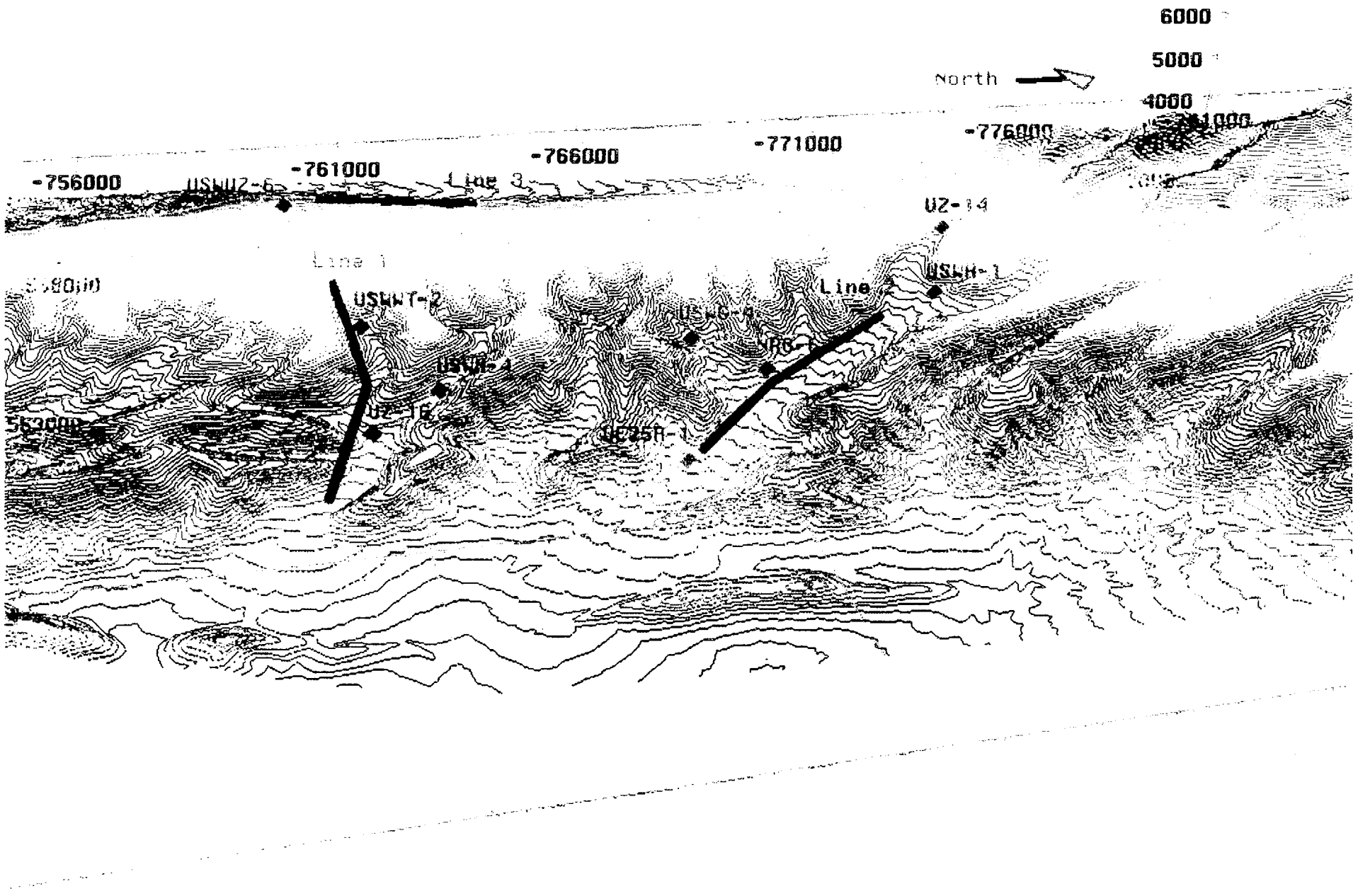

Figure 1. Topographic map of Yucca Mountain showing the location of seismic lines 1, 2, and 3 (in red) acquired in 1993, and some well locations (blue). Multi-offset, 9-component VSP was acquired in WT-2 and NRG-6 in 1993 also.

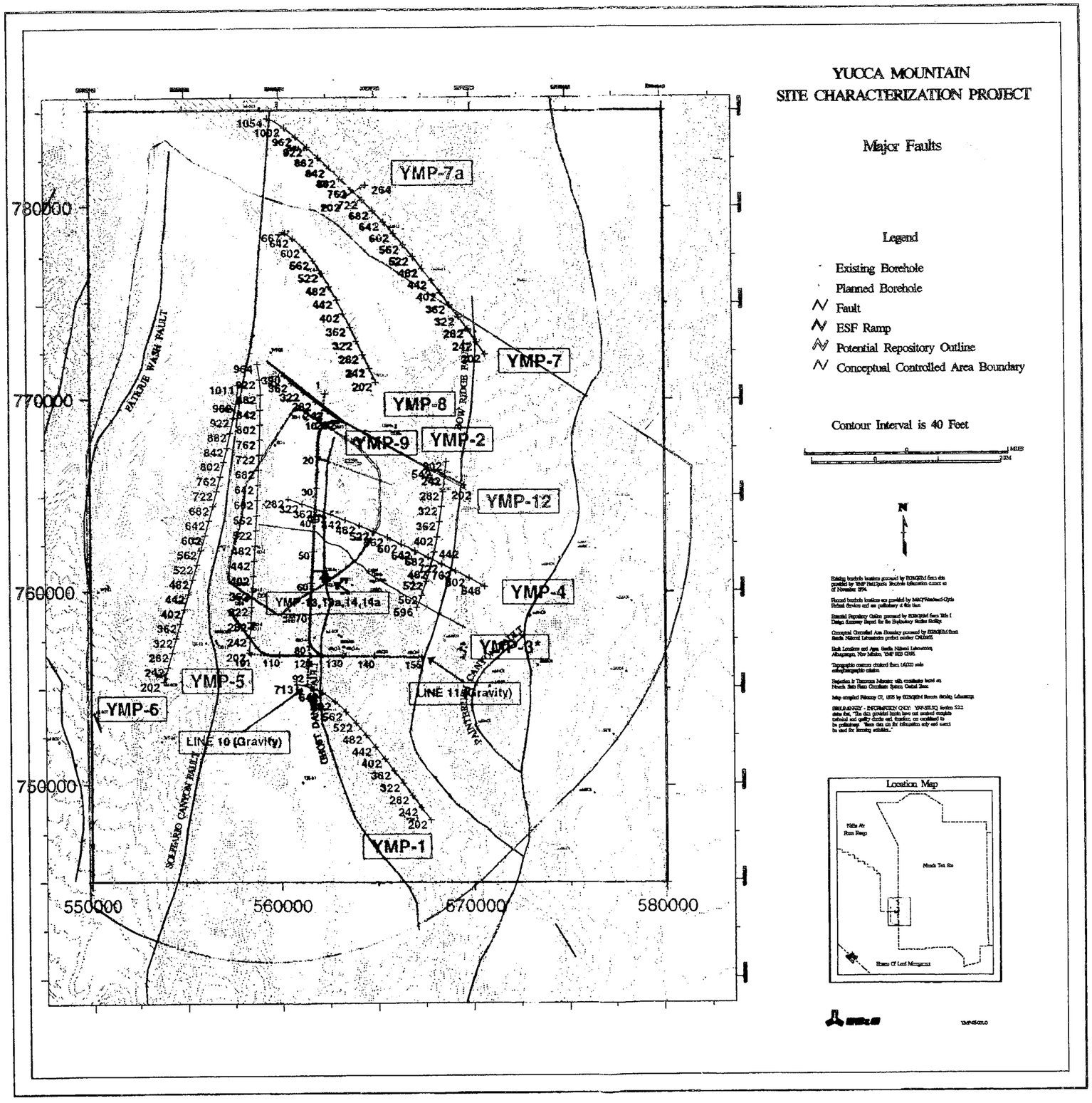

Figure 2a. Common Depth Point (CDP) locations for each of the seismic lines listed in Table 2. Data for YMP-3 is not shown because it did not have useable data. YMP-13a, 13b, 14a, and 14b are located on the UZ-7a well pad (see Figure 2b). Also shown are the station locations for the gravity only Lines 10 and 11. Coordinates are Nevada State Plane (feet East and North).

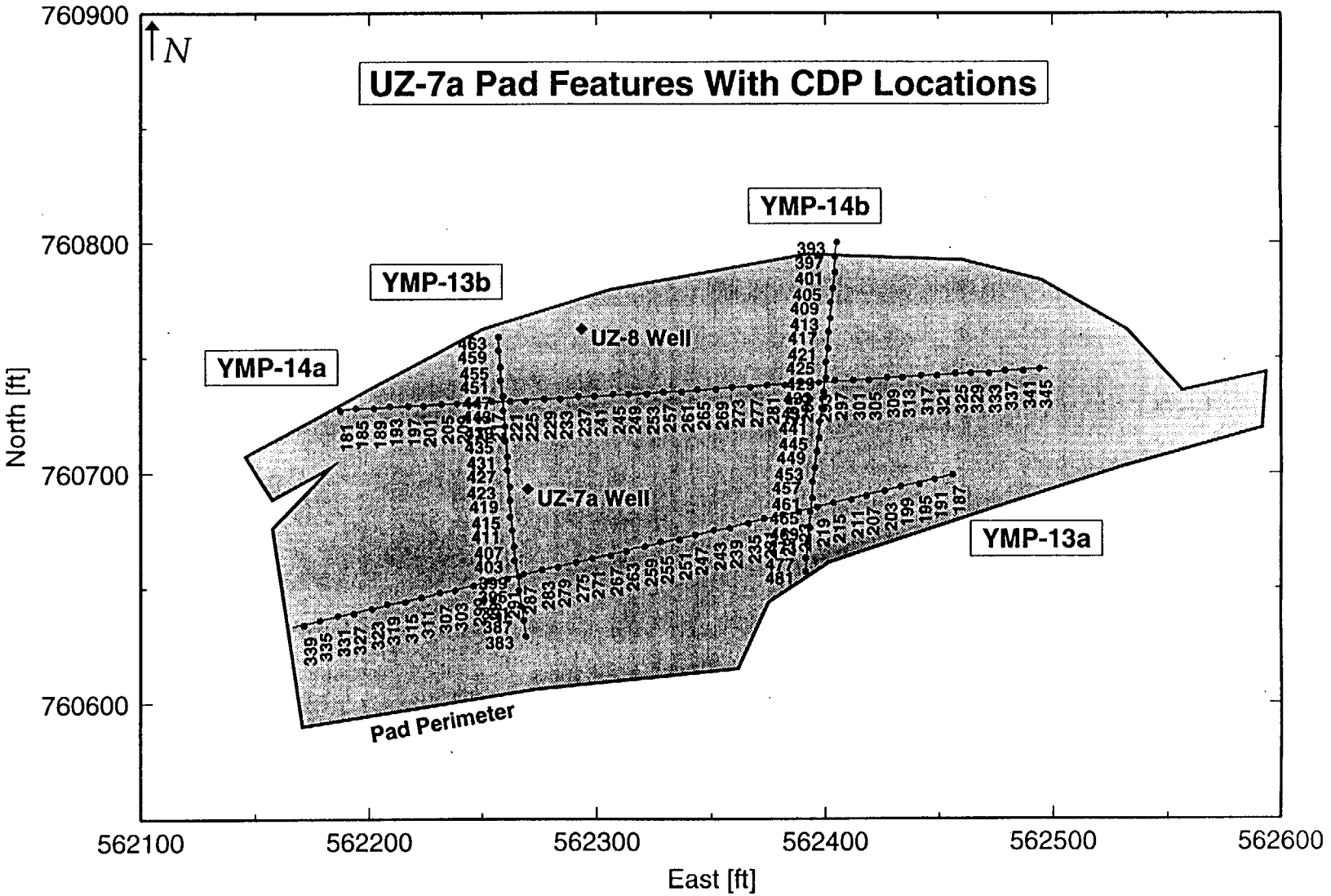

Figure 2b. Detailed map of the UZ-7a well pad showing CDP stations for YMP-13a, 13b, 14a, and 14b. Coordinates are Nevada State Plane (feet East and North).

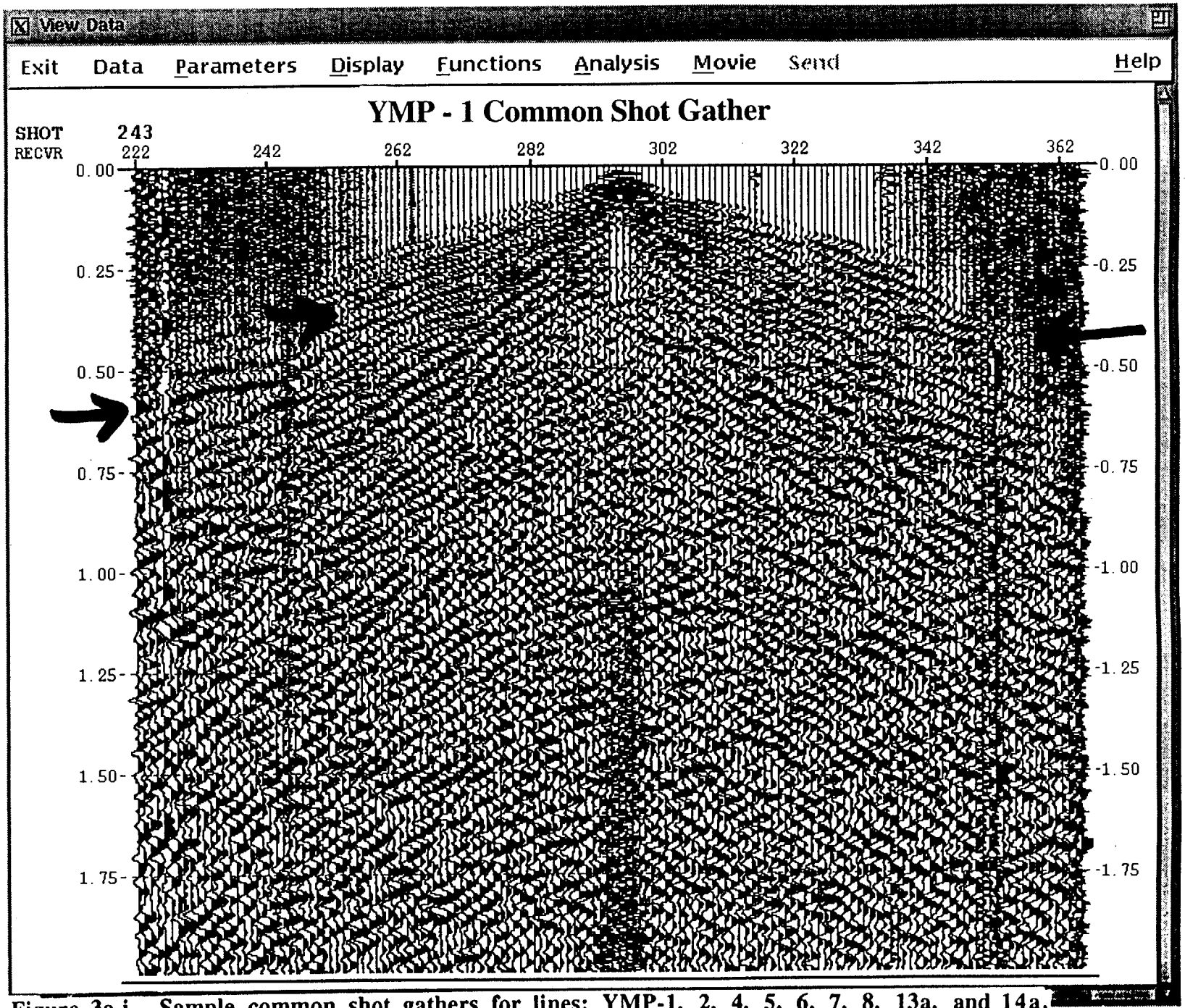

Figure 3a-i. Sample common shot gathers for lines: YMP-1, 2, 4, 5, 6, 7, 8, 13a, and 14a, respectively. Arrows indicate seismic reflectors. Note reflected energy on YMP-13a and strong air-waves on both YMP-13a and 14a.

Figure 3a.

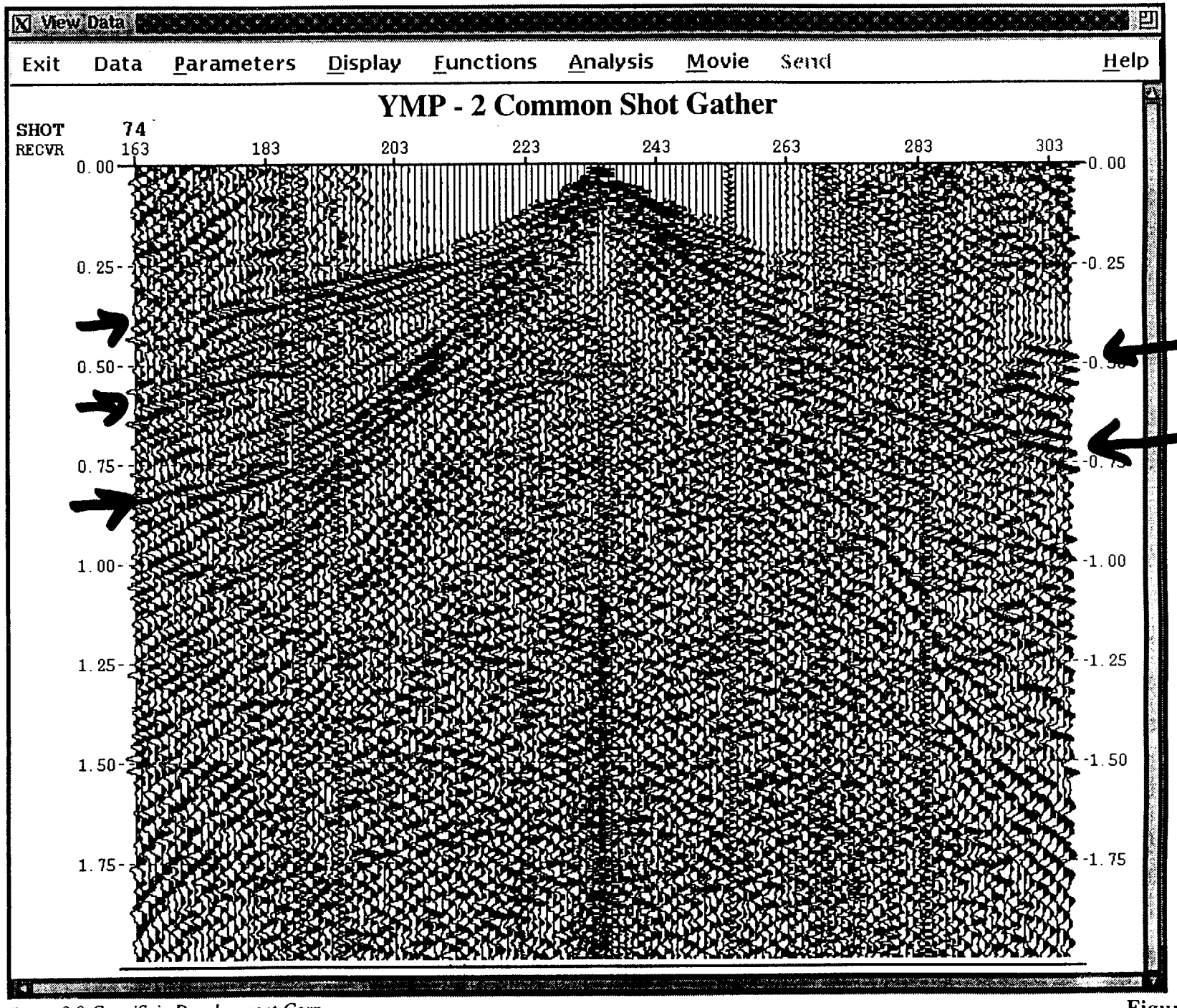

Focus 3.0 CogniSeis Development Corp.

Figure 3b.

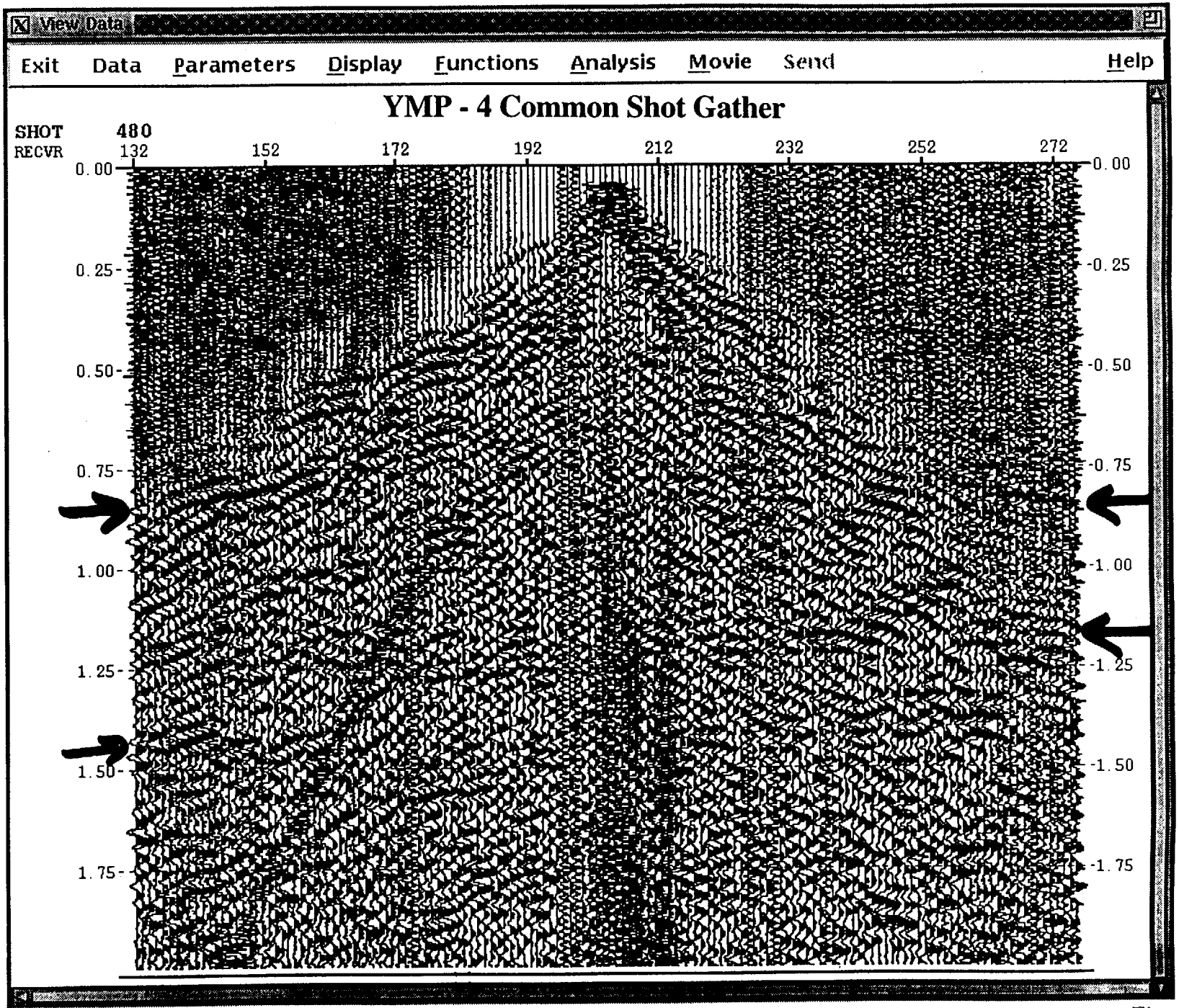

Focus 3.0 CogniSeis Development, Inc.

Figure 3c.

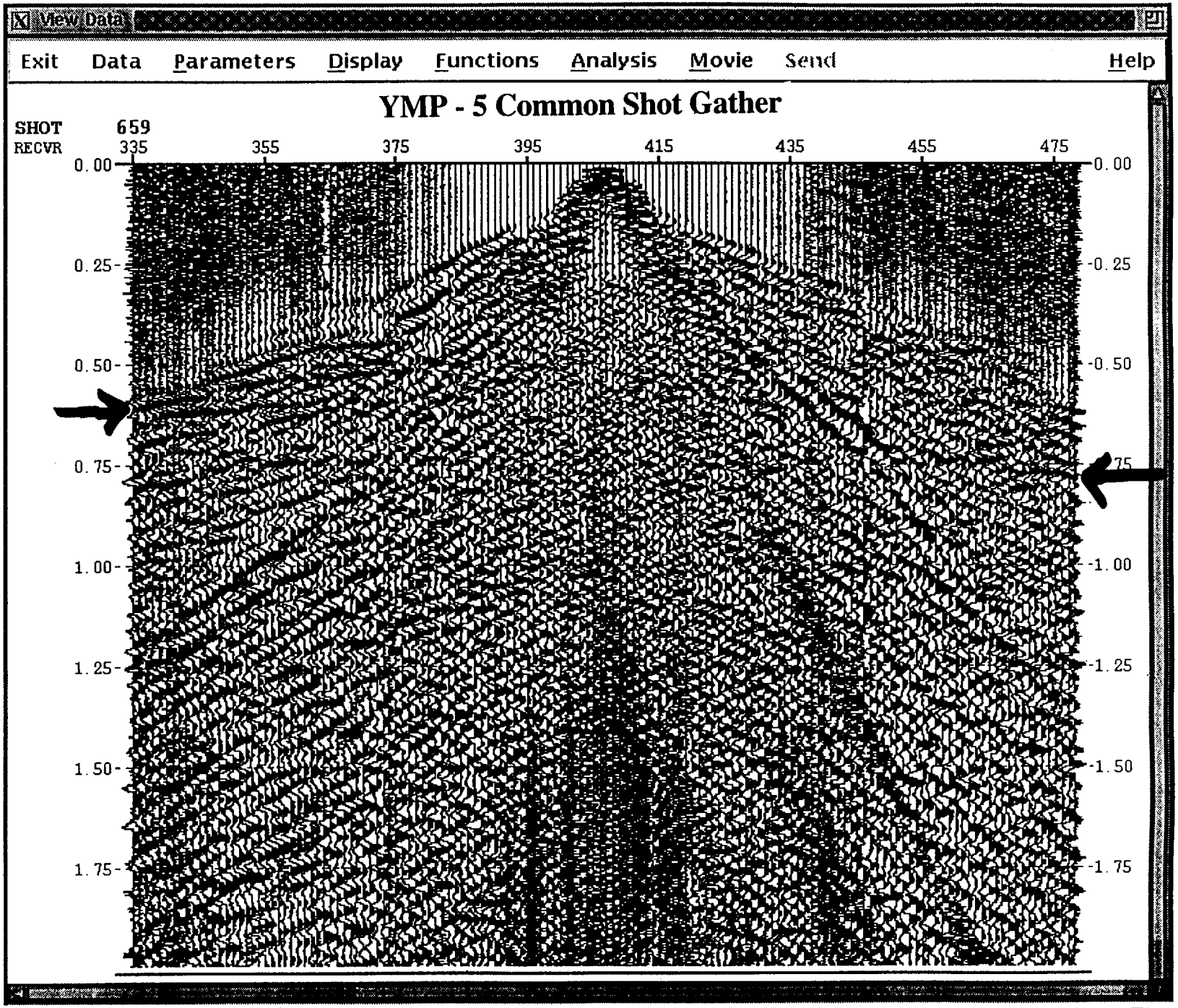

Focus 3.0 CogniSeis Development, Inc.

Figure 3d.

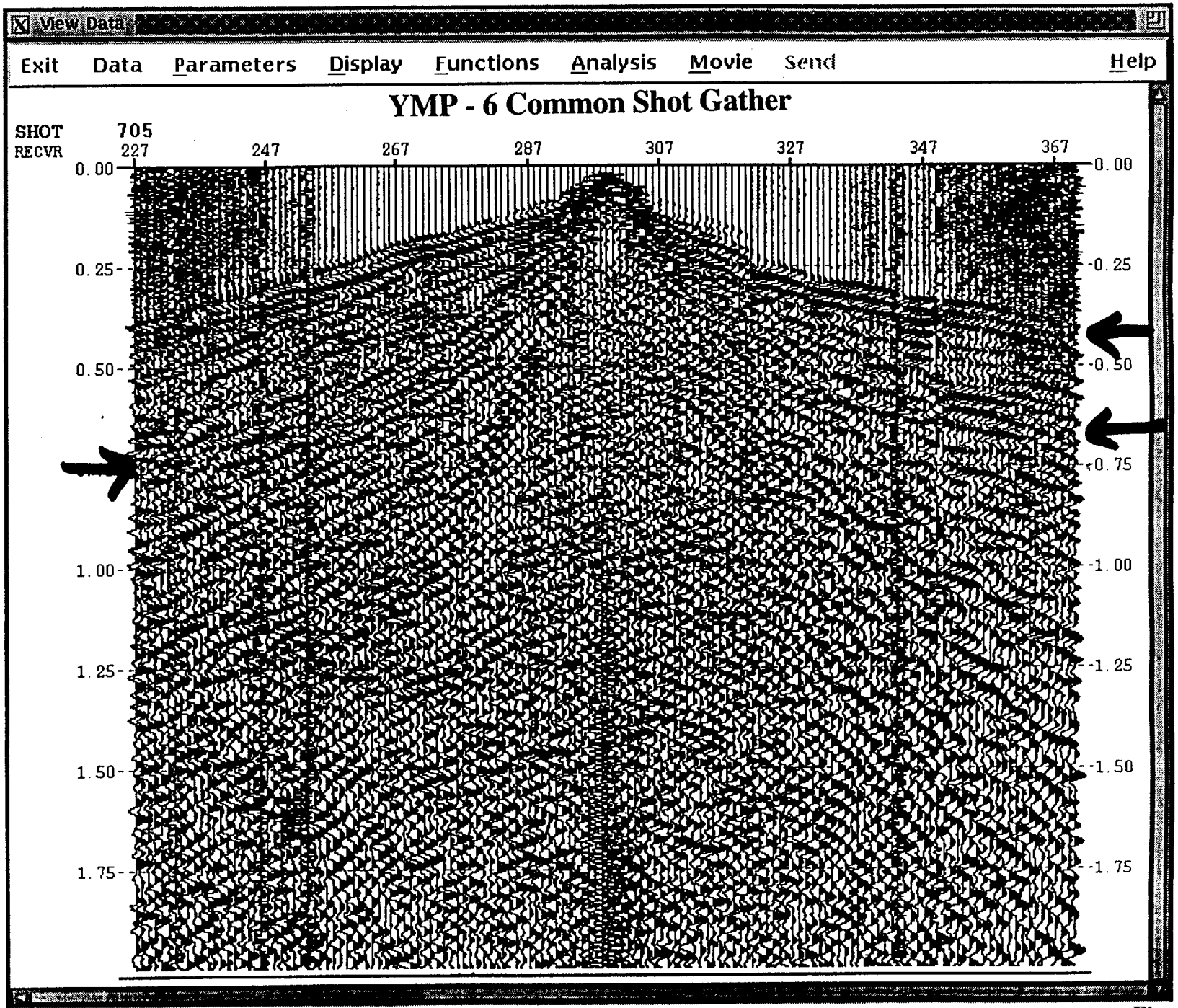

Focus 3.0 CogniSeis Development, Inc.

Figure 3e.

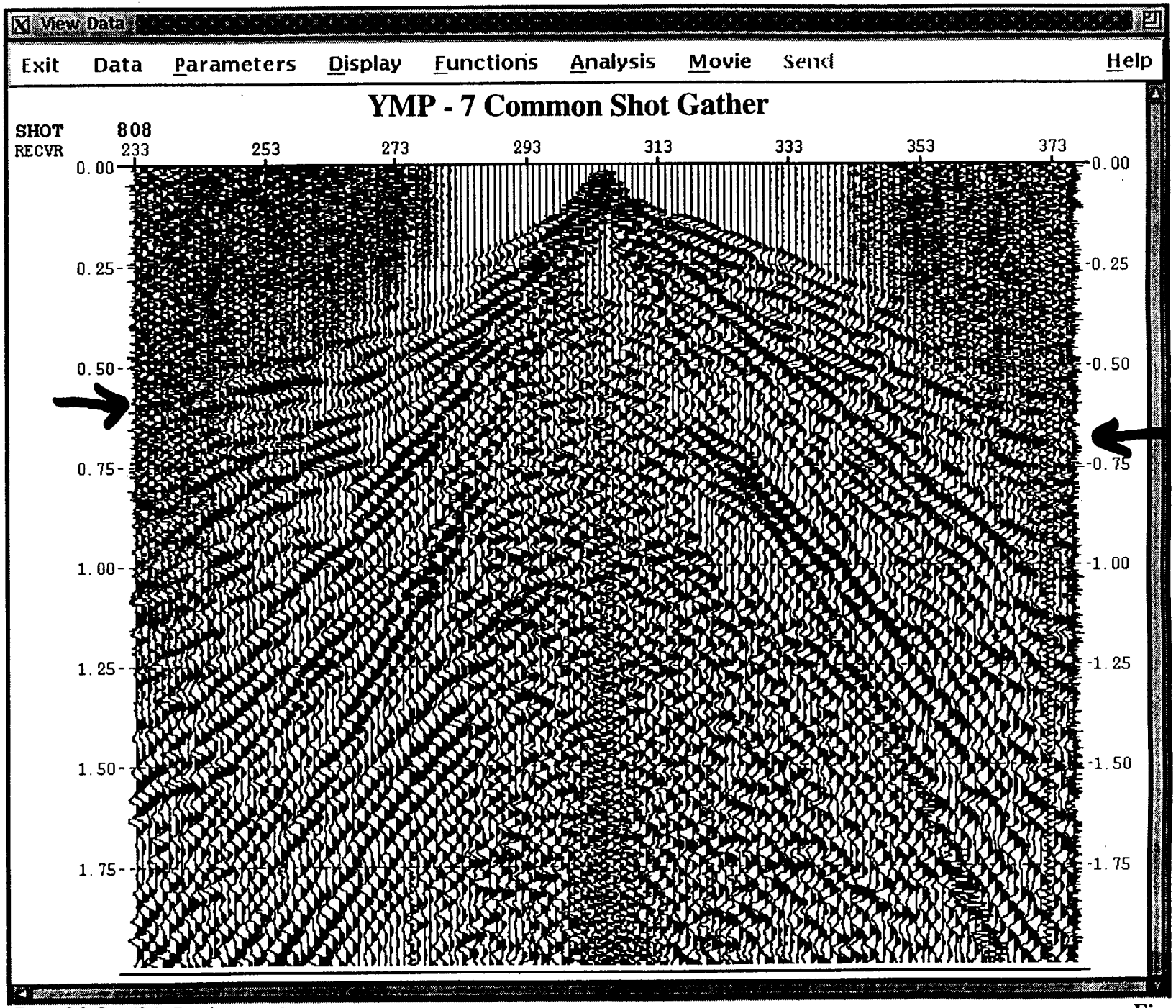

Focus 3.0 CogniSeis Development, Inc.

Figure 3f.

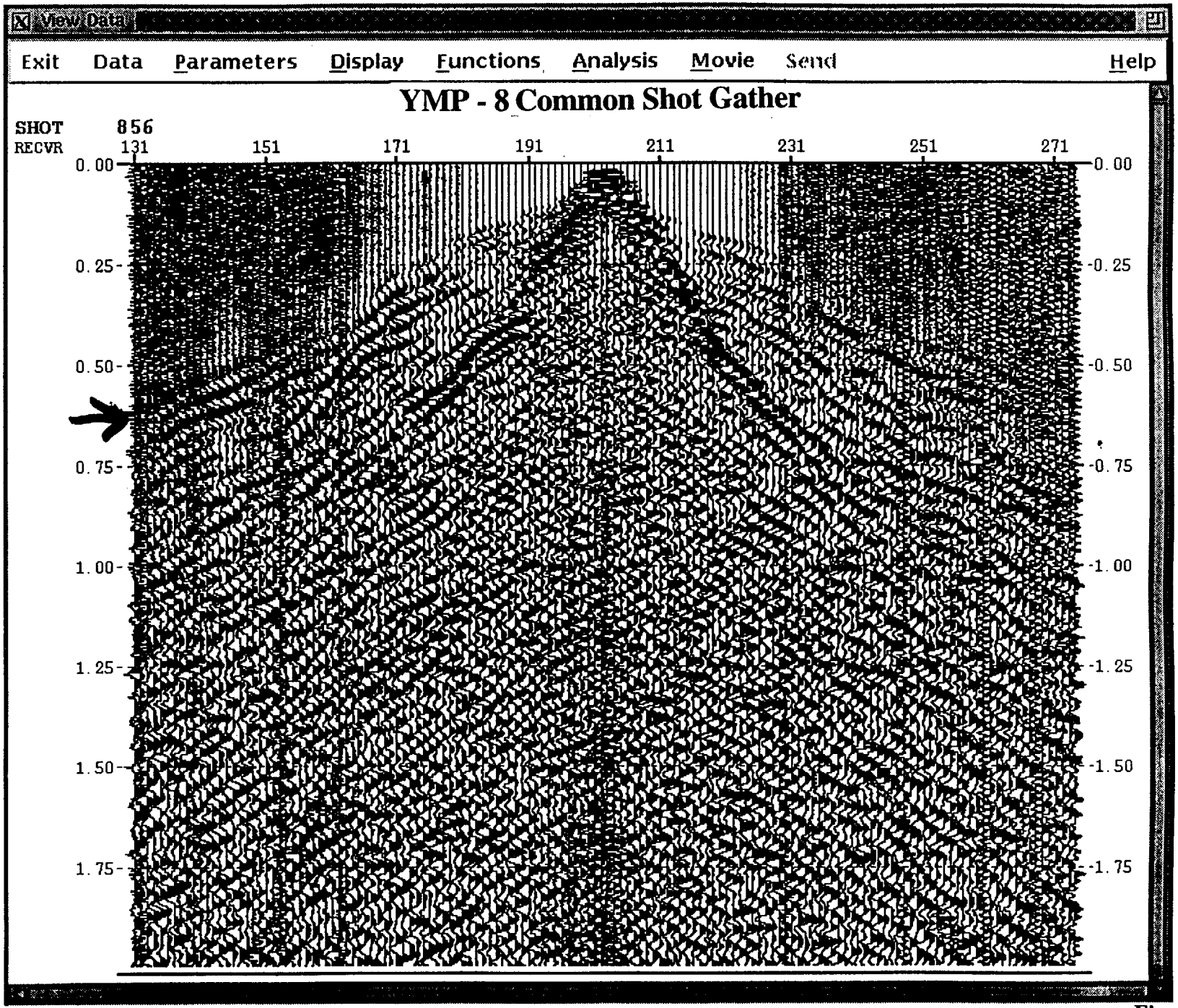

Focus 3.0 CogniSeis Development, Inc.

Figure 3g.

YMP-13a Common Shot Gathers.

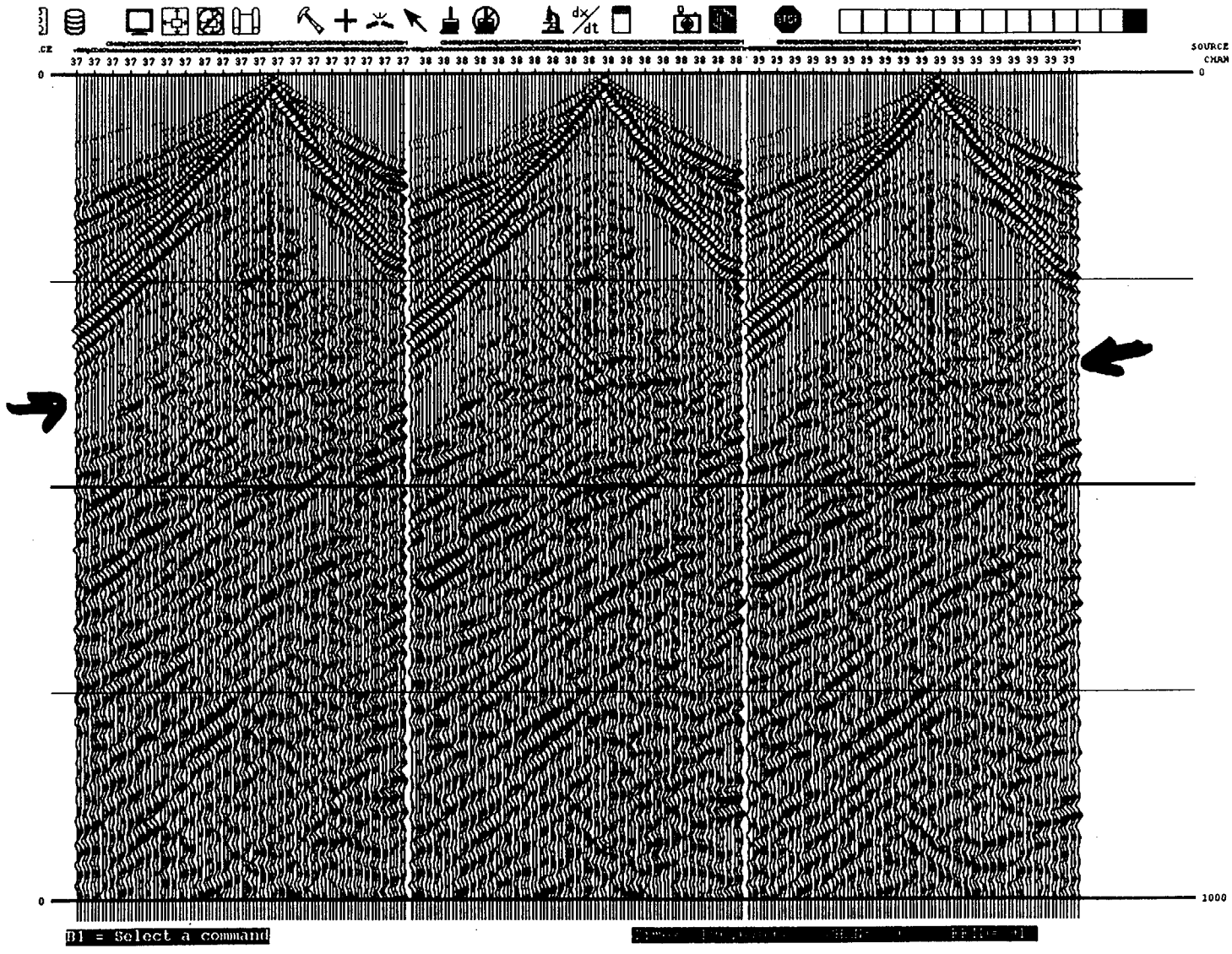

Figure 3h.

YMP-14a Common Shot Gathers.

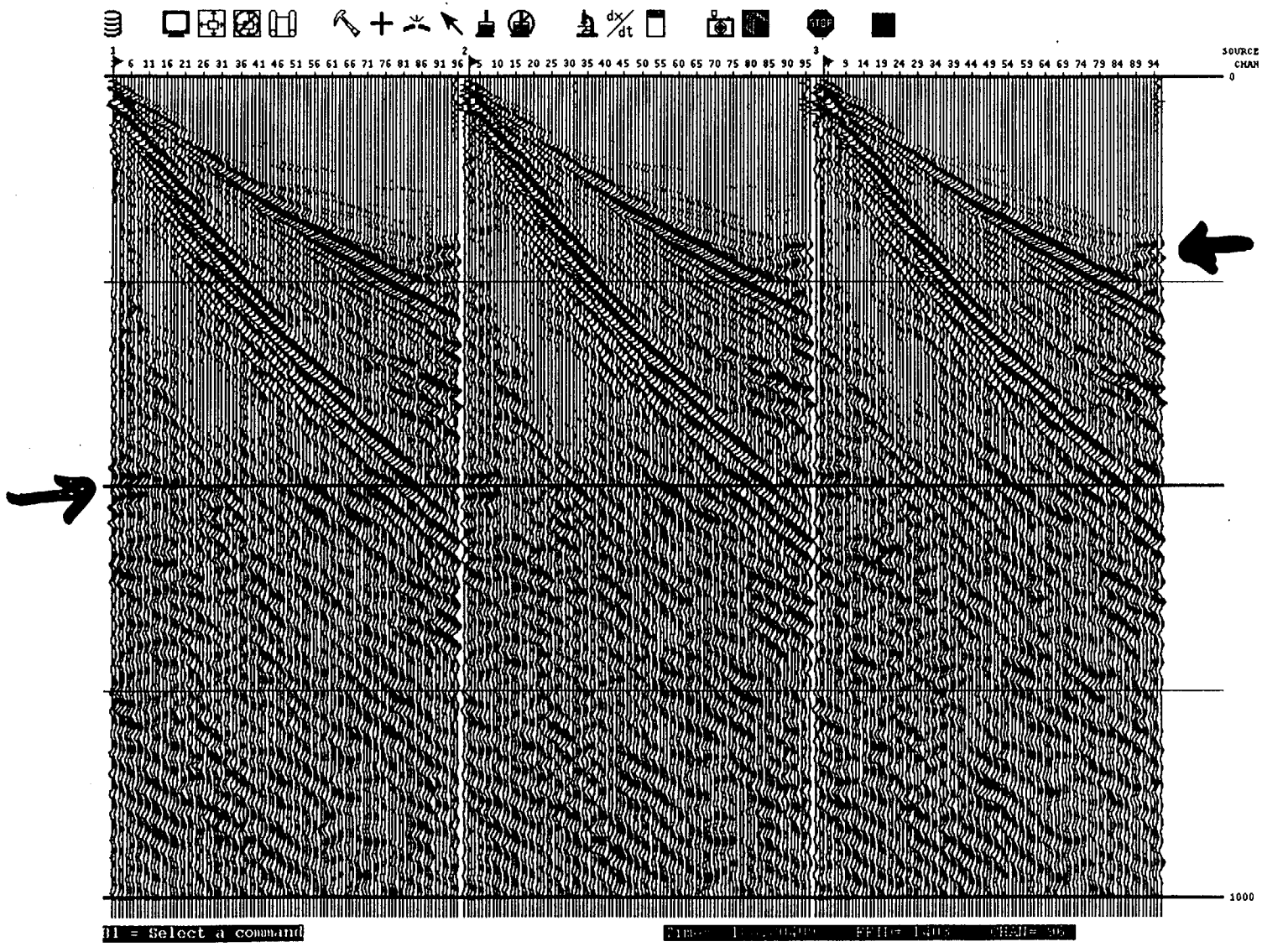

Figure 3i.

YMP-6 MIGRATED DEPTH

SOUTH **NORTH**

1 inch = 1200 feet V.E. 1:1

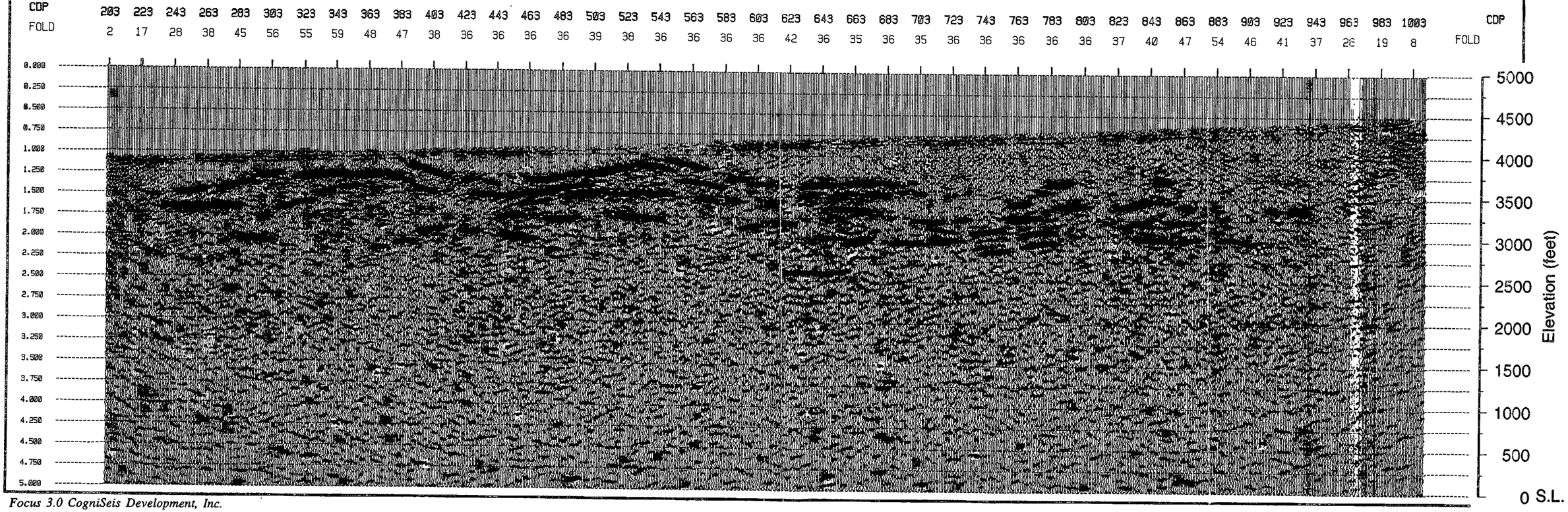

Focus 3.0 CogniSeis Development, Inc.

Figure 11d. YMP-6 highlighted reflectors in red.

Figure 11d

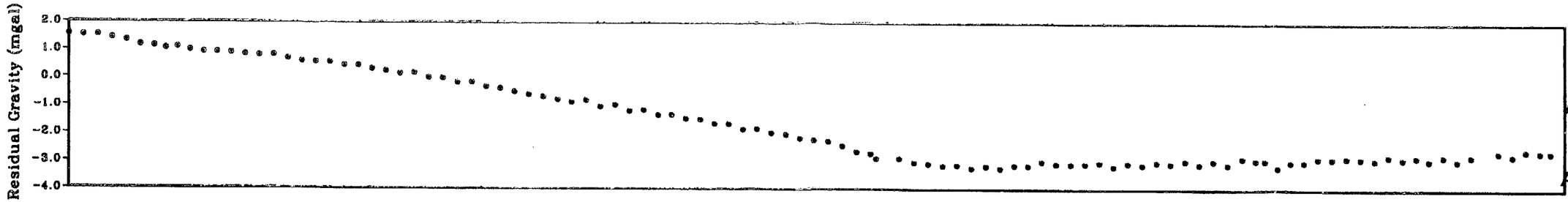

YMP-6 MIGRATED DEPTH

SOUTH **NORTH**

1 inch = 1200 feet V.E. 1:1

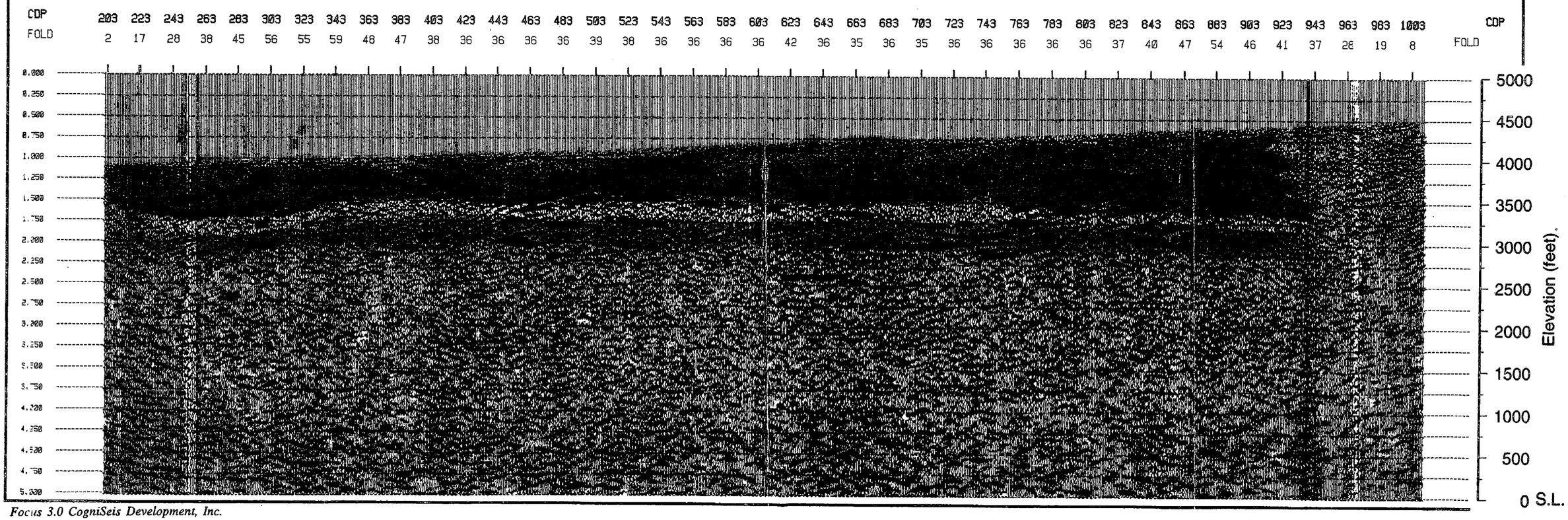

Focus 3.0 CogniSeis Development, Inc.

Figure 11e. YMP-6 interpreted section.

Figure 11e

YMP-7 STACK

NW **SE**

1 inch = 1200 feet

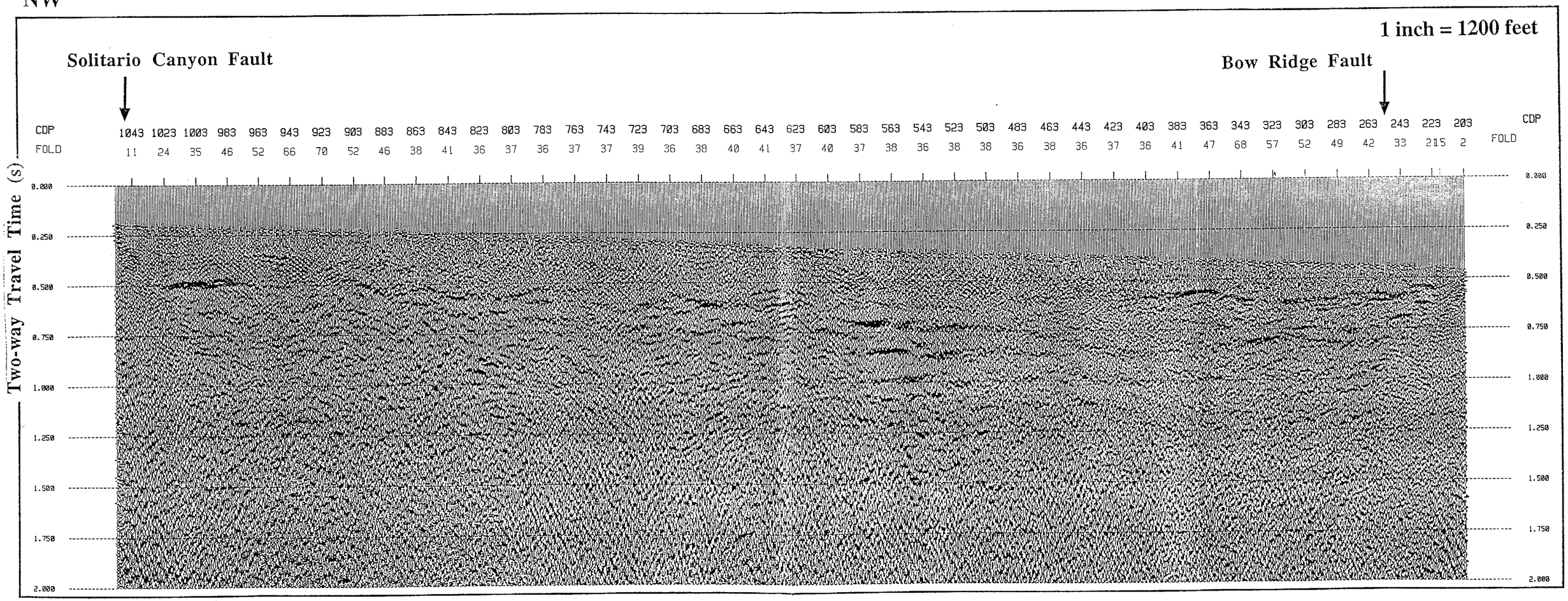

Focus 3.0 CogniSeis Development, Inc.

Figure 12a. YMP-7 stacked time section.

Figure 12a

YMP-7 MIGRATED DEPTH

NW SE

1 inch = 1200 feet V.E. 1:1

Solitario Canyon Fault

Bow Ridge Fault

CDP	1043	1023	1003	983	963	943	923	903	883	863	843	823	803	783	763	743	723	703	683	663	643	623	603	583	563	543	523	503	483	463	443	423	403	383	363	343	323	303	283	263	243	223	203	CDP
FOLD	11	24	35	46	52	66	70	52	46	38	41	36	37	36	37	37	39	36	38	40	41	37	40	37	38	36	38	38	36	38	36	37	36	41	47	68	57	52	49	42	33	21	2	FOLD

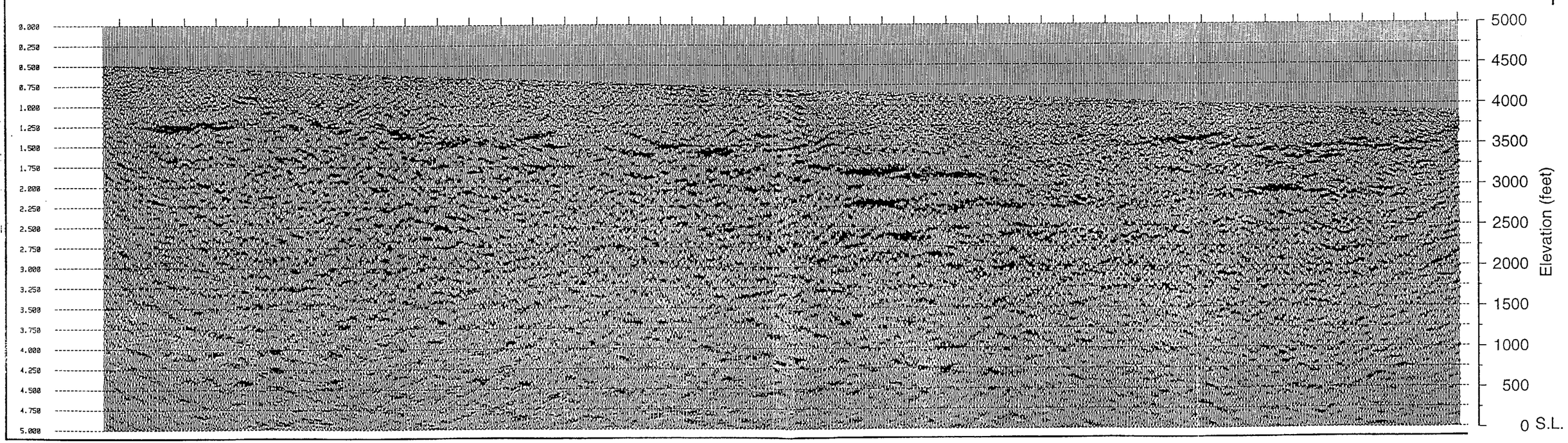

Focus 3.0 CogniSeis Development, Inc.

Figure 12b. YMP-7 migrated depth section.

Figure 12b

YMP-7 LYNX GEOLOGIC MODEL

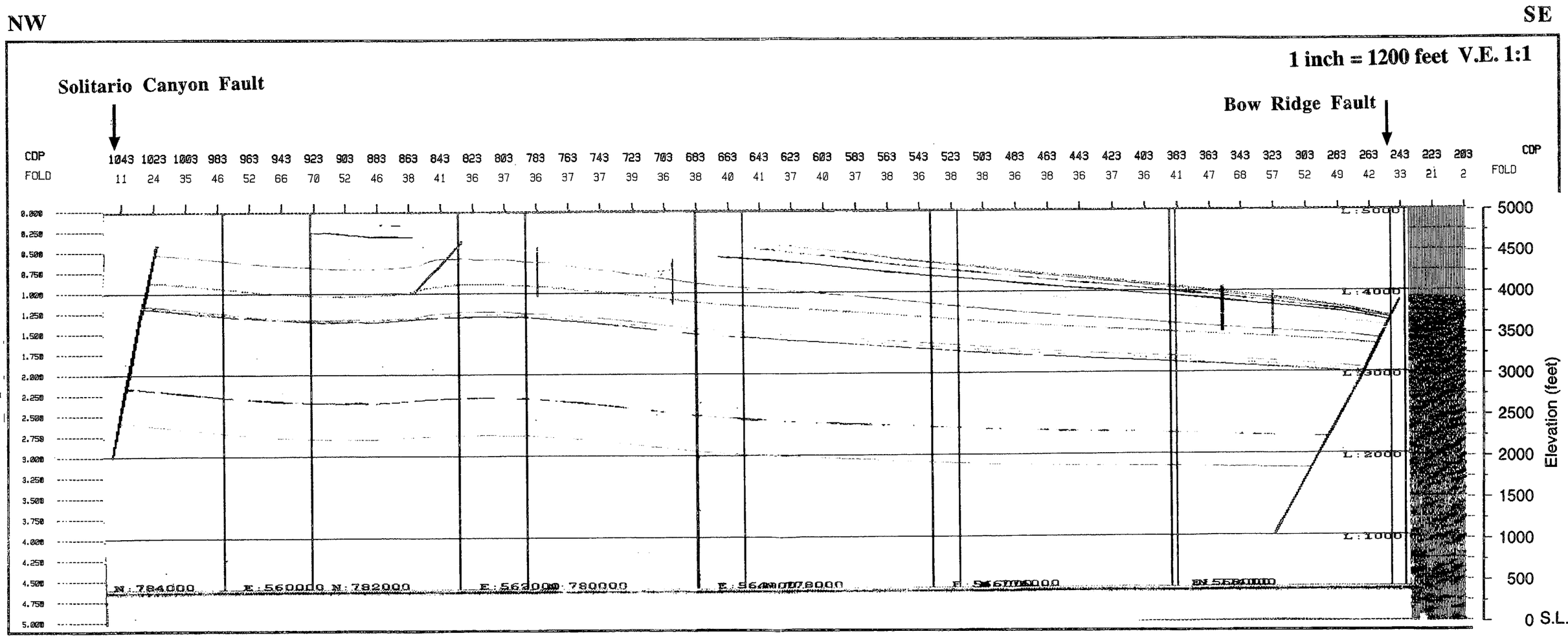

Figure 12c

Figure 12c. YMP-7 Lynx geologic model.

YMP-7 MIGRATED DEPTH

NW **SE**

1 inch = 1200 feet V.E. 1:1

Solitario Canyon Fault

Bow Ridge Fault

CDP	1043	1023	1003	983	963	943	923	903	883	863	843	823	803	783	763	743	723	703	683	663	643	623	603	583	563	543	523	503	483	463	443	423	403	383	363	343	323	303	283	263	243	223	203	CDP
FOLD	11	24	35	46	52	66	70	52	46	38	41	36	37	36	37	37	39	36	38	40	41	37	40	37	38	36	38	38	36	38	36	37	36	41	47	68	57	52	49	42	33	21	2	FOLD

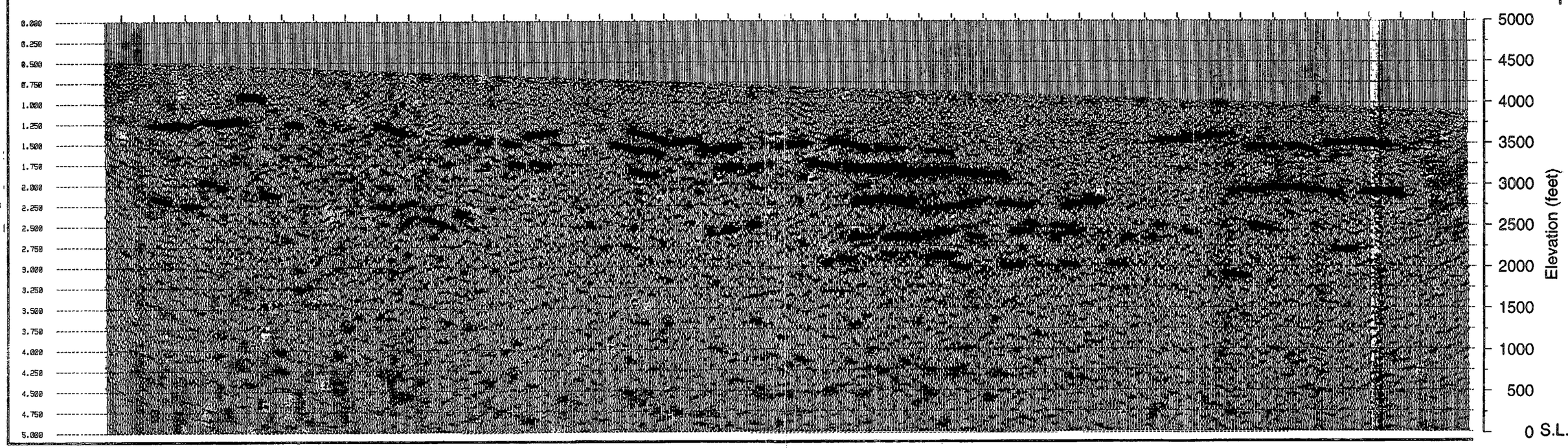

Focus 3.0 CogniSeis Development, Inc.

Figure 12d. YMP-7 highlighted reflectors in red.

Figure 12d

YMP-5 MIGRATED DEPTH

SOUTH **NORTH**

1 inch = 1200 feet V.E. 1:1

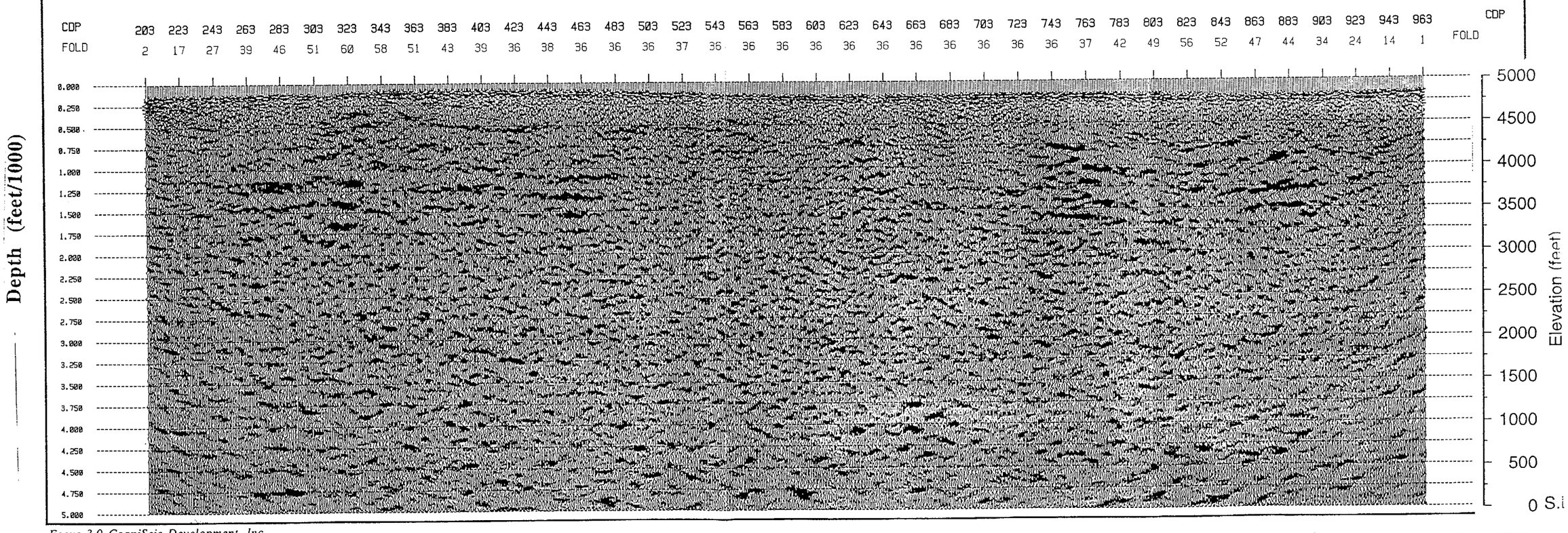

Focus 3.0 CogniSeis Development, Inc.

Figure 10b. YMP-5 migrated depth section.

Figure 10b

YMP-5 LYNX GEOLOGIC MODEL

SOUTH **NORTH**

1 inch = 1200 feet V.E. 1:1

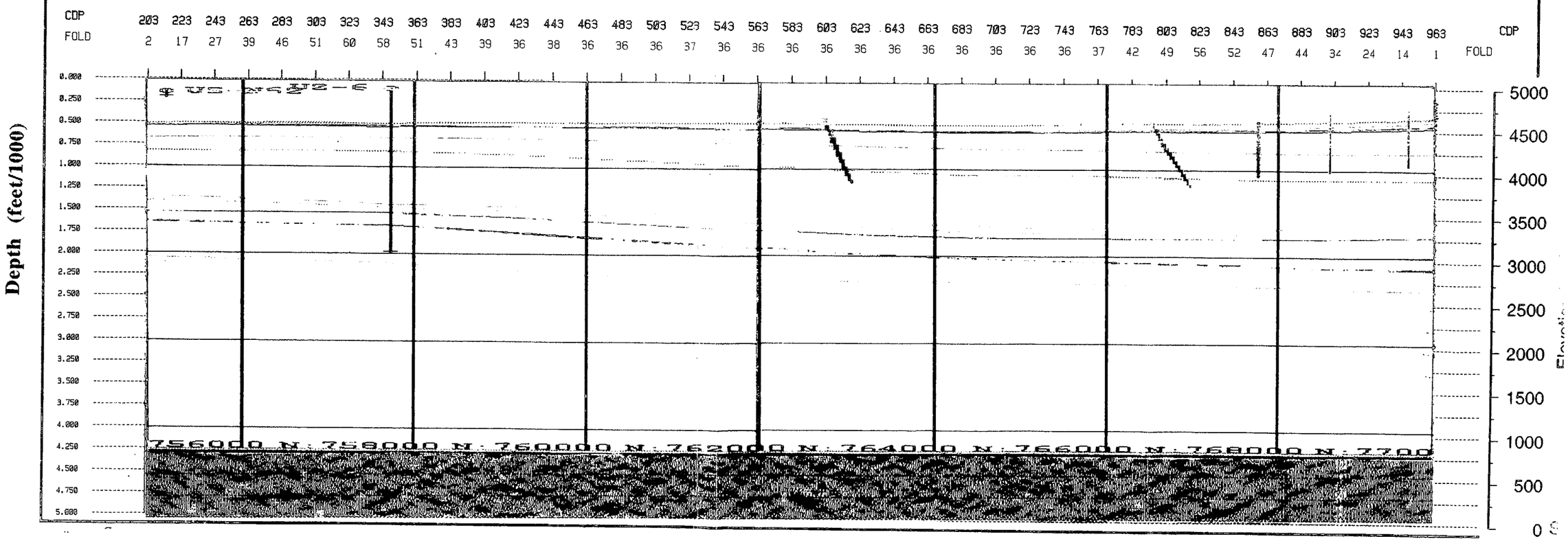

Figure 10c. YMP-5 Lynx geologic model.

Figure 10c

YMP-5 MIGRATED DEPTH

SOUTH **NORTH**

1 inch = 1200 feet V.E. 1:1

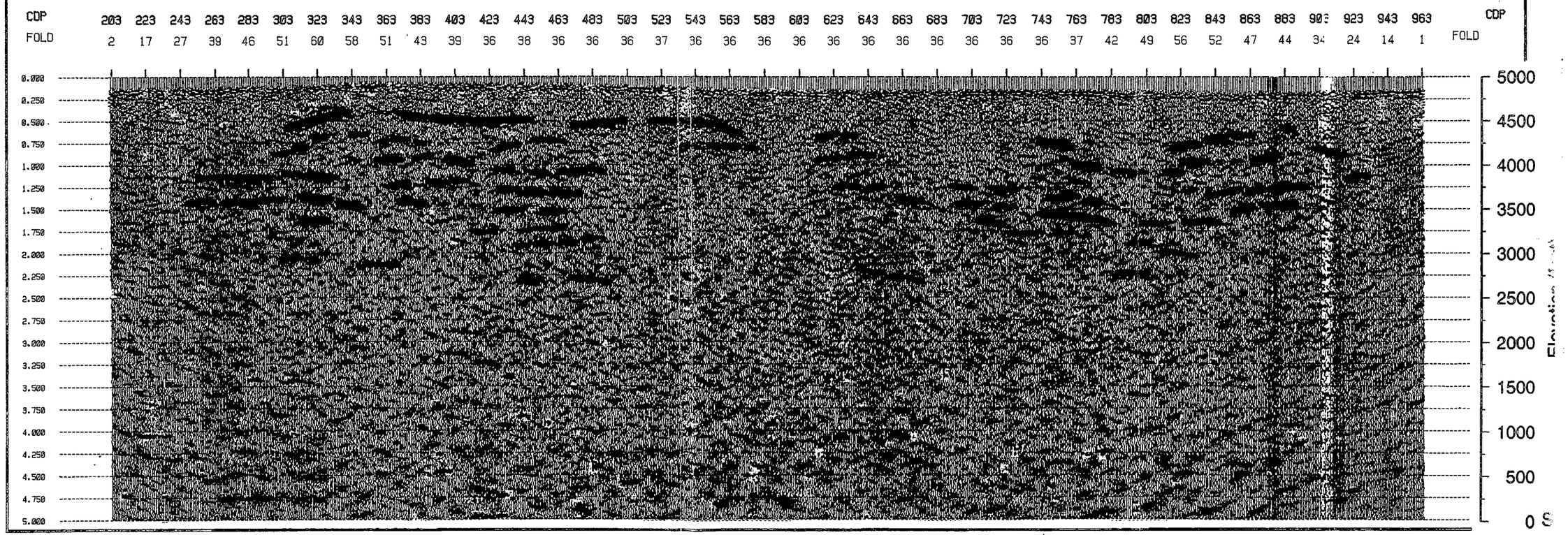

Focus 3.0 CogniSeis Development, Inc.

Figure 10d

Figure 10d. YMP-5 highlighted reflectors in red.

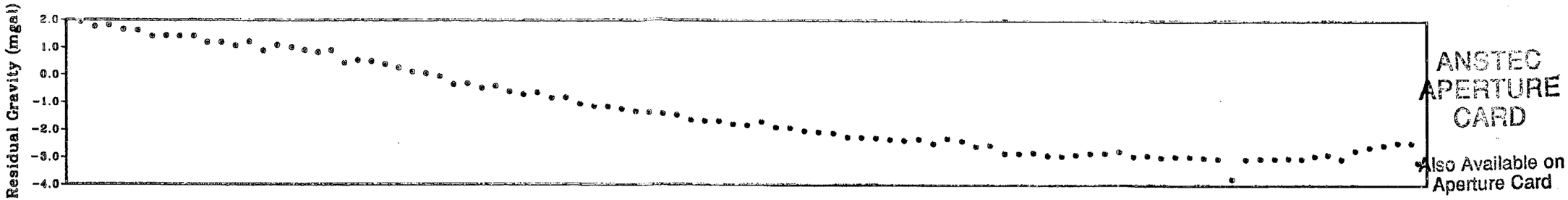

YMP-5 MIGRATED DEPTH

SOUTH **NORTH**

1 inch = 1200 feet V.E. 1:1

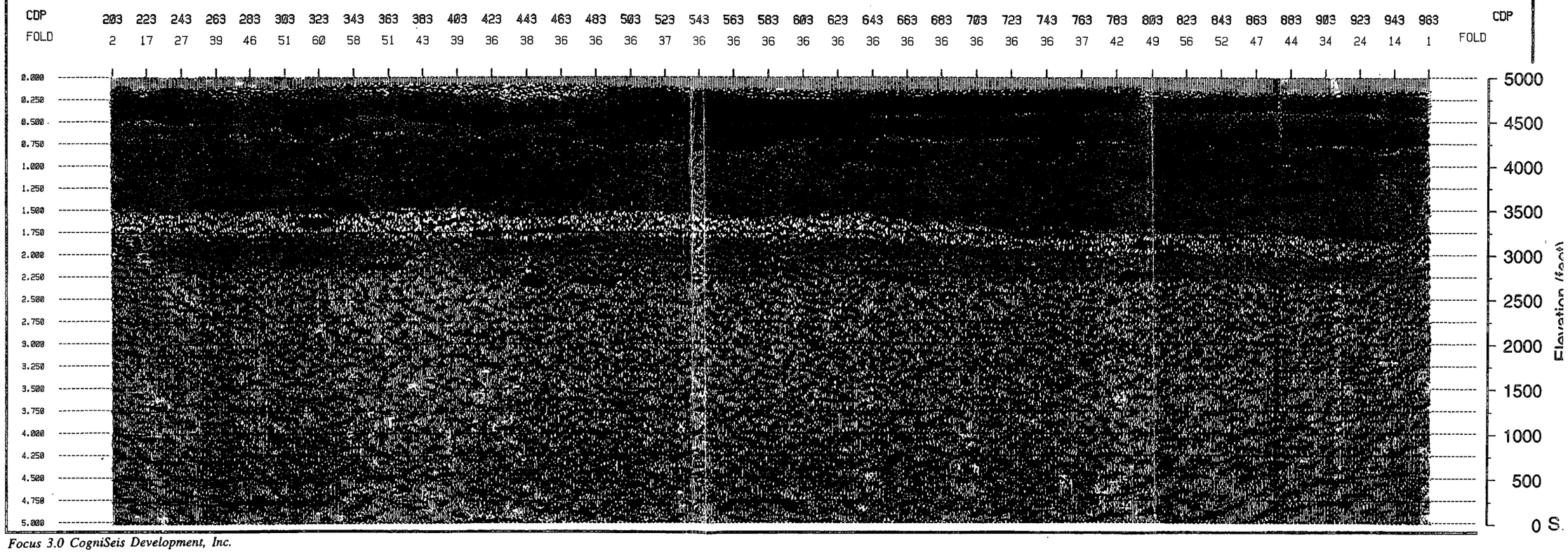

Focus 3.0 CogniSeis Development, Inc.

Figure 10e. YMP-5 interpreted section.

Figure 10e

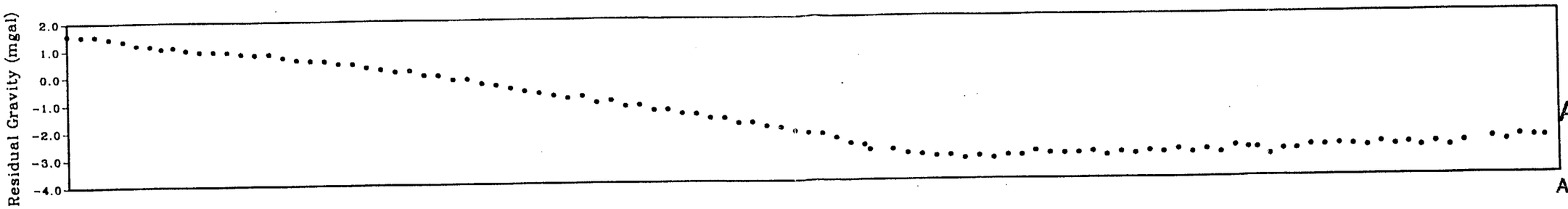

YMP-6 STACK

SOUTH **NORTH**

1 inch = 1200 feet

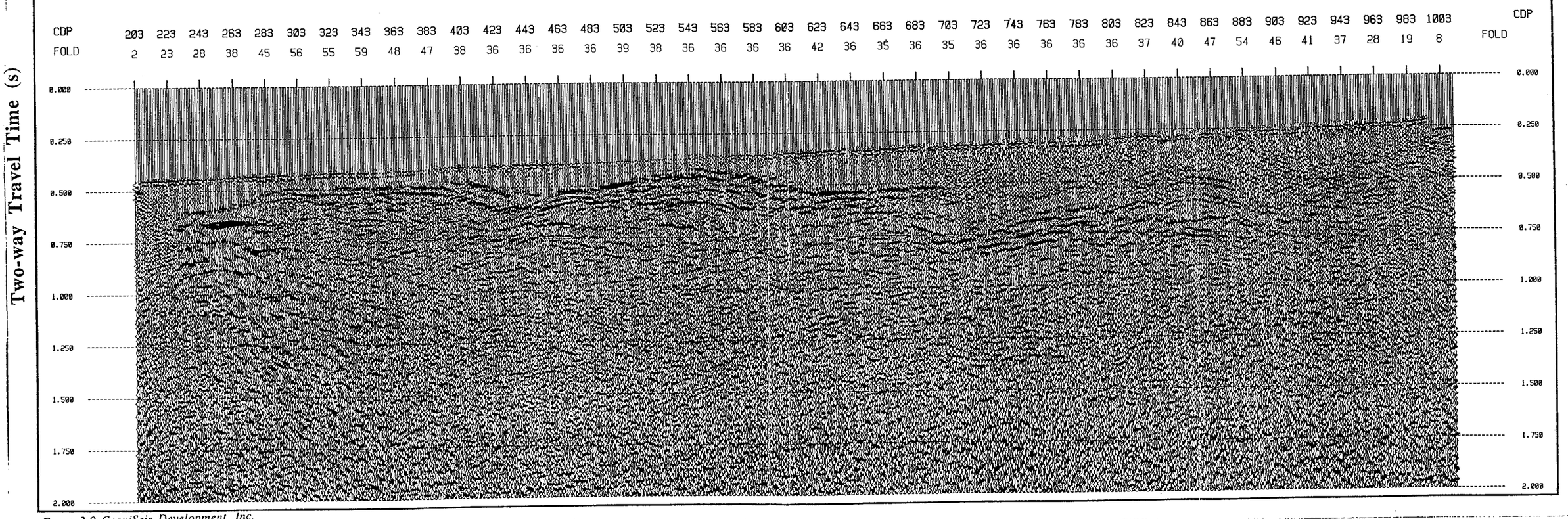

Focus 3.0 CogniSeis Development, Inc.

Figure 11a

Figure 11a. YMP-6 stacked time section with residual gravity.

YMP-6 MIGRATED DEPTH

SOUTH **NORTH**

1 inch = 1200 feet V.E. 1:1

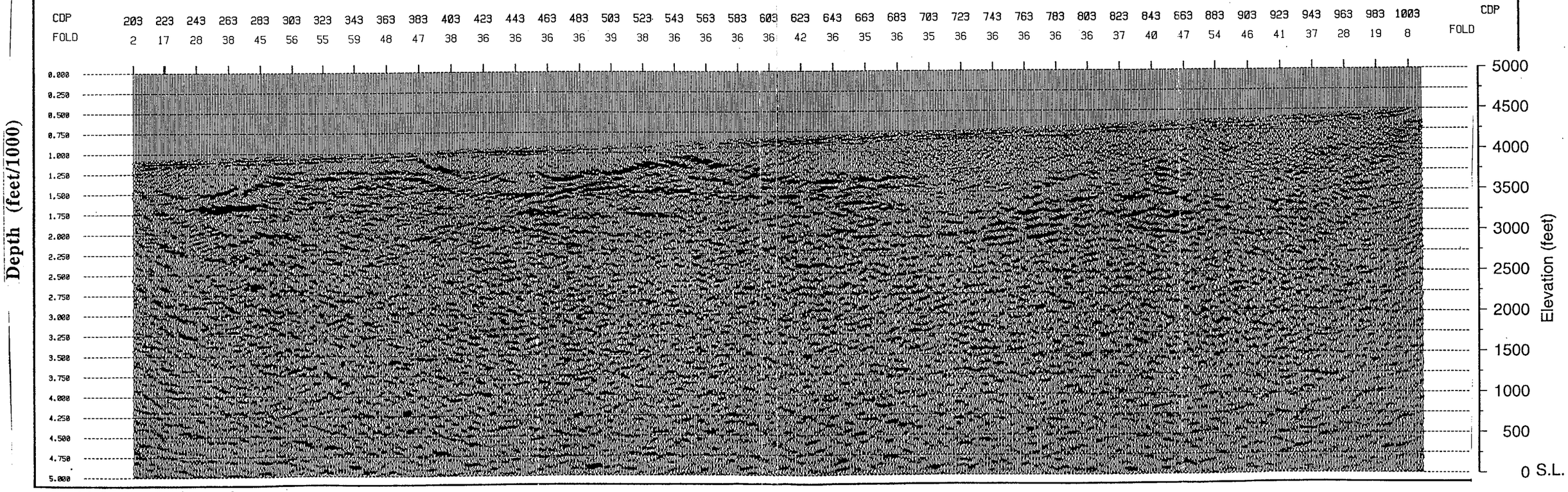

Focus 3.0 CogniSeis Development, Inc.

Figure 11b

Figure 11b. YMP-6 migrated depth section.

YMP-6 LYNX GEOLOGIC MODEL

SOUTH **NORTH**

1 inch = 1200 feet V.E. 1:1

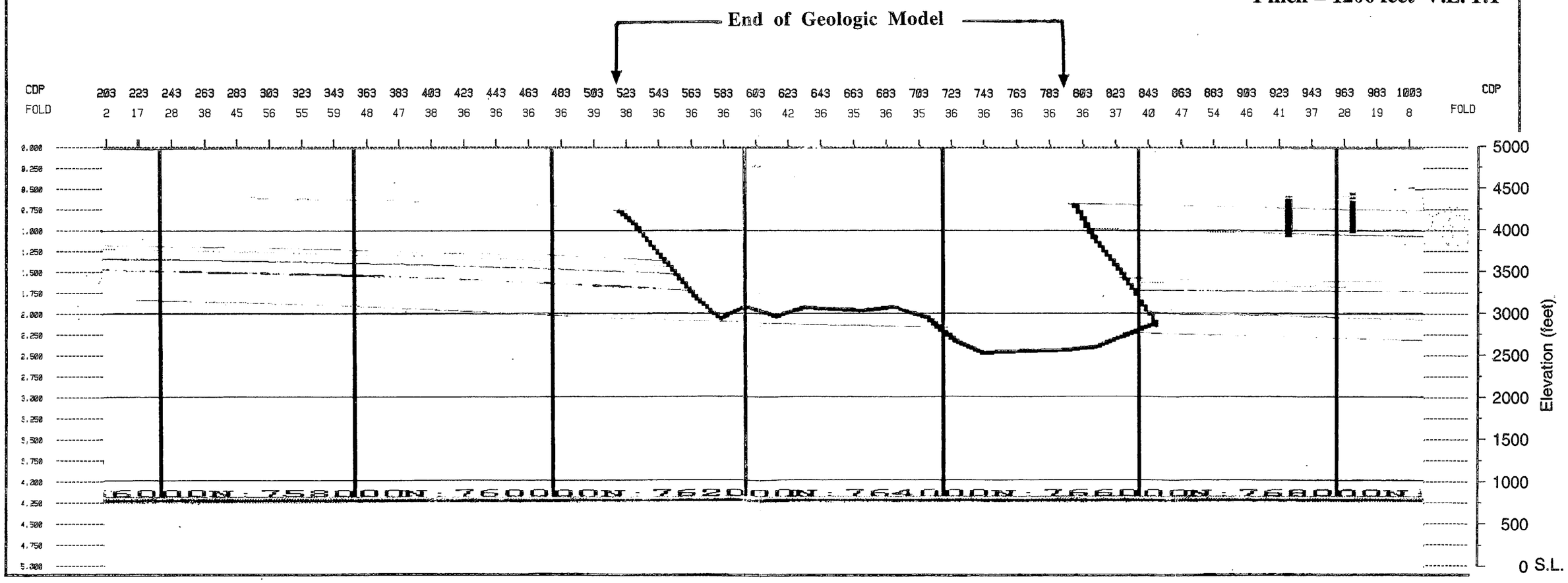

Figure 11c. YMP-6 Lynx geologic model.

Figure 11c

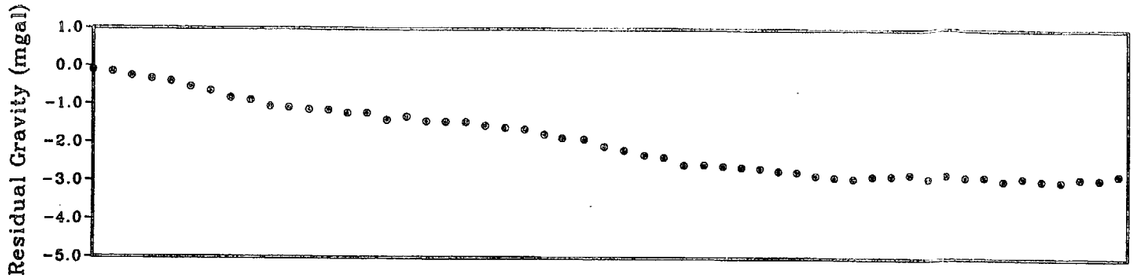

YMP-2 MIGRATED DEPTH

SOUTH **NORTH**

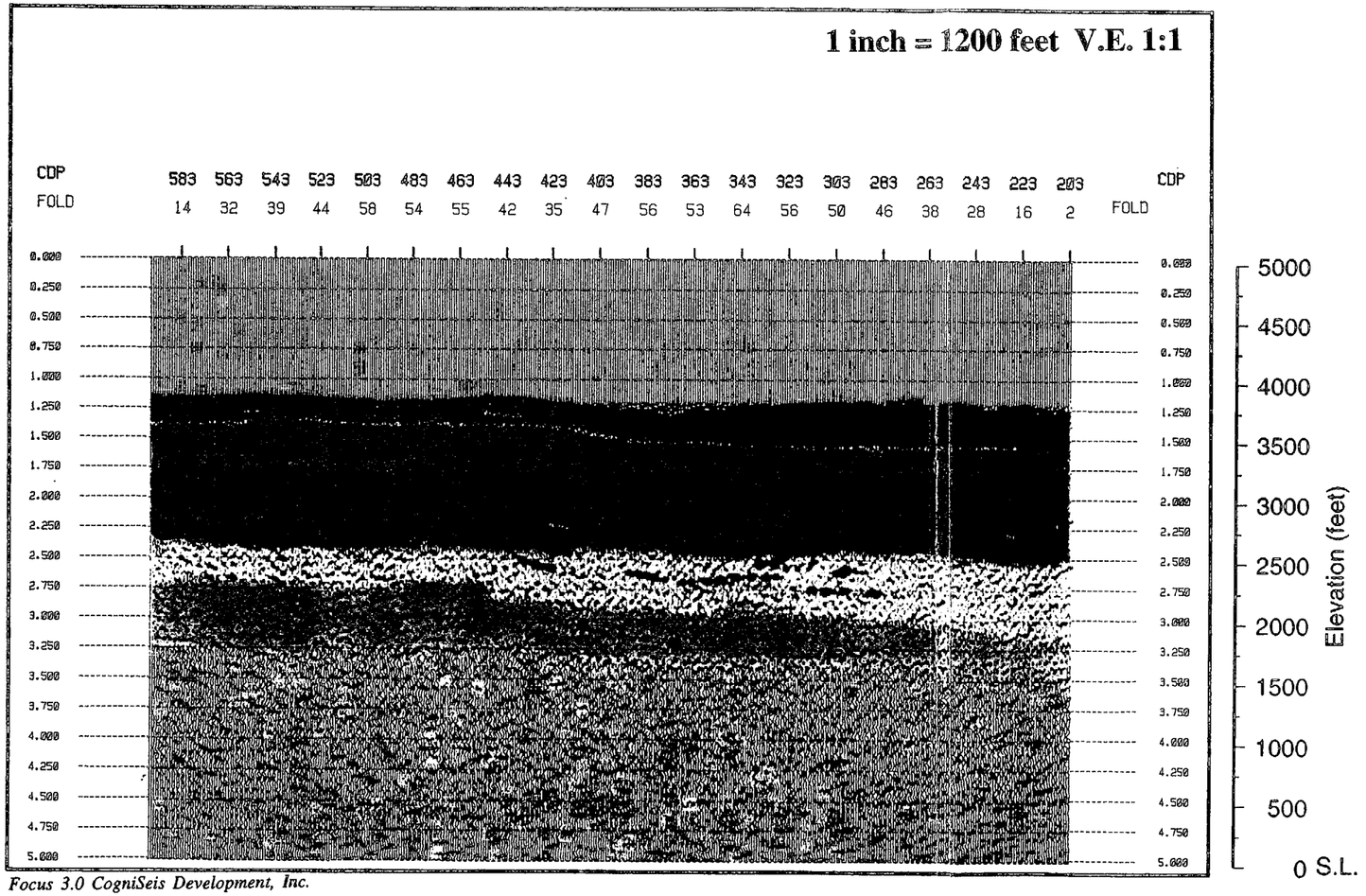

Focus 3.0 CogniSeis Development, Inc.

Figure 8e. YMP-2 interpreted section.

Figure 8e

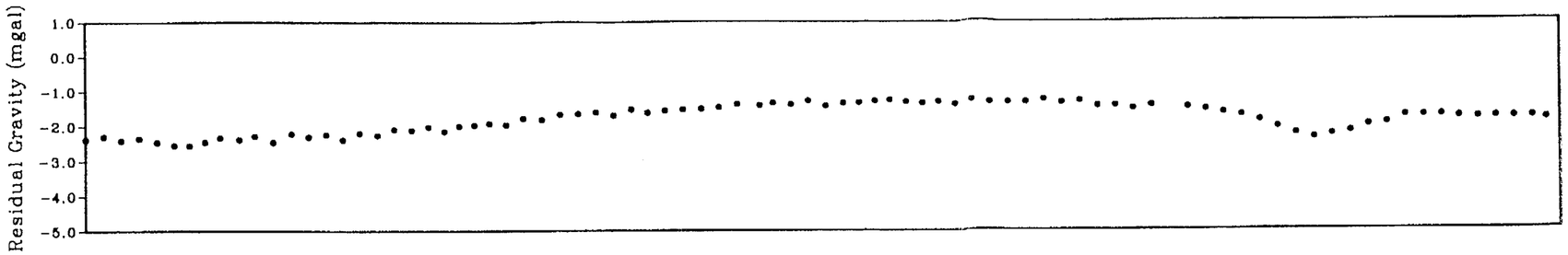

YMP-4 STACK

WEST **EAST**

1 inch = 1200 feet

Ghost Dance Fault

Bow Ridge Fault

CDP	283	303	323	343	363	383	403	423	443	463	483	503	523	543	563	583	603	623	643	663	683	703	723	743	763	783	803	823	843	CDP
FOLD	8	13	30	30	41	51	68	68	64	59	52	47	46	41	40	43	41	41	38	38	44	49	58	56	53	47	39	28	18	5	FOLD

Two-way Travel Time (s)

0.000 0.250 0.500 0.750 1.000 1.250 1.500 1.750 2.000

Focus 3.0 CogniSeis Development, Inc.

Figure 9a. YMP-4 stacked time section with residual gravity.

YMP-4 MIGRATED DEPTH

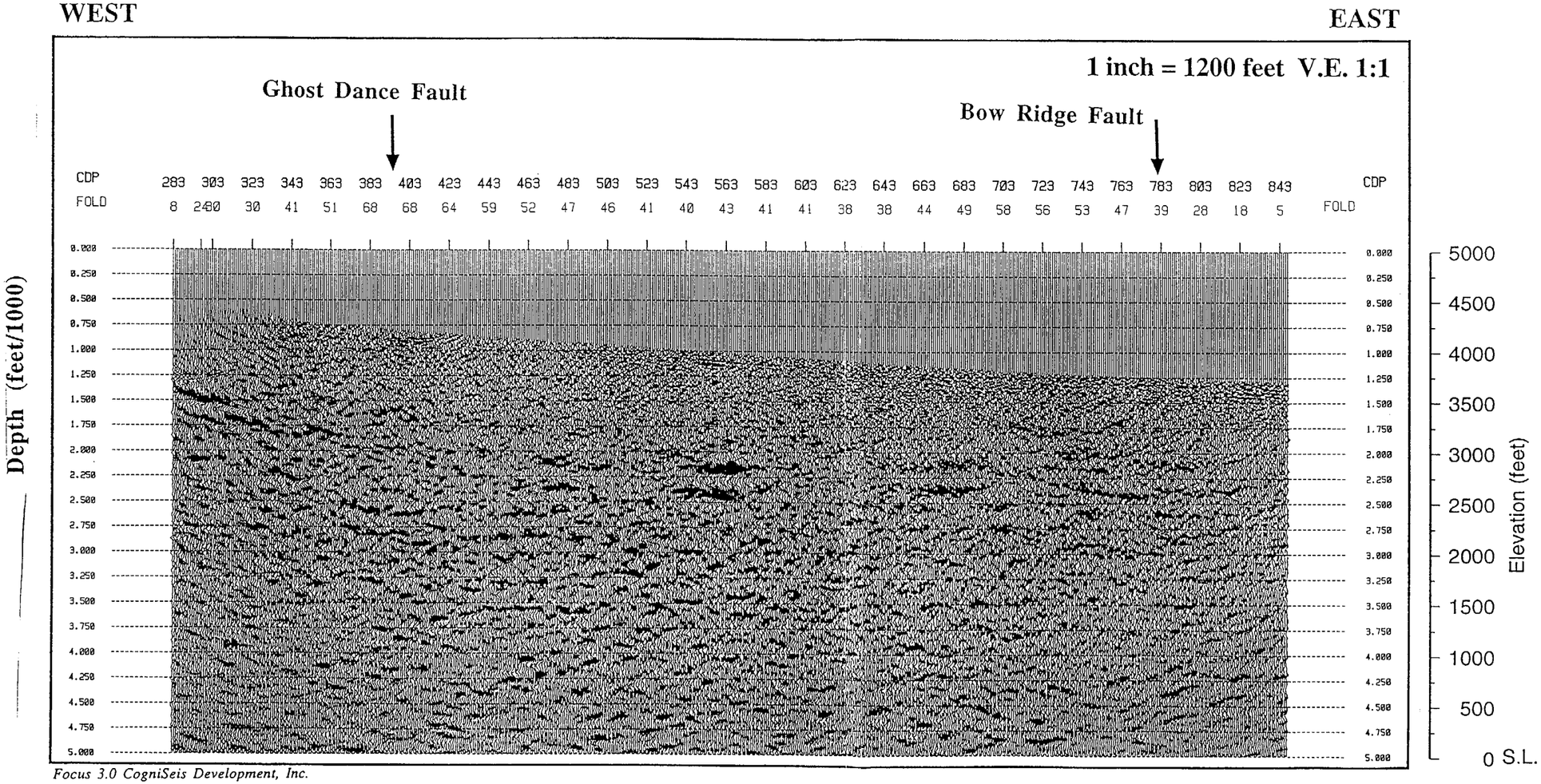

Figure 9b. YMP-4 migrated depth section.

Figure 9b

9601050003 -17

YMP-4 LYNX GEOLOGIC MODEL

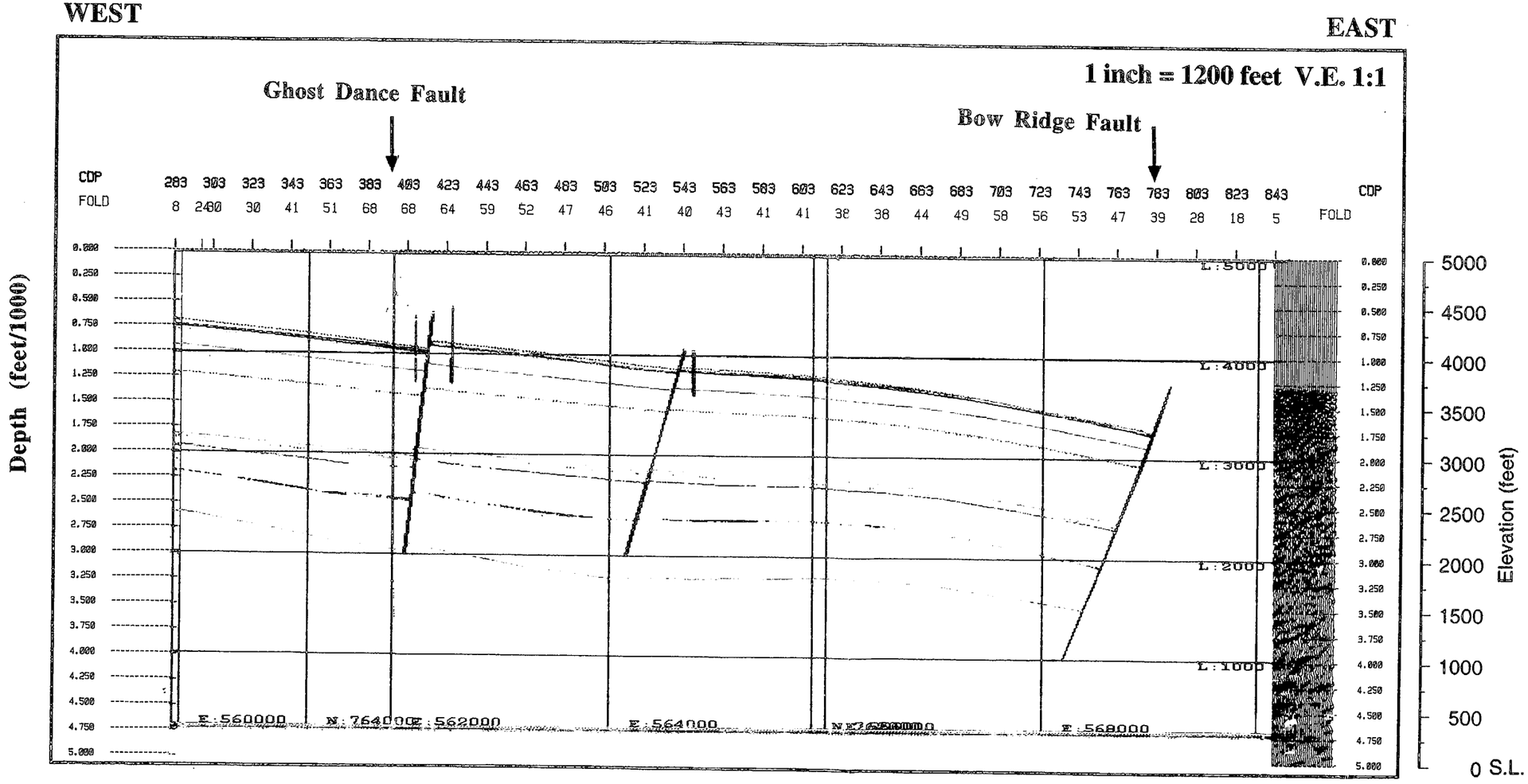

Figure 9c. YMP-4 Lynx geologic model.

Figure 9c

YMP-4 MIGRATED DEPTH

WEST **EAST**

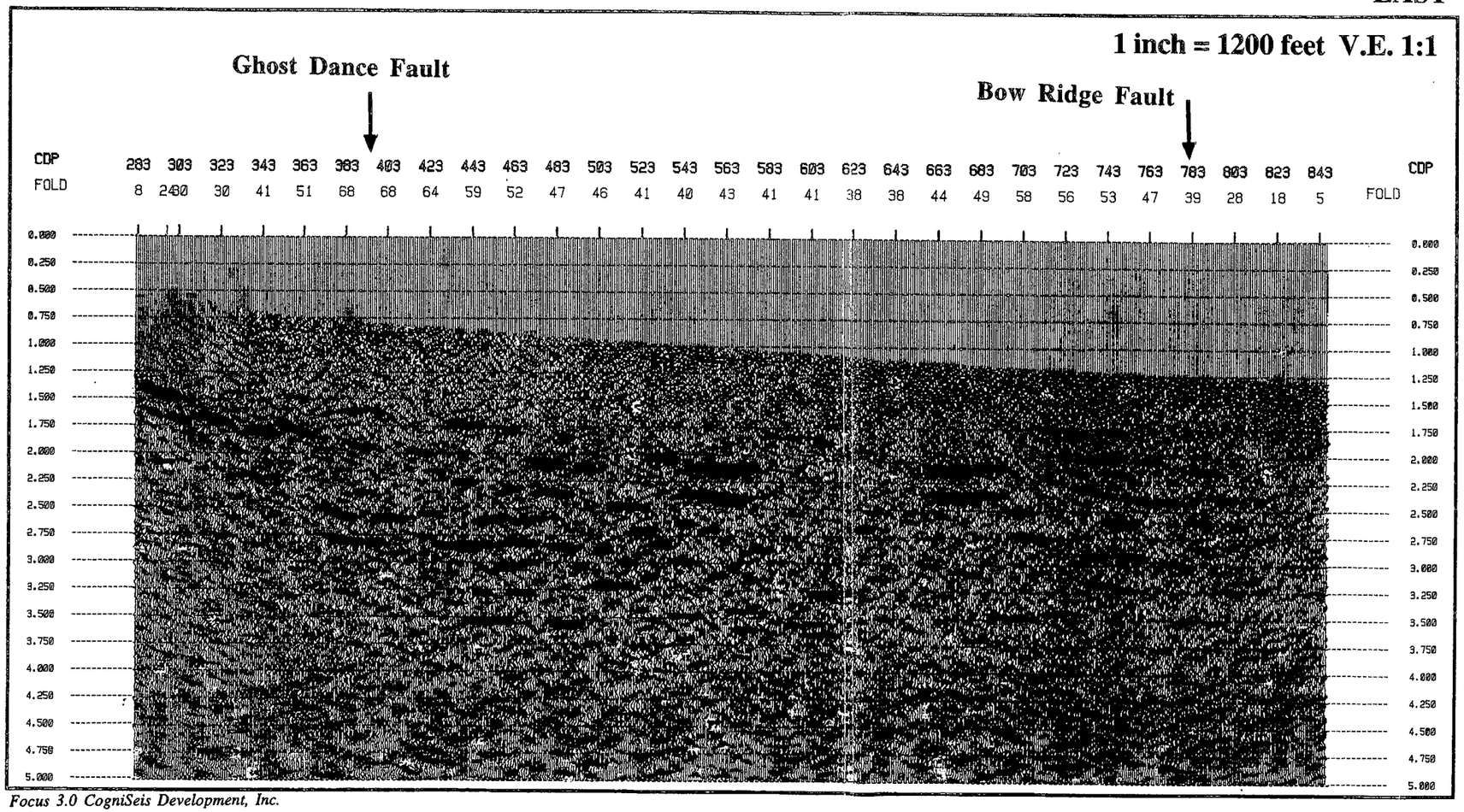

Focus 3.0 CogniSeis Development, Inc.

Figure 9d. YMP-4 highlighted reflectors in red.

Figure 9d

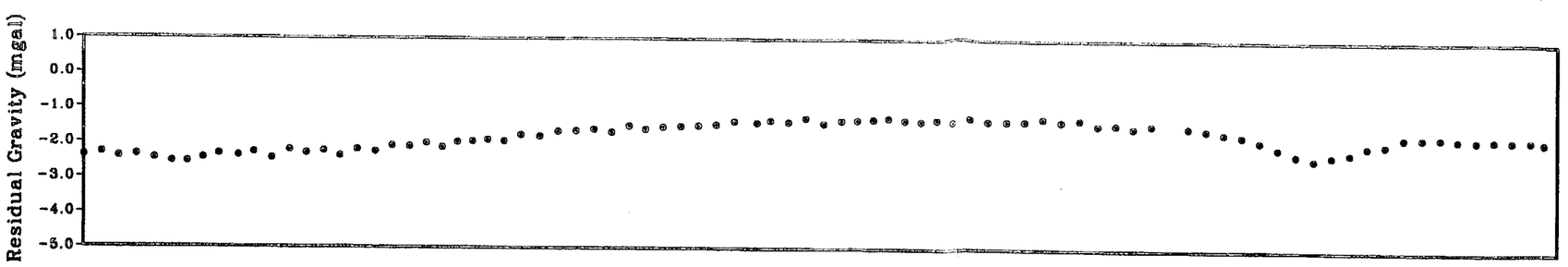

YMP-4 MIGRATED DEPTH

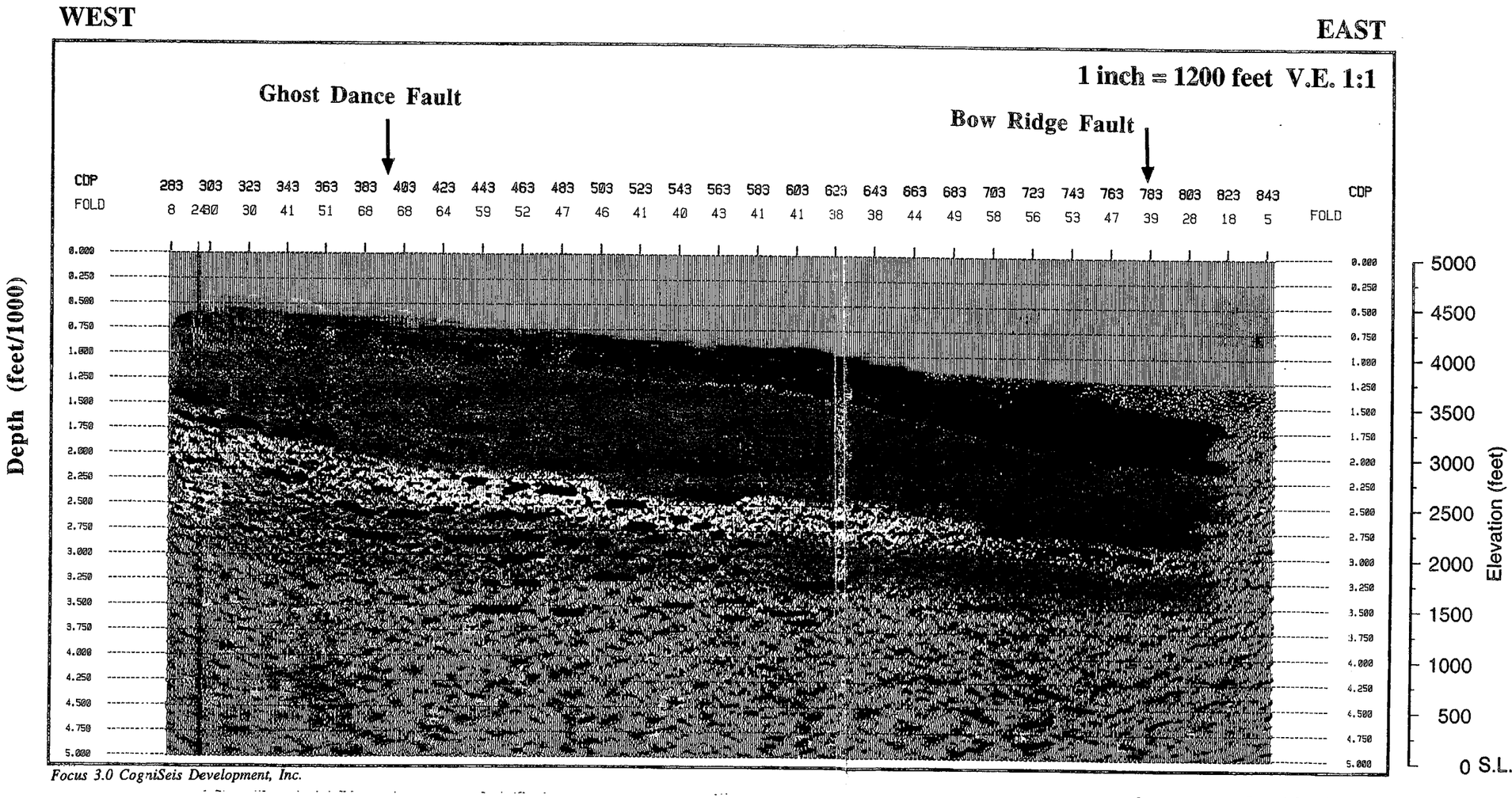

Figure 9e. YMP-4 interpreted section.

Figure 9e

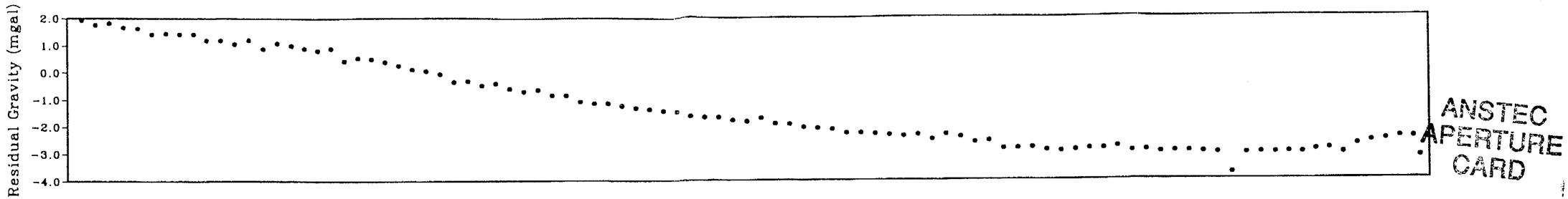

YMP-5 STACK

SOUTH **NORTH**

1 inch = 1200 feet

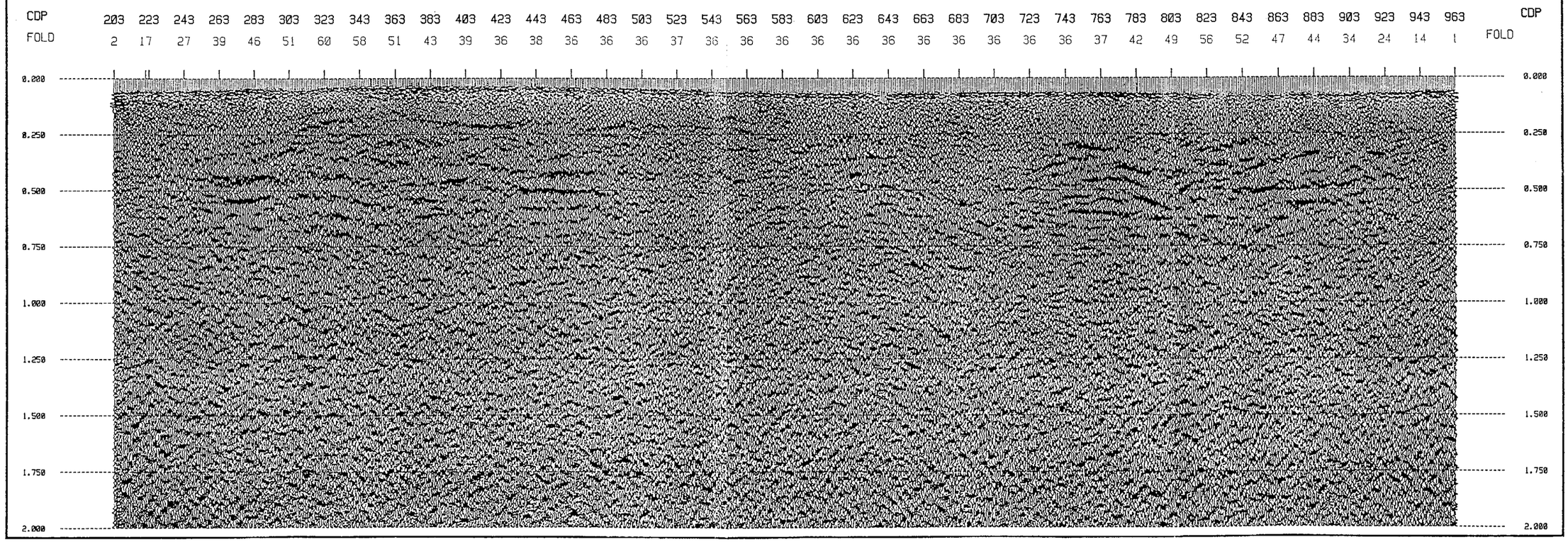

Focus 3.0 CogniSeis Development, Inc.

Figure 10a. YMP-5 stacked time section with residual gravity.

Figure 10a

YMP - 1 NMO Corrected CDP Supergather 454-456

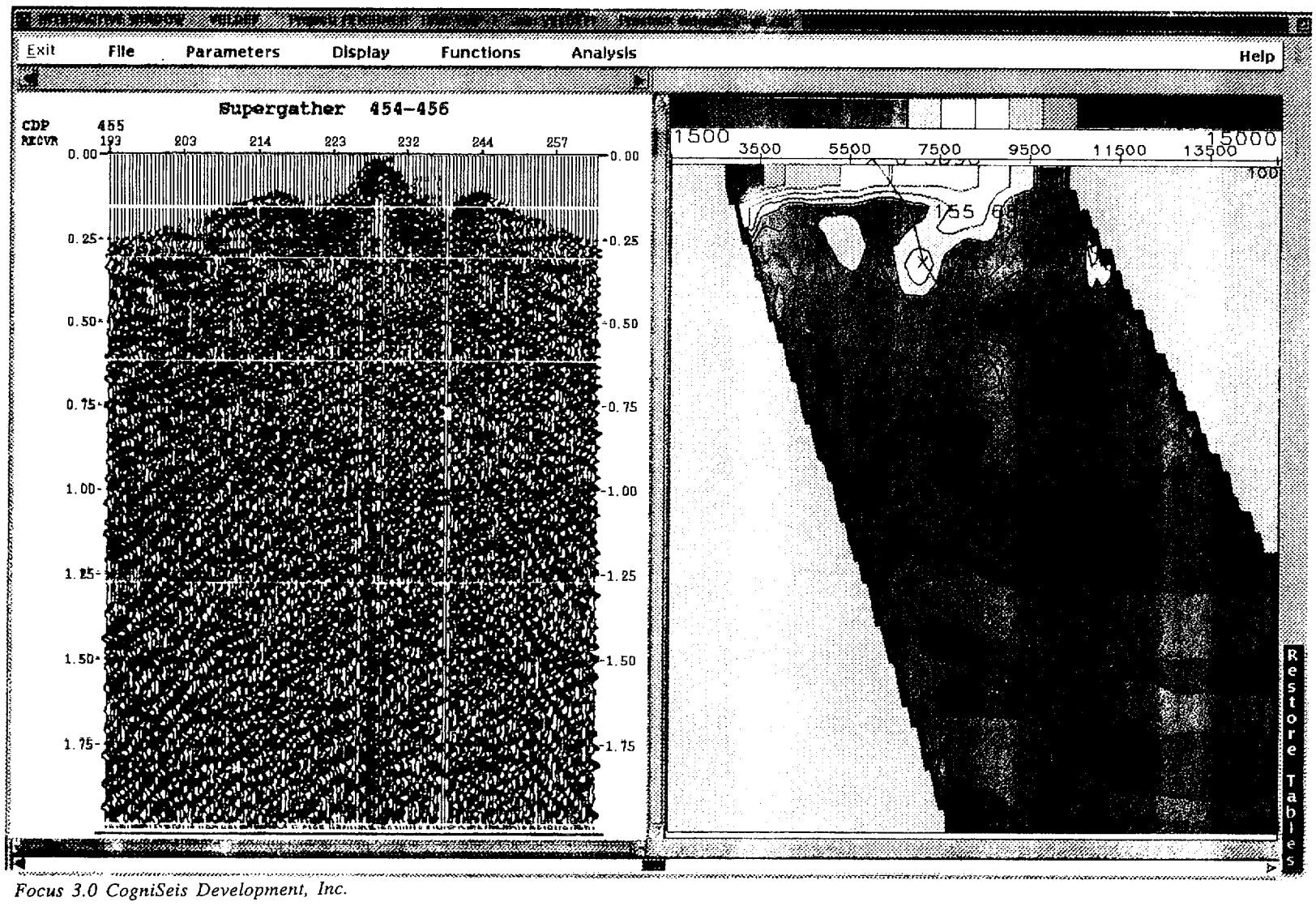

Focus 3.0 CogniSeis Development, Inc.

YMP-1 Stacked CDP Gathers 445-465

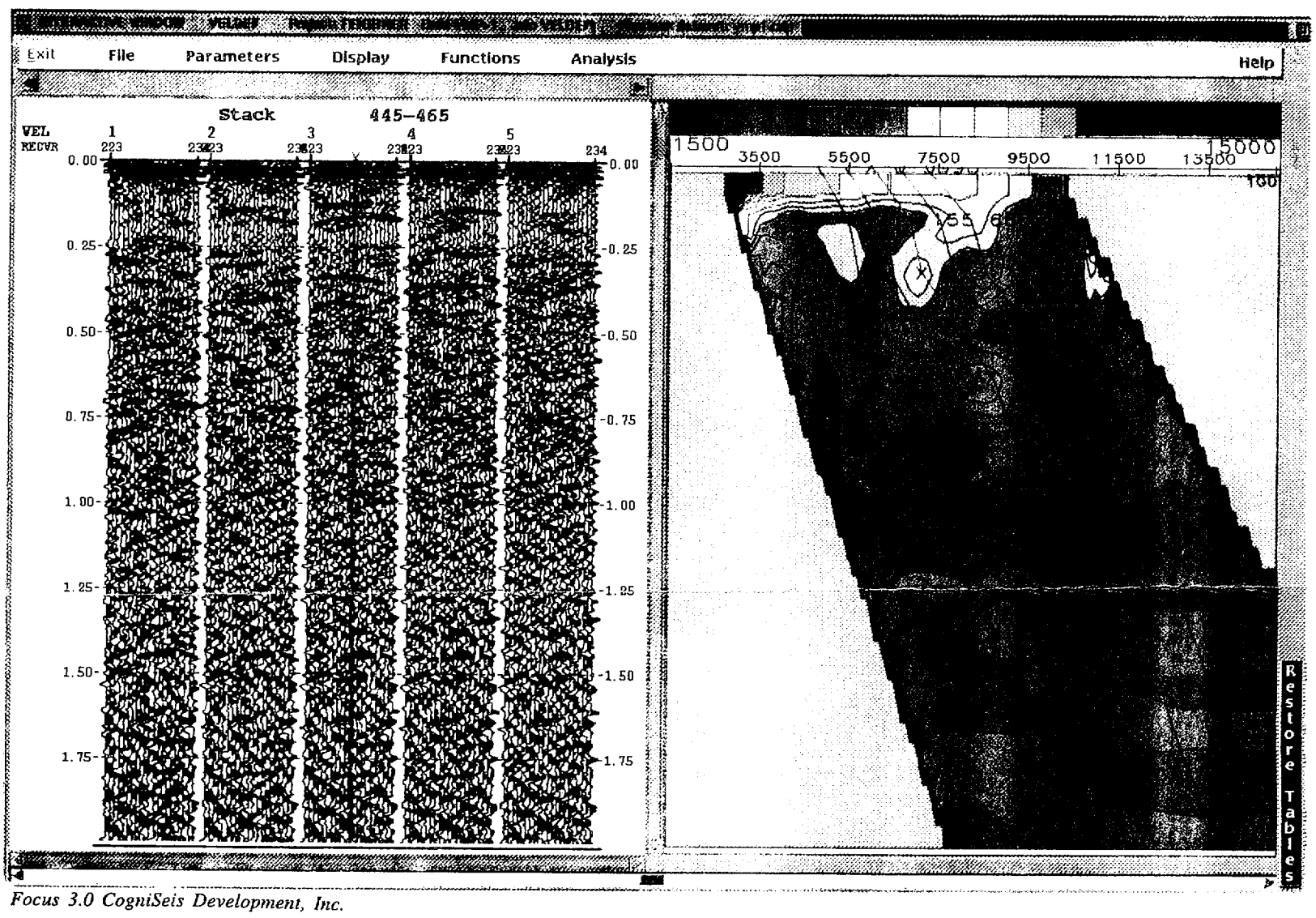

Focus 3.0 CogniSeis Development, Inc.

Figure 4. Example of the interactive velocity analysis program VELDEF. Top figure is a Normal Moveout (NMO) corrected CDP gather with the indicated stacking velocity function on the right. The yellow lines on the left indicate flat lying events that will be stacked. The bottom figure is a stack of the CDP gathers with the picked velocity function in red. Also shown are alternative stacks with slower and faster velocities for comparison.

YMP - 1 Stacking Velocities

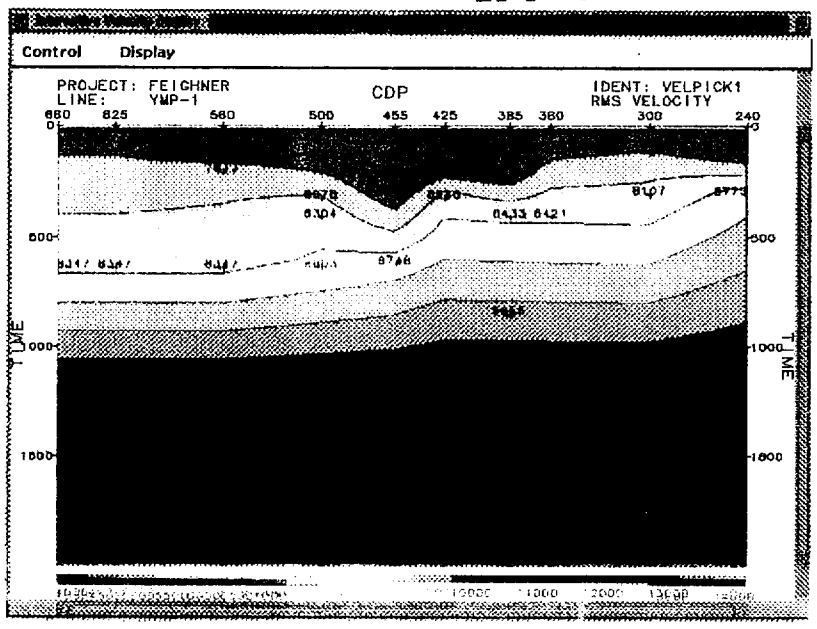

YMP - 2 Stacking Velocities

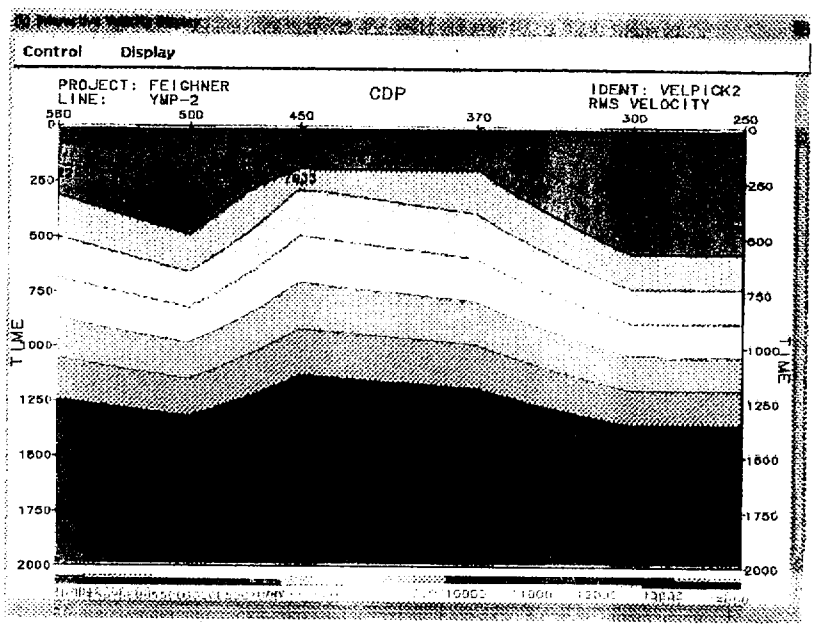

YMP - 4 Stacking Velocities

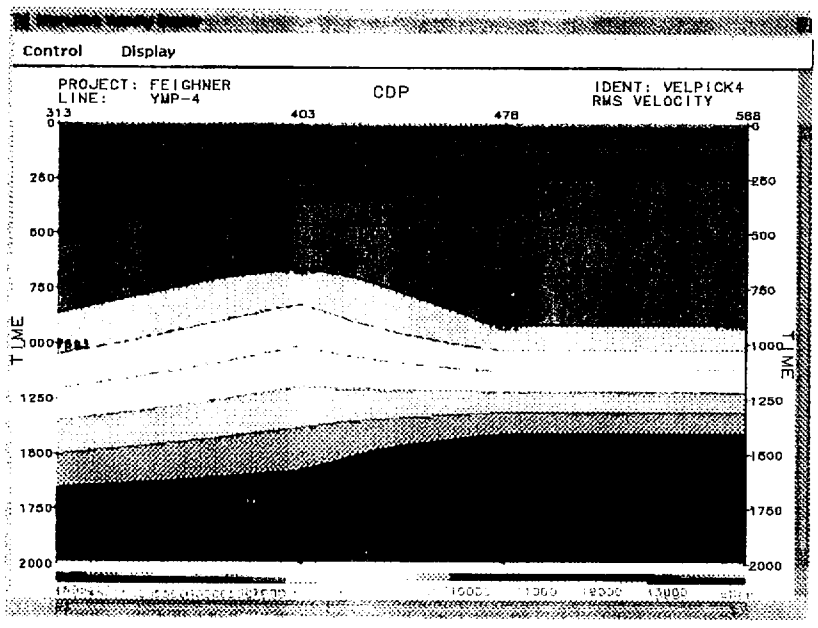

YMP - 5 Stacking Velocities

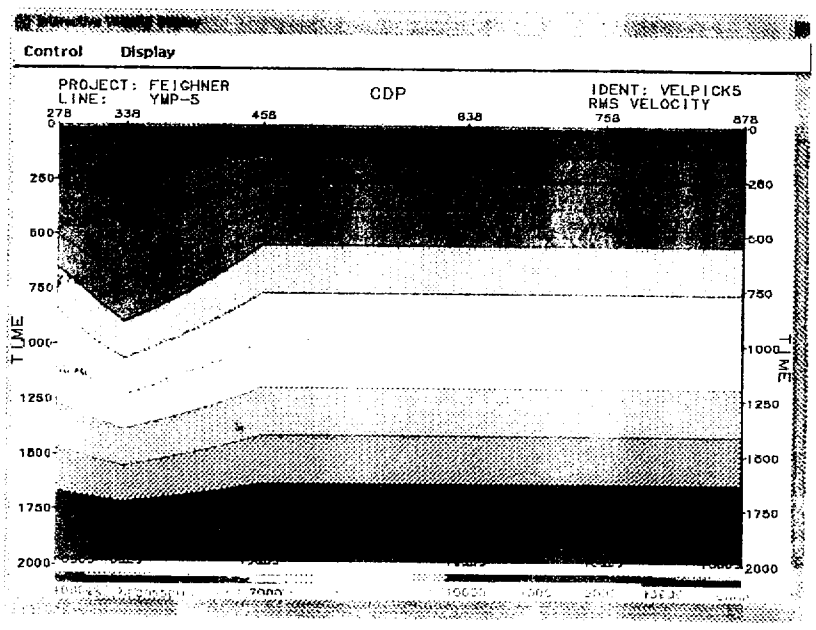

YMP - 6 Stacking Velocities

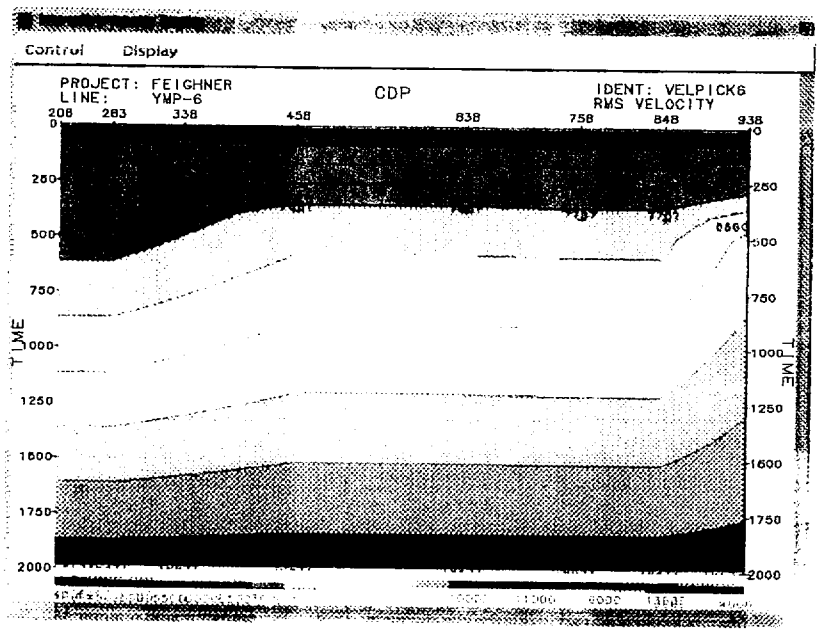

YMP - 7 Stacking Velocities

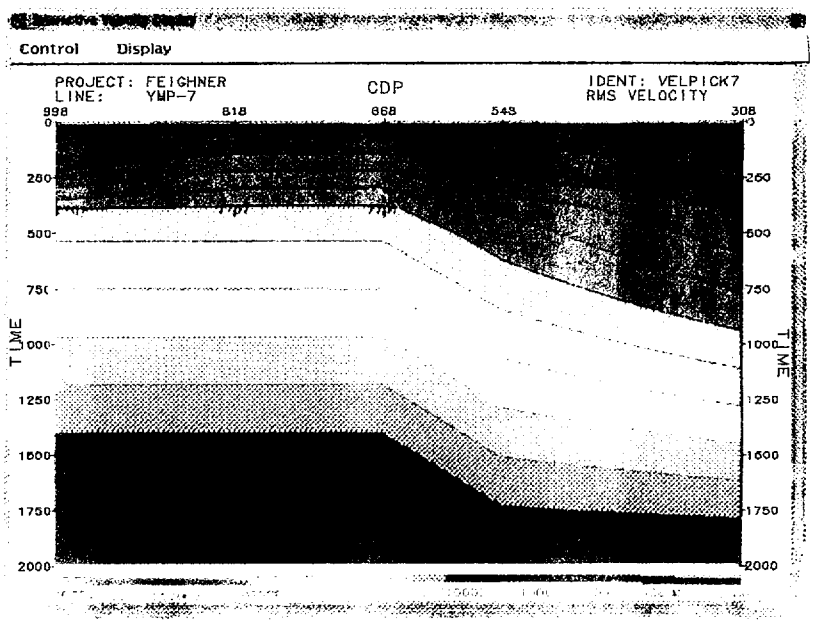

YMP - 7a Stacking Velocities

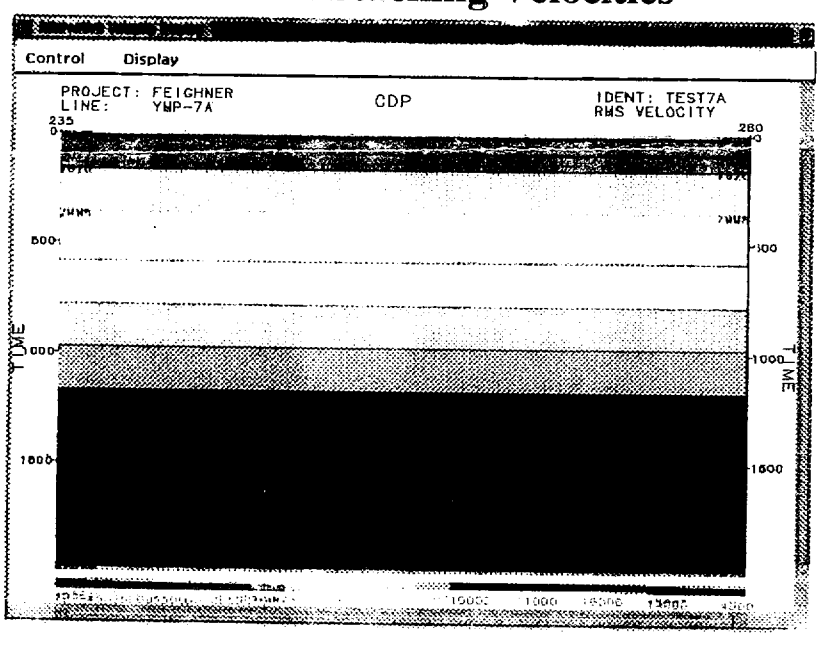

YMP - 8 Stacking Velocities

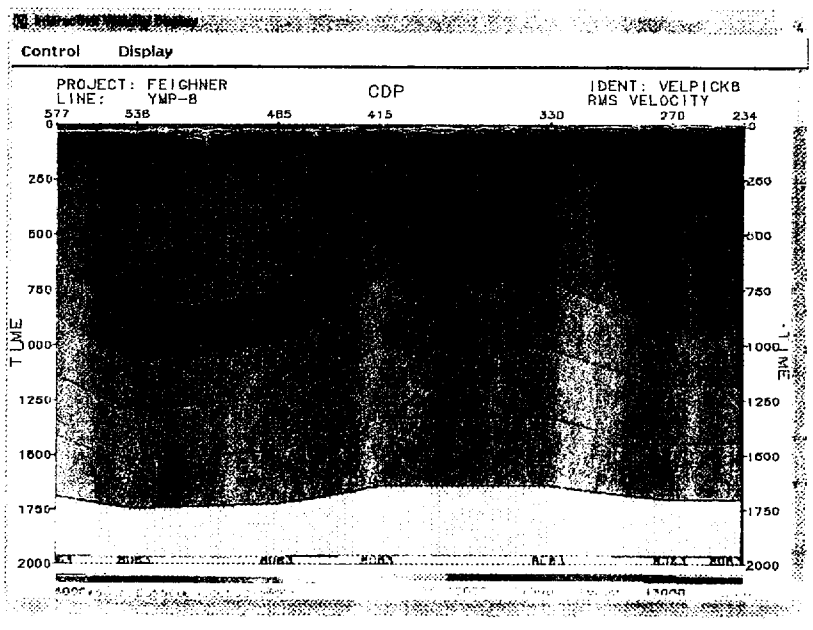

Figure 5. Stacking velocities and migration functions used in data processing.

YMP - 9 Stacking Velocities

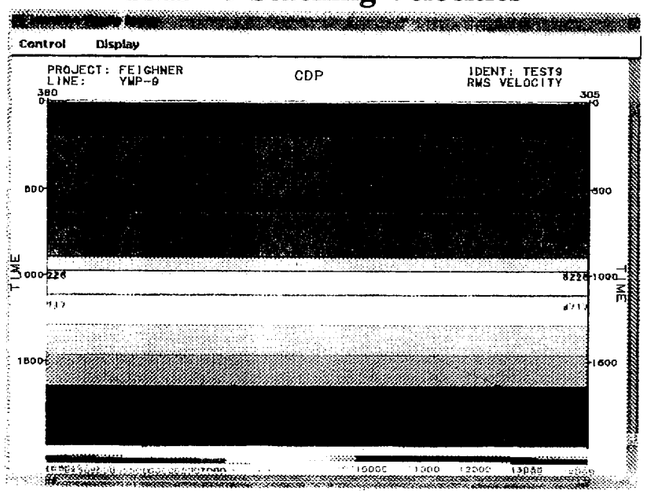

YMP - 12 Stacking Velocities

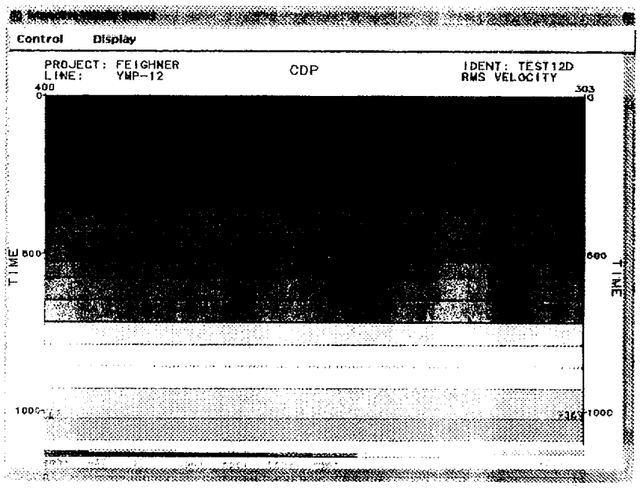

Migration Velocity Function (Example YMP-1)
Function hung from the Surface
Function used on all the lines, except YMP-12

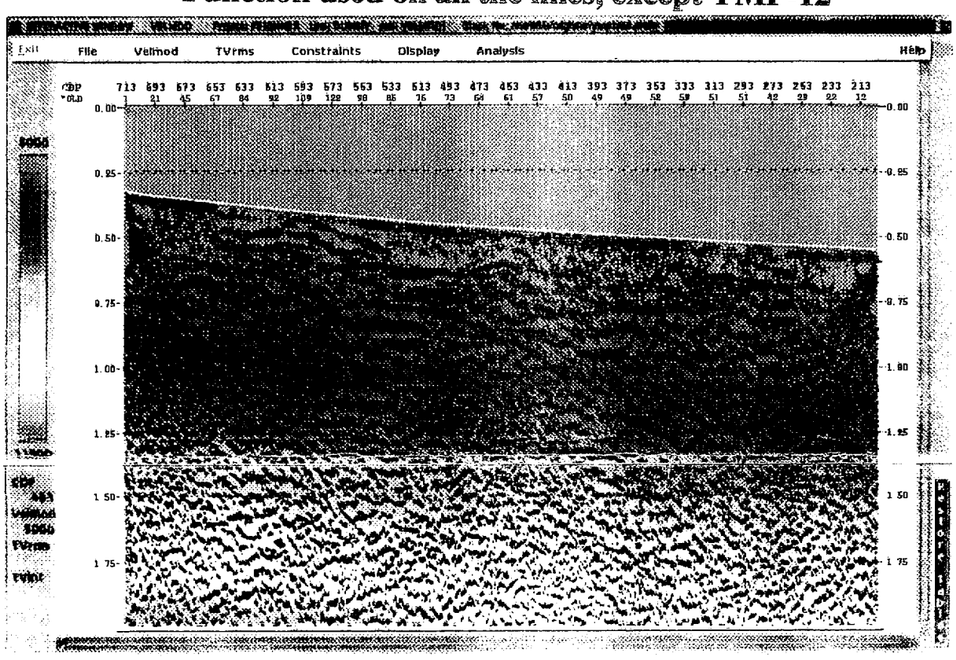

YMP-12 Migration Velocity Function

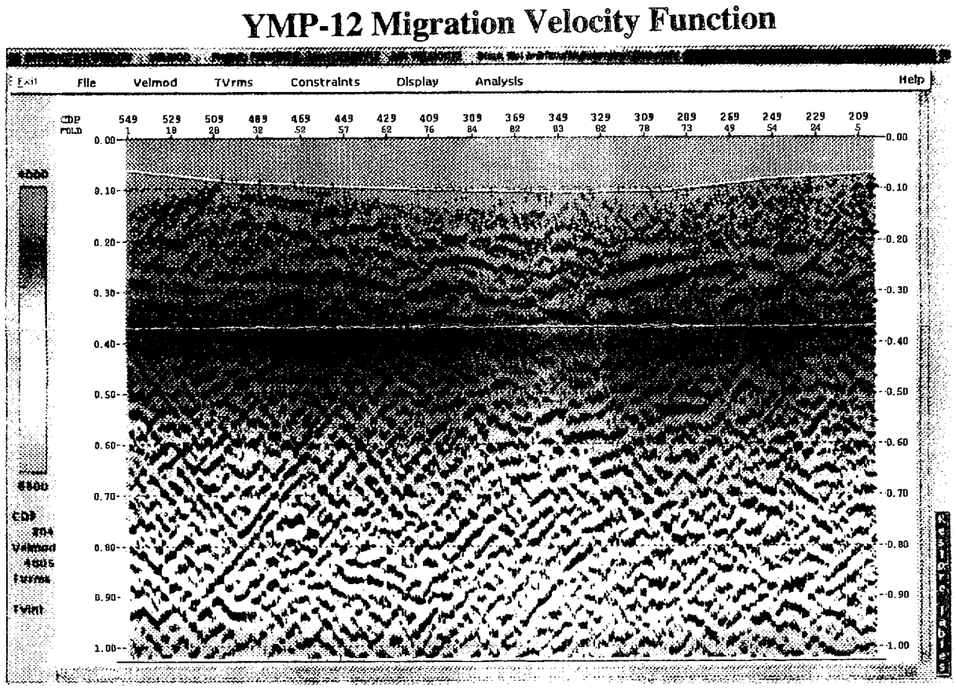

Figure 5 (continued).

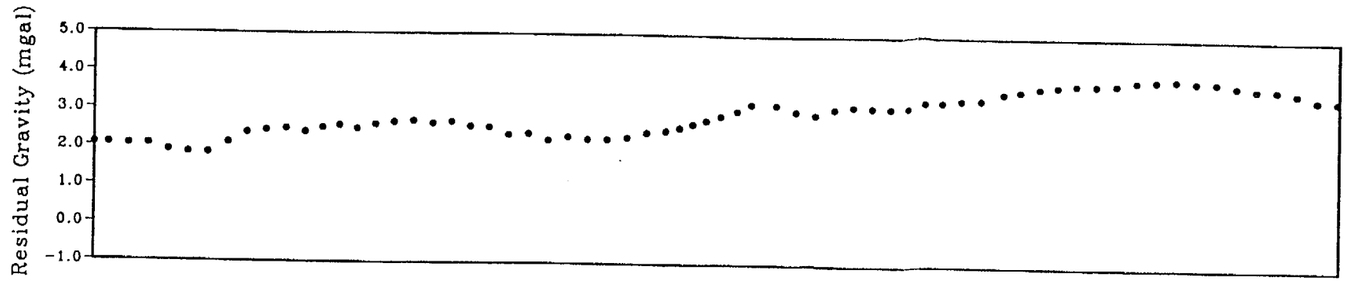

YMP-1 STACK

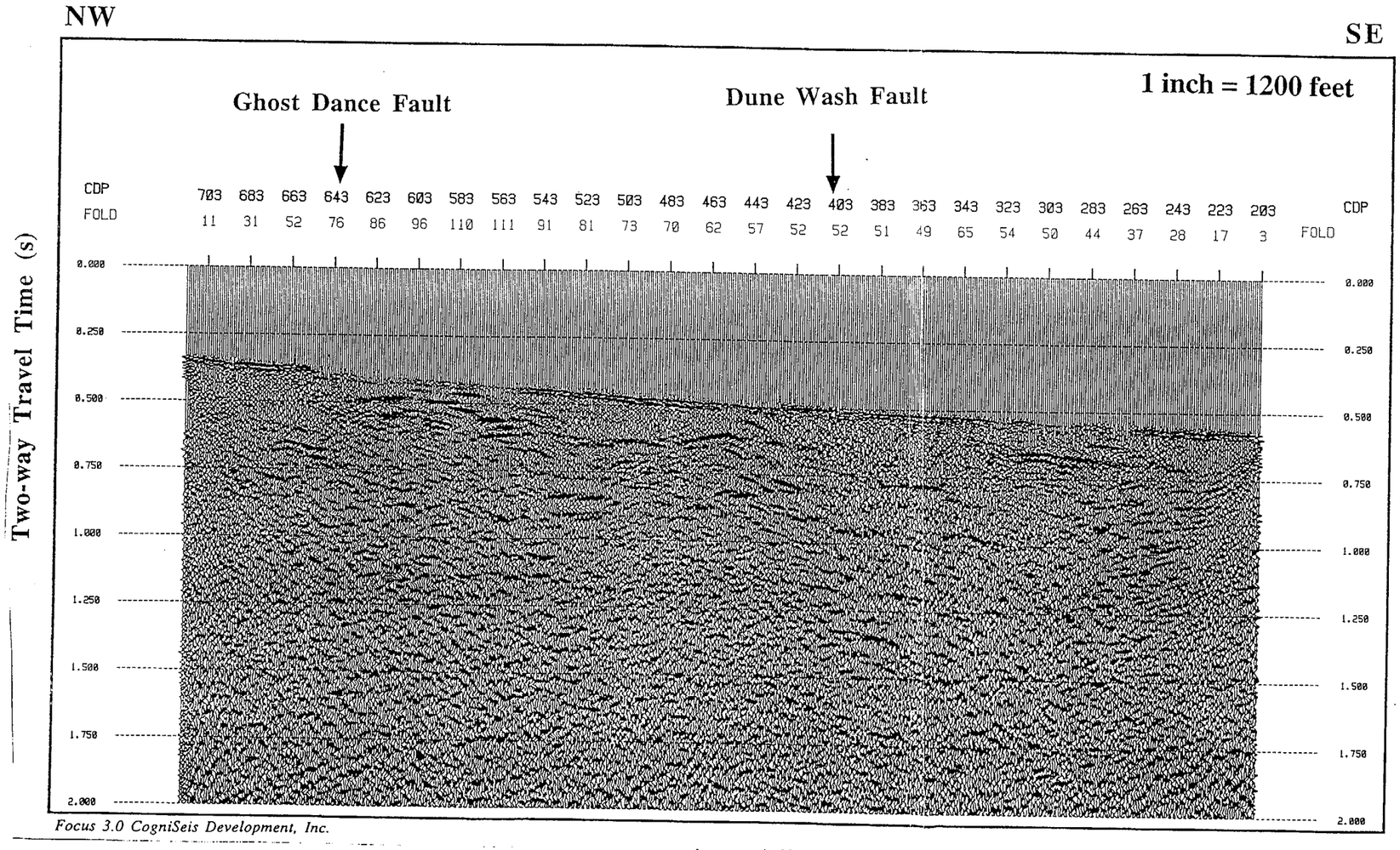

Figure 7a. YMP-1 stacked time section with residual gravity.

YMP-1 MIGRATED DEPTH

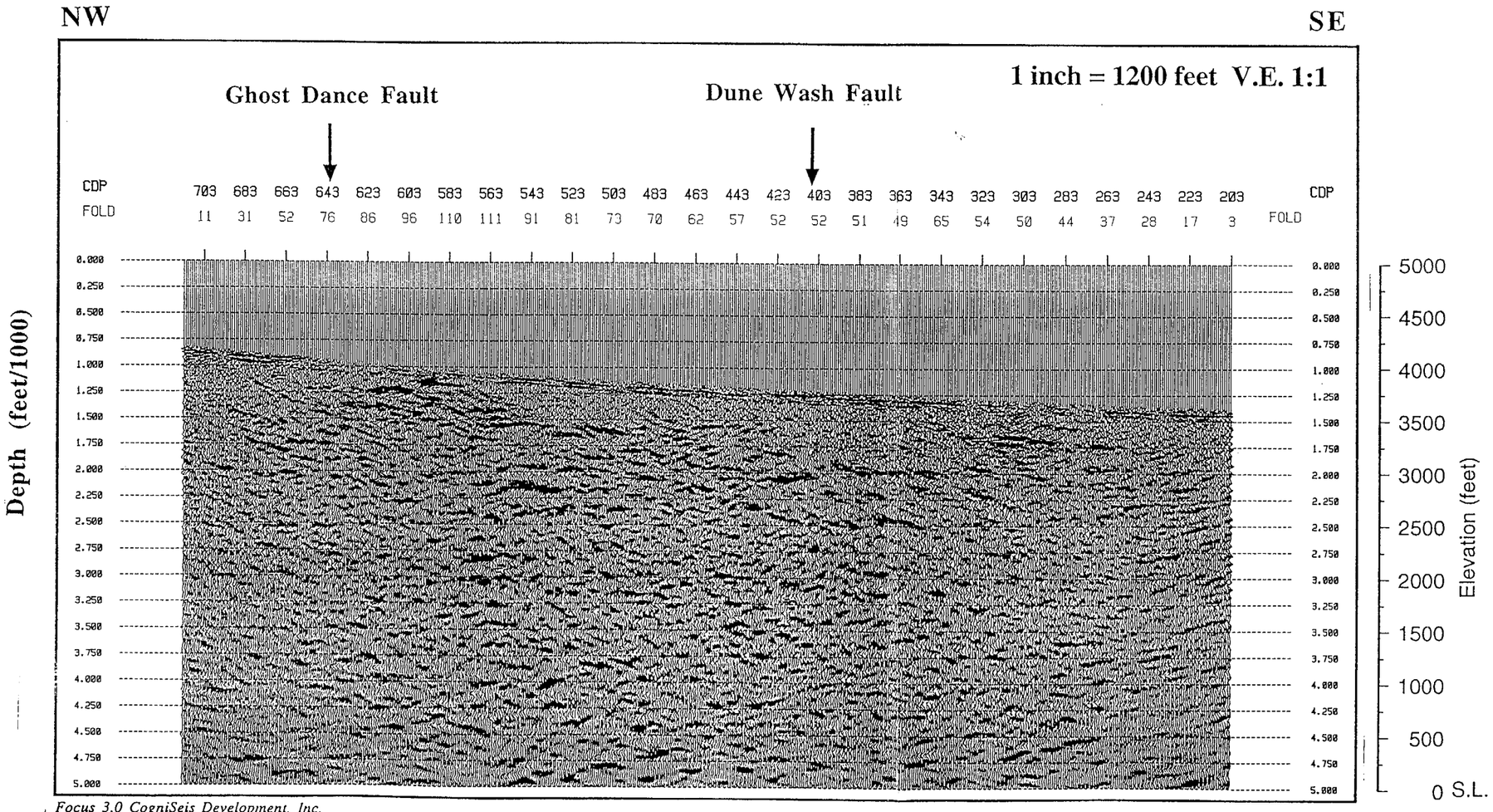

Figure 7b. YMP-1 migrated depth section.

Figure 7b

Special Processing Comparison (Example YMP - 1)

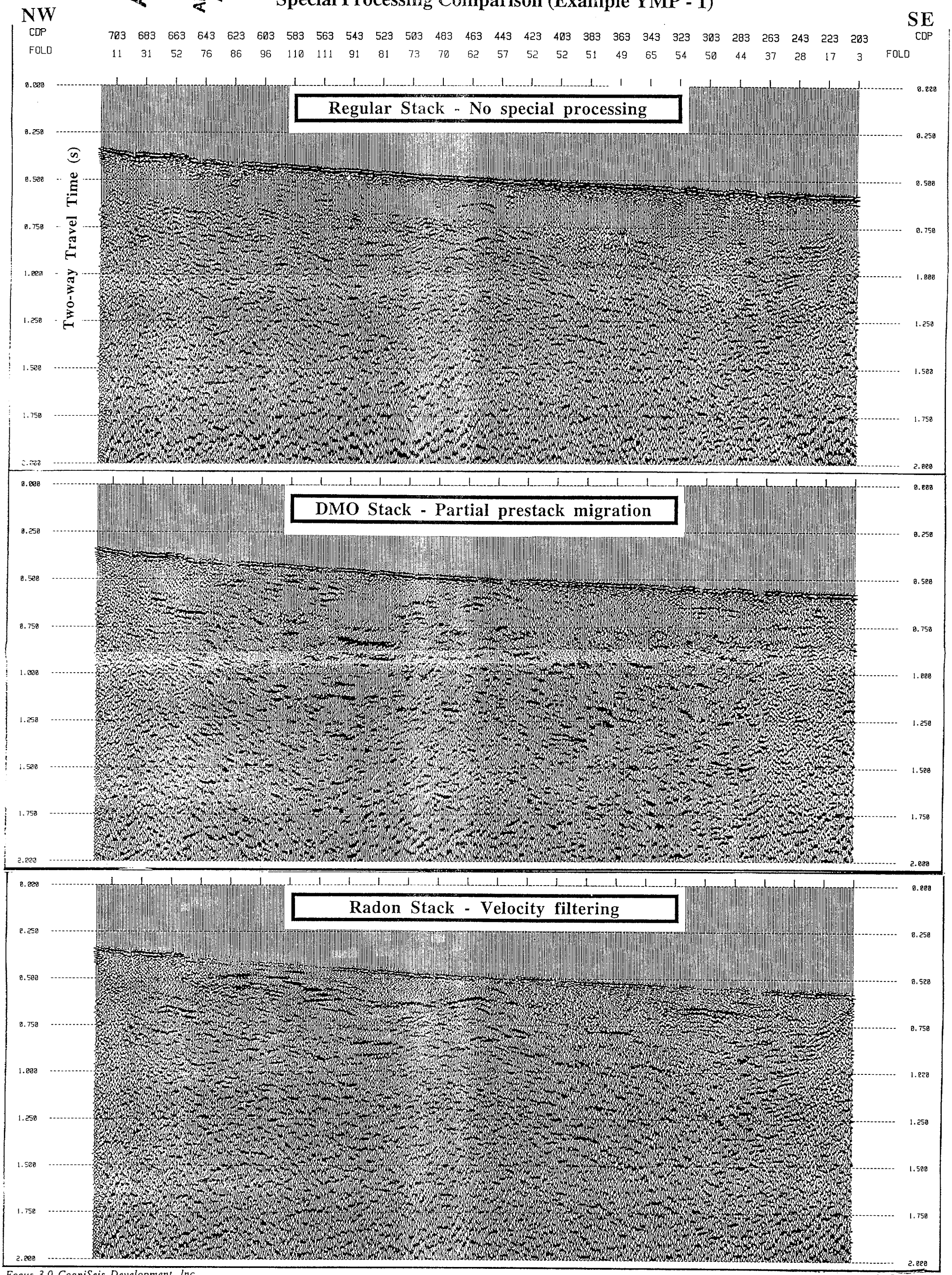

Focus 3.0 CogniSeis Development, Inc.

1 inch = 1200 feet

Figure 6. Special processing comparison of YMP-1. Top figure is a regular stack with no special processing applied. Middle figure is a Dip Moveout (DMO) stack and the bottom is a Radon velocity filter stack. The Radon stack consistently produced the best section and was used as a standard part of the processing flow for all the lines.

YMP-1 LYNX GEOLOGIC MODEL

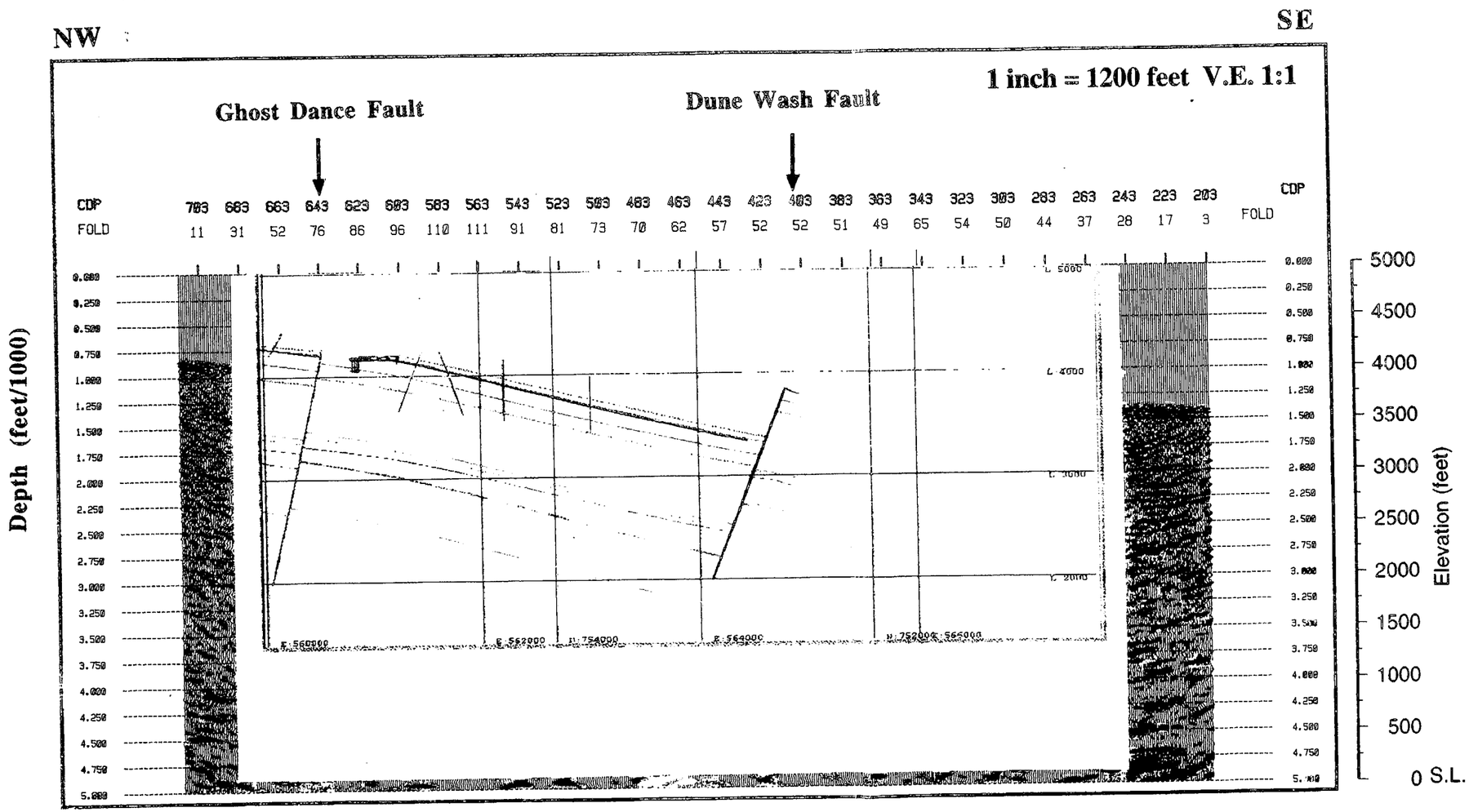

Figure 7c. YMP-1 Lynx geologic model.

YMP-1 MIGRATED DEPTH

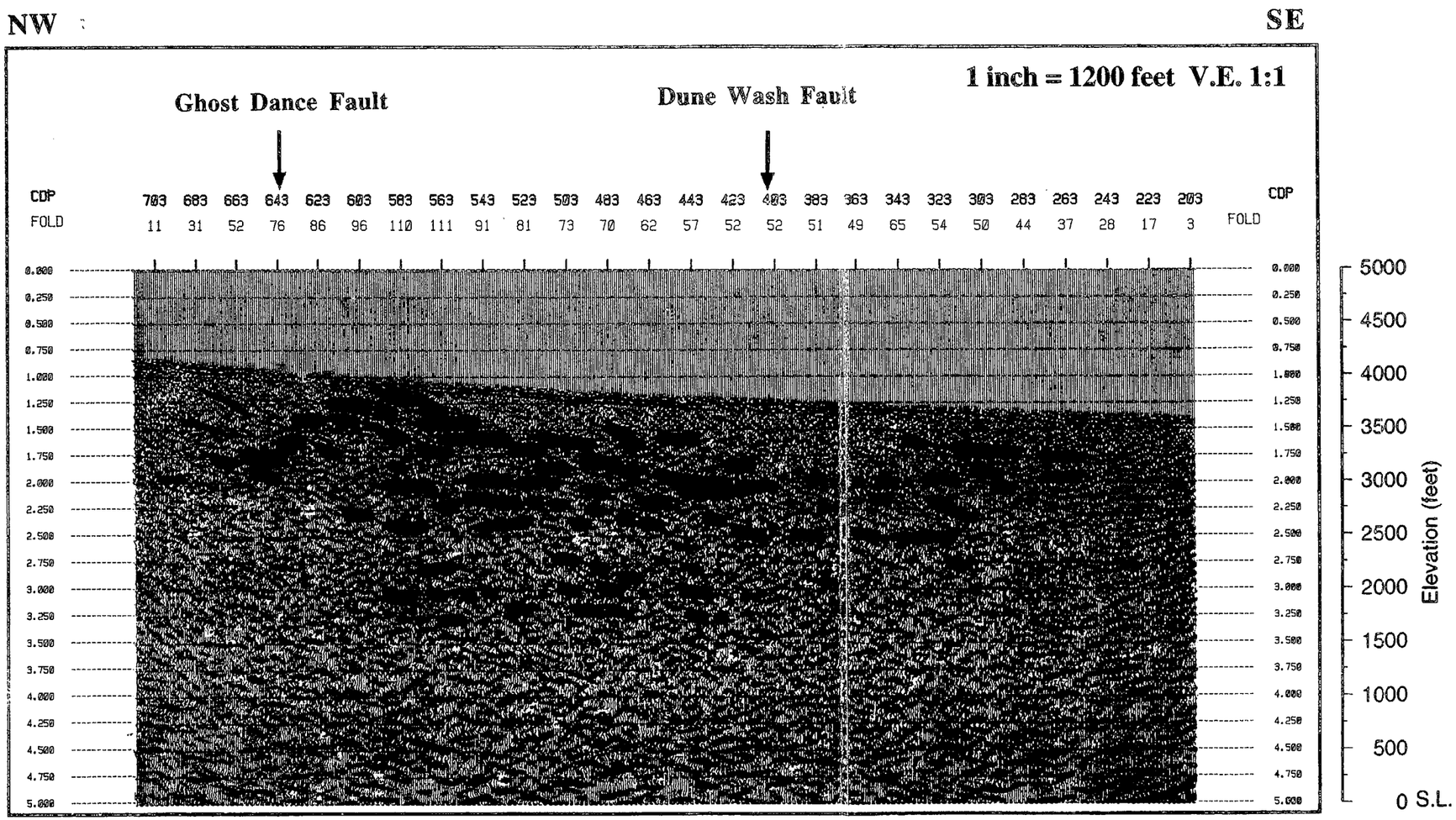

Focus 3.0 CogniSeis Development, Inc.

Figure 7d. YMP-1 highlighted reflectors in red.

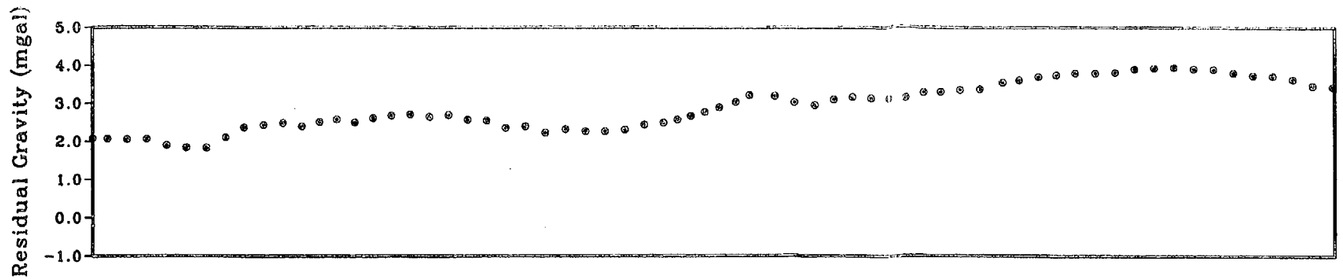

YMP-1 MIGRATED DEPTH

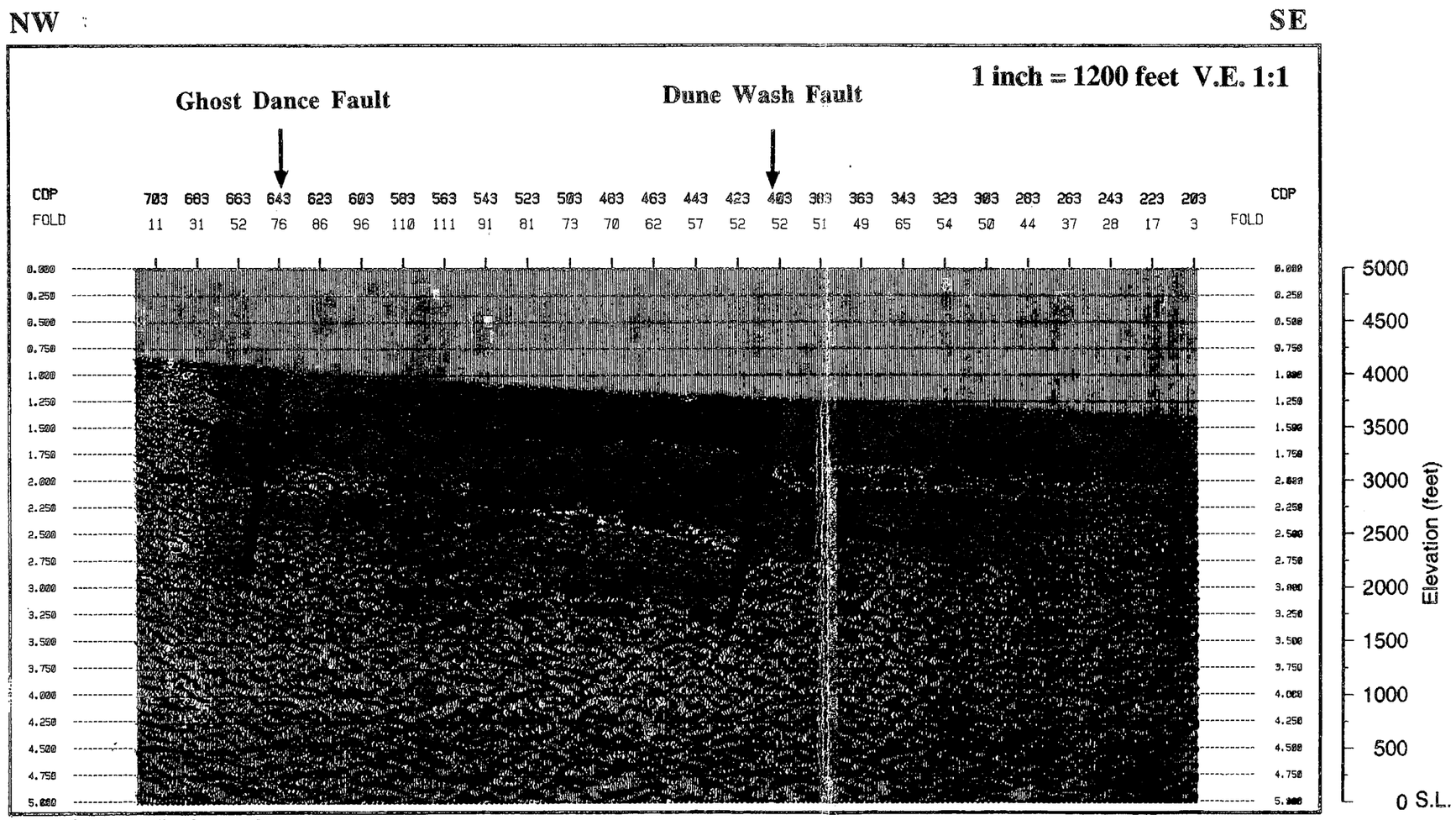

Focus 3.0 CogniSeis Development, Inc.

Figure 7e. YMP-1 interpreted section.

Figure 7e

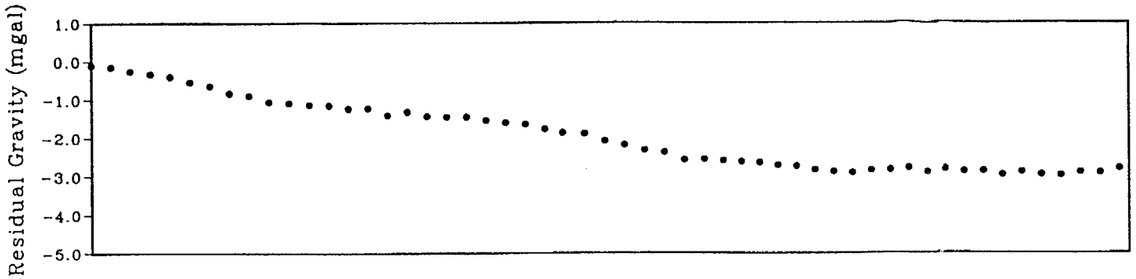

YMP-2 STACK

SOUTH **NORTH**

1 inch = 1200 feet

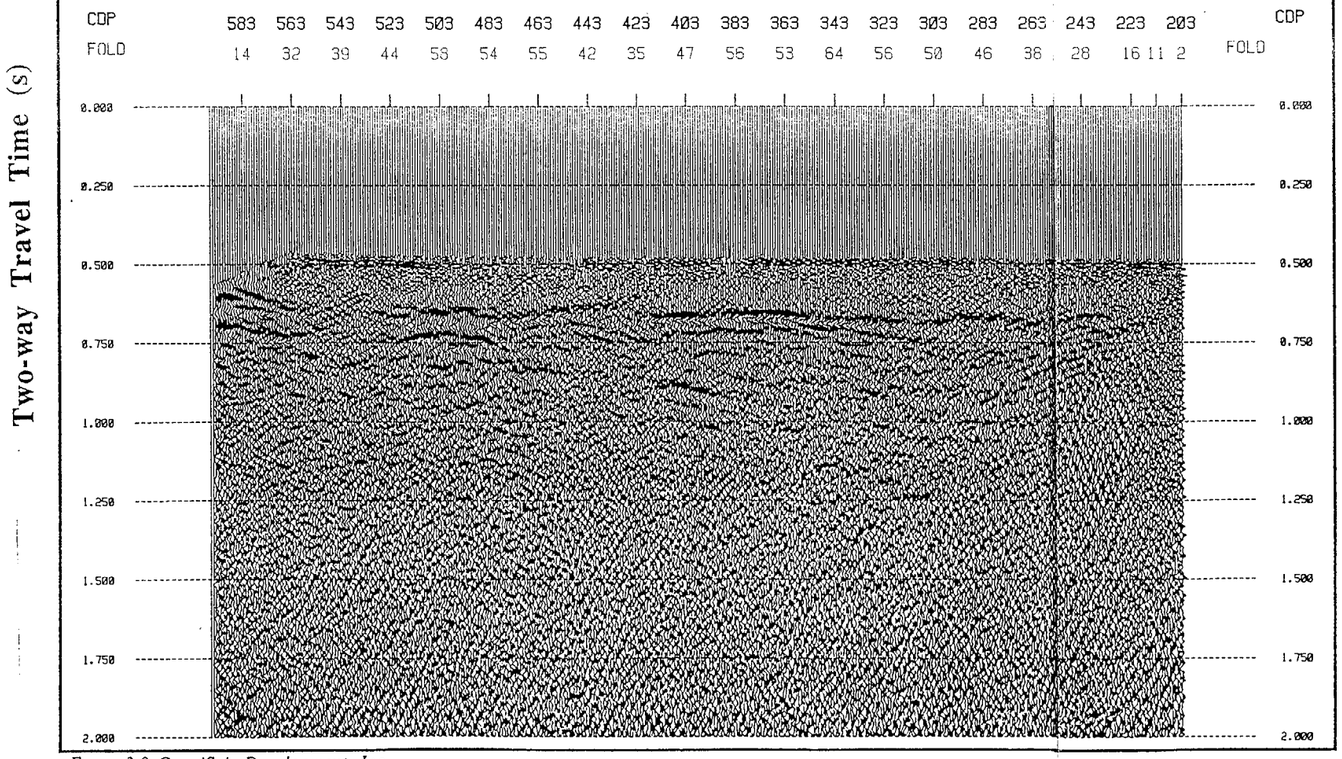

Focus 3.0 CogniSeis Development, Inc.

Figure 8a. YMP-2 stacked time section with residual gravity.

Figure 8a

YMP-2 MIGRATED DEPTH

SOUTH **NORTH**

1 inch = 1200 feet V.E. 1:1

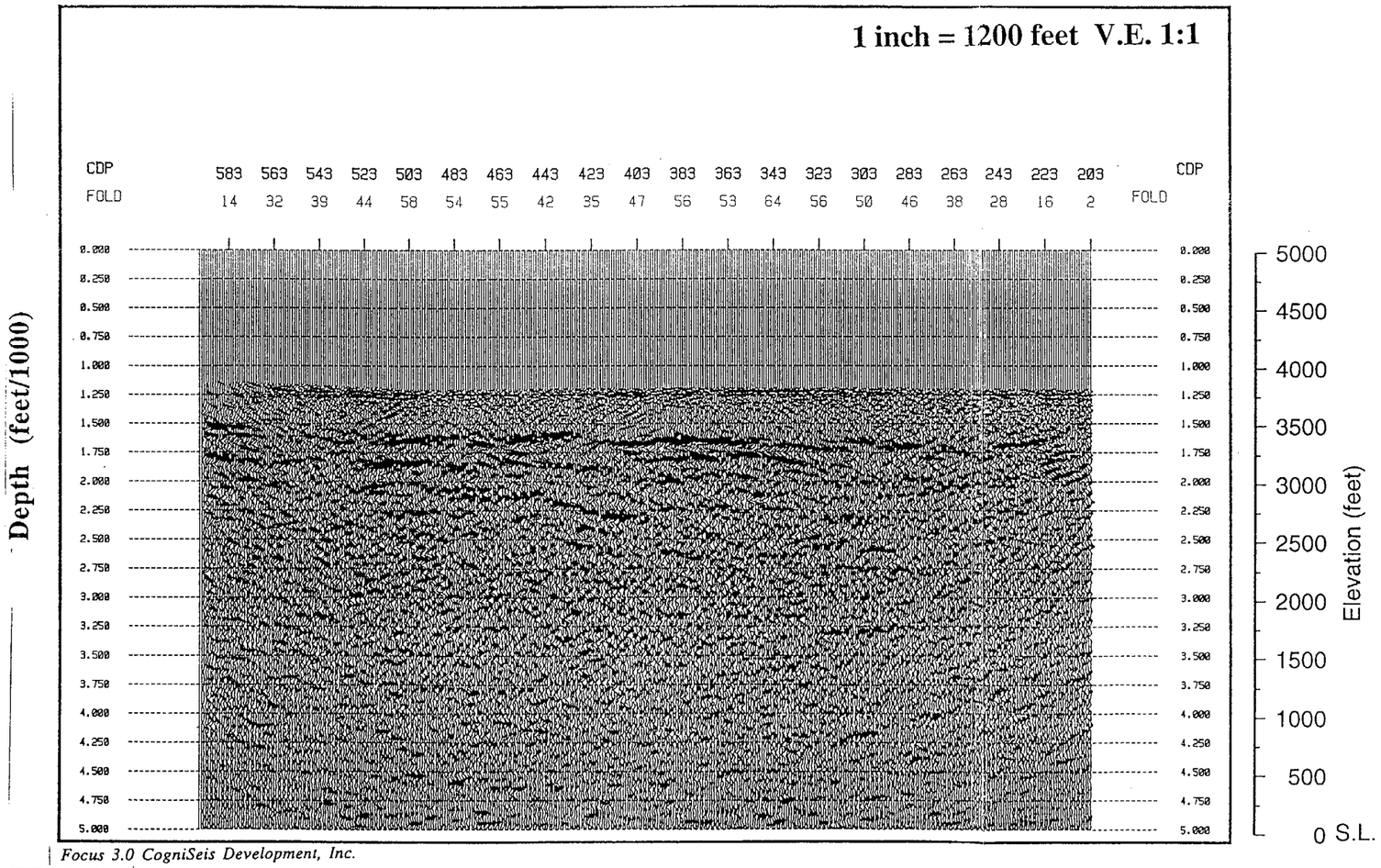

Figure 8b. YMP-2 migrated depth section.

YMP-2 LYNX GEOLOGIC MODEL

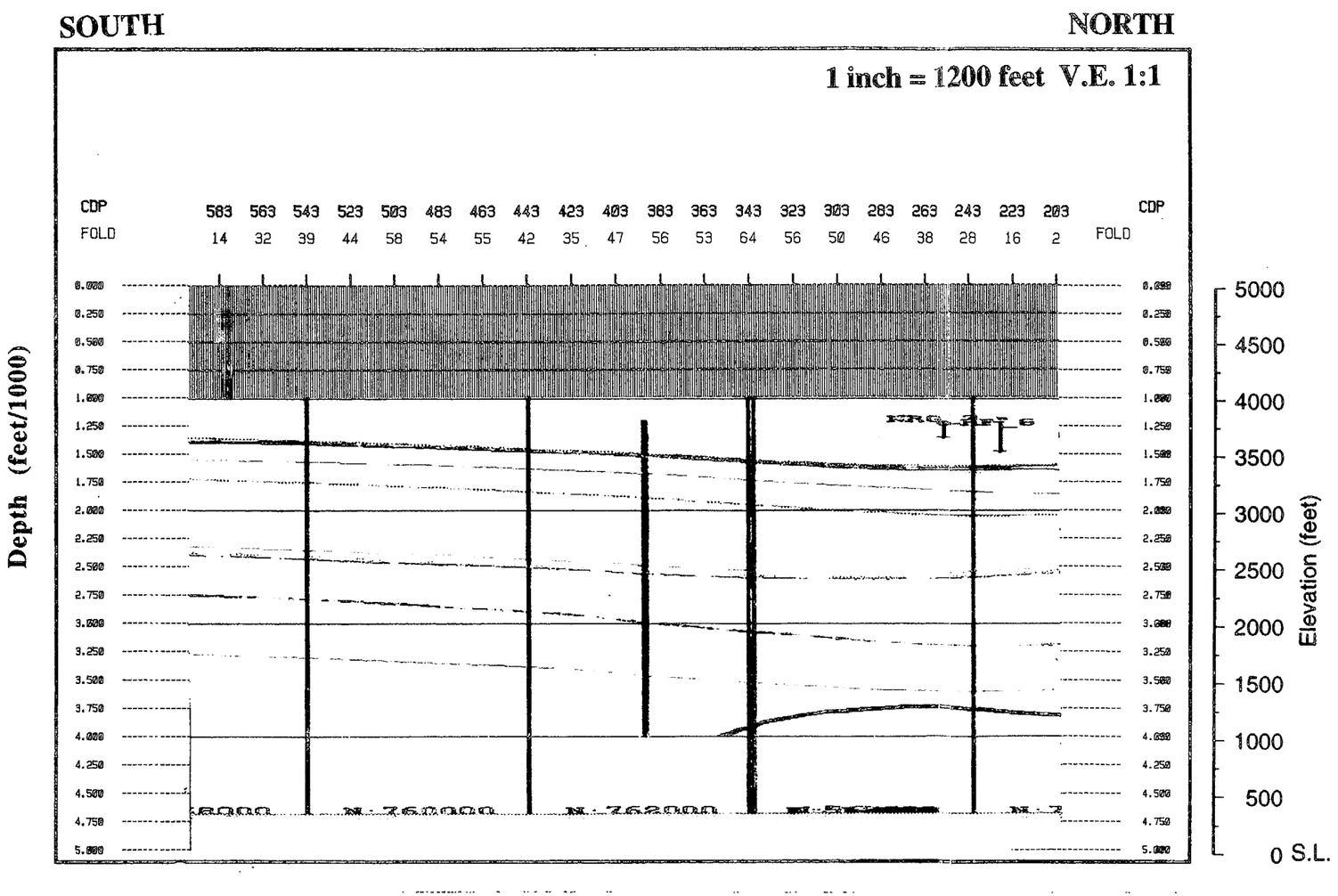

Figure 8c. YMP-2 Lynx geologic model.

Figure 8c

 -33

YMP-2 MIGRATED DEPTH

SOUTH **NORTH**

1 inch = 1200 feet V.E. 1:1

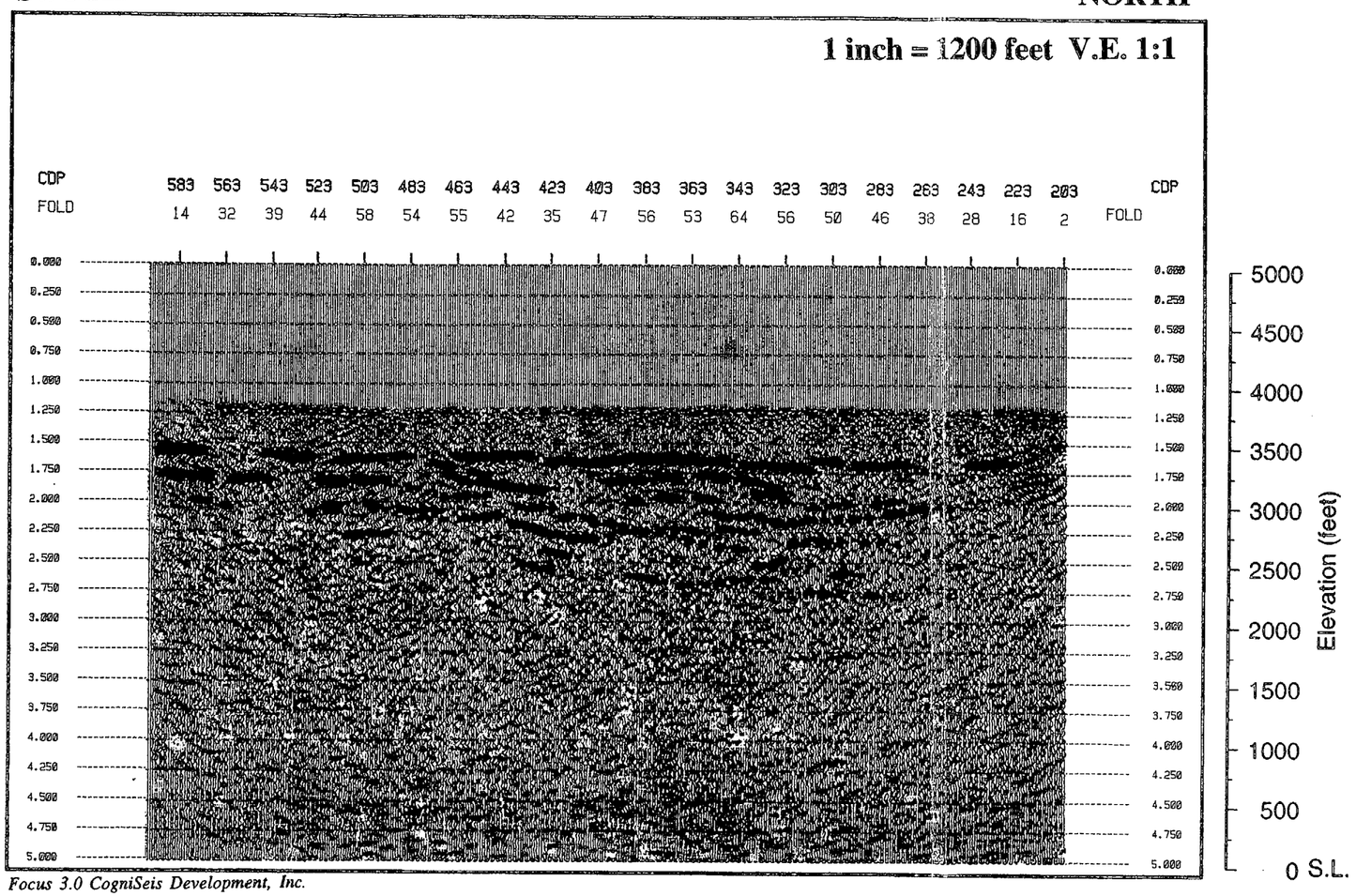

Focus 3.0 CogniSeis Development, Inc.

Figure 8d. YMP-2 highlighted reflectors in red.

Figure 8d

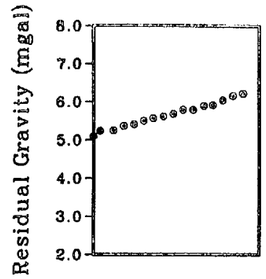

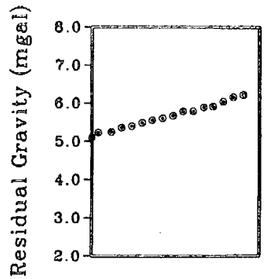

YMP-7A STACK

MIGRATED

MIGRATED

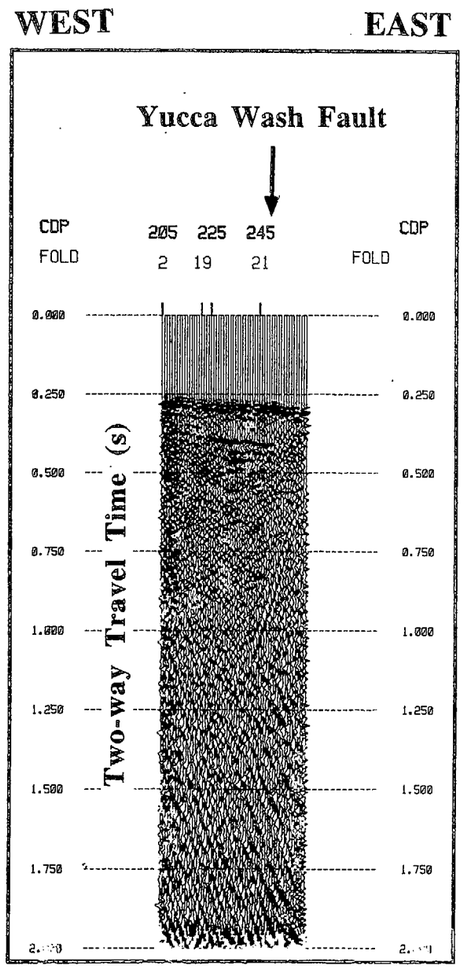

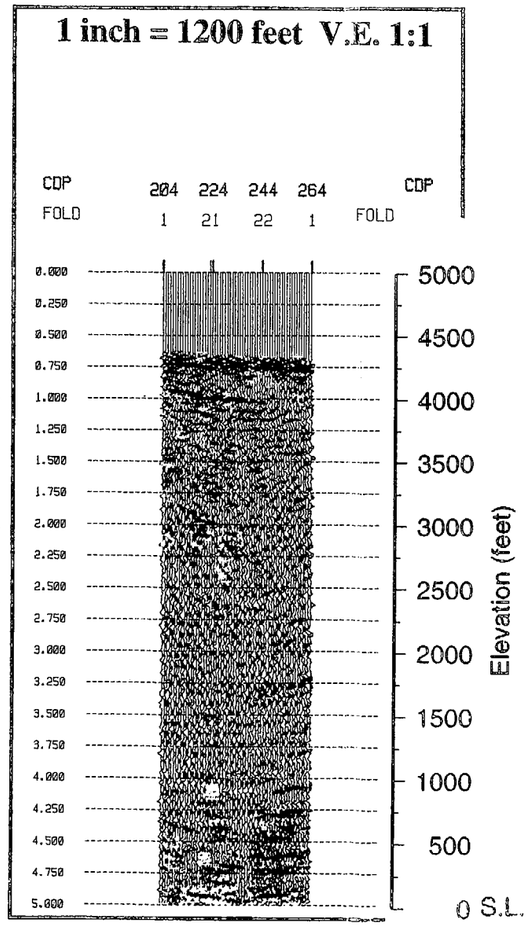

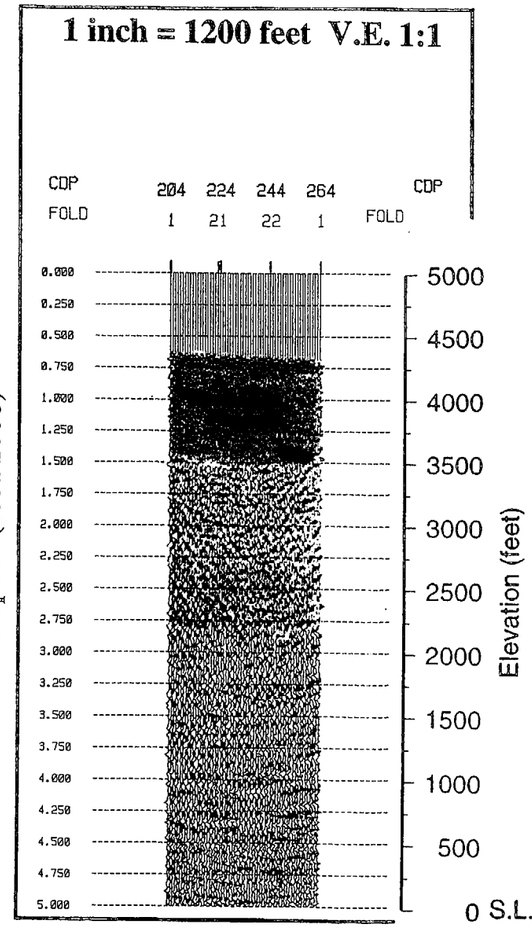

Focus 3.0 CogniSeis Development, Inc.

Figure 13. YMP-7a stacked time section with residual gravity, migrated depth section, and interpreted section with highlighted reflectors in red.

YMP-7 MIGRATED DEPTH

NW **SE**

1 inch = 1200 feet V.E. 1:1

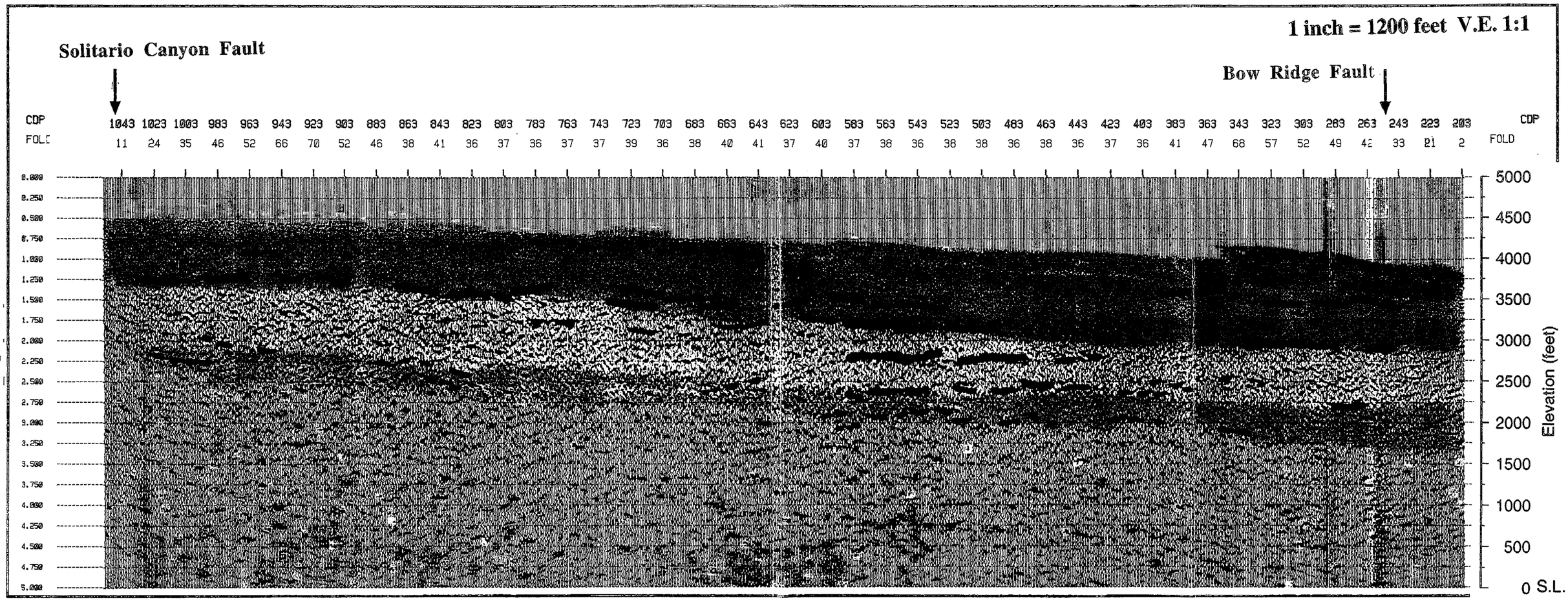

Focus 3.0 CogniSeis Development, Inc.

Figure 12e. YMP-7 interpreted section.

Figure 12e

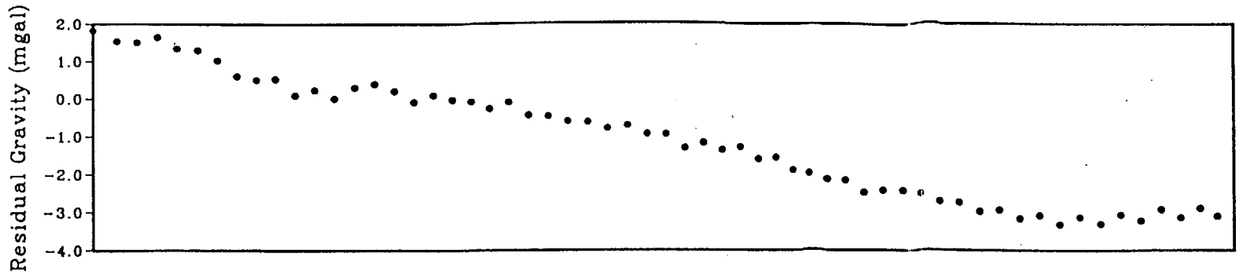

YMP-8 STACK

NW **SE**

1 inch = 1200 feet

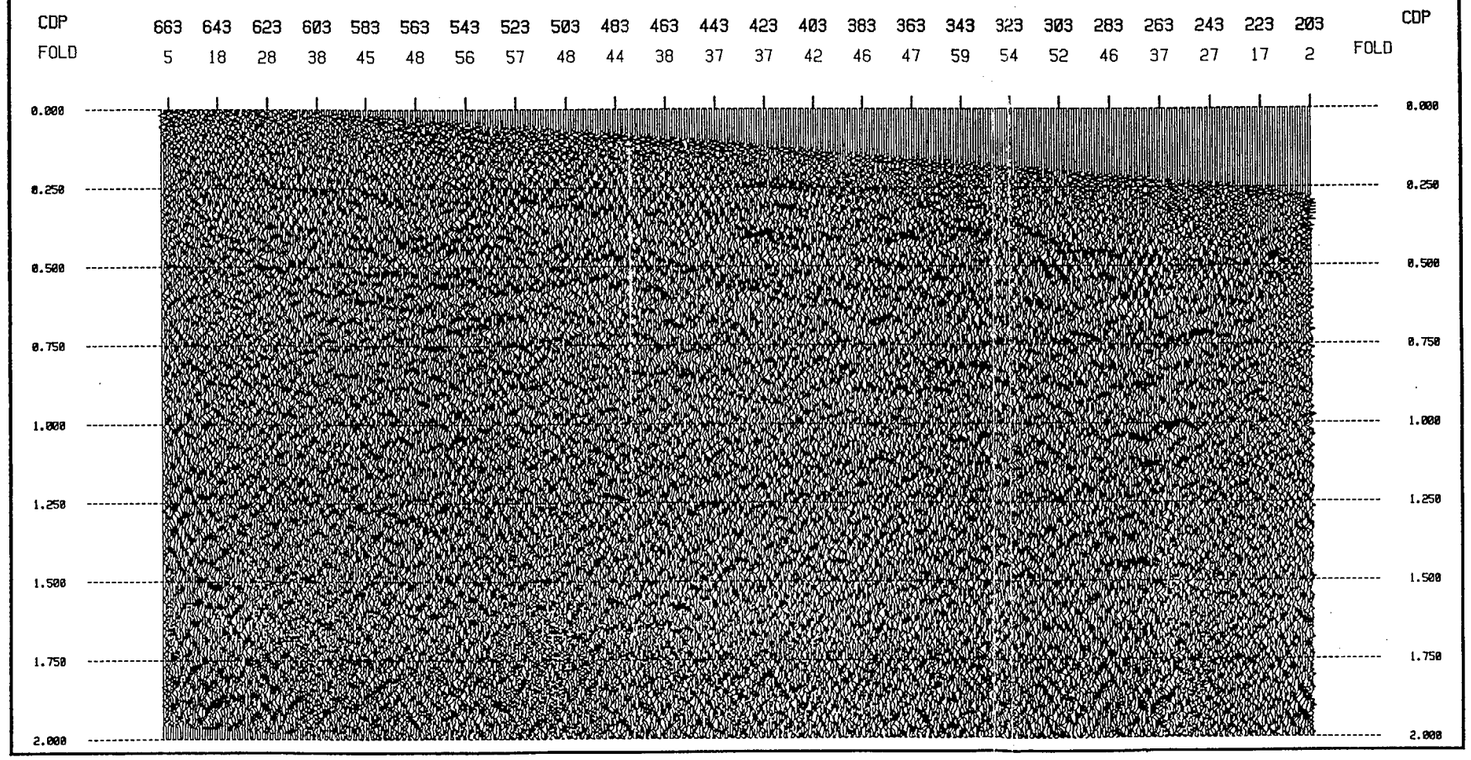

Focus 3.0 CogniSeis Development, Inc.

Figure 14a. YMP-8 stacked time section with residual gravity.

Figure 14a

YMP-8 MIGRATED DEPTH

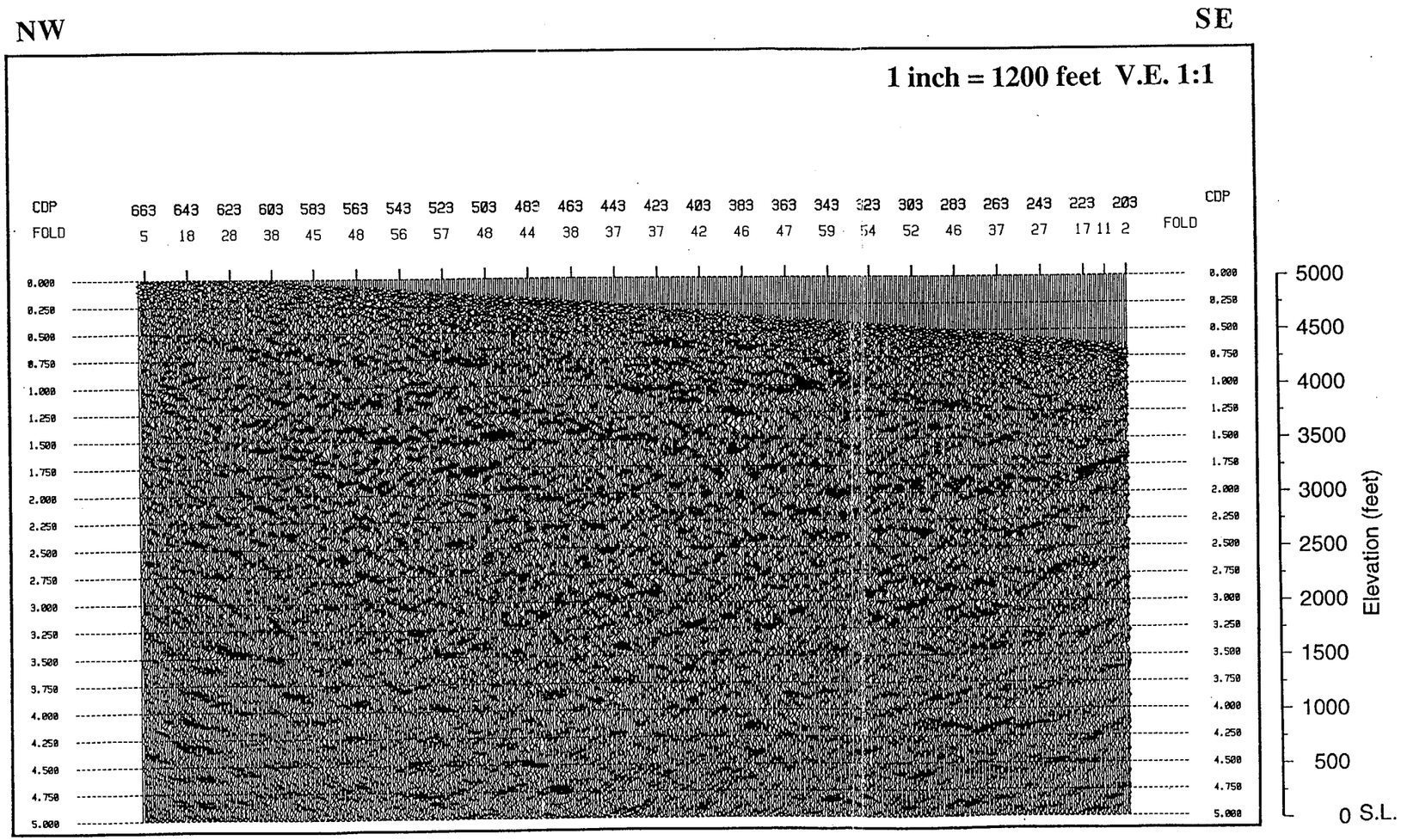

Figure 14b. YMP-8 migrated depth section.

YMP-8 LYNX GEOLOGIC MODEL

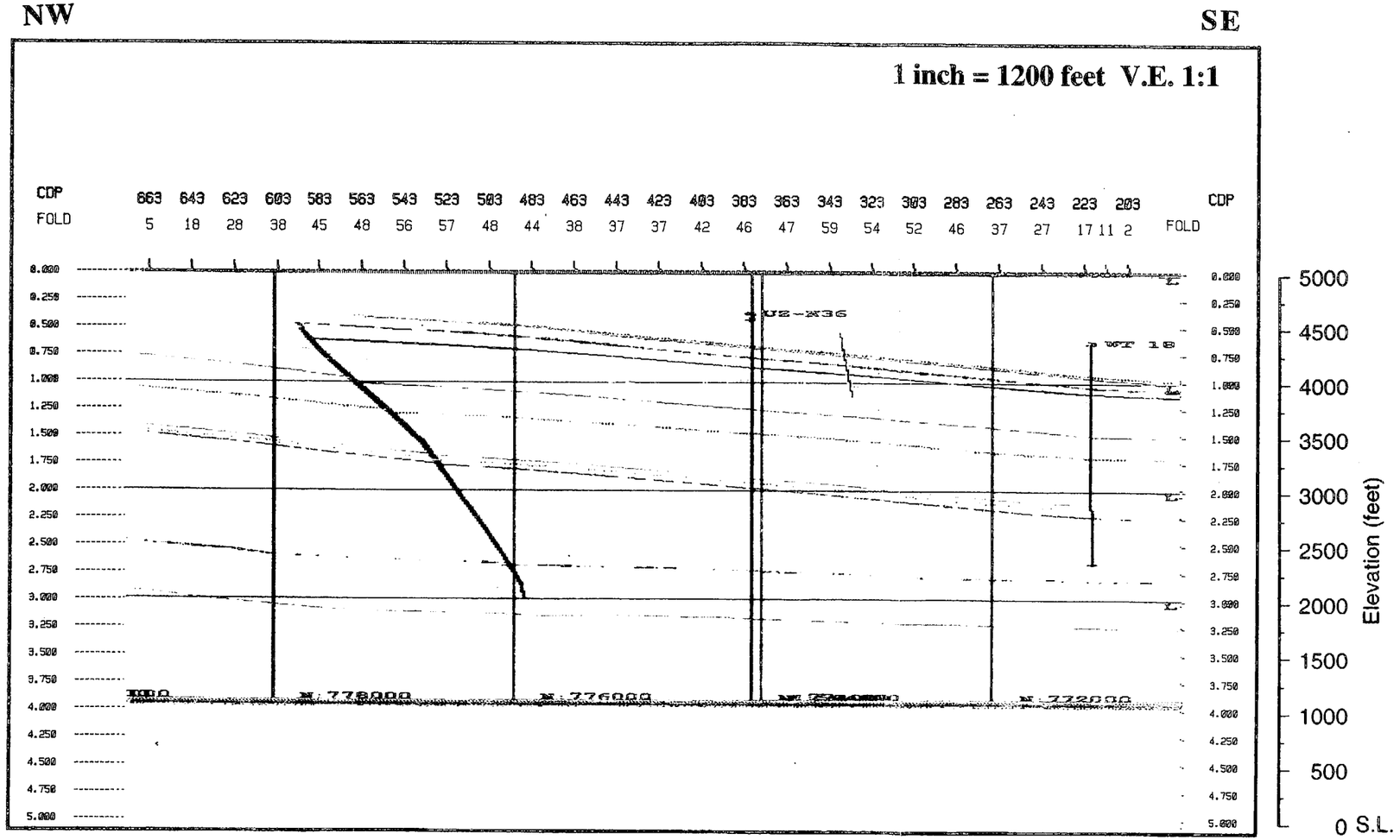

Figure 14c. YMP-8 Lynx geologic model.

Figure 14c

YMP-8 MIGRATED DEPTH

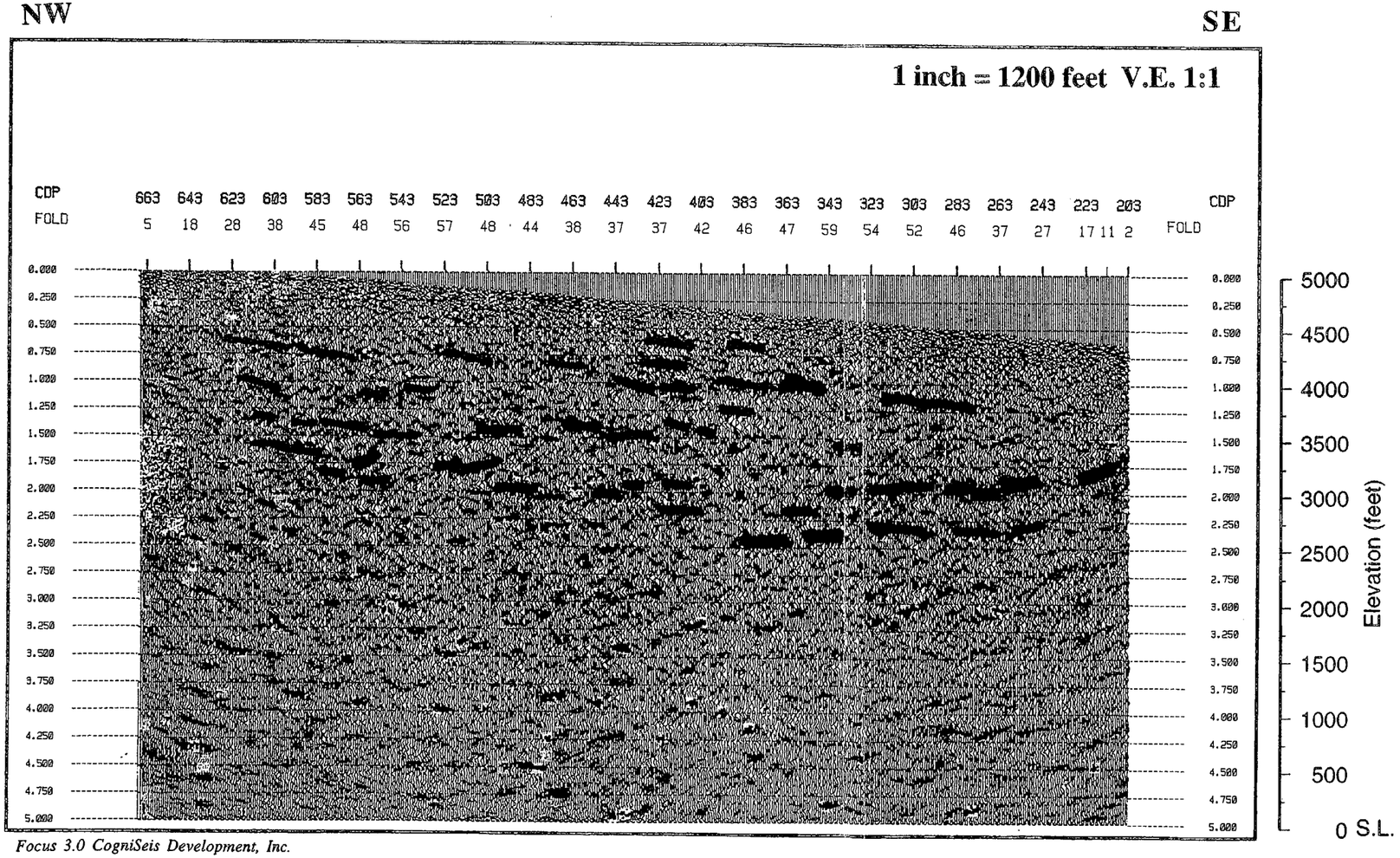

Focus 3.0 CogniSeis Development, Inc.

Figure 14d. YMP-8 highlighted reflectors in red.

Figure 14d

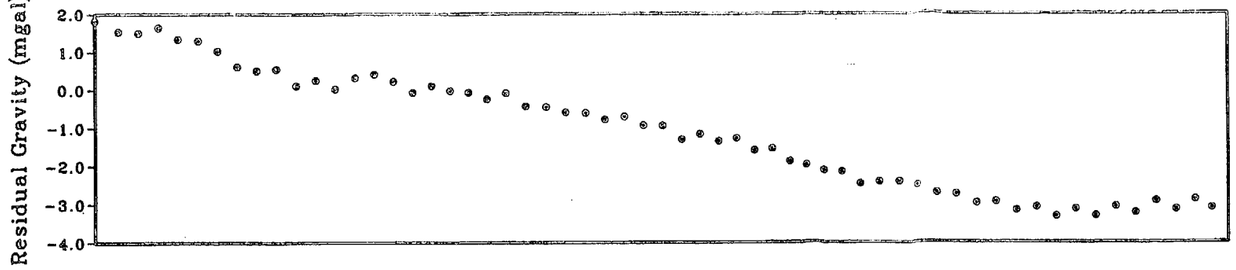

YMP-8 MIGRATED DEPTH

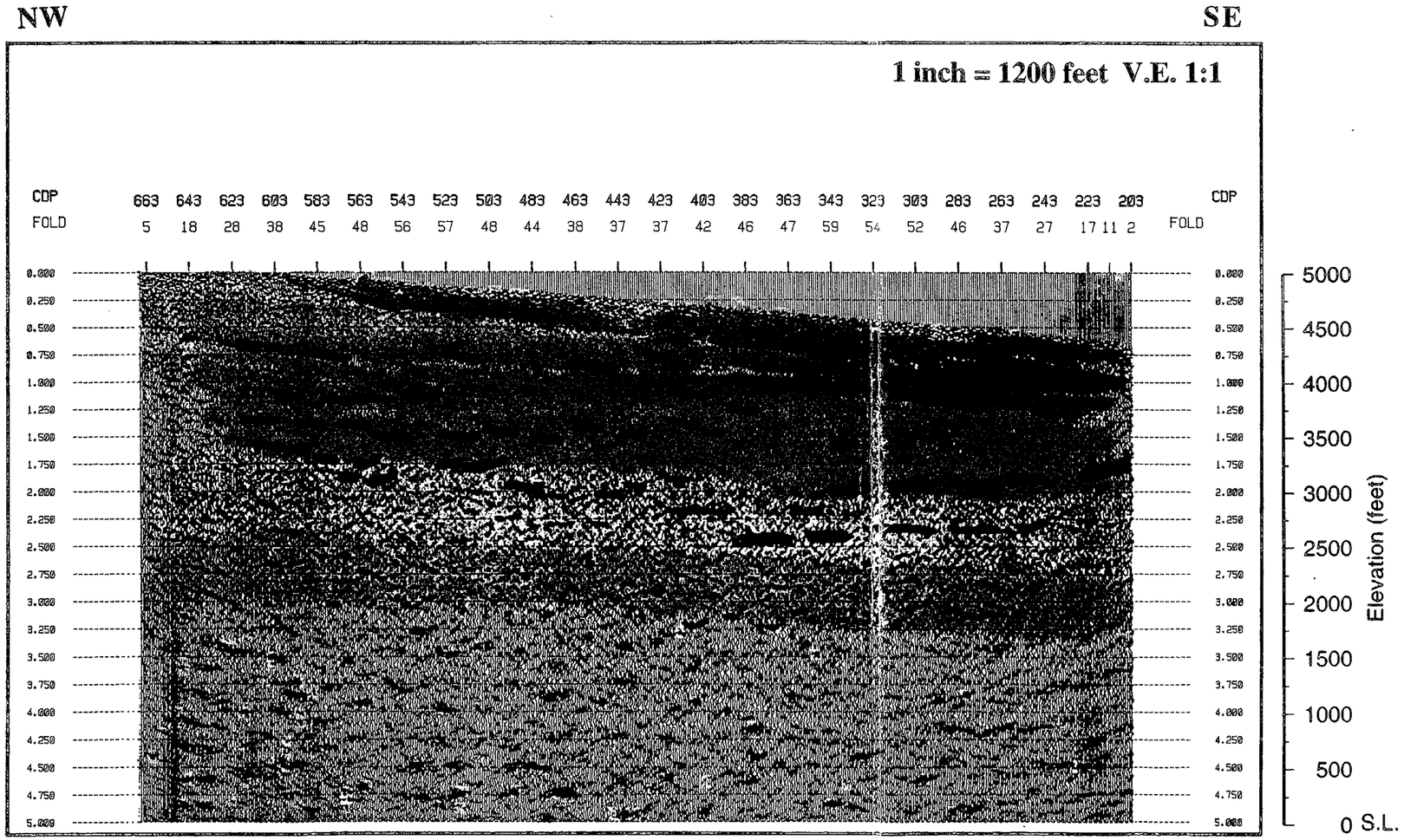

Focus 3.0 Cogniseis Development, Inc.

Figure 14e. YMP-8 interpreted section.

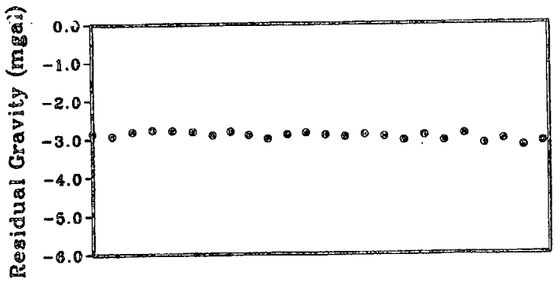

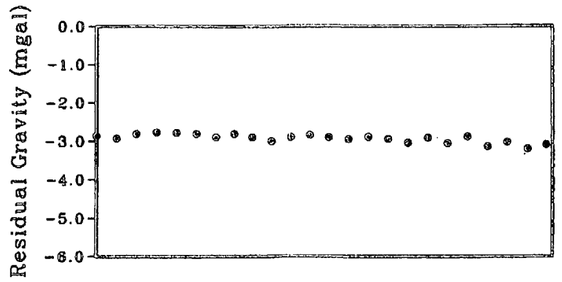

YMP-9 STACK

YMP-9 MIGRATED DEPTH

YMP-9 MIGRATED DEPTH

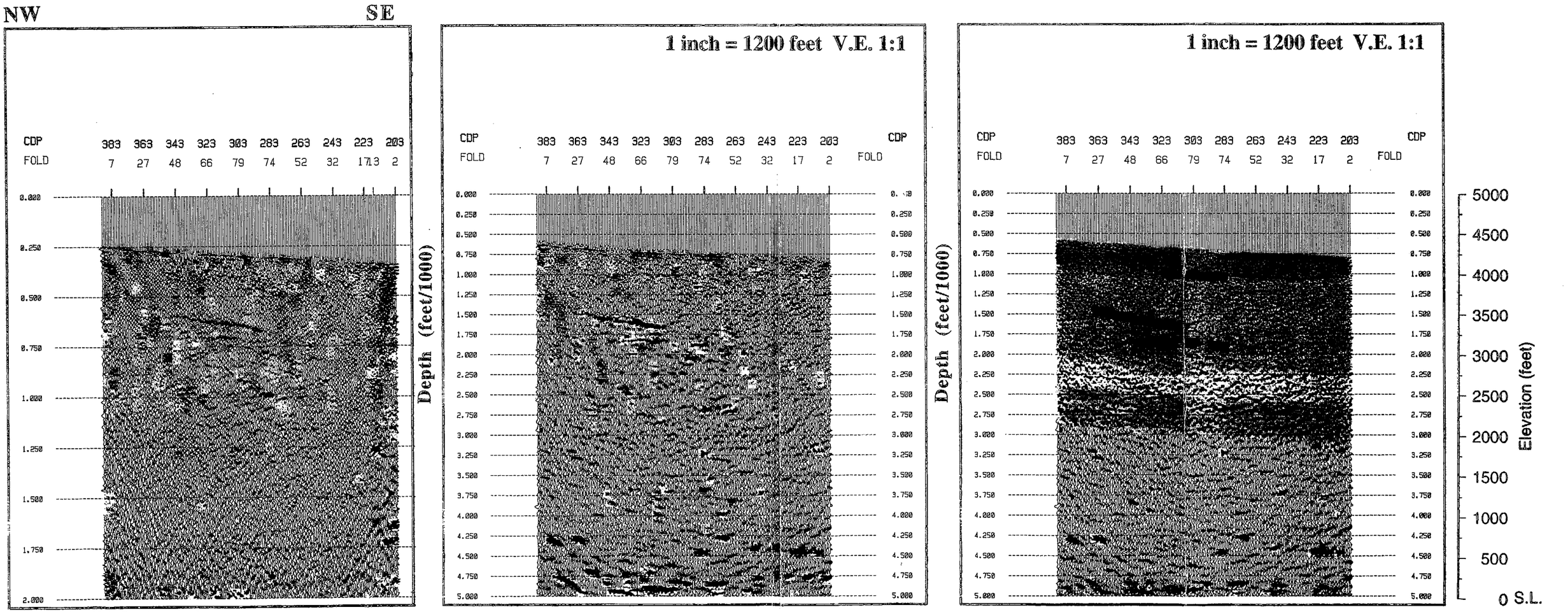

Focus 3.0 CogniSeis Development, Inc.

Figure 15. YMP-9 stacked time section with residual gravity, migrated depth section, and interpreted section with highlighted reflectors in red.

Figure 15

YMP-12 STACK

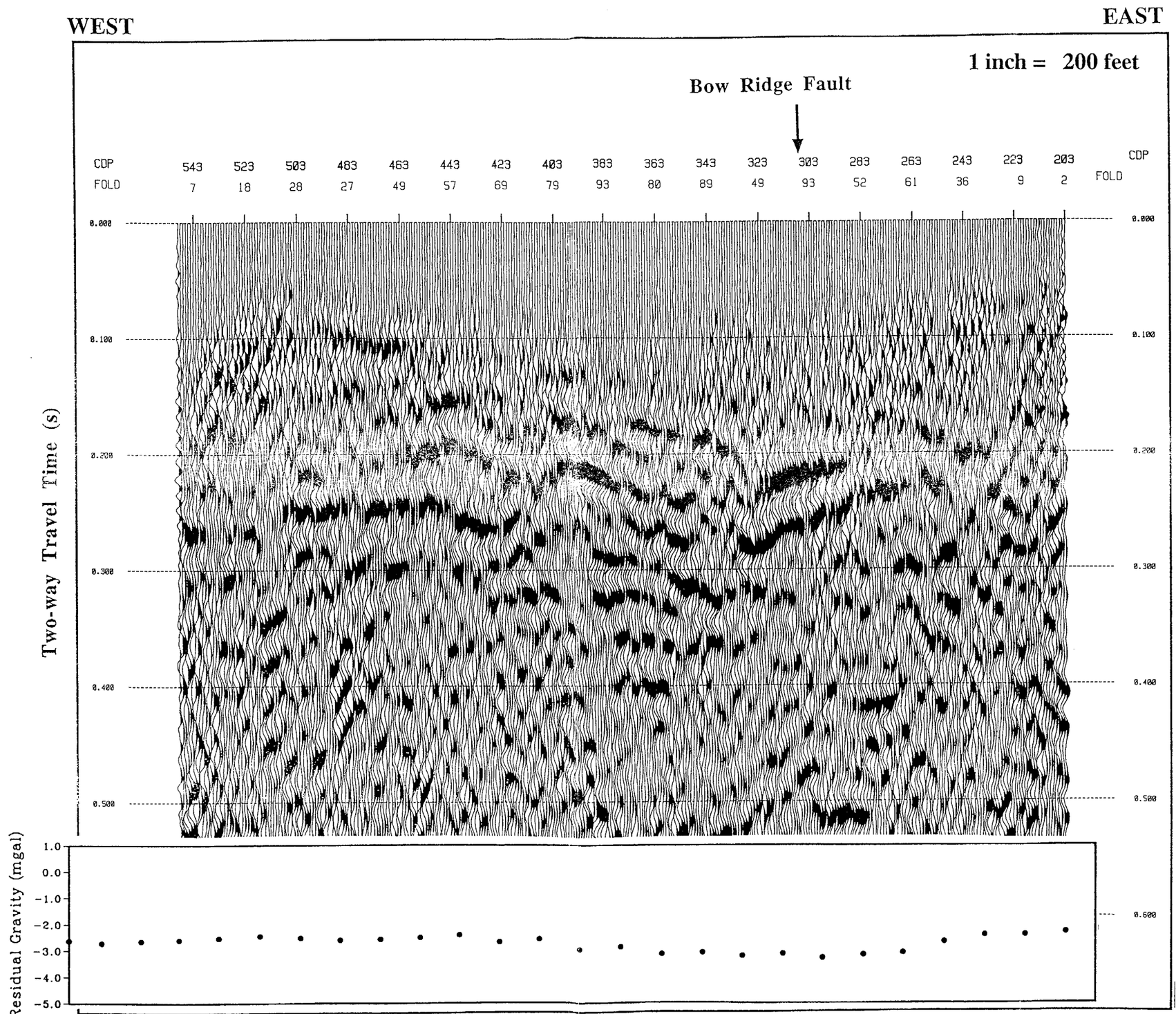

Figure 16a. YMP-12 stacked time section with residual gravity.

Figure 16a

YMP-12 STACK

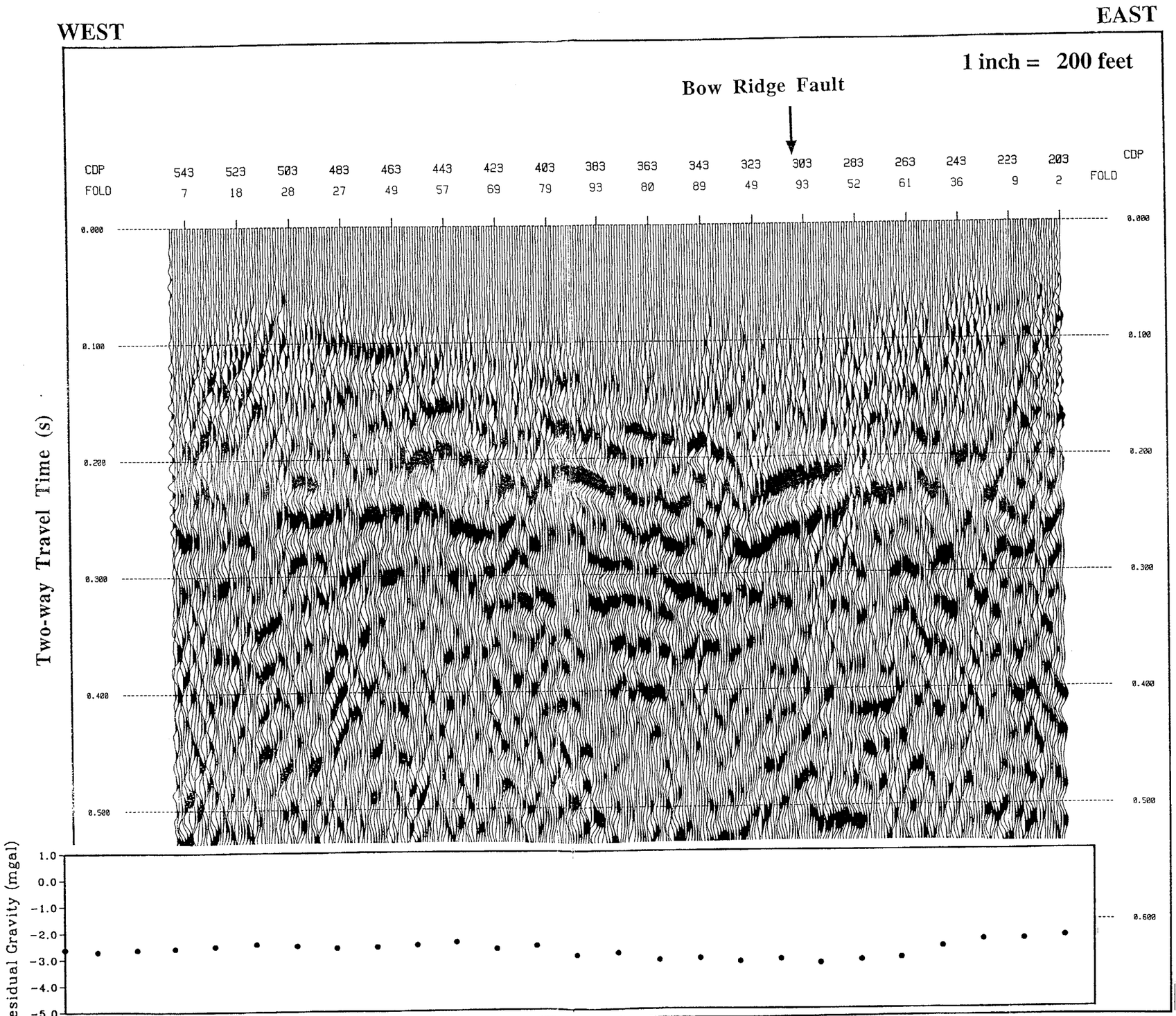

Figure 16a. YMP-12 stacked time section with residual gravity.

Figure 16a

YMP-12 MIGRATED DEPTH

WEST **EAST**

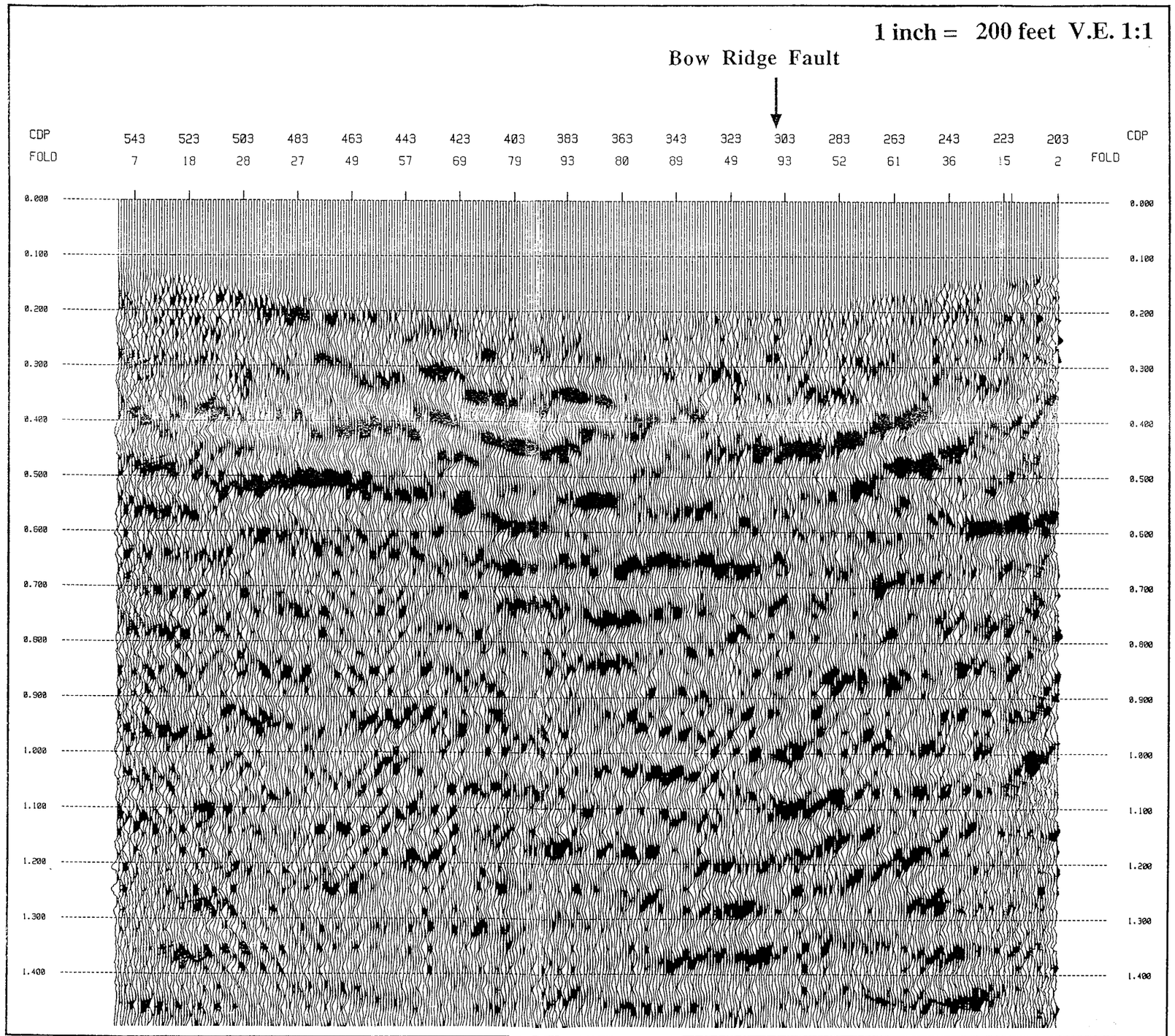

Focus 3.0 CogniSeis Development, Inc.

Figure 16b. YMP-12 migrated depth section.

Figure 16b

YMP-12 GEOLOGIC MODEL

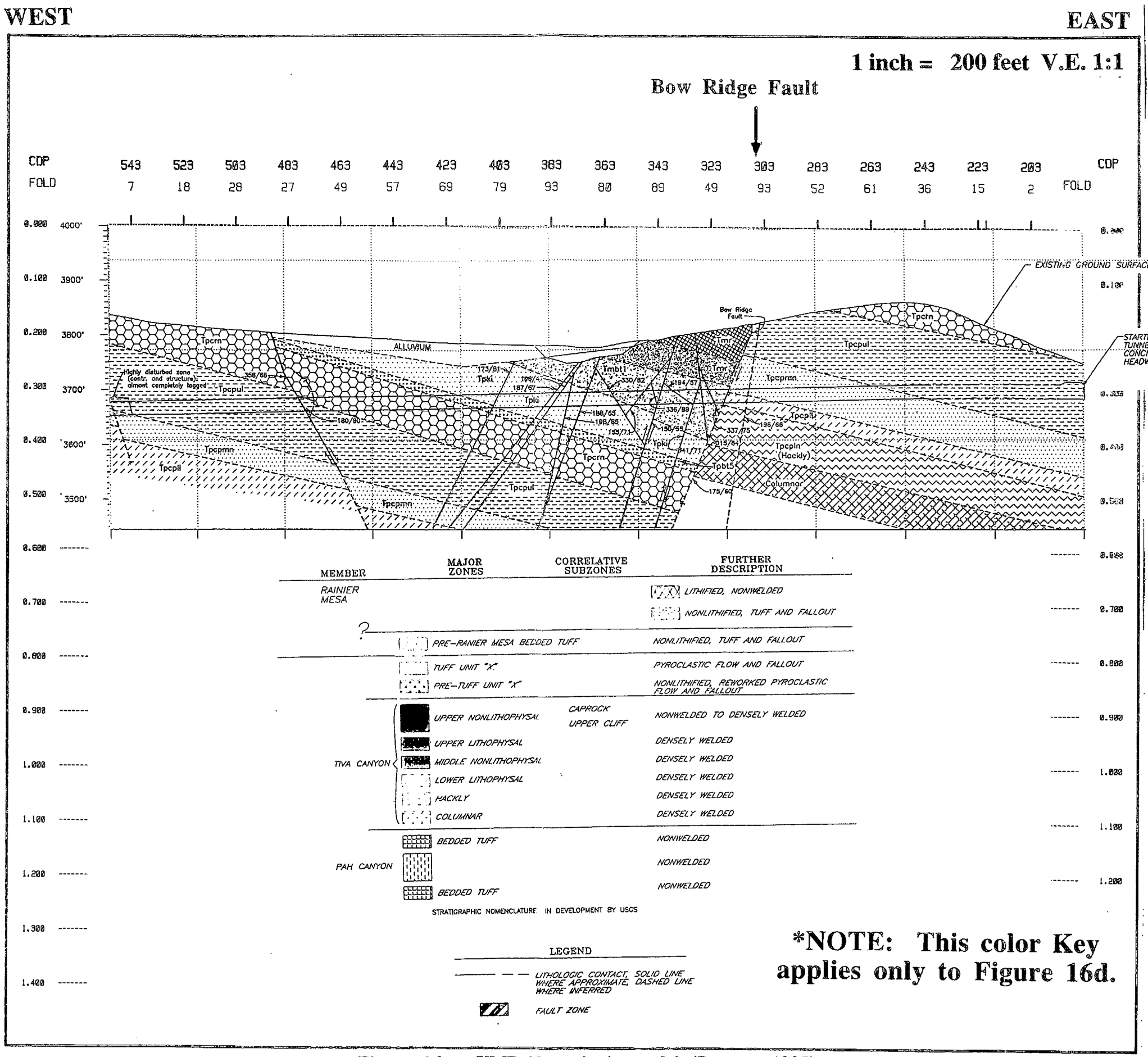

Figure 16c. YMP-12 geologic model (Beason, 1995).

Figure 16c

YMP-12 MIGRATED DEPTH

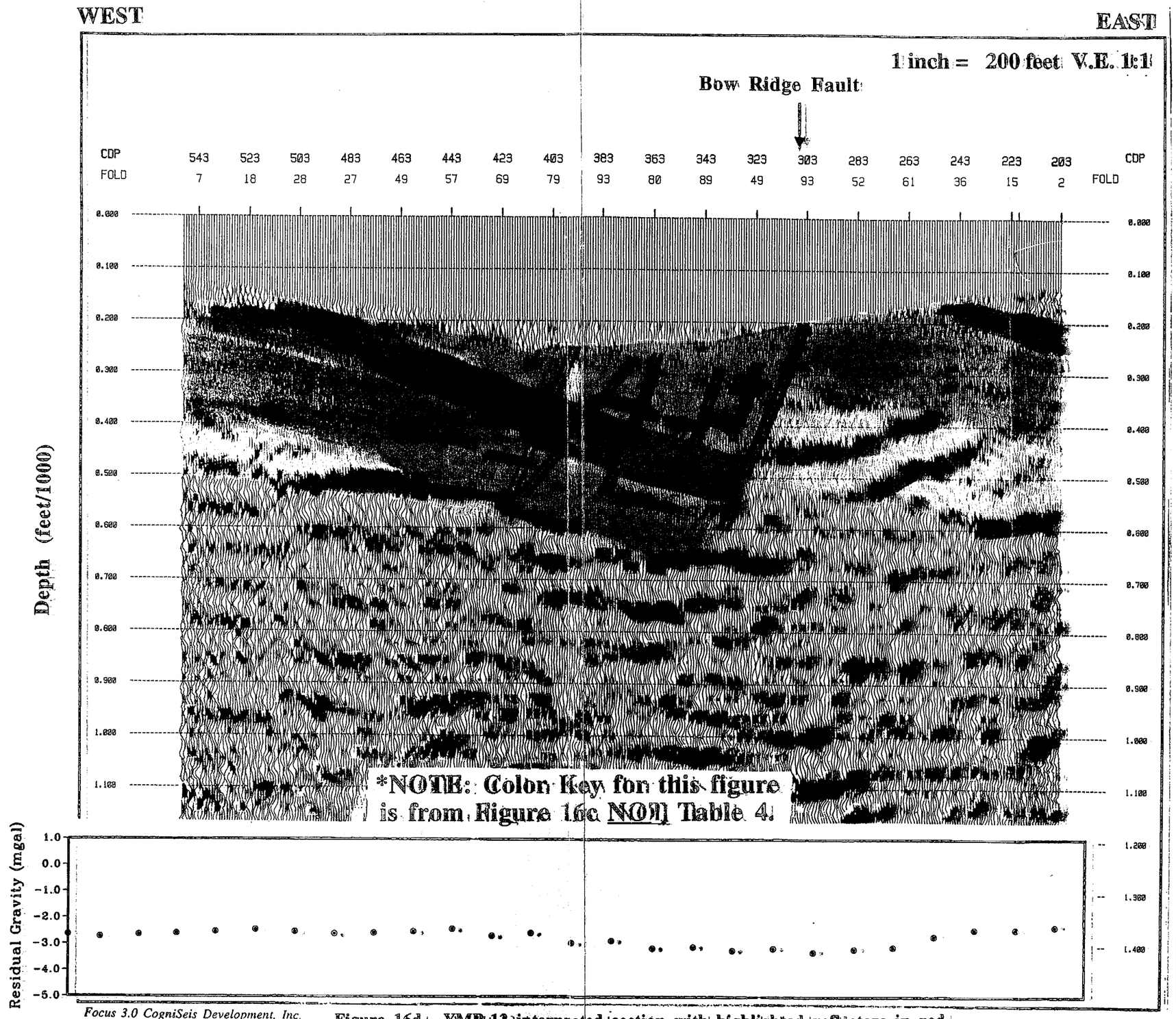

Focus 3.0 CogniSeis Development, Inc.

Figure 16d. YMP-12 interpreted section with highlighted reflectors in red.

Figure 16d!

YMP 13a

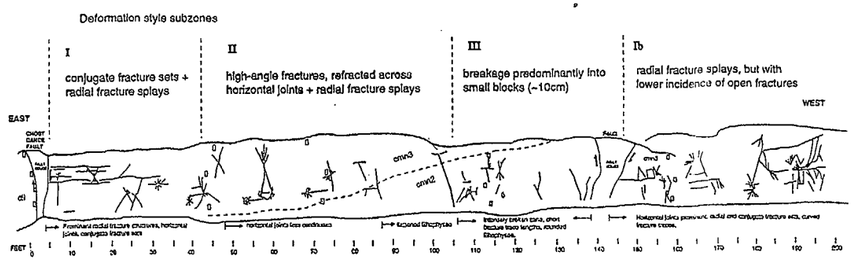

East

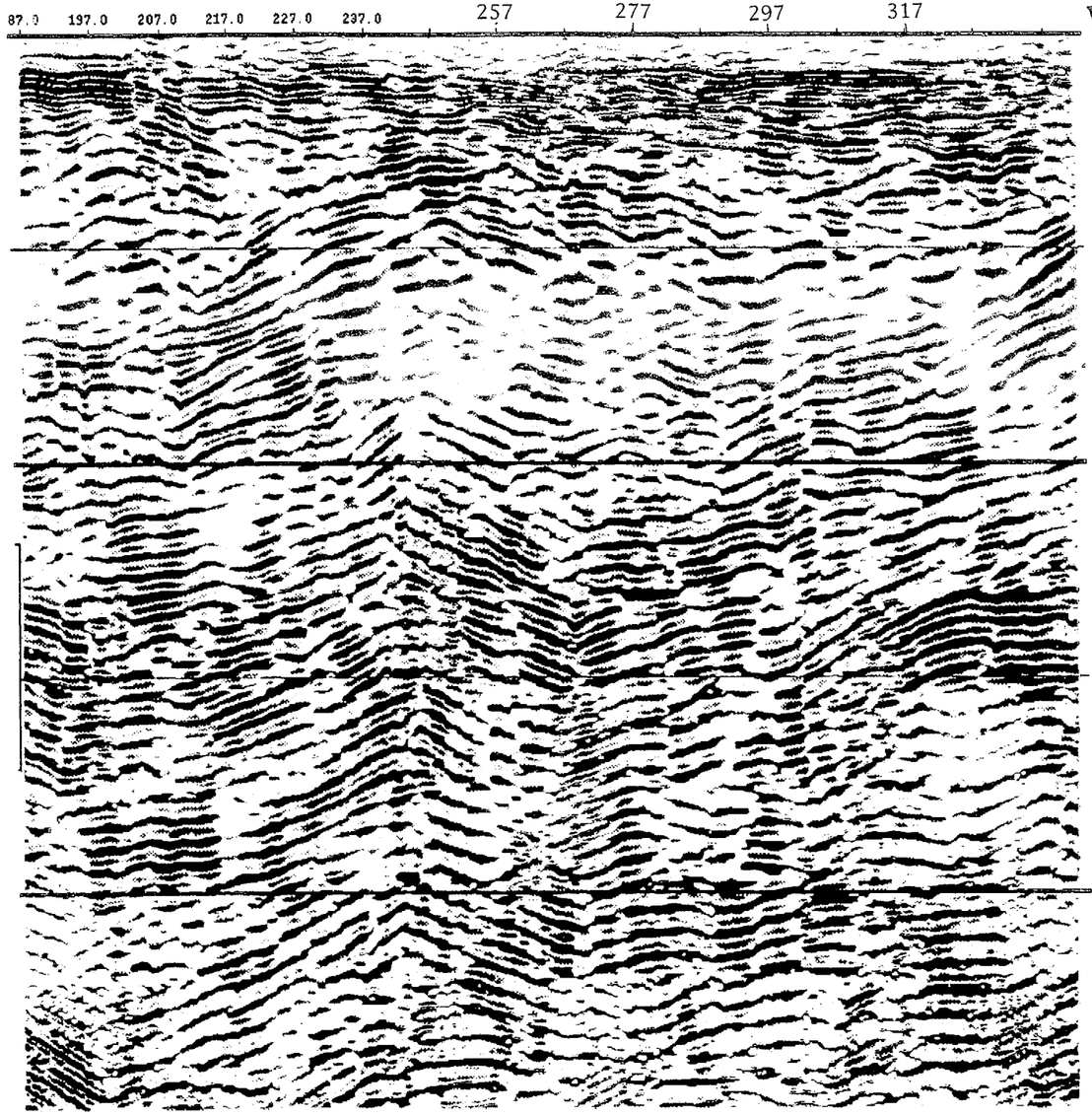

Figure 17a. YMP-13a depth section. For lines YMP-13a, 13b, 14a, and 14b, 2500 feet of data is shown and the CDP interval is 3 feet.

Figure 17a.

YMP 13a

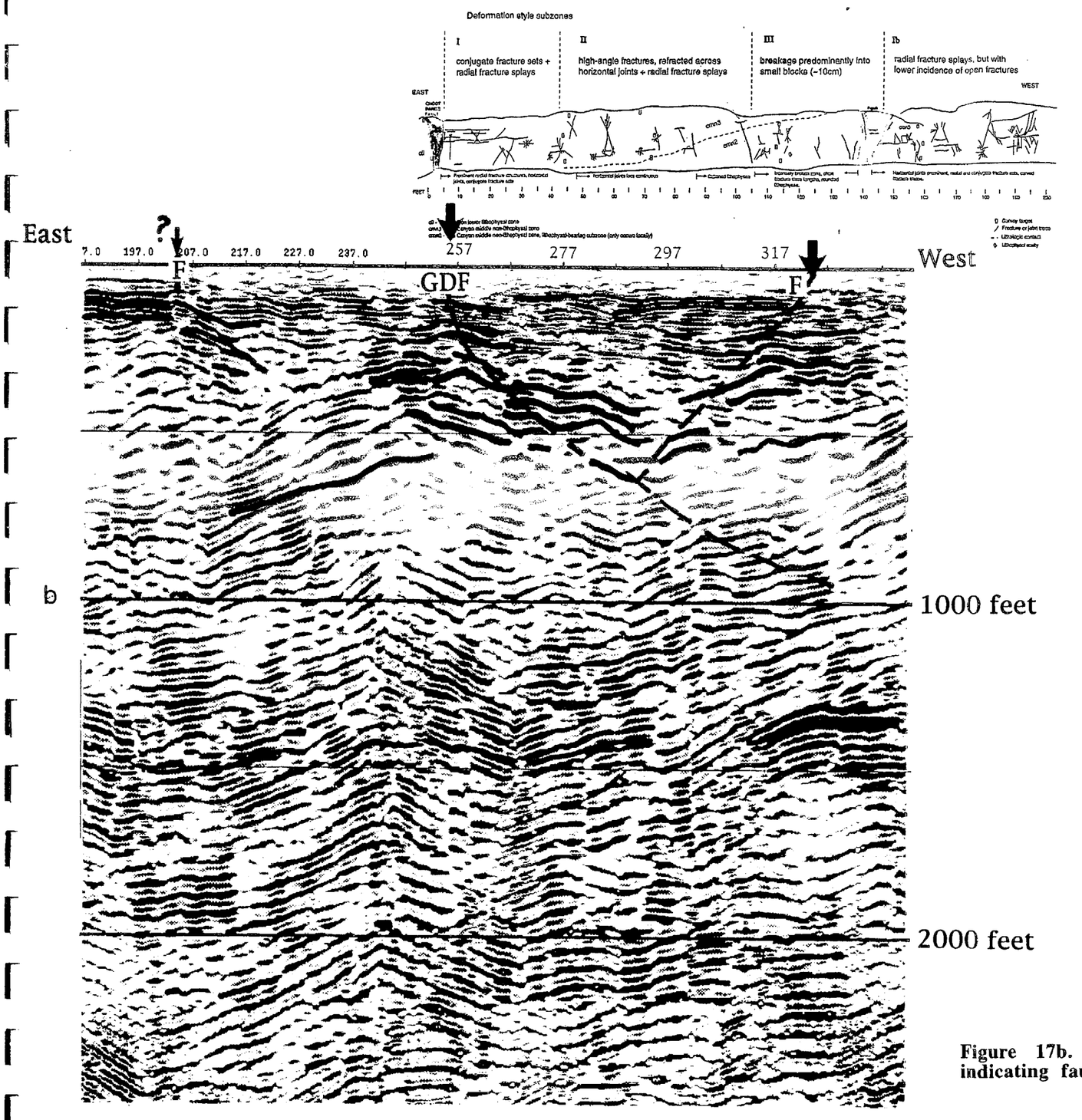

Figure 17b. YMP-13a interpreted depth section with arrows indicating faults.

Figure 17b.

YMP 13b

South North

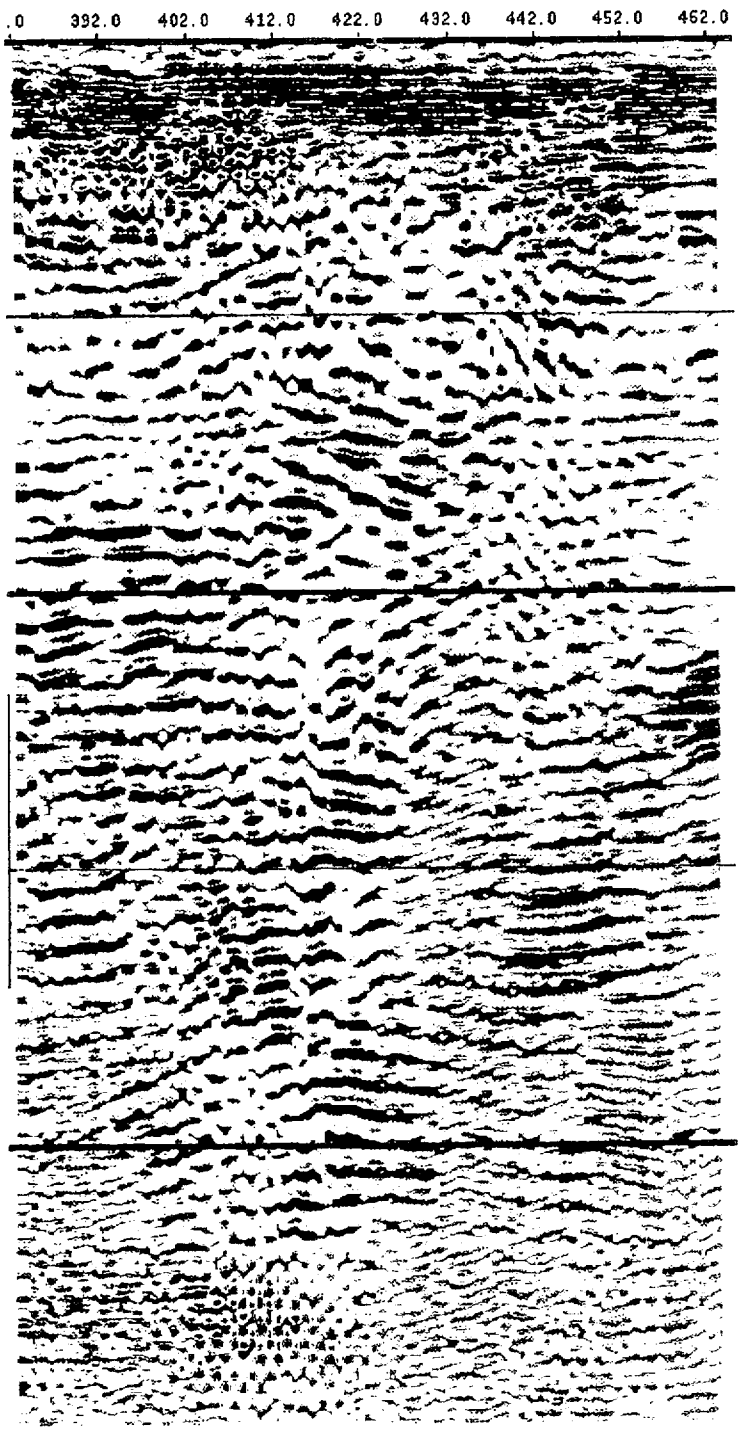

YMP 13b

South North

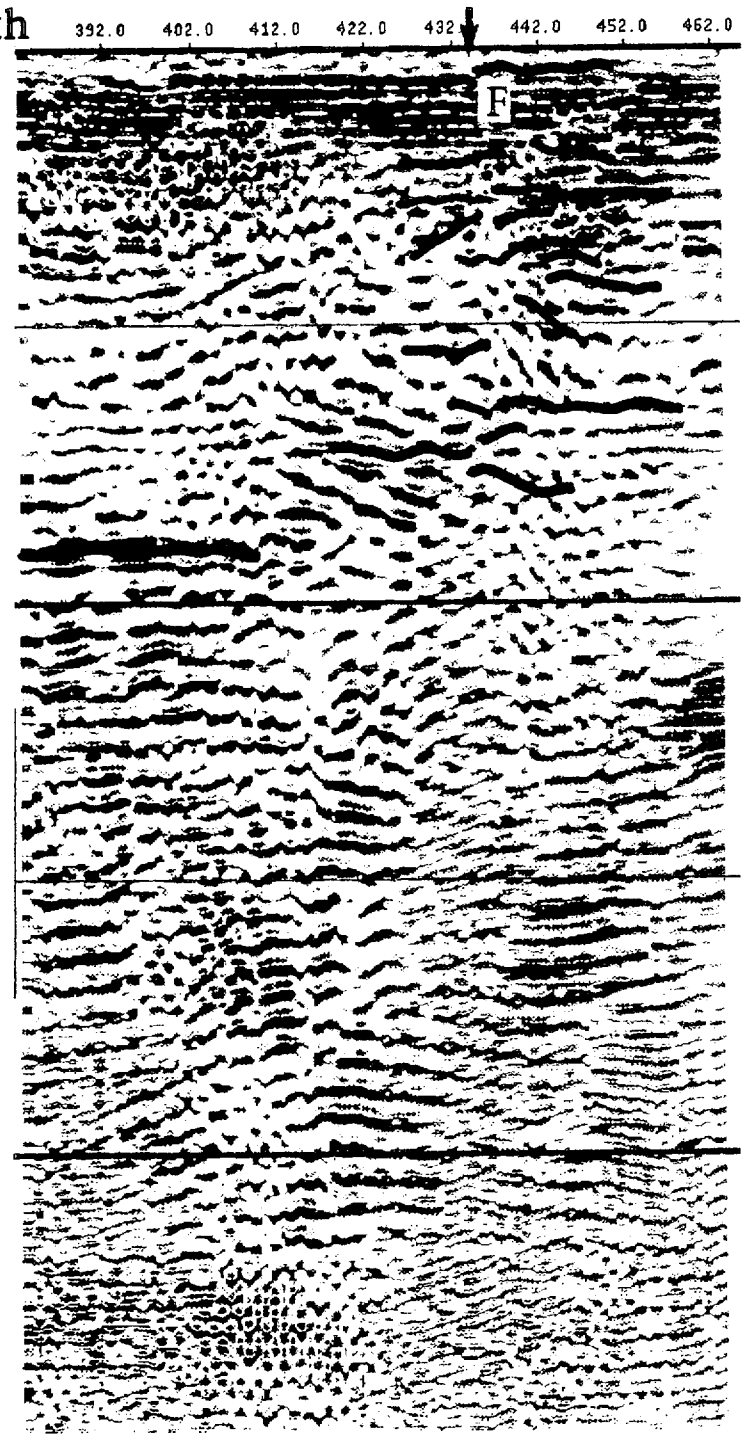

Figure 18. (a) YMP-13b depth section; (b) interpreted depth section with arrows indicating faults.

Figure 18.

East

West

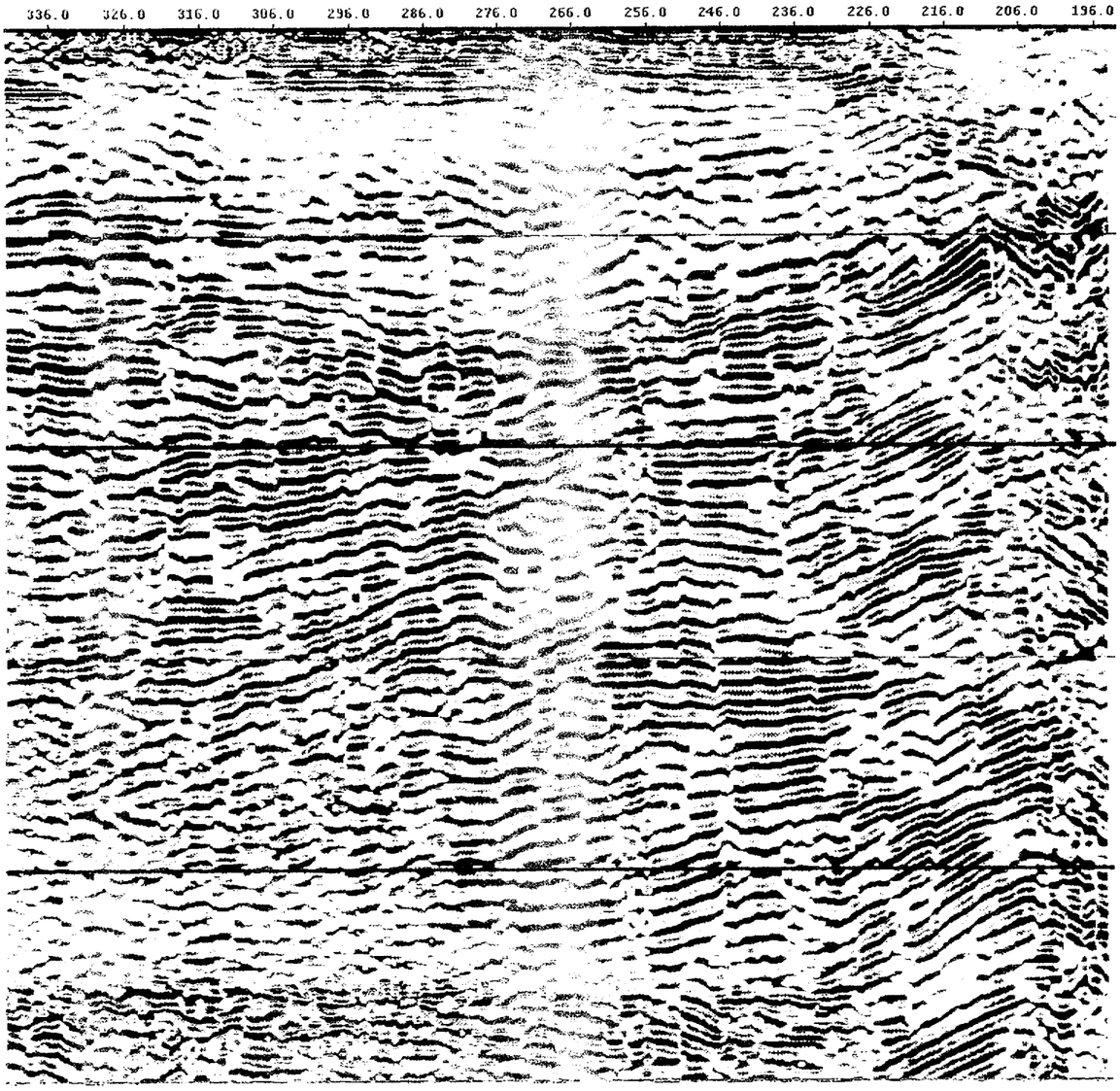

a

1000 feet

2000 feet

YMP 14a

East

West

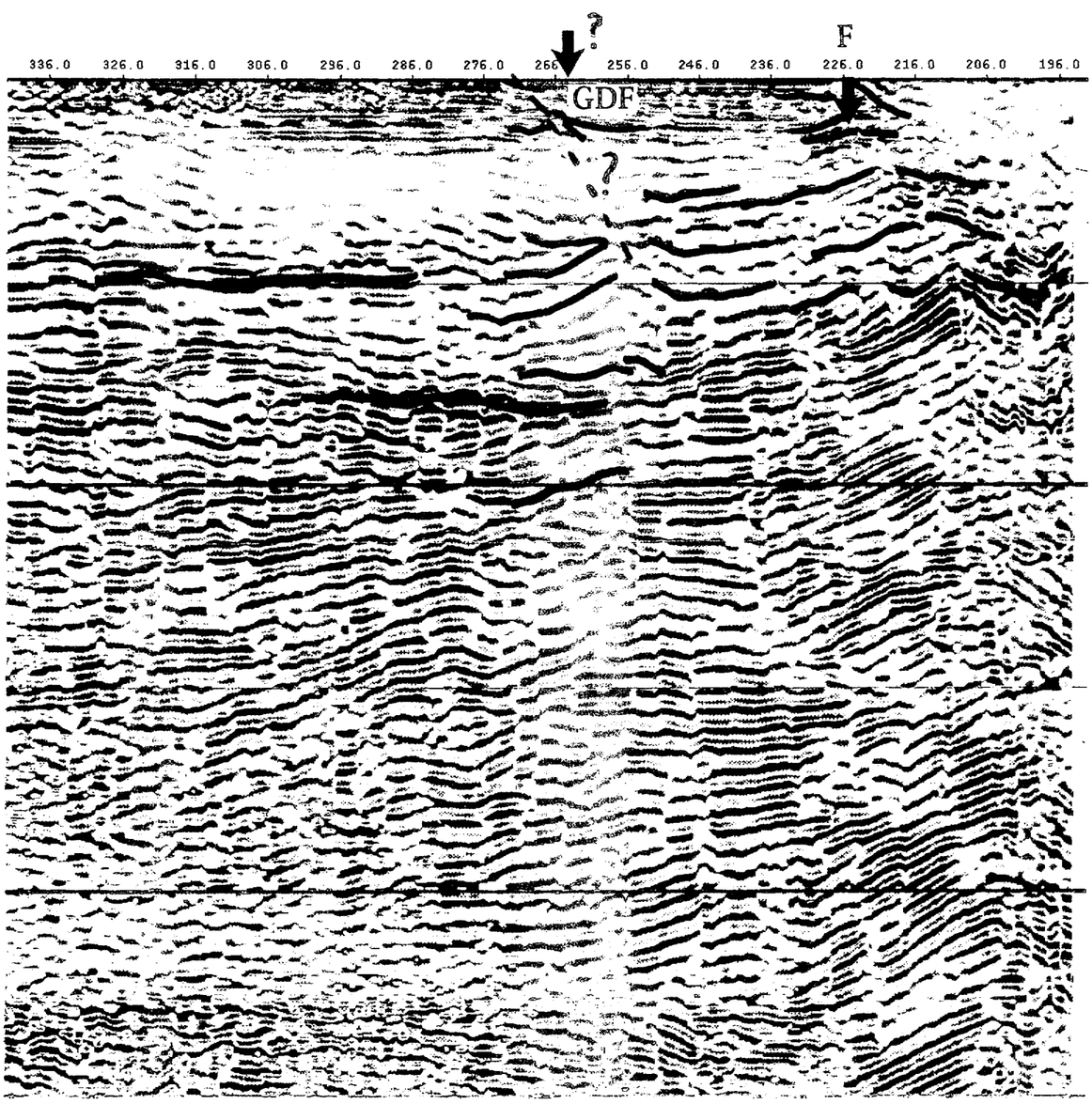

b

1000 feet

2000 feet

Figure 19. (a) YMP-14a depth section; (b) interpreted depth section.

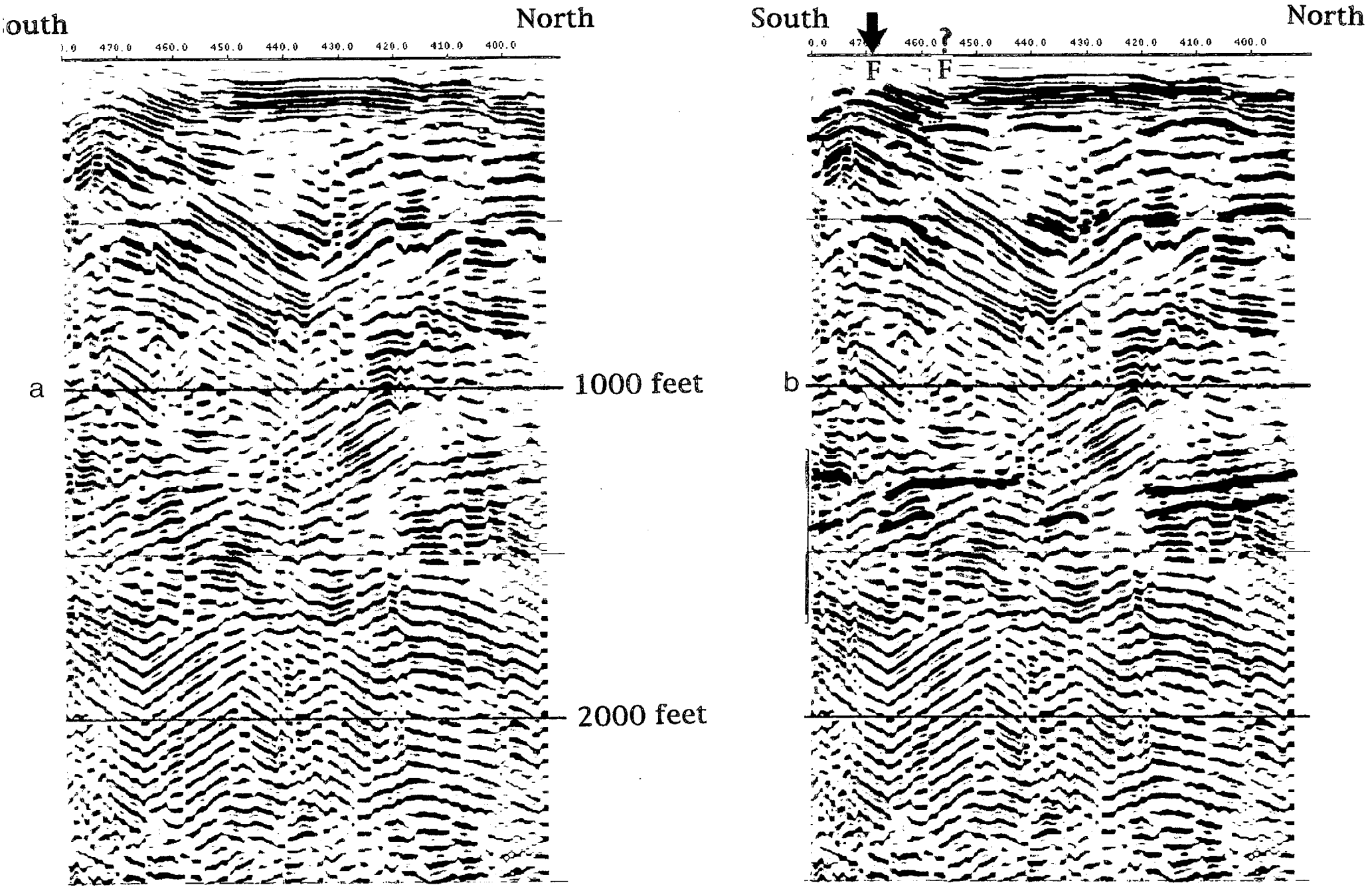

Figure 20. (a) YMP-14b depth section; (b) interpreted depth section with arrows indicating faults.

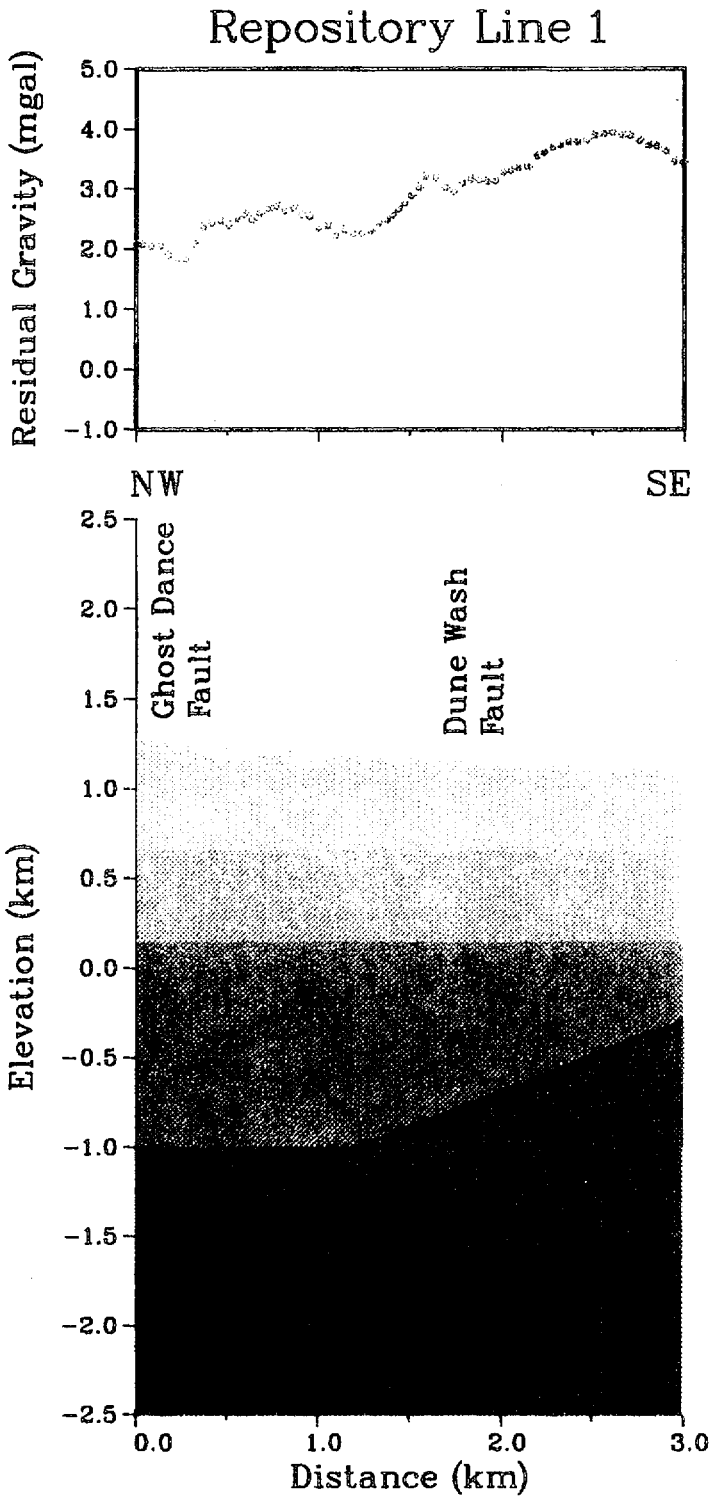

Figure G1. Cross section along repository line 1. The lower panel shows the density structure, with the red area being basement and the yellow, green, and blue areas showing the sedimentary fill, with the density anomaly varying from $-0.5\ gm/cm^3$ at the surface to $-0.2\ gm/cm^3$ at the contact with basement. No vertical exaggeration. The upper panel shows the residual gravity anomalies along the line, which is the Bouguer anomaly minus the effects of regional and basement structure.

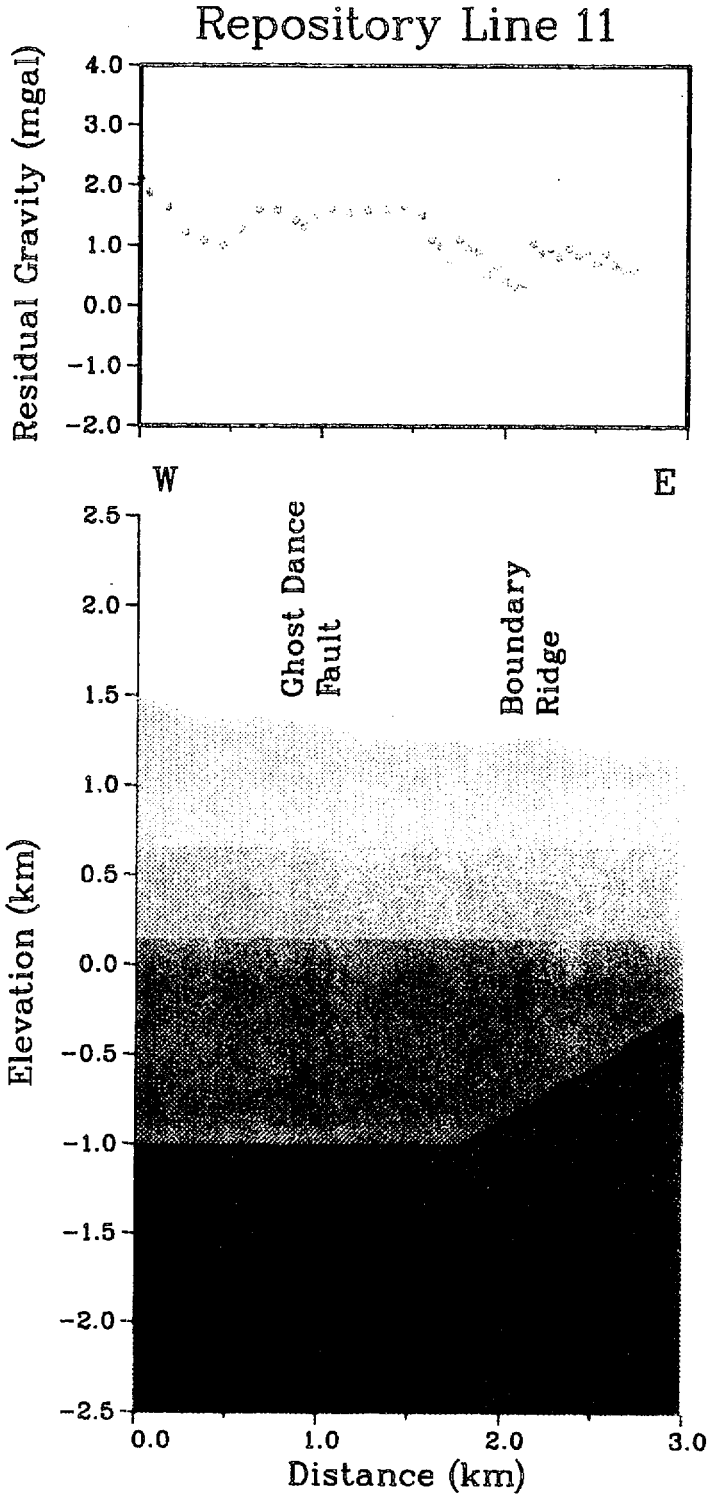

Figure G2. Cross section along repository line 11. The lower panel shows the density structure, with the red area being basement and the yellow, green, and blue areas showing the sedimentary fill, with the density anomaly varying from $-0.5\ gm/cm^3$ at the surface to $-0.2\ gm/cm^3$ at the contact with basement. No vertical exaggeration. The upper panel shows the residual gravity anomalies along the line, which is the Bouguer anomaly minus the effects of regional and basement structure.

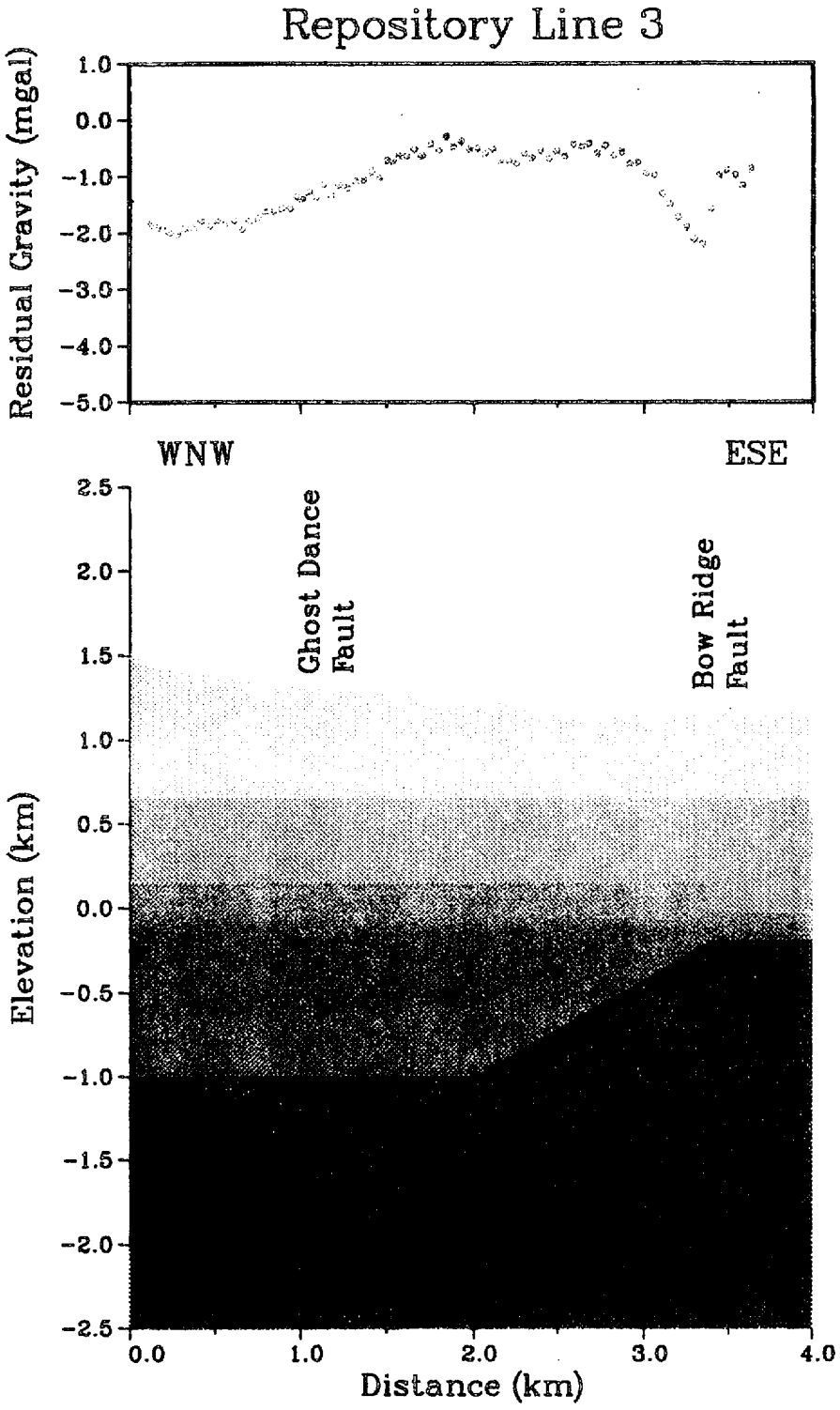

Figure G3. Cross section along repository line 3. The lower panel shows the density structure, with the red area being basement and the yellow, green, and blue areas showing the sedimentary fill, with the density anomaly varying from $-0.5\ gm/cm^3$ at the surface to $-0.2\ gm/cm^3$ at the contact with basement. No vertical exaggeration. The upper panel shows the residual gravity anomalies along the line, which is the Bouguer anomaly minus the effects of regional and basement structure.

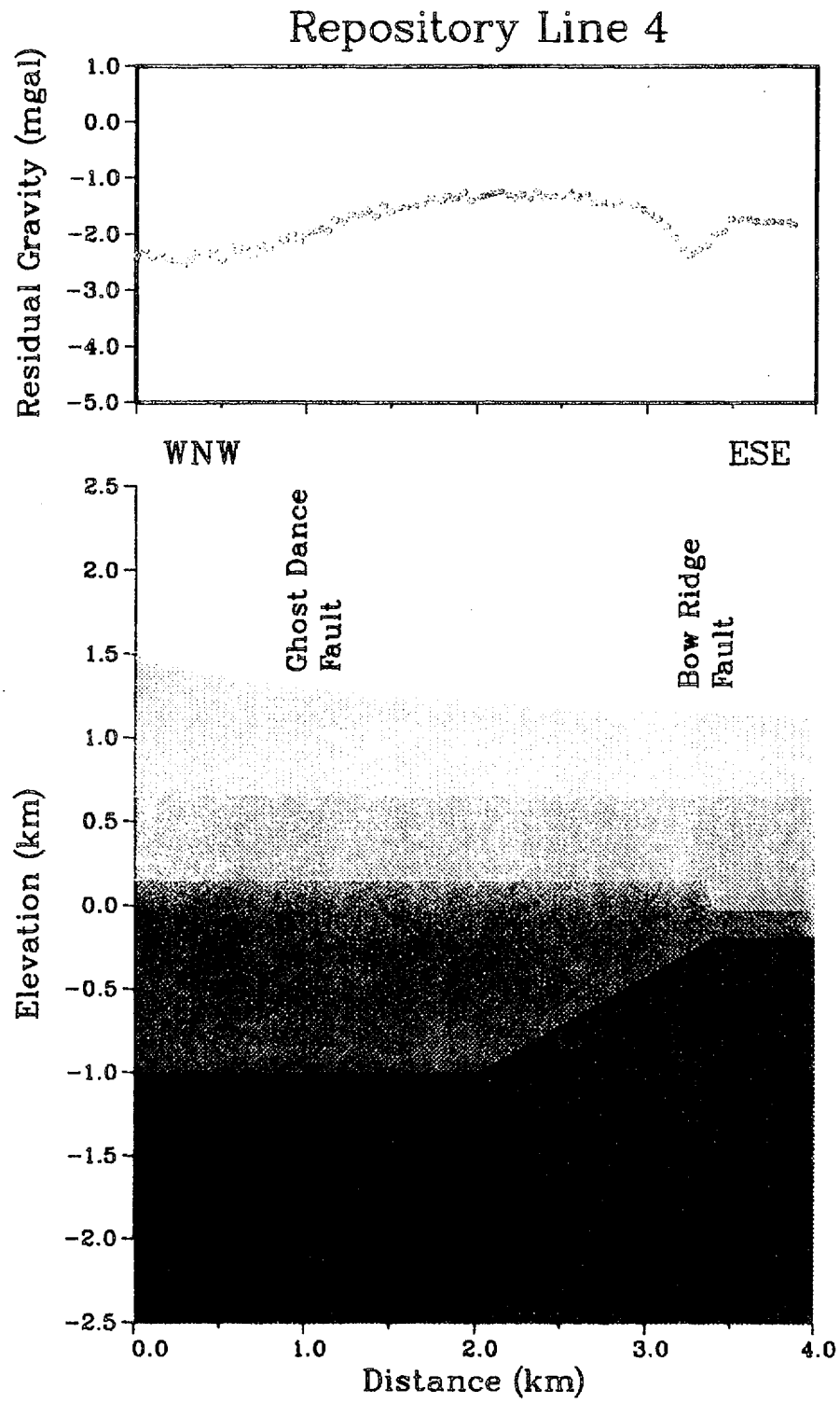

Figure G4. Cross section along repository line 4. The lower panel shows the density structure, with the red area being basement and the yellow, green, and blue areas showing the sedimentary fill, with the density anomaly varying from $-0.5\ gm/cm^3$ at the surface to $-0.2\ gm/cm^3$ at the contact with basement. No vertical exaggeration. The upper panel shows the residual gravity anomalies along the line, which is the Bouguer anomaly minus the effects of regional and basement structure.

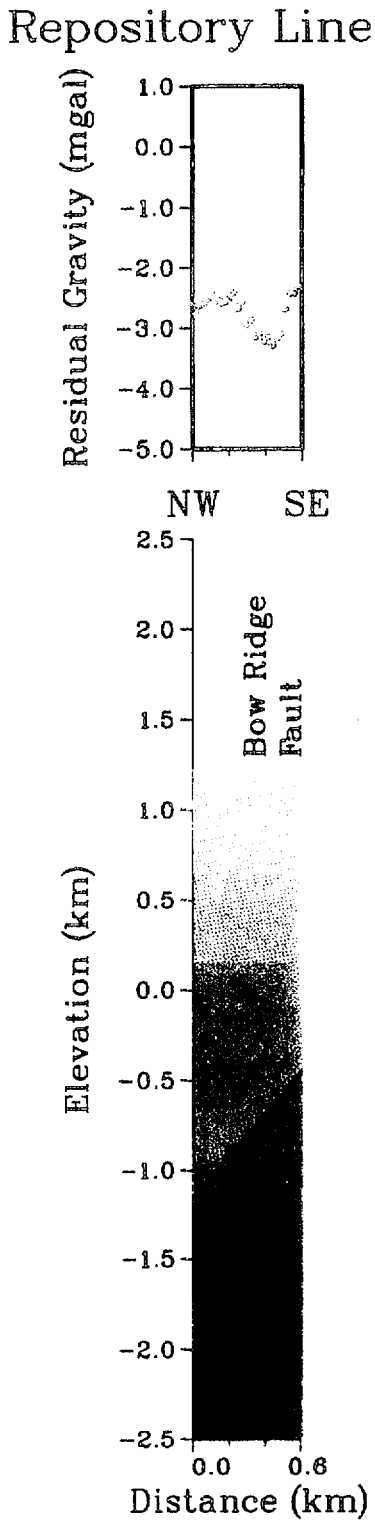

Figure G5. Cross section along repository line 12. The lower panel shows the density structure, with the red area being basement and the yellow, green, and blue areas showing the sedimentary fill, with the density anomaly varying from $-0.5\ gm/cm^3$ at the surface to $-0.2\ gm/cm^3$ at the contact with basement. No vertical exaggeration. The upper panel shows the residual gravity anomalies along the line, which is the Bouguer anomaly minus the effects of regional and basement structure.

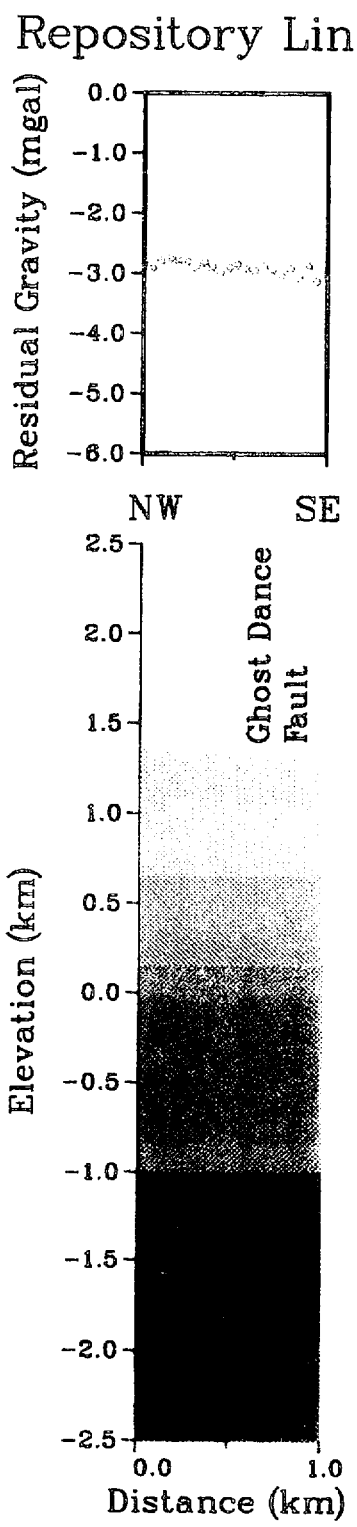

Figure G6. Cross section along repository line 9. The lower panel shows the density structure, with the red area being basement and the yellow, green, and blue areas showing the sedimentary fill, with the density anomaly varying from $-0.5\ gm/cm^3$ at the surface to $-0.2\ gm/cm^3$ at the contact with basement. No vertical exaggeration. The upper panel shows the residual gravity anomalies along the line, which is the Bouguer anomaly minus the effects of regional and basement structure.

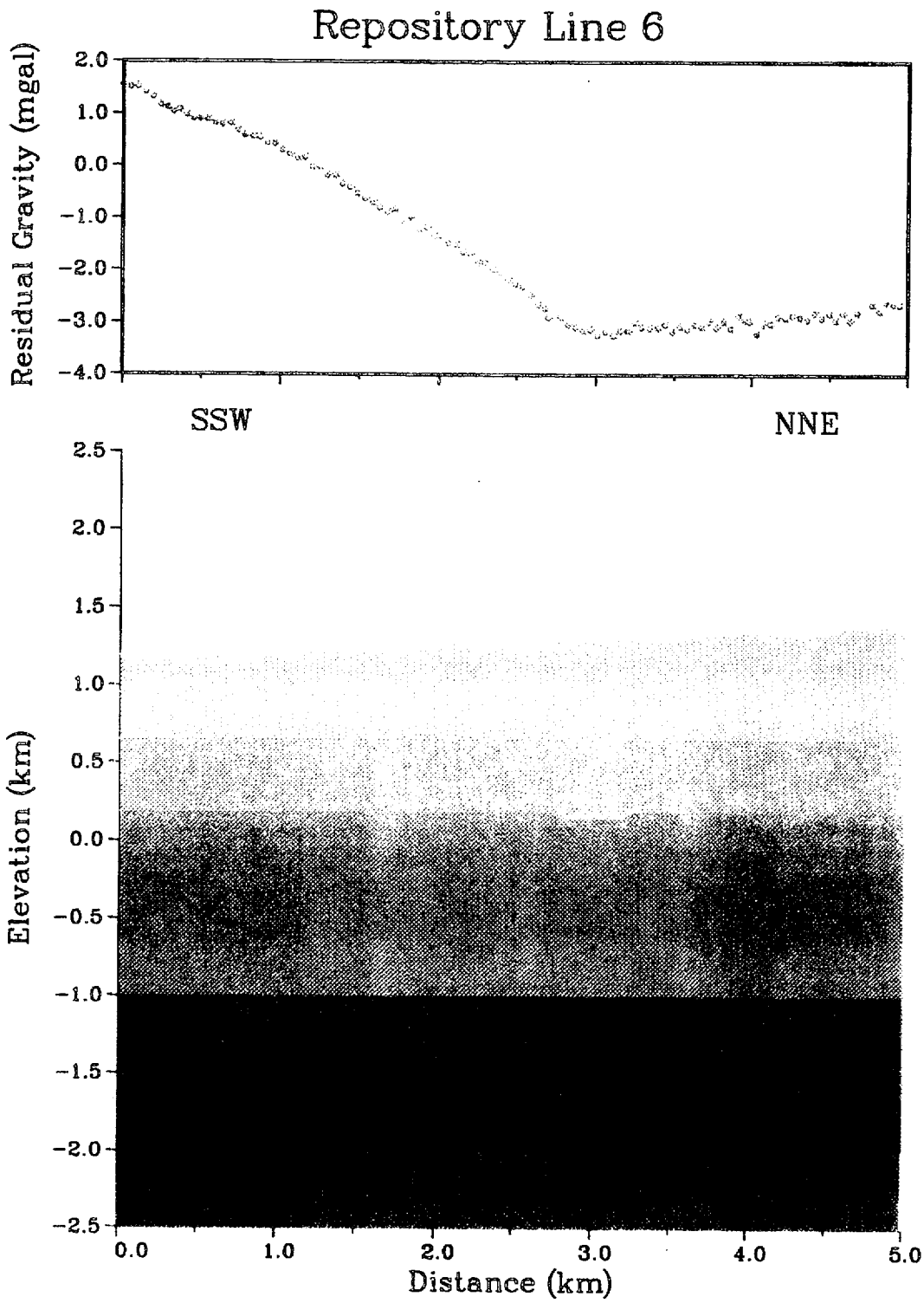

Figure G7. Cross section along repository line 6. The lower panel shows the density structure, with the red area being basement and the yellow, green, and blue areas showing the sedimentary fill, with the density anomaly varying from $-0.5\ gm/cm^3$ at the surface to $-0.2\ gm/cm^3$ at the contact with basement. No vertical exaggeration. The upper panel shows the residual gravity anomalies along the line, which is the Bouguer anomaly minus the effects of regional and basement structure.

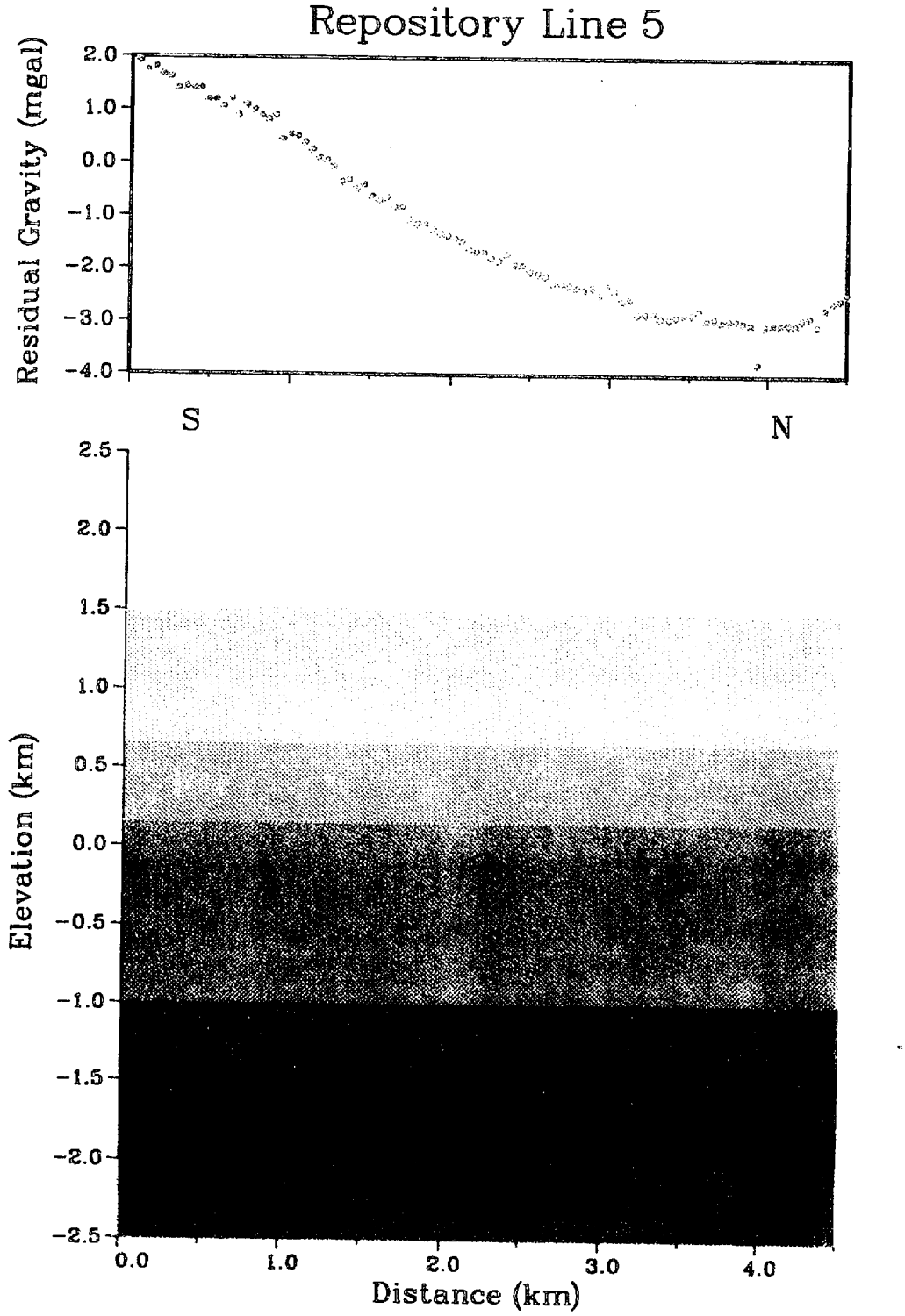

Figure G8. Cross section along repository line 5. The lower panel shows the density structure, with the red area being basement and the yellow, green, and blue areas showing the sedimentary fill, with the density anomaly varying from $-0.5\ gm/cm^3$ at the surface to $-0.2\ gm/cm^3$ at the contact with basement. No vertical exaggeration. The upper panel shows the residual gravity anomalies along the line, which is the Bouguer anomaly minus the effects of regional and basement structure.

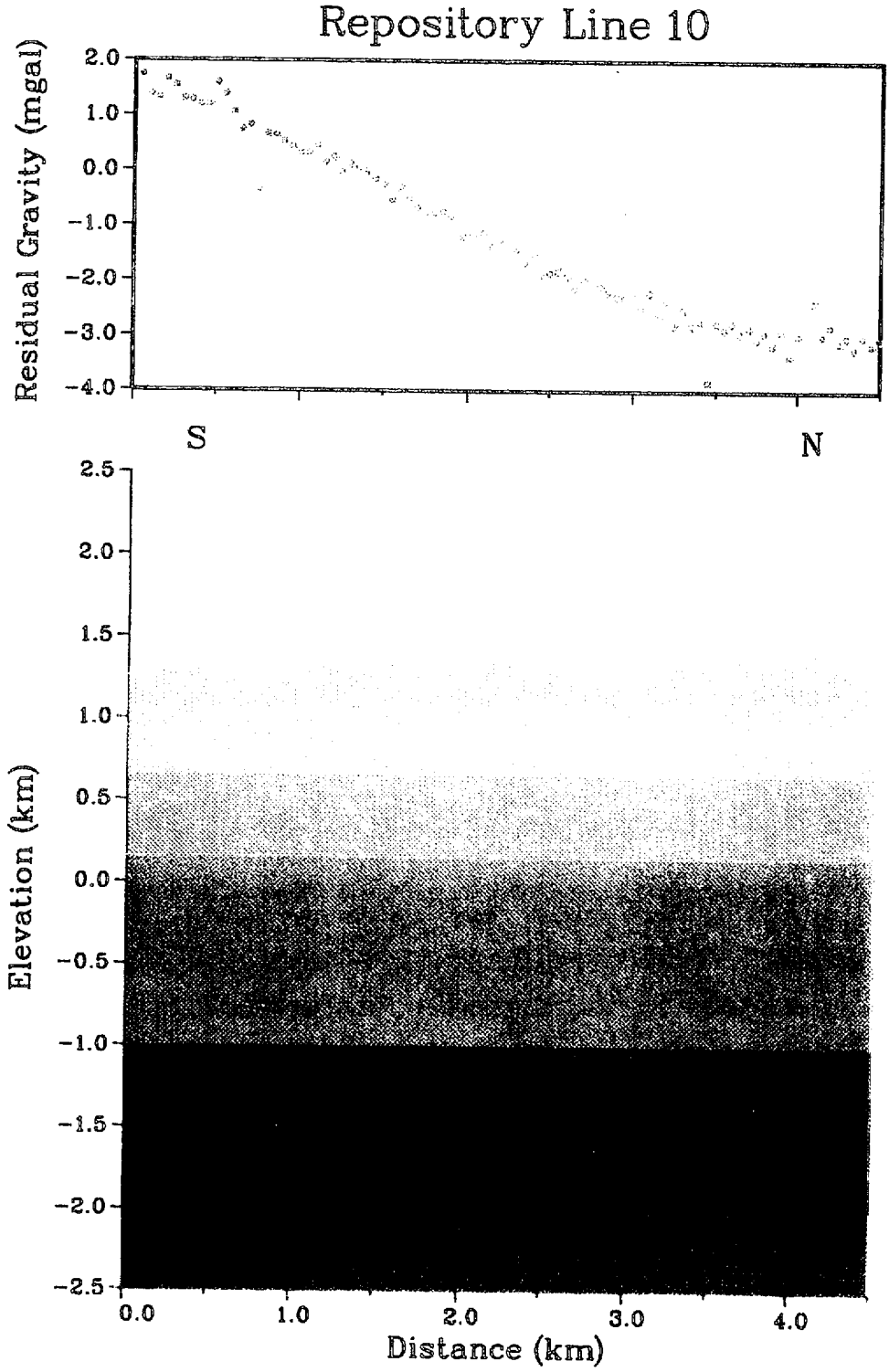

Figure G9. Cross section along repository line 10. The lower panel shows the density structure, with the red area being basement and the yellow, green, and blue areas showing the sedimentary fill, with the density anomaly varying from $-0.5\ gm/cm^3$ at the surface to $-0.2\ gm/cm^3$ at the contact with basement. No vertical exaggeration. The upper panel shows the residual gravity anomalies along the line, which is the Bouguer anomaly minus the effects of regional and basement structure.

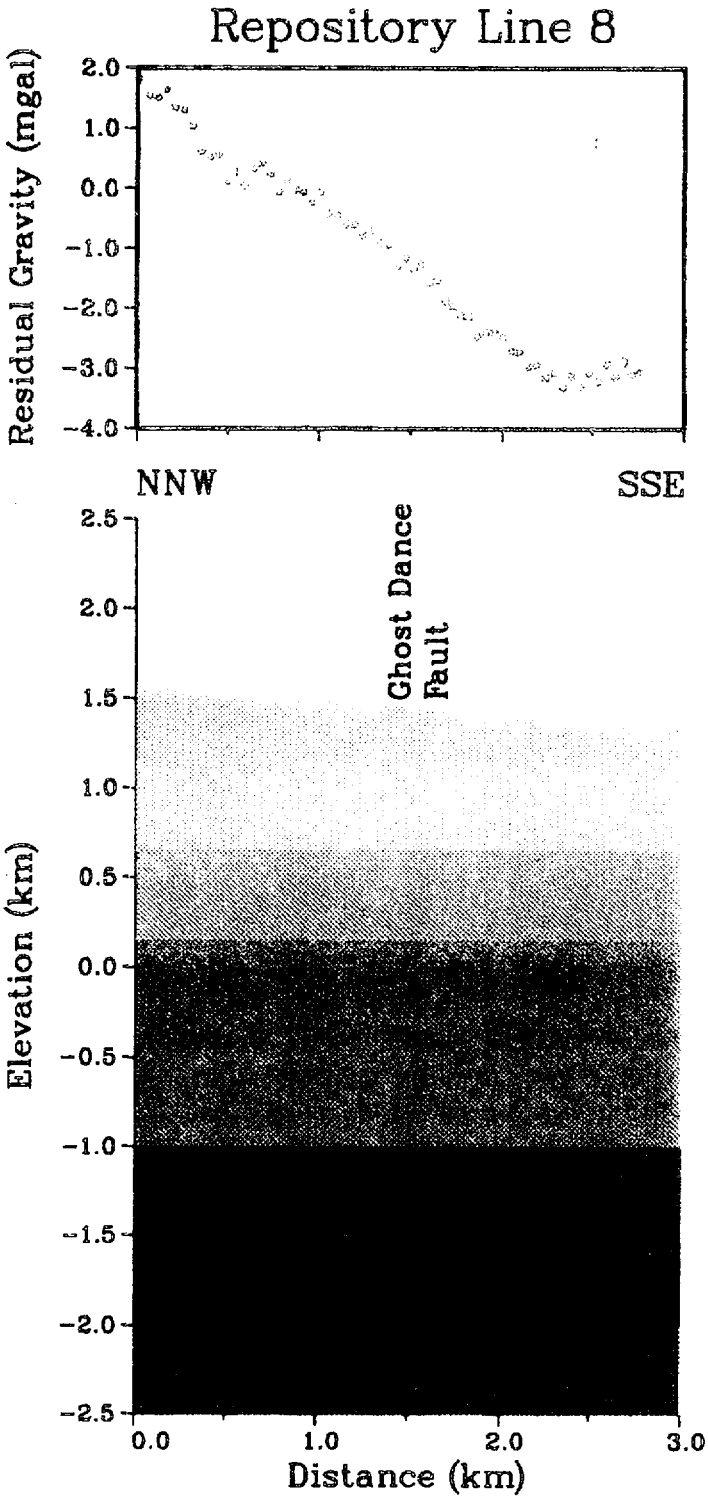

Figure G10. Cross section along repository line 8. The lower panel shows the density structure, with the red area being basement and the yellow, green, and blue areas showing the sedimentary fill, with the density anomaly varying from $-0.5\ gm/cm^3$ at the surface to $-0.2\ gm/cm^3$ at the contact with basement. No vertical exaggeration. The upper panel shows the residual gravity anomalies along the line, which is the Bouguer anomaly minus the effects of regional and basement structure.

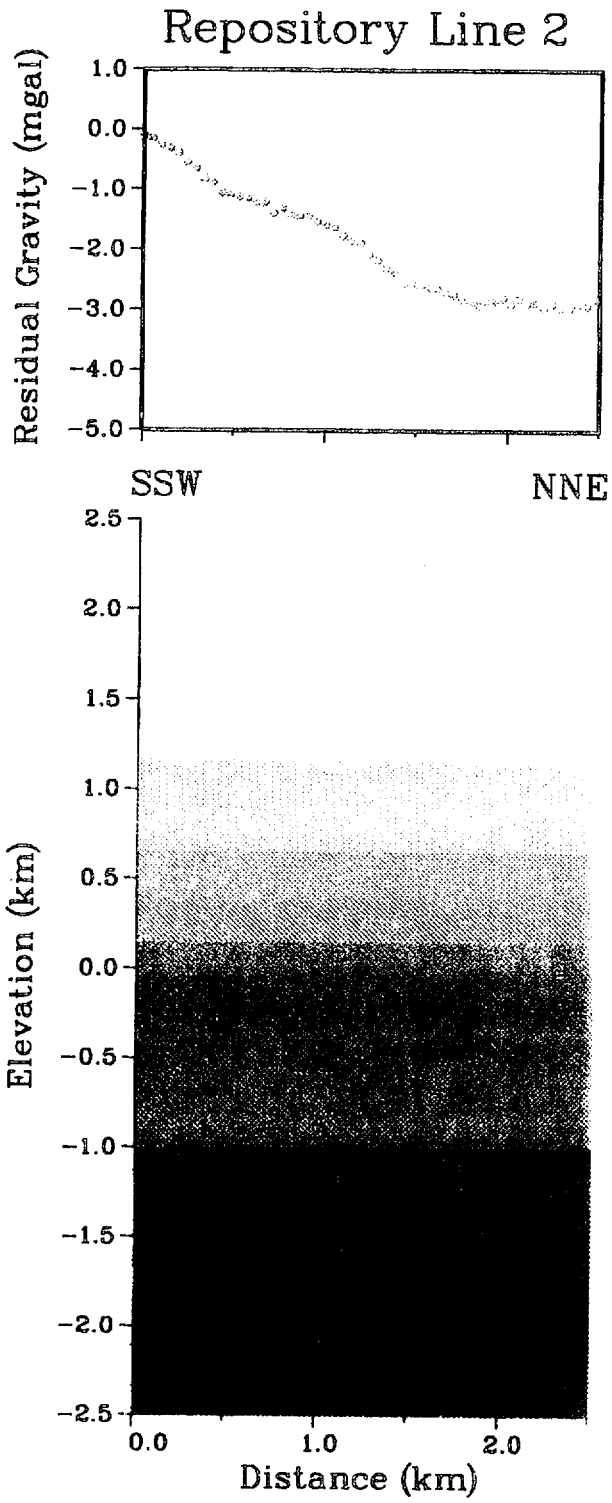

Figure G11. Cross section along repository line 2. The lower panel shows the density structure, with the red area being basement and the yellow, green, and blue areas showing the sedimentary fill, with the density anomaly varying from $-0.5\ gm/cm^3$ at the surface to $-0.2\ gm/cm^3$ at the contact with basement. No vertical exaggeration. The upper panel shows the residual gravity anomalies along the line, which is the Bouguer anomaly minus the effects of regional and basement structure.

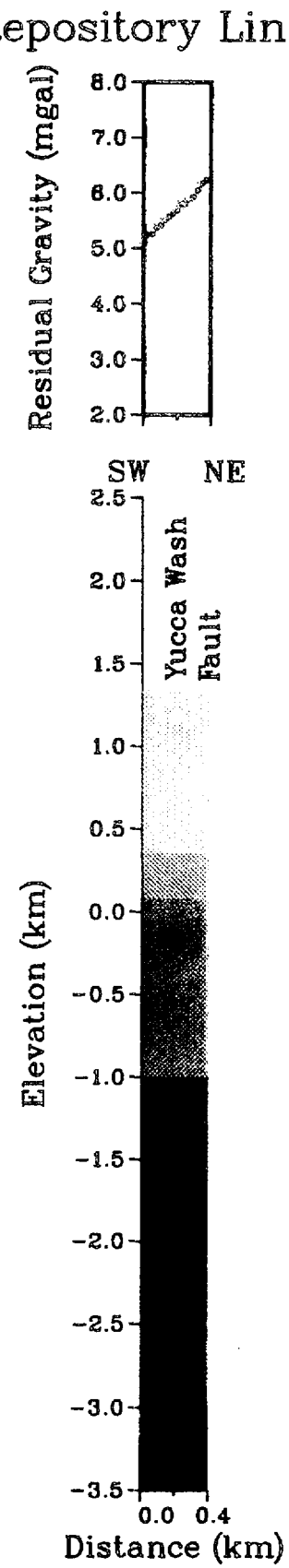

Figure G12. Cross section along repository line 7a. The lower panel shows the density structure, with the red area being basement and the yellow, green, and blue areas showing the sedimentary fill, with the density anomaly varying from $-0.5\ gm/cm^3$ at the surface to $-0.2\ gm/cm^3$ at the contact with basement. No vertical exaggeration. The upper panel shows the residual gravity anomalies along the line, which is the Bouguer anomaly minus the effects of regional and basement structure.

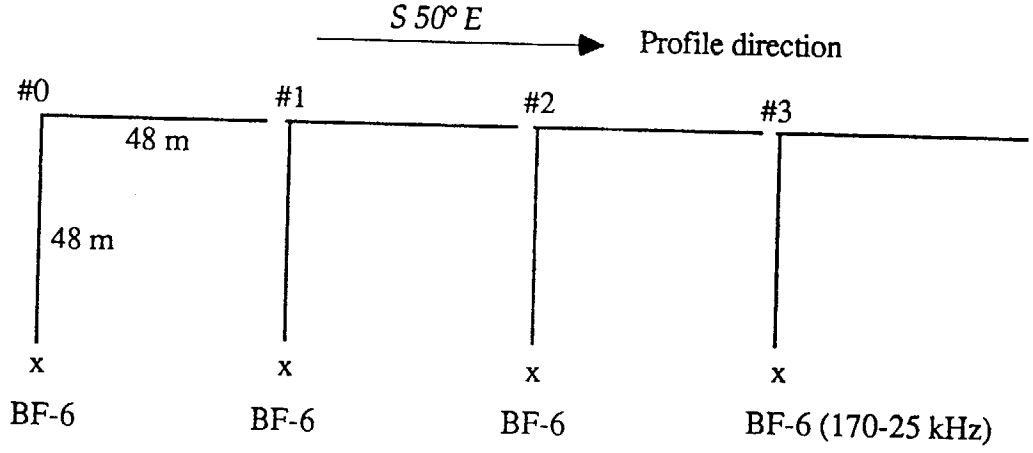

MT field set up

Figure MT1. MT field set-up.

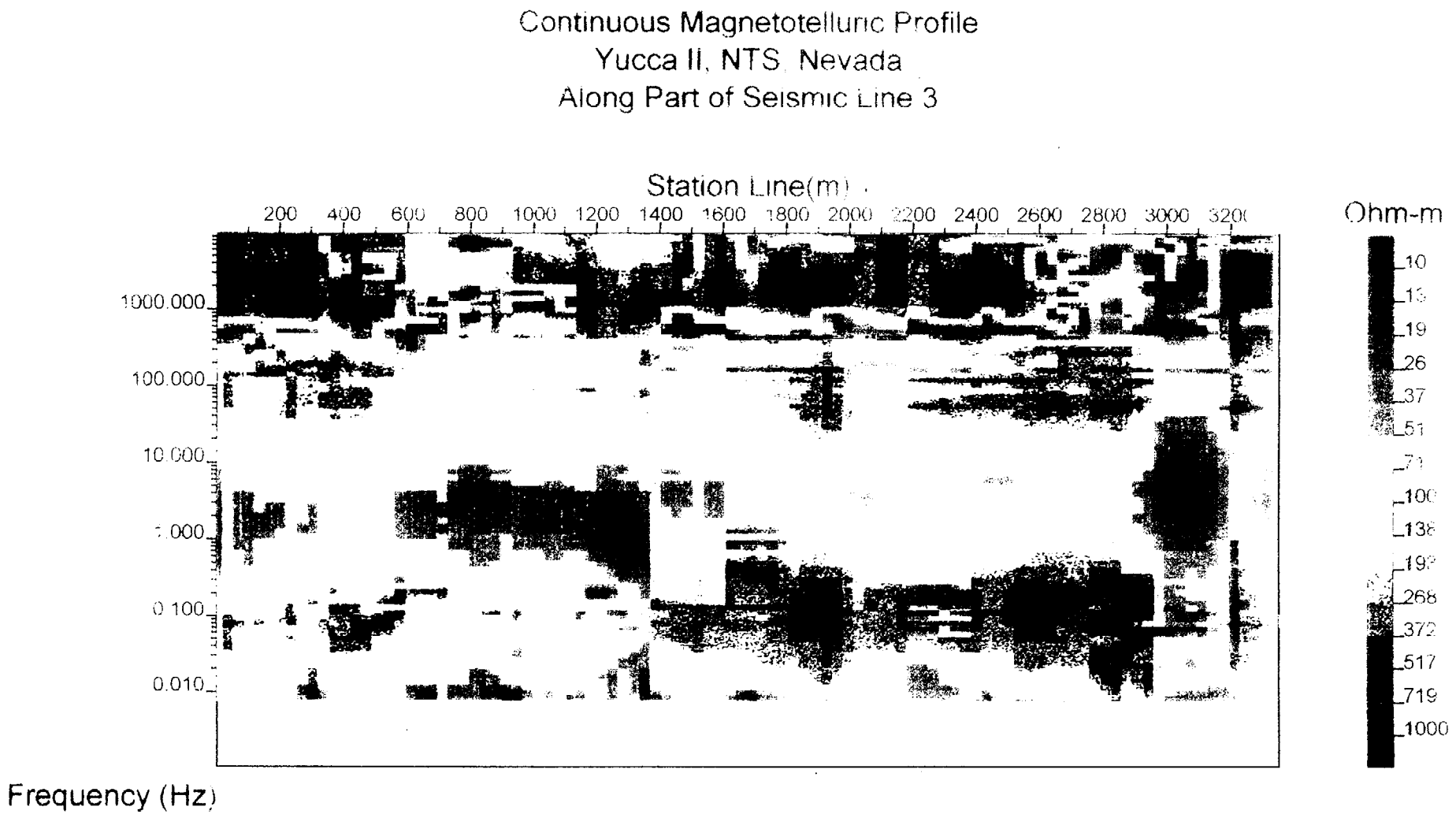

Figure MT2. Raw XY apparent resistivity data.

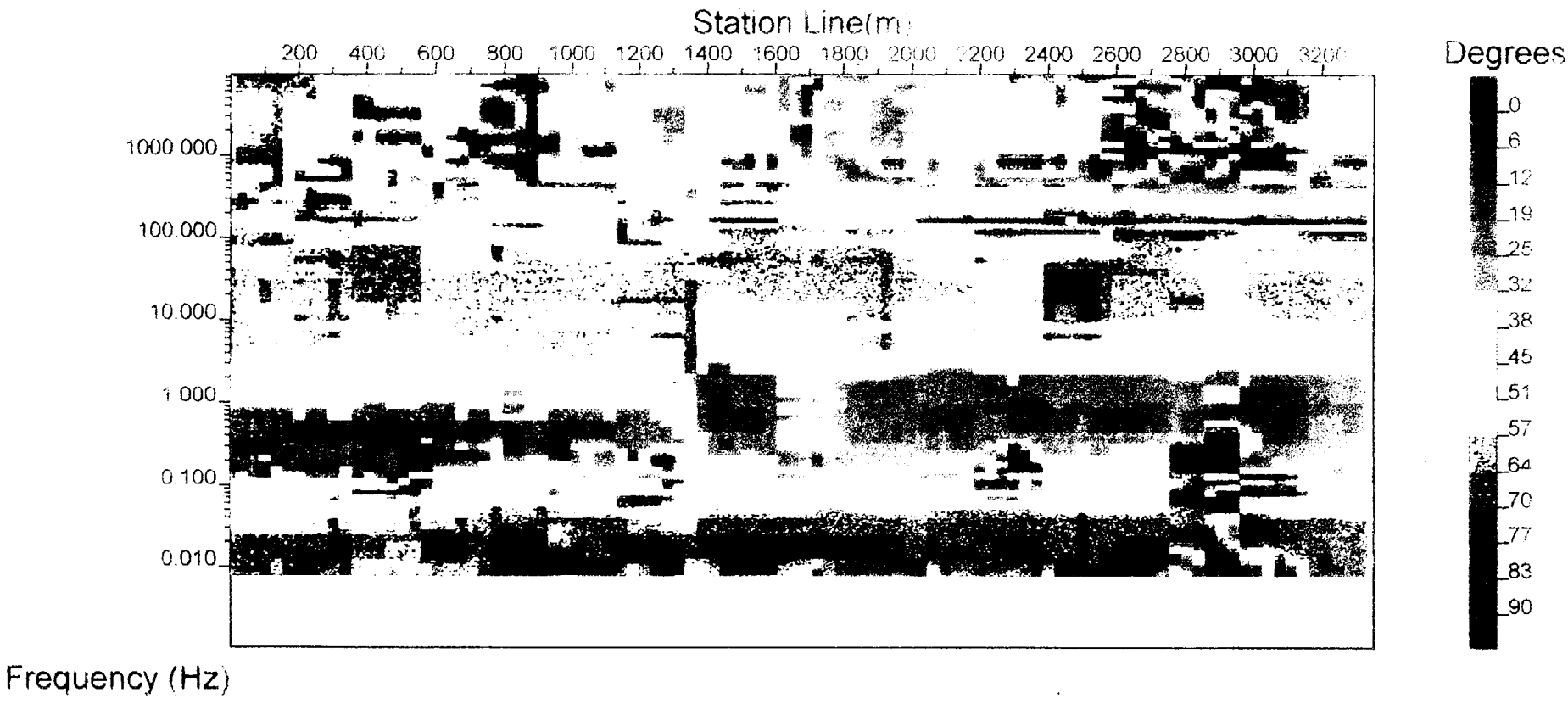

Figure MT3. Raw XY phase data.

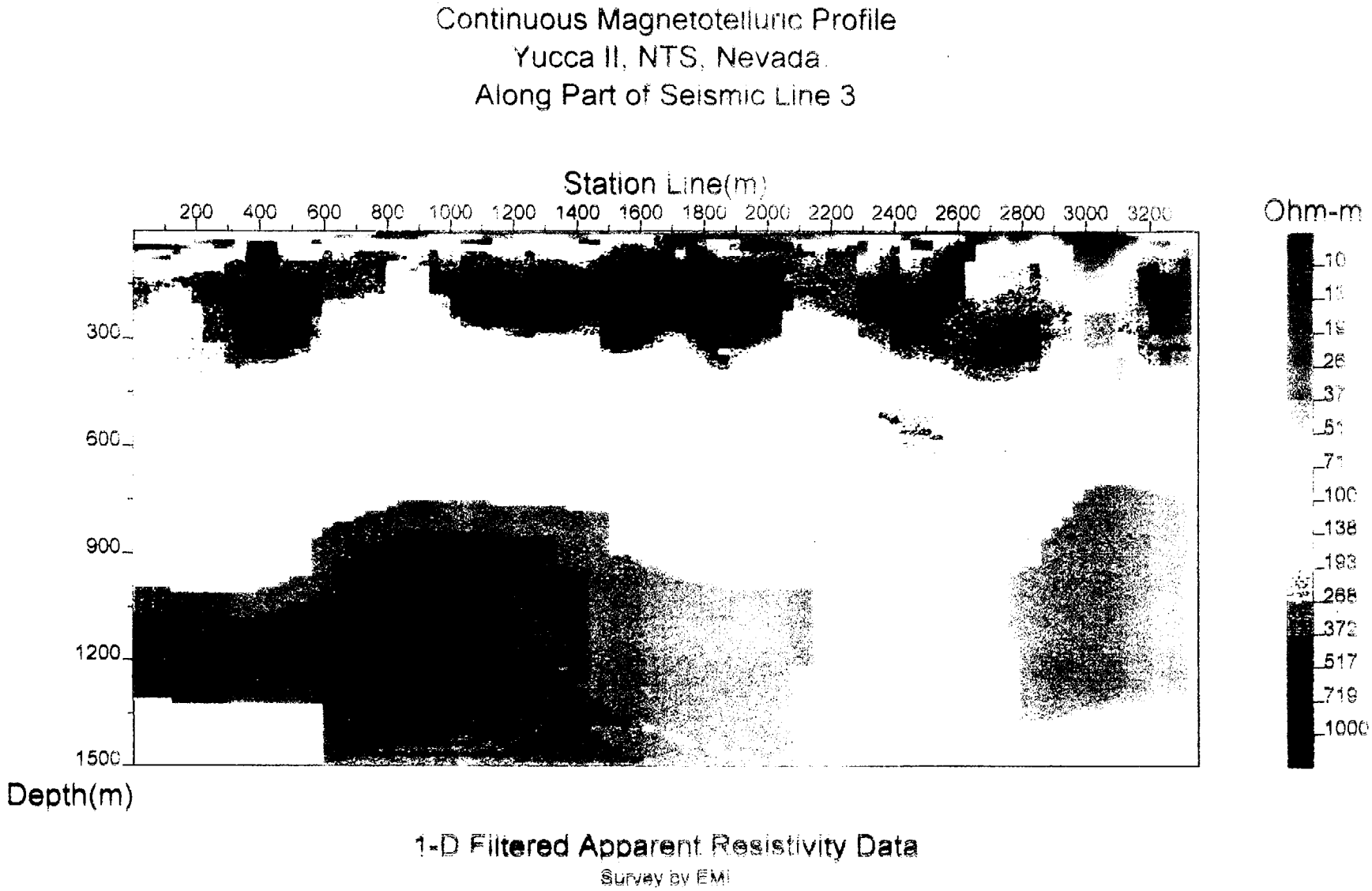

Figure MT4. 1-D filtered apparent resistivity data.

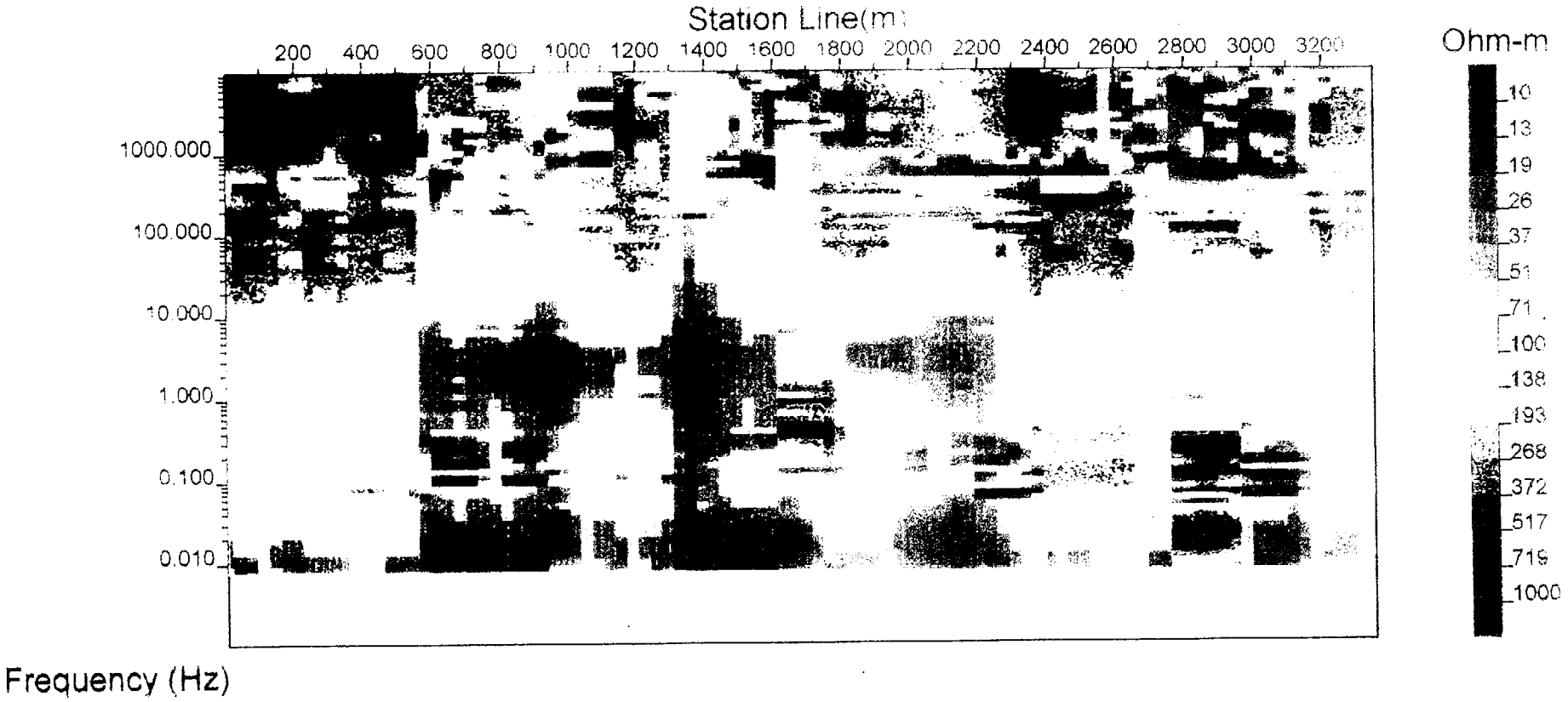

Figure MT5. Raw YX apparent resistivity data.

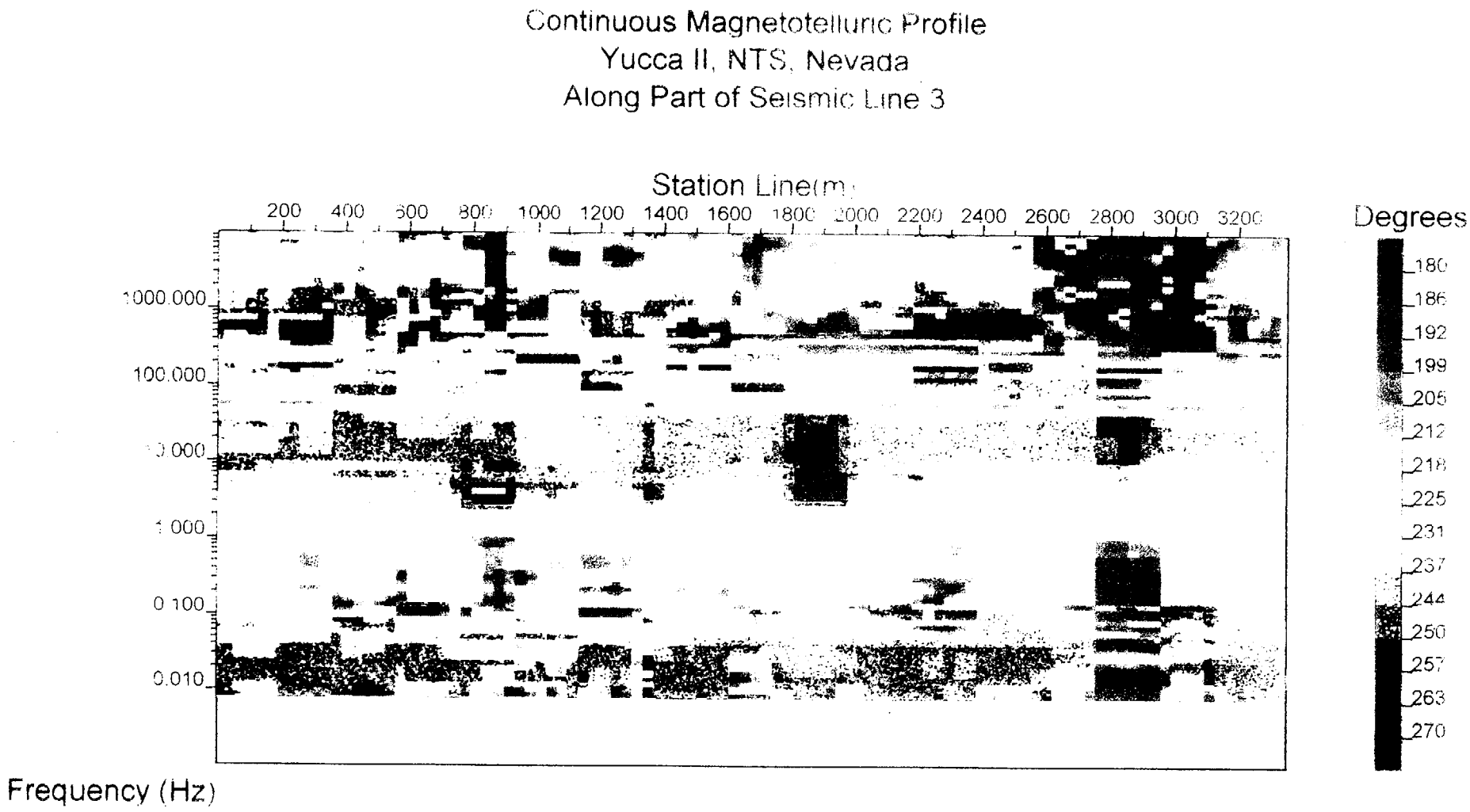

Figure MT6. Raw YX phase data.

Engineering Geoscience

University of California, Berkeley
414 Hearst Mining Bldg.
Berkeley, CA 94720

MT Data for: torquil

Date: 09/07/95

Geotools
MT Workstation

by

Geotools Corporation
5808 Balcones Dr. Suite 202
Austin, Texas 78731 USA
(512) 454-0679

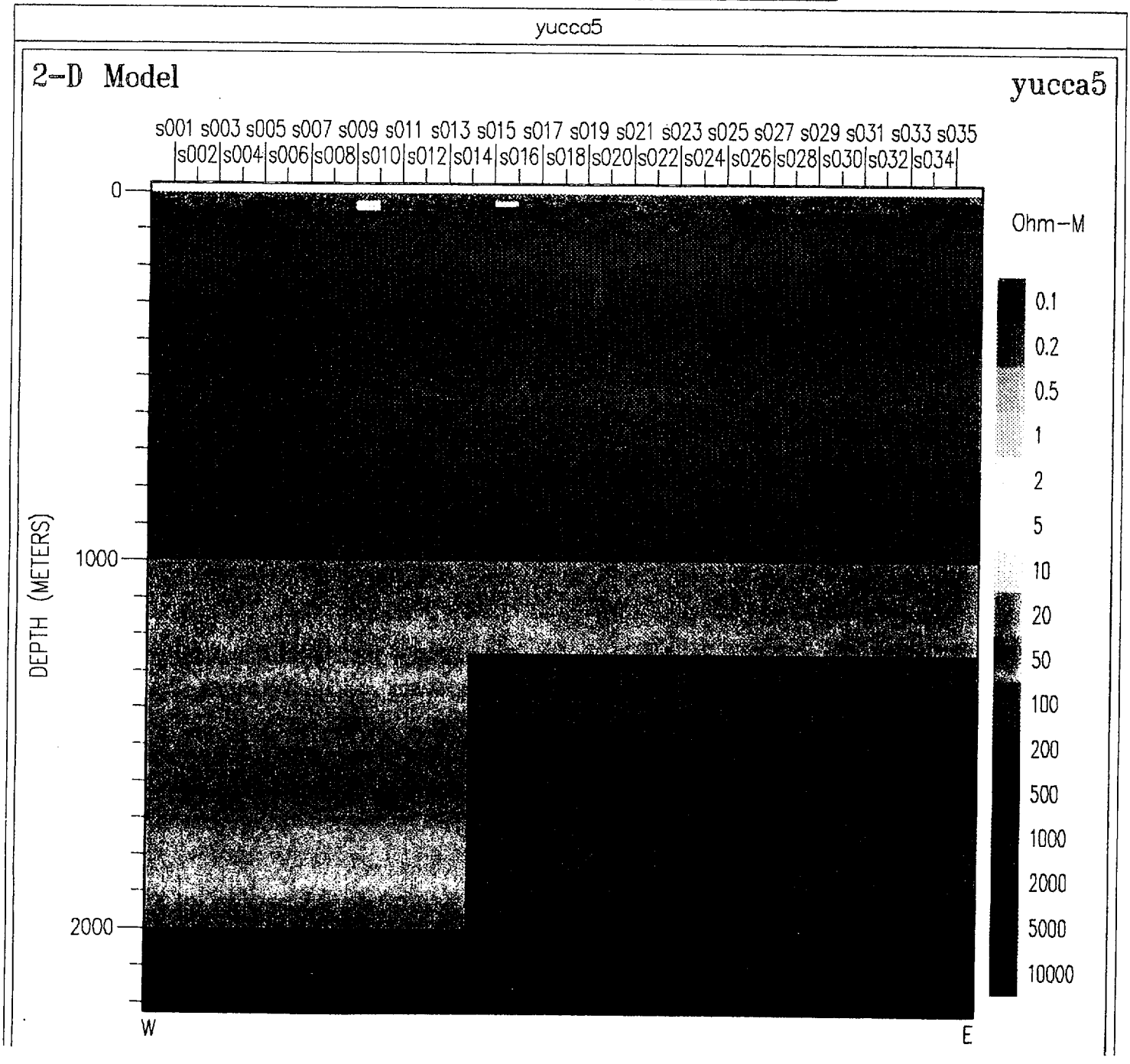

Figure MT7. 2-D resistivity model.

Engineering Geoscience

University of California, Berkeley
414 Hearst Mining Bldg.
Berkeley, CA 94720

MT Data for: torquil

Date: 09/07/95

Geotools
MT Workstation

by

Geotools Corporation
5808 Balcones Dr. Suite 202
Austin, Texas 78731 USA
(512) 454-0679

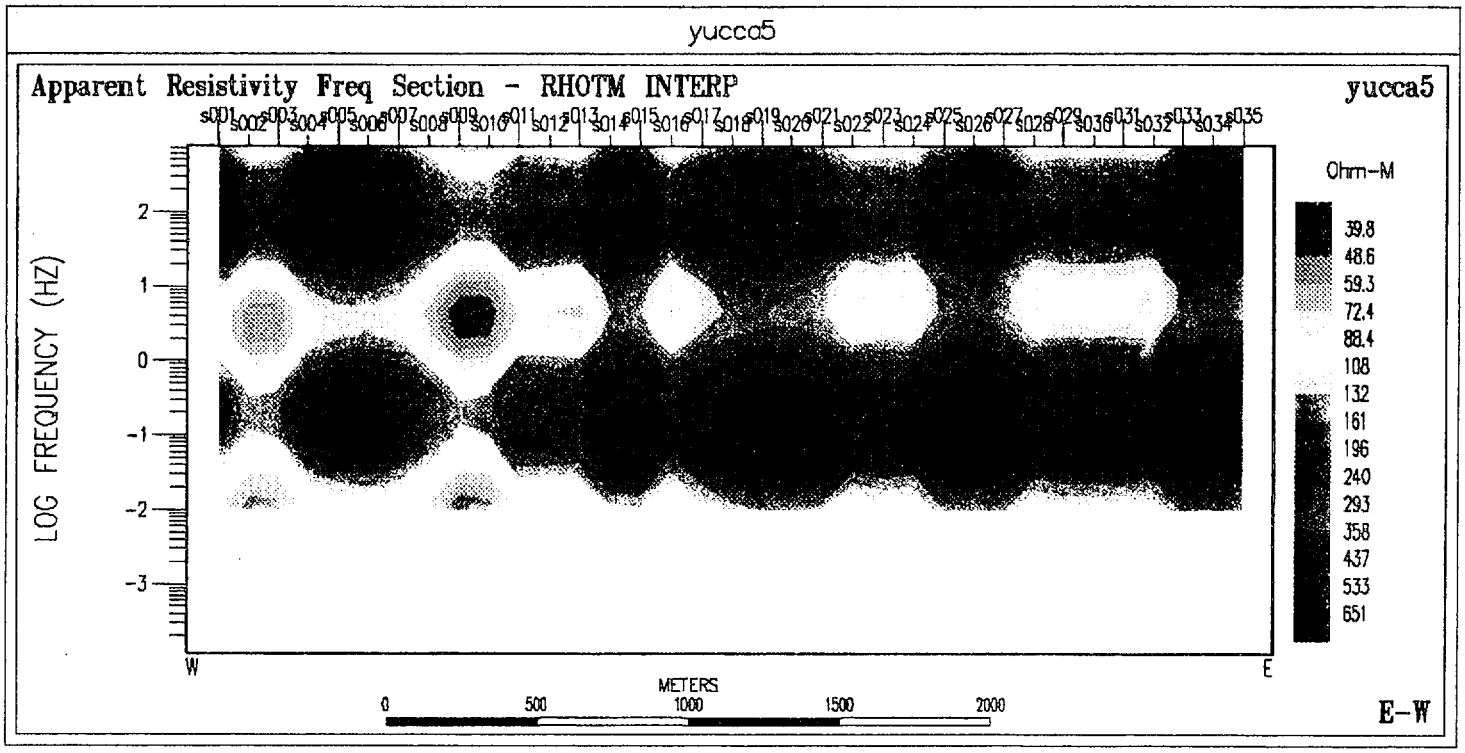

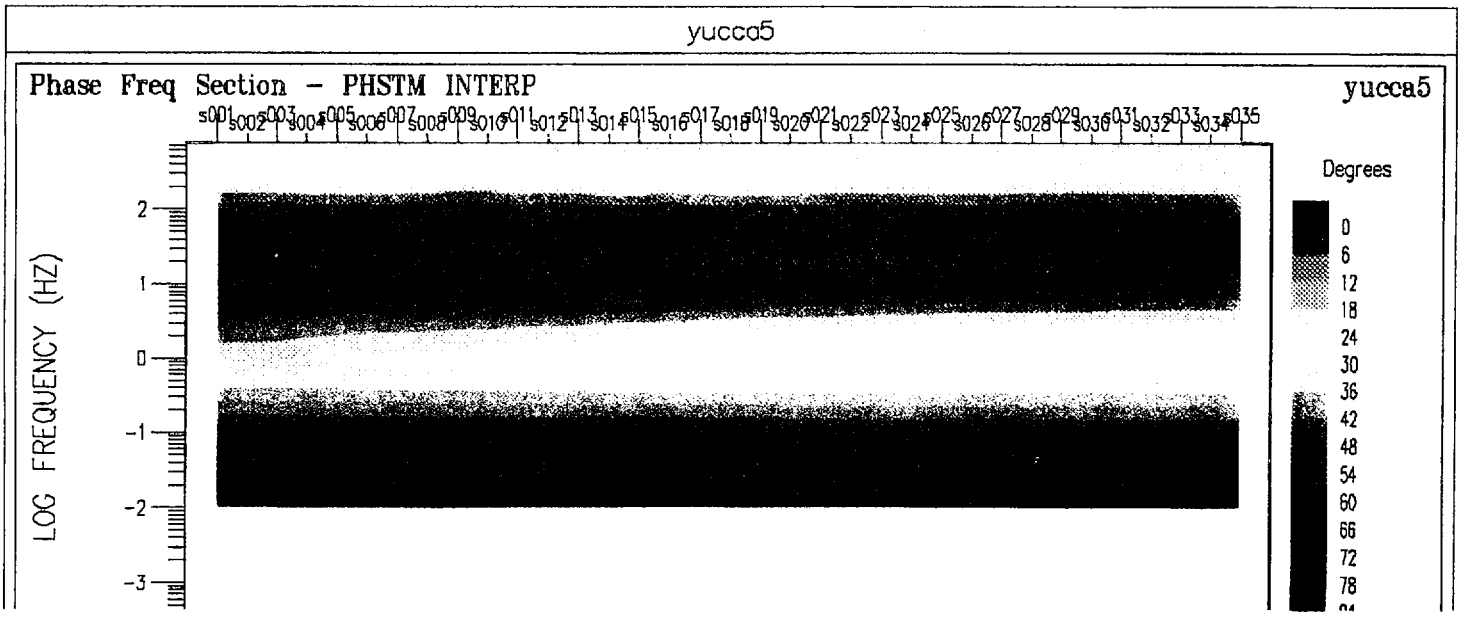

Figure MT8. XY apparent resistivity section.

Engineering Geoscience

University of California, Berkeley
414 Hearst Mining Bldg.
Berkeley, CA 94720

MT Data for: torquil

Date: 09/07/95

Geotools
MT Workstation

by

Geotools Corporation
5808 Balcones Dr. Suite 202
Austin, Texas 78731 USA
(512) 454-0679

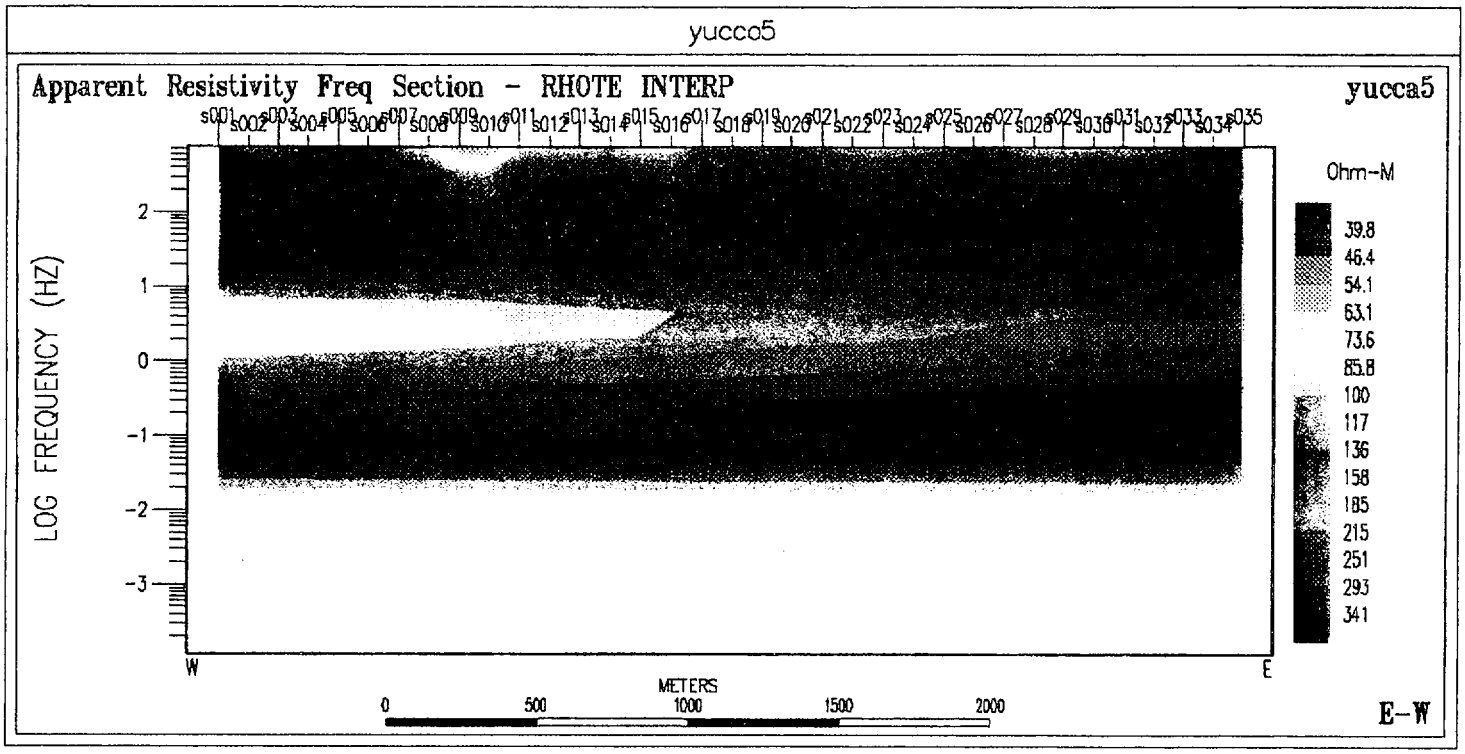

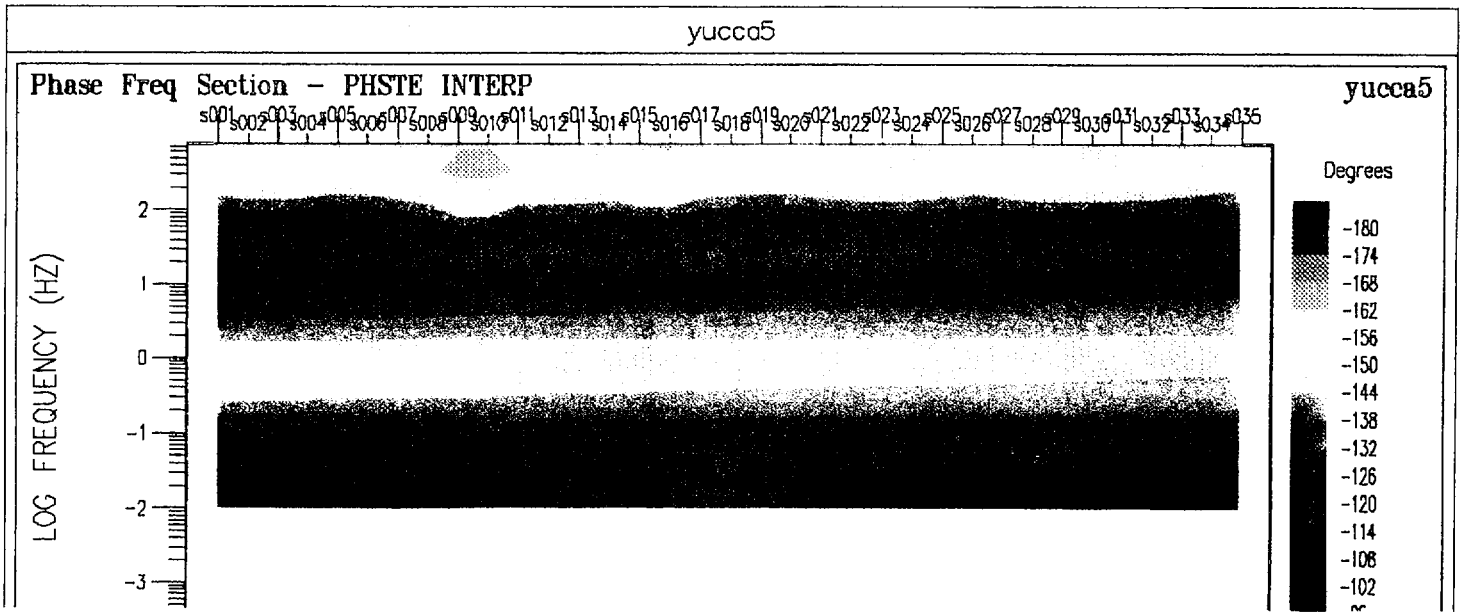

Figure MT9. YX apparent resistivity section.